

NASA CR-

141708

Contract Number NAS 9-13859
DRL Number T-956
Line Item Number 3
DRD Number MA-129T
Harris Report Number 9300-75-001

PERFORMANCE ANALYSIS OF WIDEBAND DATA AND TELEVISION CHANNELS

Final Report

JANUARY 1975



Prepared for
National Aeronautics and
Space Administration
Johnson Space Center
Houston, Texas

Prepared by
Advanced Programs
Department

N75-19481

Unclas
G3/32 13449

(NASA-CR-141708) PERFORMANCE ANALYSIS OF
WIDEBAND DATA AND TELEVISION CHANNELS Final
Report, Feb. 1974 - Jan. 1975 (Harris Corp.,
Melbourne, Fla.) 211 p HC \$7.25 CSCL 17B



HARRIS
COMMUNICATIONS AND
INFORMATION HANDLING

HARRIS CORPORATION Electronic Systems Division*
P.O. Box 37, Melbourne, Florida 32901 305/727-4000
*(formerly RADIATION)

TECHNICAL REPORT STANDARD TITLE PAGE

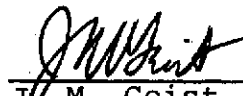
1. Report No.		2. Government Accession No.		3. Recipient's Catalog No.	
4. Title and Subtitle PERFORMANCE ANALYSIS OF WIDEBAND DATA AND TELEVISION CHANNELS				5. Report Date 31 January 1975	
				6. Performing Organization Code	
7. Author(s) Thomas H. Gee and John M. Geist				8. Performing Organization Report No. 9300-75-001	
9. Performing Organization Name and Address Advanced Programs Department Harris Corp., Electronic Systems Div. Melbourne, Florida 32901				10. Work Unit No.	
				11. Contract or Grant No. NAS 9-13859	
12. Sponsoring Agency Name and Address NASA Johnson Space Center Houston, Texas 77058 Technical Monitor: G. D. Arndt				13. Type of Report and Period Covered Final Report Feb. 1974-Jan. 1975	
				14. Sponsoring Agency Code	
15. Supplementary Notes					
16. Abstract <p>This report addresses several aspects of Space Shuttle Communications, and is concerned chiefly with the return link (Shuttle-to-ground) relayed through a satellite repeater (TDRS). The repeater exhibits nonlinear amplification and an amplitude-dependent phase shift.</p> <p>Models are developed for various link configurations, and computer simulation programs based on these models are described. Certain analytical results on system performance are also obtained. These analytical and simulation tools are then applied to several study tasks.</p> <p>For the system parameters assumed, the results indicate approximately 1 dB degradation relative to a link employing a linear repeater. While this degradation is dependent upon the repeater, filter bandwidths, and modulation parameters used, the programs can accommodate changes to any of these quantities. Thus the programs can be applied to determine the performance with any given set of parameters, or used as an aid in link design.</p>					
17. Key Words (Selected by Author(s)) Space Shuttle TDRS Satellite Repeater Nonlinearity				18. Distribution Statement	
19. Security Classif. (of this report) Unclassified		20. Security Classif. (of this page) Unclassified		21. No. of Pages 211	
				22. Price*	

Contract Number NAS 9-13859
DRL Number T-956
Line Item Number 3
DRD Number MA-129T

PERFORMANCE ANALYSIS OF WIDEBAND DATA
AND TELEVISION CHANNELS
FINAL REPORT

January 1975

Prepared by


J. M. Geist
Project Engineer

Approved by


C. L. Mohre
Director

Prepared for
National Aeronautics and
Space Administration
Johnson Space Center
Houston, Texas

Prepared by
Advanced Programs
Department

TABLE OF CONTENTS

<u>Paragraph</u>	<u>Title</u>	<u>Page</u>
	GLOSSARY	vii
1.0	INTRODUCTION	1-1
1.1	Simulation Philosophy	1-1
1.2	Description of Study Tasks	1-2
1.3	Principal Results and Recommendations for Further Investigation.	1-3
1.4	Organization of the Report	1-4
1.5	Acknowledgements	1-5
2.0	MATHEMATICAL MODEL OF THE RETURN LINK	2-1
2.1	RF Signals and Baseband Representation	2-1
2.2	Repeater Model	2-2
2.3	Signal Formats	2-5
2.3.1	High Rate Data Channels	2-5
2.3.2	Multiplexed Data and Television Channels	2-8
2.4	Ground Receivers	2-9
2.4.1	Receivers for High Rate PSK Signals.	2-9
2.4.2	Receiver for TV-PSK FDM/FM Signal	2-11
2.5	Summary	2-15
2.6	References	2-15
3.0	ANALYTICAL RESULTS	3-1
3.1	TWT Effects on Sine Wave Plus Gaussian Noise	3-1
3.2	TWT Effects on PSK Detection	3-9
3.2.1	Single-Sample Error Probability	3-11
3.2.2	Density Function of the Mixer Output	3-16
3.3	The FDM/FM Link at High Signal-to-Noise Ratios	3-23
3.4	References	3-31
4.0	SIMULATION OF THE RETURN LINK	4-1
4.1	General Considerations	4-1
4.2	High-Rate PSK Simulations	4-2
4.3	FDM/FM Simulation	4-6
4.4	Reference	4-21
5.0	QUANTITATIVE RESULTS FOR STUDY TASKS	5-1
5.1	Performance of the FDM/FM Link	5-1
5.2	Performance of High Rate Digital Links	5-4
5.3	Performance of the Analog TV/FM Link	5-10
5.4	Filtering and TWT Effects on Spread-Spectrum Signals	5-13

TABLE OF CONTENTS (Continued)

<u>Paragraph</u>	<u>Title</u>	<u>Page</u>
5.5	Blackout Reduction at Ku-Band	5-23
5.6	Degradation Due to Repeater Nonlinearity . .	5-24
5.7	References	5-29

APPENDICES

A	Equivalent Baseband Representation of an RF System	A-1
B	Representation of Nonlinearities	B-1
C	Implementation of Digital Filters	C-1
D	Filter Generation Programs and Their Use . .	D-1
E	Use of the Simulation Programs	E-1

LIST OF ILLUSTRATIONS

<u>Figure</u>	<u>Title</u>	<u>Page</u>
2.0-1	General Block Diagram of the Return Link . . .	2-1
2.2-1	Typical TWT Characteristics	2-4
2.2-2	AM-to-PM Conversion Characteristic	2-6
2.3.1-1	NRZ-L PSK Power Spectrum	2-7
2.3.1-2	Split-Phase PSK Power Spectrum	2-7
2.3.2-1	Baseband FDM Signal Spectrum	2-8
2.4.1-1	Receiver for the High-Rate NRZ-L PSK Signal. . .	2-10
2.4.2-1	RF Demodulator for FDM/FM Signal	2-11
2.4.2-2	Phase-Locked Loop	2-12
2.4.2-3	Baseband Model of the Phase-Locked Loop. . . .	2-13
2.4.2-4	Linearized Baseband PLL Model	2-14
2.5-1	Baseband Model of the NRZ-L PSK Link	2-16
2.5-2	Baseband Model of the Split-Phase PSK Link . .	2-16
2.5-3	Baseband Model of the FDM/FM Link	2-17
3.1-1	Envelope and Phase Moments for Sine Wave Plus Gaussian Noise	3-3
3.1-2	Normalized Average, Mean Square, and Standard Deviation of TWT Output Amplitude, $\beta = 0.44$. .	3-6
3.1-3	Average Output Phase and $\gamma, \beta = 0.44$	3-7
3.1-4	RMS Phase Jitter at TWT Output, $\beta = 0.44$. . .	3-8
3.2-1	Discrete-Time Model of PSK Communication Link	3-10
3.2.1-1	PSK Signal Phasor Representations	3-12
3.2.1-2	Equal-Probability Loci for Input Signal Phasor $A = 0.44E_{SAT}$	
3.2.1-3	Single-Sample Error Probability for Ideal Hard Limiter	3-15
3.2.1-4	Single-Sample Error Probability for TWT of Figure 2.2-1, $\beta = 0.44$	3-17
3.2.2-1	Domain and Range of the Transformation (E, ϕ) \rightarrow (r, s)	3-19
3.2.2-2	Density Function of $\cos \phi$ at $\rho = 0$ dB	3-21
3.2.2-3	Density Function of v for TWT of Figure 2.2-1 at $\rho = 0$ dB and $\beta = 0.44$	3-22
3.3-1	Model of FDM/FM Communication Link	3-24
3.3-2	PSK Detector	3-28
4.2-1	Organization of the NRZ-L PSK Simulation Program	4-3
4.2-2	Pseudorandom Data Sequence Generator	4-4
4.2-3	Frequency Response of Lowpass Equivalent of Wideband TDRS Input Filter	4-5
4.2-4	Frequency Response of Lowpass Equivalent of Narrowband TDRS Input Filter	4-7
4.3-1	Organization of the FDM/FM Simulation Program	4-8

LIST OF ILLUSTRATIONS (Continued)

<u>Figure</u>	<u>Title</u>	<u>Page</u>
4.3-2	Signal Options in FDM/FM Simulation Program .	4-9
4.3-3	Frequency Response of Lowpass Premultiplexing Filter (Eighth-Order Chebyshev)	4-11
4.3-4	Frequency Response of Bandpass Premultiplex- ing Filter (Fourth-Order Butterworth). . . .	4-12
4.3-5	Frequency Response of the IF Filter Lowpass Equivalent	4-14
4.3-6	Implementation of the Loop Filter	4-13
4.3-7	Frequency Response of the Linearized PLL . . .	4-16
4.3-8	PLL FM Demodulator Characteristic	4-17
4.3-9	Phase-Locked Loop 3-dB Point as a Function of Loop Gain	4-18
4.3-10	Power Measurements for Determination of Test- Tone-to-Noise Ratio	4-20
5.1-1	Establishing PSK Synchronization by Inspection	5-2
5.1-2	Test Tone-to-Noise Ratio at Demultiplexing Filter Output	5-5
5.1-3	PSK Error Probability for the FDM/FM Signal. .	5-6
5.1-4	PLL RMS Tracking Error	5-7
5.2-1	Simulated Performance of NRZ-L PSK System . .	5-9
5.2-2	Simulated Performance of Split-Phase PSK System	5-11
5.3-1	Output Test Tone-to-Noise Ratio for Analog TV/FM Signal, Downlink SNR = 20 dB	5-12
5.3-2	PLL RMS Tracking Error, Downlink SNR = 20 dB	5-14
5.4-1	Simplified Model of the Forward Link	5-13
5.4-2	Model for Degradation Calculations	5-16
5.4-3	Lower Bound to Degradation for Ideal Filter- ing of a Baseband Pseudorandom Signal. . .	5-19
5.4-4	Generator for PN Sequence of Length 2047 . .	5-20
5.4-5	Bounds on Degradation for a Filter-TWT Cascade	5-22
5.6-1	A Typical TWT Characteristic and Its Linear Equivalent at Operating Point A	5-26
5.6-2	Model of a Linear Repeater Link. (a) Linear Repeater Link. (b) Equivalent Model. (c) One-Sided Power Spectral Density of $n_{eq}(t)$	5-27
5.6-3	Test Tone-to-Noise Ratio at Lowpass Demulti- plexing Filter Output for FDM/FM Signal, Downlink SNR = 15 dB	5-30

LIST OF ILLUSTRATIONS (Continued)

<u>Figure</u>	<u>Title</u>	<u>Page</u>
5.6-4	Comparison of TWT and Linear Repeater for NRZ-L PSK Signal, Downlink $E_b/N_0 = 10$ dB. .	5-31
5.6-5	Comparison of TWT and Linear Repeater for Split-Phase PSK Signal, Downlink $E_b/N_0 = 10$ dB	5-32
A-1	Bandpass System	A-1
A-2	System Input Passband	A-1
A-3	Equivalent Baseband System	A-2
A-4	Filter Transformations	A-5
B-1	Quadrature Model of a TWT Nonlinearity. . . .	B-3
C-1	Effect of Lowpass-to-Bandpass Transformation	C-5
E-1	Sample Input Deck for FDM/FM Simulation . . .	E-5
E-2	Sample Input Deck for NRZ-L PSK Simulation .	E-22

LIST OF TABLES

<u>Table</u>	<u>Title</u>	<u>Page</u>
3.2.1-1	Adjustment Factor and Phase Offset	3-16
5.1-1	System Performance as a Function of PLL Gain	5-8
5.2-1	Correlator Phase for Various SNR's	5-10
5.4-1	Forward Link Spectrum-Spreading Parameters .	5-15

GLOSSARY

This glossary summarizes symbols and abbreviations used generally throughout the text. Symbols which are defined and used only within a brief development are omitted, as are symbols whose use is in agreement with universal engineering practice.

A	Amplitude of a transmitted (uplink) signal
C	Chip rate of a PN sequence
c	Signal amplitude on a virtual channel
d(t)	Baseband data signal
E	TWT input voltage
E_{sat}	Saturating drive level of TWT
E(t)	Envelope of signal at repeater input
F(.)	TWT amplitude nonlinearity
f(.)	Normalized TWT amplitude nonlinearity
f_{sc}	PSK subcarrier frequency (FDM/FM signal)
$\Delta f_1, \Delta f_2$	Zero-to-peak RF deviations (FDM/FM signal)
G	Phase-locked loop gain
G(.)	AM-to-PM conversion characteristic
g(.)	Normalized AM-to-PM conversion characteristic
K	Gain of linear repeater
N_o	One-sided uplink noise power spectral density
P_E	Bit error probability
Q(.)	Complementary error function
R	Data rate
R_o	TWT output voltage at saturation

T	Duration of a bit (Sections 2 and 3) Duration of a simulation run (Section 4.3) Sampling interval (Appendix C)
$u(t)$	Analog baseband message (FDM/FM signal)
$v(t)$	FDM baseband (analog and PSK)
$x_1(t)$	Uplink transmitted signal
$x_2(t)$	Downlink transmitted signal
$y_1(t)$	Uplink received signal
$y_2(t)$	Downlink received signal
z_o	One-sided downlink noise power spectral density
α	Correlator phase offset at PSK receiver
β	TWT backoff; i.e., fraction of saturating input level at which tube is driven
β_1, β_2	RF deviation ratios (FDM/FM signal)
$\phi(t)$	Phase of signal at repeater input
$\psi(t)$	Phase of transmitted (uplink) signal
ρ	Signal-to-noise ratio Cross-correlation between two binary signals (Section 5.4)

SECTION 1.0
INTRODUCTION

1.0

INTRODUCTION

The diverse capabilities and missions planned for the Space Shuttle require flexible and reliable communications between the Orbiter and ground. In the Spaceflight Tracking and Data Network (STDN) of the future, one of the alternative configurations for Shuttle communications will be to relay the signals through the Tracking and Data Relay Satellite (TDRS). This study addresses the problem of Shuttle communications through TDRS and is concerned chiefly with the return link (Orbiter to TDRS to ground). The major objectives of this study are to develop models and techniques which can be used to determine the effects on system performance of the nonlinear amplification by the repeater.

Over the past several years, considerable study has been devoted to the problem of communication through a nonlinear satellite repeater. Most of this work has addressed the situation in which several users, either frequency- or code-multiplexed, simultaneously access the satellite via high-power uplinks. In the Shuttle return link, however, the transmitter is onboard the Shuttle, rather than at a ground station; therefore, the uplink is power limited and additive noise must be considered on the uplink as well as the downlink. The Shuttle utilizes single-access TDRS channels. Thus amplitude variations at the repeater input are due entirely to the effects of additive noise and not to interference by other users.

Exact analysis of communication systems having nonlinear components is usually possible only if some special form of the nonlinearity is assumed. It was desired in this study to develop models and techniques which could be used for general repeater characteristics and not be limited to given functional forms. This suggested the use of a flexible, modular digital computer simulation of the communication system. Once written, this simulation could be applied to determine answers to specific problems of interest in the Shuttle communication system.

1.1

Simulation Philosophy

Developing the mathematical model of a system and writing the corresponding computer simulation program is only one step in the simulation approach to solving the problem. It is equally important to develop a simulation philosophy which recognizes the limitations as well as the capabilities of the simulation program. For example, it is relatively straightforward to write a computer simulation program for a digital communication system and to apply this program in Monte Carlo fashion to determine the error probability of

the system. However, if error probabilities on the order of 10^{-4} are of interest, then the simulation program must process on the order of 10^6 bits, to obtain measurements of reasonable confidence. If the program is sufficiently complicated, this leads to enormous run times and this direct approach is not a cost-effective method to solve the problem. In this study, reasonable efforts have been made to make the simulation programs as efficient as possible without sacrificing the convenience of modularity. However, the communication system being modelled is, itself, so complex that the run times prohibit direct Monte Carlo measurements of low error probabilities. The usefulness of these simulations, therefore, generally lies elsewhere than in direct measurement of the quantities of interest.

In many cases, some measurements taken by Monte Carlo simulations will be useful. For example, in determining the degradation due to the use of a nonlinear repeater, the user might reason that the effects of the nonlinearity are felt most seriously at low input signal-to-noise ratios. Therefore, measurements of degradation under this condition, say, at error probabilities of 10^{-2} , would furnish lower bounds to degradation at error probabilities of actual interest.

Another useful feature of the simulation programs developed in this study is the capability to plot the waveform at various points in the receiver. By making use of this option, the user can obtain a visual display of the effects on the waveform of narrowing filter bandwidths, changing nonlinear characteristics, varying modulation parameters, and so forth. This information can yield considerable insight into the effects of various components on overall system performance.

1.2 Description of Study Tasks

The contract Statement of Work delineates six specific areas of investigation under this study. Task 1 is concerned with the performance of an FDM/FM communication link in which an analog television signal is frequency multiplexed with a PSK signal. The composite signal frequency modulates an RF carrier and is transmitted through the nonlinear repeater to ground. The problem is to determine the effects of the repeater on appropriate performance parameters, namely, signal-to-noise ratio for the analog portion of the signal and error probability for the PSK portion of the signal.

Task 2 is concerned with a pure digital data signal which directly phase shift keys the RF carrier. Two formats are of interest: a 100 Mb/s NRZ-L format and a 30 Mb/s split-phase (also called biphas-L) format.

The system of interest in Task 3 is essentially the same as that in Task 1 except that the digital portion of the signal is removed. That is, an analog video signal frequency modulates the RF carrier for transmission over the repeater channel.

Unlike the other tasks, Task 4 is concerned with the forward link. The signal on the forward link is a pure digital signal consisting of command data, synchronization data and digitized voice. In order to satisfy international regulations on the received power density at the earth's surface, the spectrum of the signal is spread by mixing with a pseudorandom sequence of appropriate chip rate. Task 4 is concerned with the determination of the degradation when such a spread spectrum signal is passed through the filters and nonlinearity in the TDRS repeater.

Task 5 addresses the problem of blackout due to the formation of plasma on the outside surface of a vehicle as it reenters the earth's atmosphere. The degree of attenuation due to the plasma is a function of the signal frequency as well as several other factors; the task is specifically concerned with reduction of the blackout effect by the use of a K_u -band carrier*.

The final task, Task 6, is concerned with the overall degradation in link performance due to the presence of a nonlinear repeater in the link. In this task, the performance results compiled in Tasks 1, 2 and 3 are compared with the expected performance when an equivalent linear repeater is used.

1.3 Principal Results and Recommendations for Further Investigation

The chief products of this study are the mathematical models developed for the transmission of Shuttle signals through a nonlinear repeater, and the computer simulation programs derived from these models. These can be valuable tools in the analysis and overall system design of the Shuttle return link. The programs themselves are extremely flexible. The characteristics of the repeater nonlinearity, filter transfer functions, and modulation parameters of the signals are all variable either on input or by relatively simple modifications to the programs. This flexibility is especially significant in view of the fact that many of the parameters of the actual link, such as TDRS characteristics, are not yet clearly defined. In fact, one of the most important

*During the course of the study, the Technical Monitor directed that this task be de-emphasized in order to devote more time to the other five tasks.

uses of these programs could be in helping to determine appropriate specifications for TDRS.

With regard to the principal tasks of interest in this study, performance of the system has been evaluated using the simulation programs and the results verified where possible by analytical means. In general, the conclusion is that use of the nonlinear repeater leads to approximately 1 dB degradation with respect to an equivalent linear repeater. These results are conditioned on the use of specific repeater characteristics, filters and modulation parameters. However, these characteristics are typical of those which are expected to be used in the actual link. As the link characteristics become available, they can easily be built into the programs.

In their present form, the models depend heavily on the assumption of a single carrier centered in the receive band of the repeater. Since the possibility exists of a tracking beacon being sent on a separate carrier, it would be useful to generalize the model to accept two carriers. Another useful extension of this work would be to implement synchronization subsystems in the receivers (synchronization is now effectively hardwired). Implementation of carrier, subcarrier and bit synchronizers would permit study of the effects of the nonlinearity on the ability to synchronize, to track doppler variations, and so forth.

Other areas in which further investigation would be profitable are the effects of the nonlinearity on performance of coded communication systems, study of structure and performance of optimum receivers for nonlinearly relayed signals, and refinement and simplification of the analytical results developed in this study.

Finally, an important area of future work is to carefully monitor the progress of the TDRS program and make appropriate changes and modifications to the simulation programs developed in this study in order that these programs may continue to be useful in analyzing performance of the Shuttle-TDRS-ground link.

1.4 Organization of the Report

In Section 2, a mathematical model of the return link is developed. This section specifies the details of the repeater characteristics, the signal formats of interest and the appropriate receivers. The models developed in this section form the basis for the computer simulation programs discussed subsequently.

In Section 3, a number of analytical results on performance of both the digital and the FDM/FM signals are developed. These results are included chiefly because of the insight they give into the underlying mathematical structure of the system.

The simulation programs themselves are discussed in Section 4. This section shows how the models developed in Section 2 are organized into software modules in the simulation programs. It also discusses various considerations of programming such as the selection of sampling rates, the implementation of filters, and so forth.

The results of the efforts on the six tasks discussed earlier are contained in Section 5. Tasks 1, 2, 3 and 6 rely heavily on the use of the simulation programs. It should be stressed that the results reported on these tasks are for specific filters, specific repeater characteristics and specific modulation parameters. They should be considered more as examples of the use of the simulation programs than as results of general significance.

The report concludes with several appendices. The first three contain mathematical details supporting developments in the main body of the text. The remaining appendices contain program listings, detailed run time information, instructions on use of the programs, and other documentation of the software.

1.5 Acknowledgements

The authors acknowledge with appreciation the technical guidance and many helpful suggestions of the Technical Monitor, Dr. G. D. Arndt, and his associates at Johnson Space Center. Several of our colleagues at HARRIS Electronic Systems Division have made significant contributions to this work. Among them, special mention is due to M. A. Harrell, who accomplished most of the computer programming and operation during the course of the study.

SECTION 2.0

MATHEMATICAL MODEL OF THE RETURN LINK

2.0

MATHEMATICAL MODEL OF THE RETURN LINK

This section develops the mathematical model which subsequently leads to analytical and simulation results on performance of the return link, which is diagrammed in Figure 2.0-1. First, signal flow through the system is discussed in general, then the three system components are discussed in detail separately.

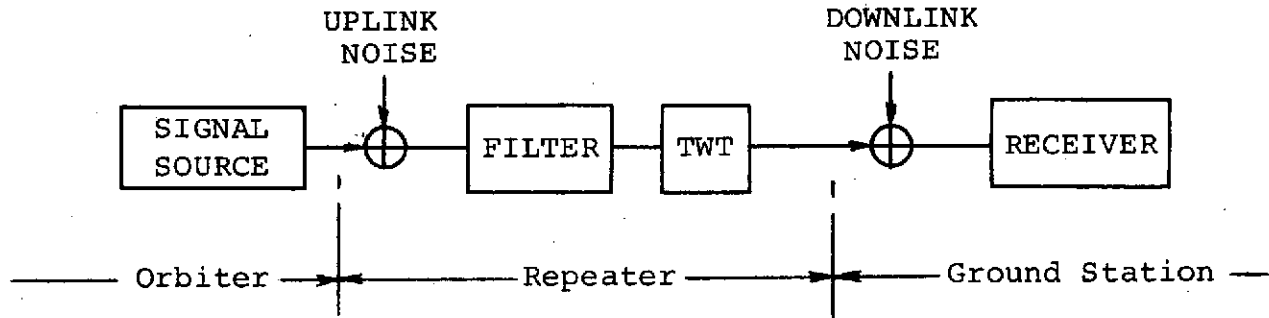


FIGURE 2.0-1. GENERAL BLOCK DIAGRAM OF THE RETURN LINK

2.1

RF Signals and Baseband Representation

For the situations of interest in this study, the signal source emits a narrowband signal of constant amplitude and modulated phase, situated in the center of the repeater's receive band:

$$\begin{aligned} x_1(t) &= A \cos [\omega_1 t + \psi(t)] \\ &= \text{Re} \{ A e^{j\psi(t)} e^{j\omega_1 t} \} \end{aligned}$$

This signal is received in the presence of narrowband Gaussian noise, represented as

$$\begin{aligned} n_1(t) &= n_{1c}(t) \cos \omega_1 t - n_{1s}(t) \sin \omega_1 t \\ &= \text{Re} \{ N_1(t) e^{j\omega_1 t} \} \end{aligned}$$

where $N_1(t) = n_{1c}(t) + j n_{1s}(t)$. Therefore, the repeater input can be represented as

$$y_1(t) = \text{Re} \{ E(t) e^{j\phi(t)} e^{j\omega_1 t} \}$$

where $E(t) = |A e^{j\psi(t)} + N_1(t)|$ and $\phi(t) = \angle (A e^{j\psi(t)} + N_1(t))$.

In Appendix A, it is shown that the bandpass filtering of this narrowband signal performed by the repeater input filter is equivalent to lowpass filtering its complex envelope $E(t)\exp(j\phi(t))$ by a lowpass equivalent of the bandpass filter. Therefore, the Traveling Wave Tube (TWT) input is given by

$$Y_T(t) = \text{Re}\{\hat{E}(t)e^{j\hat{\phi}(t)} e^{j\omega_1 t}\}$$

where $\hat{E}(t)e^{j\hat{\phi}(t)} = h_{LP}(t) * [E(t)e^{j\phi(t)}]$

$h_{LP}(t)$ denoting the impulse response of the equivalent lowpass filter, and $*$ representing the convolution operator.

The effect of the TWT is to nonlinearly scale the amplitude and to rotate the phase by an amount dependent on the amplitude. In addition, the carrier frequency is shifted to a different value for transmission to ground. Thus, the repeater output can be written

$$x_2(t) = \text{Re}\{F(\hat{E}(t))e^{j[\hat{\phi}(t)+G(\hat{E}(t))]} e^{j\omega_2 t}\}$$

The addition of downlink noise and filtering in the RF and IF stages of the ground receiver can be handled in the same fashion as in the uplink, leading to a detector input of the form

$$Y_D(t) = \text{Re}\{R(t)e^{j\theta(t)} e^{j\omega_2 t}\}$$

The detector itself performs some function on the complex envelope $R(t)\exp(j\theta(t))$; for example, an ideal limiter-discriminator furnishes $\theta(t)$ as output.

It is apparent from the foregoing discussion that all the operations on RF signals performed by the various system components can be emulated at baseband by operations on complex envelopes. Appendix A contains a more thorough and rigorous discussion of baseband modeling. Subsequent sections of this chapter will address the specific complex envelope operations performed by each component of the system. Since the characteristics of the repeater place constraints on the types of signals which can be used, the repeater is discussed first.

2.2 Repeater Model

The repeater in Figure 2.0-1 is the Tracking and Data Relay Satellite (TDRS) which, as currently envisioned, will provide a variety of user modes and frequencies for both forward (ground-to-user) and return (user-to-ground) links [2-1].

The modes of interest in this study are the single access modes at Ku-band. For this service, the user may elect to employ either a wideband mode, with 225 MHz bandwidth at $f_c=15.0085$ GHz, or a narrowband mode with 88 MHz bandwidth at either 14.94 GHz or 15.077 GHz. After passing through the repeater input filter, the signal undergoes amplification by a TWT, and is then transmitted to ground (at a different carrier frequency). Spurious response at harmonics of the carrier frequency are effectively suppressed by a "zonal filter" of extremely broad bandwidth at the TWT output.

Over a fairly wide frequency range, the effects of TWT amplification of an RF signal can be represented as amplitude scaling and phase rotation by nonlinear functions of the input amplitude [2-2], [2-3]. That is, if the TWT input is

$$y(t) = E(t) \cos[\omega_c t + \phi(t)]$$

then the TWT output will be

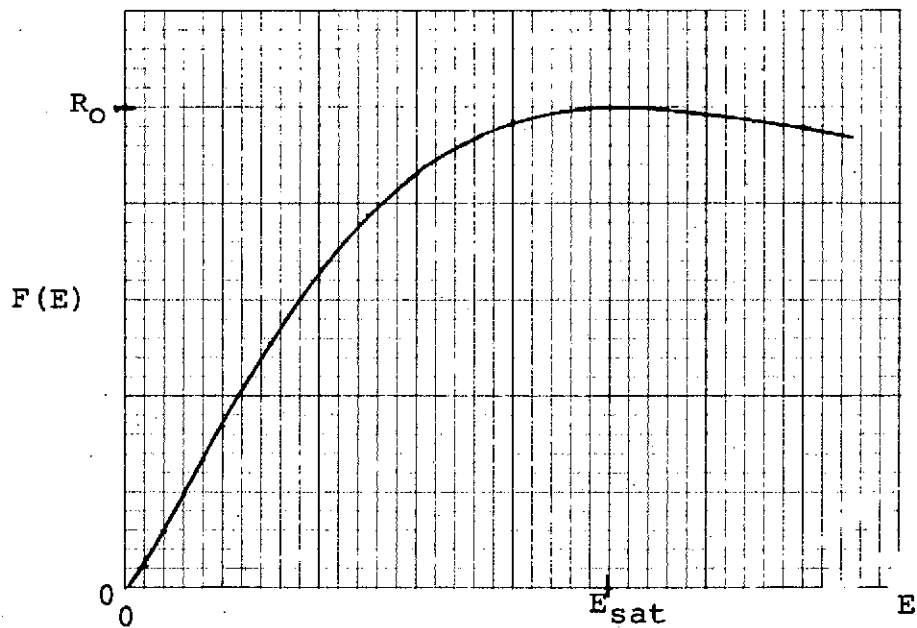
$$z(t) = F(E(t)) \cos[\omega_c t + \phi(t) + G(E(t))] \quad (2.2-1)$$

Because of the amplitude-dependent phase term $G(E(t))$ in the TWT output, the tube is said to exhibit AM-to-PM conversion. It is important to note from the form of Equation (2.2-1) that the nonlinearity can be represented purely in terms of its effects on the complex envelope of the input; i.e.,

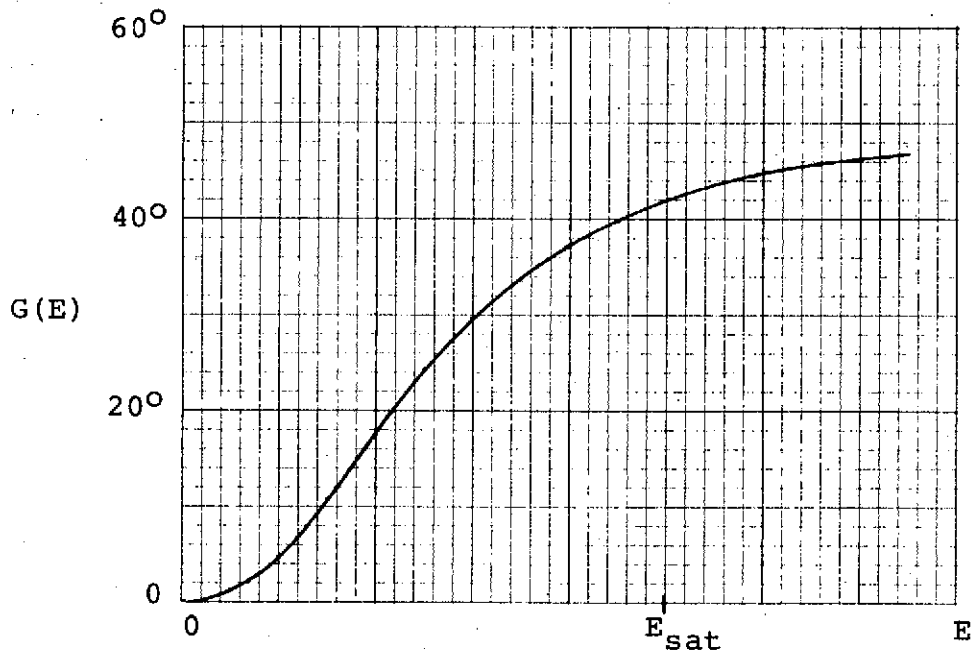
$$E(t)e^{j\phi(t)} \rightarrow F(E(t))e^{j[\phi(t)+G(E(t))]}$$

Thus, the actual repeater consisting of the cascade of a bandpass input filter, a nonlinearity, and a wideband zonal filter, can be modeled as the cascade of a lowpass filter operating on the complex envelope, followed by the operations of $F(\cdot)$ and $G(\cdot)$. Further discussion of this and alternate representations of nonlinearities is contained in Appendix B.

Typical functions $F(\cdot)$ and $G(\cdot)$ are illustrated in Figure 2.2-1. These curves are interpolated from actual TWT measured data supplied by the Technical Monitor. The input amplitude E_{sat} at which $F(E)$ is maximum is called the saturating drive level; the range $E > E_{sat}$ is called the overdrive region. There is a range of $E < E_{sat}$ over which the function is reasonably linear. When an amplitude-modulated signal, or several simultaneous signals, access the TWT, it is normally operated in this linear region in order to minimize distortion or intermodulation responses. However, when a single constant-envelope signal drives the TWT, it can be operated at or near saturation, unless the additive input noise causes appreciable envelope variation.



(a)



(b)

FIGURE 2.2-1. TYPICAL TWT CHARACTERISTICS

(a) Amplitude Nonlinearity. (b) AM-to-PM Conversion

The AM-to-PM conversion characteristic $G(\cdot)$ is redrawn in Figure 2.2-2 with the input amplitude represented in decibels below the saturating value. The characteristic is closely approximated by a straight line over a range of several decibels. AM-to-PM conversion is often specified in a number of degrees per decibel; this TWT exhibits approximately $30^\circ/\text{dB}$ AM-to-PM conversion over the range -11 dB to 0 dB, with less severe AM-to-PM conversion at lower input levels.

The TWT characteristics shown in Figure 2.2-1 are representative of commonly-used TWTs, and these characteristics are employed to obtain the data reported in the sequel. However, the mathematical models developed in the study are general, and the computer programs which have been written allow the specification of arbitrary $F(\cdot)$ and $G(\cdot)$.

Another important repeater configuration which can be accommodated by this model is that in which the received signal is hard-limited at low level prior to amplification by the TWT. The limiting removes amplitude variation so that AM-to-PM conversion is not present, and the limiter-TWT cascade appears as a hard limiter with no AM-to-PM conversion. This configuration is often used in multiple-access satellite repeaters.

2.3 Signal Formats

Two general signal formats are of interest in the return link: a high rate PSK signal and a frequency multiplexed signal consisting of analog television and 1.92 Mb/s PSK data. These signal formats are discussed in detail in this section.

2.3.1 High Rate Data Channels

The pure data signal may assume one of two forms. In one case, digital data at a rate of 50 Mb/s is encoded by a convolutional encoder of code rate $1/2$, resulting in a transmission rate of 100 Mb/s. This signal is transmitted via NRZ-L PSK on a carrier at 15.0085 GHz and the wideband TDRS input bandwidth (225 MHz) is selected. The RF spectrum and the TDRS receive bandwidth are thus as illustrated in Figure 2.3.1-1.

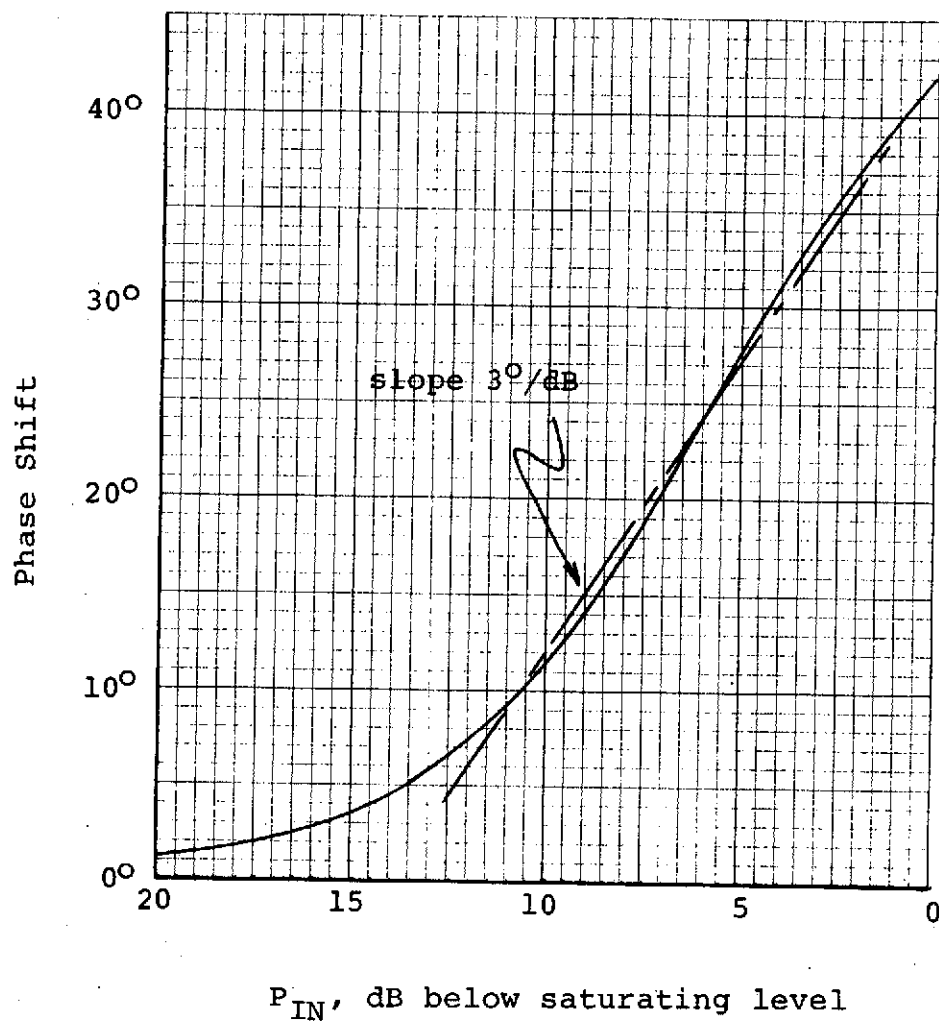


FIGURE 2.2-2. AM-TO-PM CONVERSION CHARACTERISTIC

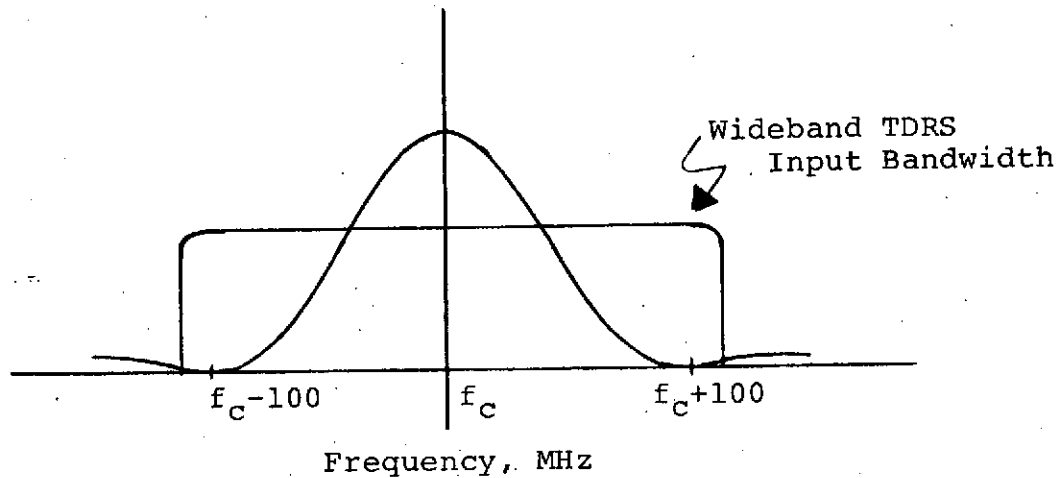


FIGURE 2.3.1-1. NRZ-L PSK POWER SPECTRUM

To see what the complex envelope of this signal is, note that the RF signal can be written

$$x_1(t) = Ad(t) \cos[\omega_c t + \psi_0]$$

where $d(t)$ is a data signal assuming the values ± 1 over each bit interval and ψ_0 is the RF phase. The complex envelope is therefore

$$X_1(t) = Ad(t) e^{j\psi_0}$$

In the alternative form, the pure data signal has a reduced data rate of 30 Mb/s and coding is not used. However, the modulation is split-phase PSK, which has roughly twice the bandwidth of NRZ PSK of the same rate. With this signal, the narrowband TDRS option is used (88 MHz input bandwidth). The RF spectrum and the TDRS receive bandwidth are illustrated in Figure 3.2.1-2.

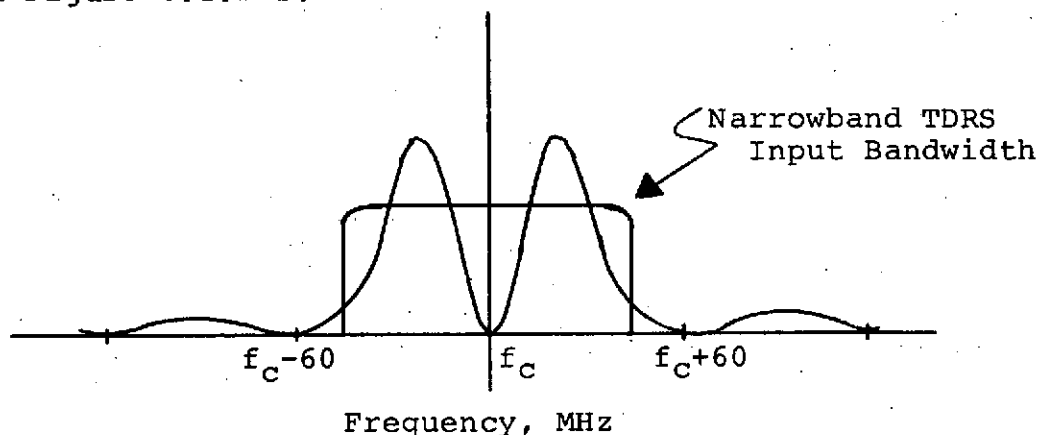


FIGURE 2.3.1-2. SPLIT-PHASE PSK POWER SPECTRUM

The RF signal is given by

$$x_1(t) = A s(t) d(t) \cos[\omega_c t + \psi_0]$$

where $d(t)$ and ψ_0 are as before, and $s(t)$ is a signal which converts NRZ data to split-phase data; i.e., $s(t)$ has the value +1 over the first half of each bit interval and -1 over the second half. The complex envelope is

$$X_1(t) = A s(t) d(t) e^{j\psi_0}$$

2.3.2 Multiplexed Data and Television Channels

For the multiplexed signal, several digital voice and telemetry channels are time-multiplexed to form a 1.92 Mb/s NRZ-L signal. This data signal phase-shift keys a sub-carrier at 8.5 MHz, which is then combined with a baseband analog TV signal whose spectrum nominally extends to 4.2 MHz. The two signals may be filtered prior to multiplexing in order to eliminate crosstalk. The composite signal spectrum is shown in Figure 2.3.2-1. This FDM signal frequency modulates a K-band carrier at 15.077 GHz. The narrowband TDRS input is used.

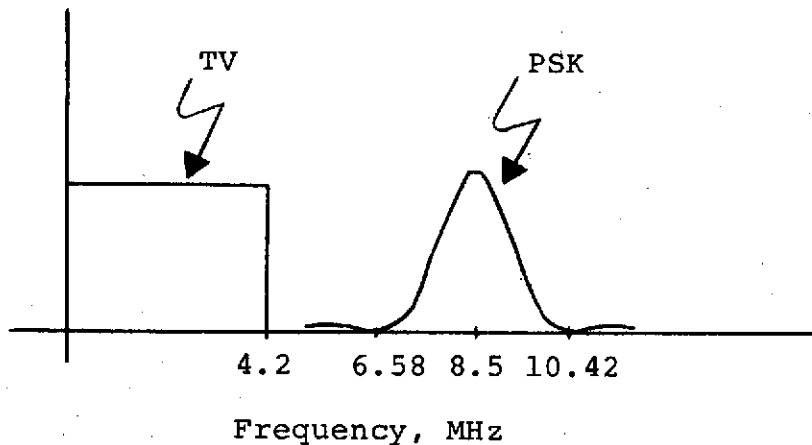


FIGURE 2.3.2-1. BASEBAND FDM SIGNAL SPECTRUM

If $u(t)$ denotes the analog TV signal, normalized to unity peak value, and $d(t)$ represents the NRZ-L data, then the baseband FDM signal is given by

$$v(t) = 2\pi\Delta f_1 u(t) + 2\pi\Delta f_2 d(t) \sin(\omega_{sc} t + \theta_{sc})$$

where Δf_1 and Δf_2 are the RF frequency deviations attributable to the TV and digital signals, respectively. The FM signal is then

$$x_1(t) = A \cos \left[\omega_c t + \int_0^t v(\tau) d\tau + \psi_0 \right]$$

and its complex envelope is

$$X_1(t) = A \exp \left\{ j \left(\int_0^t v(\tau) d\tau + \psi_0 \right) \right\} \quad (2.3.2-1)$$

2.4 Ground Receivers

This section describes the receiver structures which have been assumed for processing the signals received at the ground station. In addition, the performance measures of interest when these receivers are used are discussed.

2.4.1 Receivers for High Rate PSK Signals

It is well known [2-4] that the optimum receiver for PSK signals received in the presence of white Gaussian noise is the matched filter, a device which mixes the received signal with a phase-coherent carrier reference, integrates over a bit interval, and makes its decision according to the sign of the result. Because of the nonlinearity, the detection problem posed by this system is not exactly this classical problem. However, since it is expected that the deleterious effects of the TWT will be minor, use of the matched filter as the basis of the receiver is quite reasonable. Therefore, a receiver of the form shown in Figure 2.4.1-1 is assumed for the NRZ-L PSK signal. The filter represents the effects of all filtering in the RF and IF stages of the receiver. For simplicity, it is taken to be the same filter as that used at the TWT input; i.e., a bandpass filter of 225 MHz bandwidth. The phase of the reference signal must take into account both the original RF phase at the transmitter and the phase bias introduced by AM-to-PM conversion at the TWT. The appropriate choice to compensate for the phase bias is discussed more thoroughly in paragraph 3.2. It is worth noting here, however, that it is clear that at high SNR, the optimum phase offset must be near the average AM-to-PM shift $G(E)$, and that receiver performance will be relatively insensitive to small variations in the correlator phase about its optimum value.

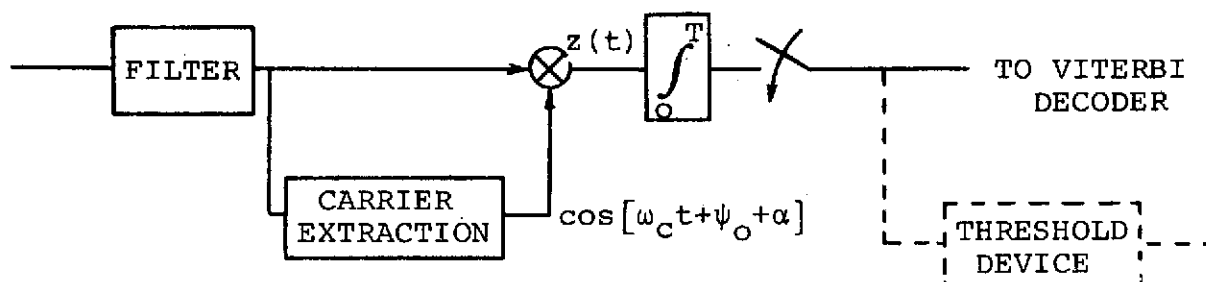


FIGURE 2.4.1-1. RECEIVER FOR THE HIGH-RATE NRZ-L PSK SIGNAL

Assuming that the signal at the filter output has the general form

$$y(t) = R(t) \cos[\omega_c t + \theta(t)]$$

the result of the indicated multiplication will be

$$z(t) = \frac{1}{2} R(t) \cos[\theta(t) - \psi_o - \alpha]$$

plus a term at frequency $2f_c$ which will ultimately disappear in the integration. Since the complex envelope of $y(t)$ is

$$Y(t) = R(t) \exp j\theta(t)$$

the result of the multiplication can be written in terms of operations on the complex envelope as

$$\begin{aligned} z(t) &= \frac{1}{2} \operatorname{Re} \{ Y(t) e^{-j(\psi_o + \alpha)} \} \\ &= \frac{1}{2} \left[\operatorname{Re} \{ Y(t) \} \cos(\psi_o + \alpha) + \operatorname{Im} \{ Y(t) \} \sin(\psi_o + \alpha) \right] \end{aligned}$$

The complex envelope $Y(t)$ itself can be obtained, as before, as the output of an equivalent lowpass filter whose input is the complex envelope of the received signal.

In the actual system, the integrator outputs at the end of each bit interval are fed to a Viterbi decoder which decodes the convolutional code and ultimately makes information bit decisions. The performance criterion of interest in this system is the probability of error in the decoder output sequence. However, consideration of encoding and decoding procedures is outside the scope of this study; accordingly, the study considers the performance of a receiver which makes hard bit decisions at the integrator

output, as illustrated in Figure 2.4.1-1. The resulting error probability as a function of SNR differs from the error probability of the coded system; however, this is a reasonable approach to estimating the degradation due to the nonlinearity.

The split-phase PSK receiver is similar to that of Figure 2.4.1-1, except that the filter has a bandwidth of 88 MHz, conforming to the narrowband TDRS input filter, and that the regenerated reference must be split-phase keyed before mixing (alternatively, the integrator may integrate separately over each half of the interval and subtract the results.) Unlike the NRZ-L signal, this signal is not coded, so that error probability in the hard-decision detector output sequence is the quantity of interest.

2.4.2 Receiver for TV-PSK FDM/FM Signal

The composite FDM/FM signal requires two stages of processing at the ground receiver. First, the RF modulation must be removed, yielding a baseband FDM/FM signal. This signal is then passed through demultiplexing filters to separate the pure baseband TV signal and the 1.92 Mb/s PSK signal at 8.5 MHz. The PSK signal then undergoes PSK detection to recover the digital information.

The RF demodulator is assumed to consist of a cascade of a filter, representing all filtering in the RF and IF stages of the receiver, a limiter, and a phase-locked loop (PLL), as shown in Figure 2.4.2-1. Suppose that the filter output can be written in the form

$$y_R(t) = R(t) \cos[\omega_c t + \theta_1(t)] \quad (2.4.2-1)$$

If the limiter is assumed to be an ideal bandpass limiter, it will remove the amplitude variation and pass

$$z(t) = \cos[\omega_c t + \theta_1(t)]$$

on to the PLL.

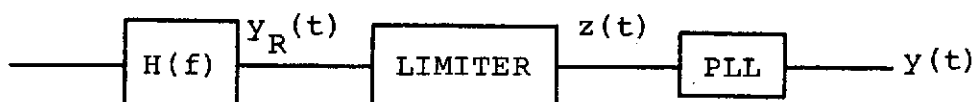


FIGURE 2.4.2-1. RF DEMODULATOR FOR FDM/FM SIGNAL

The PLL is illustrated in more detail in Figure 2.4.2-2. For simplicity, assume that the VCO quiescent frequency is ω_c , the frequency of the loop input. The VCO output is a sinusoid whose instantaneous frequency offset from ω_c is proportional to the VCO input:

$$e_3(t) = K_2 \sin[\omega_c t + \theta_2(t)]$$

where

$$\frac{d\theta_2}{dt} = K_3 e_2(t) \quad (2.4.2-2)$$

(K_2 and K_3 are constants associated with the VCO.) Therefore

$$\begin{aligned} e_1(t) &= e_3(t) \cos[\omega_c t + \theta_1(t)] \\ &= \frac{K_2}{2} \sin[\theta_1(t) - \theta_2(t)] \end{aligned} \quad (2.4.2-3)$$

plus a double-frequency term which will ultimately be suppressed by the loop filter. The filter output is therefore given by

$$e_2(t) = K_1 e_1(t) * f(t) \quad (2.4.2-4)$$

where $f(t)$ is the impulse response of the loop filter.

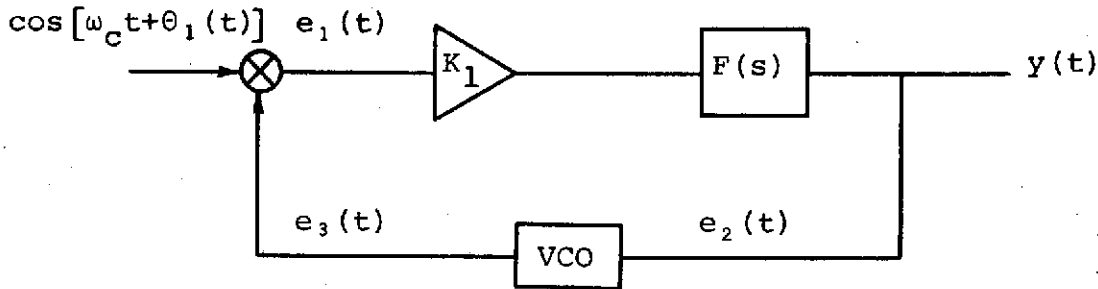


FIGURE 2.4.2-2. PHASE-LOCKED LOOP

Inserting Equation (2.4.2-3) into Equation (2.4.2-4) and combining with Equation (2.4.2-2) yields

$$\frac{d\theta_2}{dt} = \frac{K_1 K_2 K_3}{2} f(t) * \sin[\theta_1(t) - \theta_2(t)] \quad (2.4.2-5)$$

or

$$\theta_1(t) - \theta_2(t) = \theta_1(t) - \frac{K_1 K_2 K_3}{2} \int_{-\infty}^t f(s) * \sin[\theta_1(s) - \theta_2(s)] ds$$

which suggests the model of Figure 2.4.2-3, where

$$G = \frac{1}{2} K_1 K_2 K_3$$

Note that the validity of this model depends only upon the received signal's (actually signal plus noise) being representable in the form of Equation (2.4.2-1).

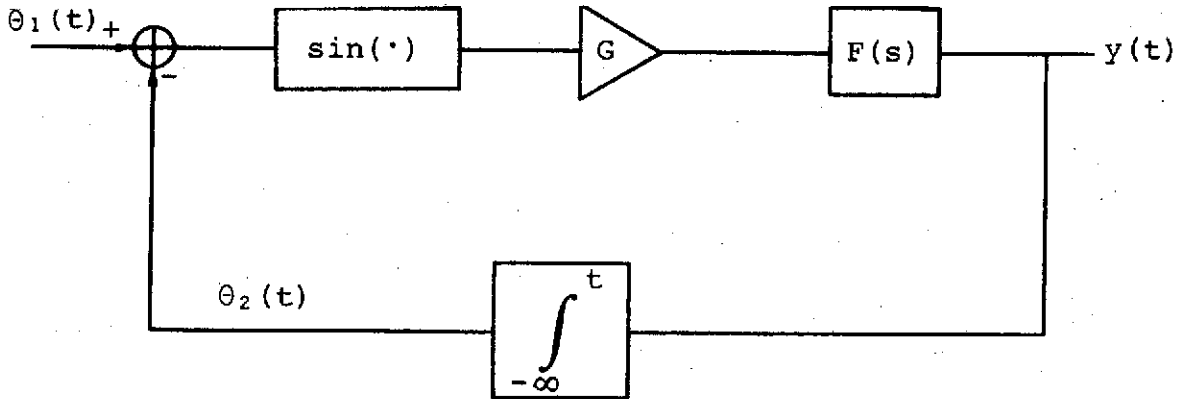


FIGURE 2.4.2-3. BASEBAND MODEL OF THE PHASE-LOCKED LOOP

As noted previously, the complex envelope of the filter output, $Y_R(t)$, can be obtained by passing the complex envelope of the received signal through an equivalent low-pass filter. The signal phase $\theta_1(t)$ can then be obtained as

$$\theta_1(t) = \tan^{-1} \left[\frac{\text{Im}\{Y_R(t)\}}{\text{Re}\{Y_R(t)\}} \right]$$

and processed through the model of Figure 2.4.2-3 to yield the RF demodulator output $y(t)$.

Phased-locked loops are usually designed to operate such that $\theta_2(t) \approx \theta_1(t)$. In this mode, $\sin[\theta_1 - \theta_2] \approx \theta_1 - \theta_2$, and the model of Figure 2.4.2-3 can be replaced by the linearized PLL model of Figure 2.4.2-4. For this model, the tools of linear feedback system theory can be applied to yield a transfer function from $\theta_1(s)$ to $\theta_2(s)$

$$\frac{\theta_2(s)}{\theta_1(s)} = \frac{GF(s)/s}{1 + GF(s)/s} \quad (2.4.2-6)$$

Of more significance in the present application is the transfer function from $\theta_1(s)$ to $Y(s)$, which is given by

$$\frac{Y(s)}{\theta_1(s)} = \frac{GF(s)}{1 + GF(s)/s}$$

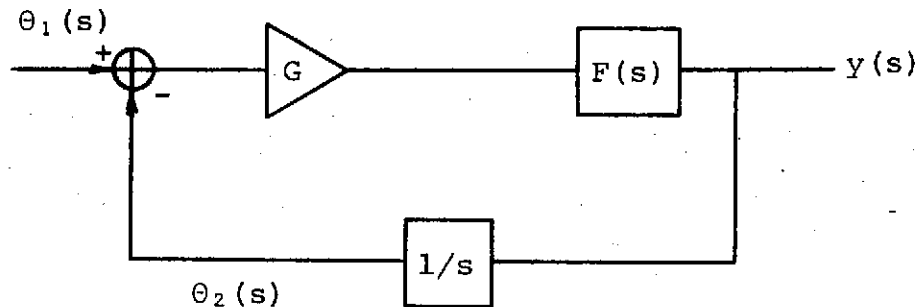


FIGURE 2.4.2-4. LINEARIZED BASEBAND PLL MODEL

More detailed information on the phase-lock loop design actually used in the simulation is given in Section 4.0, which deals with the simulation programs. For the present, assume that the PLL design is such that it functions adequately as a frequency demodulator; that is, the PLL output $y(t)$ is an estimate of the FDM signal

$$v(t) = 2\pi\Delta f_1 u(t) + 2\pi\Delta f_2 d(t) \sin(\omega_{sc}t + \theta_{sc})$$

where $u(t)$ is the analog TV signal and $d(t)$ is a 1.92 Mb/s NRZ-L binary data signal. The estimate $y(t)$ is passed through two demultiplexing filters: a lowpass filter with passband out to 4.2 MHz, and a bandpass filter centered at 8.5 MHz and wide enough to pass the PSK signal without severe distortion. The output of the PSK demultiplexing filter is then input to a matched filter PSK detector.

The appropriate performance measure for the PSK portion of the system is the error probability in the sequence at the PSK detector output. Since the TV signal is an analog signal, an output signal-to-noise measurement is appropriate. The random nature of a true TV signal makes an SNR measurement difficult, however. Instead, a commonly-used technique is to employ a test tone in the 4.2 MHz band and measure the test-tone-to-noise ratio in the demultiplexing filter output. In this approach, a very narrow-band filter is tuned to the test tone frequency and the demultiplexing filter output is passed through this filter. The power in the filter output is regarded as test-tone power, and the difference between this and the total demultiplexing filter output power is attributed to noise. The measure of performance is then the ratio of test-tone power to noise power.

2.5 Summary

Figures 2.5-1, 2.5-2, and 2.5-3 illustrate the overall system baseband models and complex envelope signal flow for the NRZ-L PSK signal, split-phase PSK signal, and FDM/FM signal, respectively. The models described in these figures are those implemented by the simulation programs to be discussed in Section 4.0.

2.6 References

- 2-1. Tracking and Data Relay Satellite System (TDRSS) Users' Guide, NASA Goddard Space Flight Center, Greenbelt, Maryland, June 10, 1974.
- 2-2. Shimbo, O., "Effects of Intermodulation, AM-PM Conversion, and Additive Noise in Multicarrier TWT Systems," Proc. IEEE, Vol. 59, pp. 230-238, February 1971.
- 2-3. Kaye, A.R., D.A. George, and M.J. Eric, "Analysis and Compensation of Bandpass Nonlinearities for Communication," IEEE Trans. Comm., Vol. COM-20, pp. 965-972, October 1972.
- 2-4. Wozencraft, J.M., and I.M. Jacobs, Principles of Communication Engineering, John Wiley and Sons, Inc., 1965.

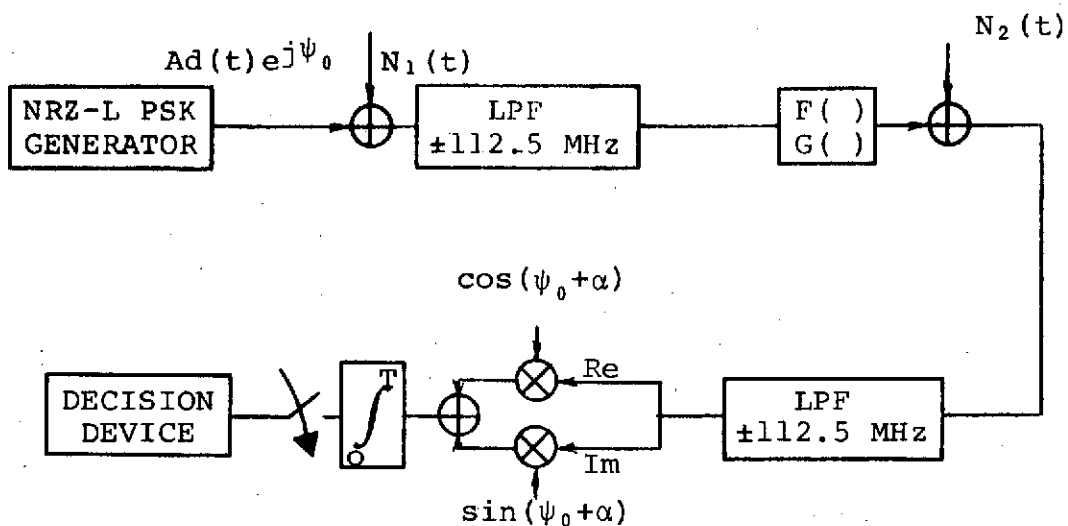


FIGURE 2.5-1. BASEBAND MODEL OF THE NRZ-L PSK LINK

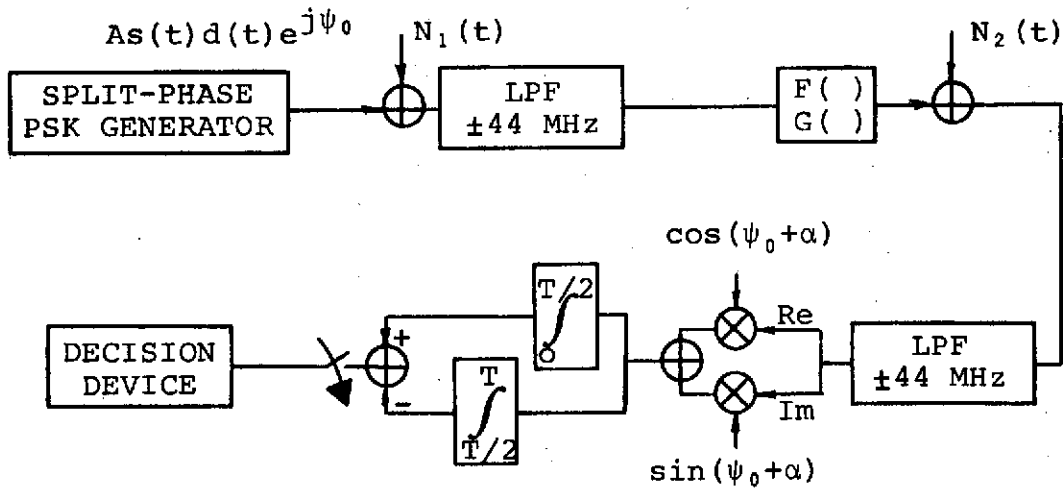


FIGURE 2.5-2. BASEBAND MODEL OF THE SPLIT-PHASE PSK LINK

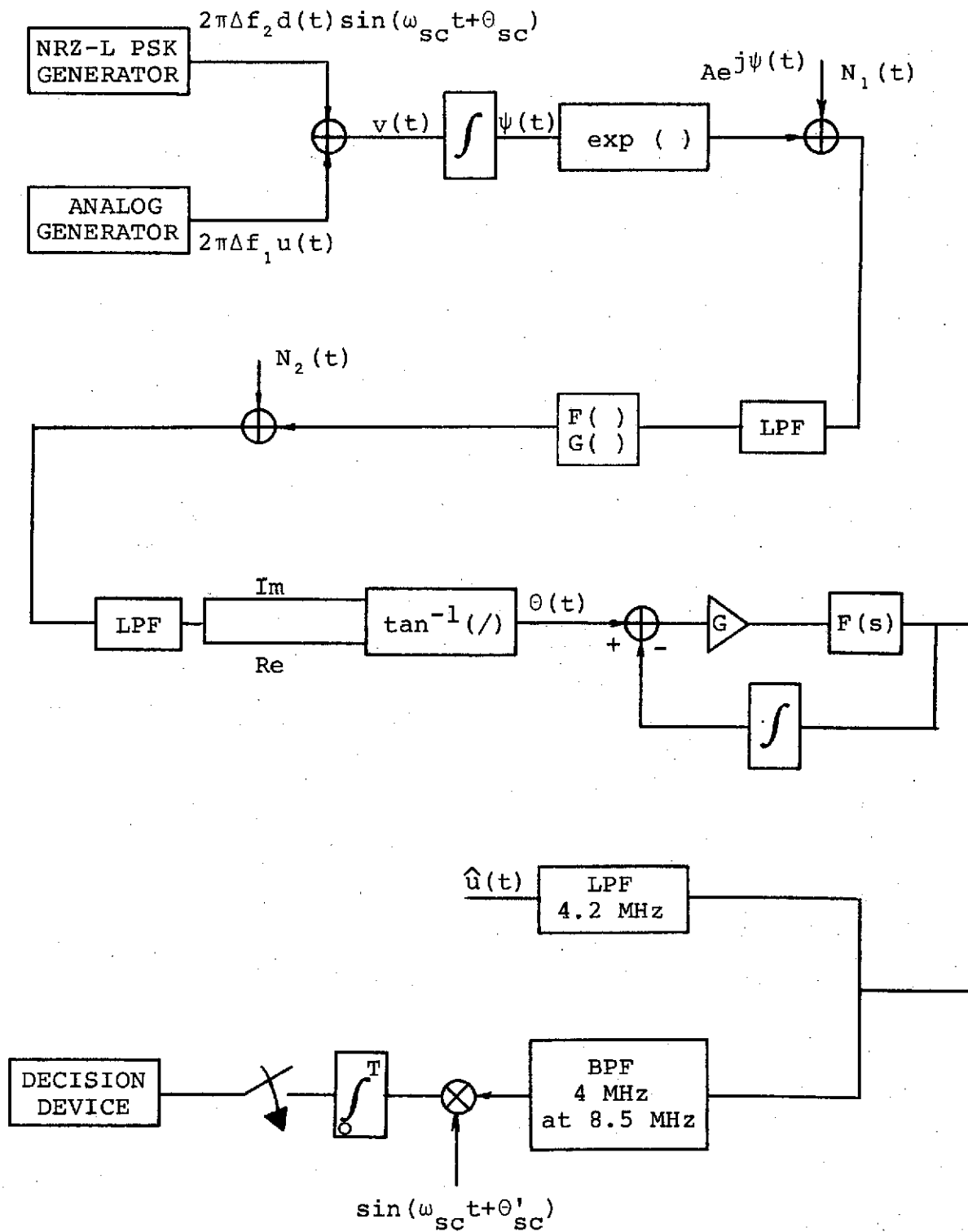


FIGURE 2.5-3. BASEBAND MODEL OF THE FDM/FM LINK

SECTION 3.0
ANALYTICAL RESULTS

3.0 ANALYTICAL RESULTS

Meaningful and accurate analytical results for non-linear operations on random processes are usually difficult to obtain. The difficulty is compounded in this study by the desire to develop techniques which are generally applicable to any TWT characteristics $F(\cdot)$ and $G(\cdot)$. Because of the difficulty of analysis, digital computer simulation was looked to as the best way to accurately predict the performance of the system.

On the other hand, even approximate analytical results are useful, both as a check on the simulation results and as indicators of the underlying mathematical structure of the nonlinear system. It is desirable, therefore, to approach the problem analytically to some extent. This section presents certain analytical results on the effects of the TWT on system performance. The approach has been to derive analytical expressions for certain statistical descriptors of the system, which are functionals of the TWT characteristics $F(\cdot)$ and $G(\cdot)$. Computer programs have then been written to evaluate these expressions for particular $F(\cdot)$ and $G(\cdot)$, which are input in the form of tables. Where possible, the correctness of the results has been verified by selection of a previously studied form for $F(\cdot)$ and $G(\cdot)$ and comparison with published results.

The first results presented consider various statistical properties of the output when the TWT input consists of a pure sine wave plus Gaussian noise. These results are then used in studying the effect of the nonlinearity on error probability of a PSK system when the TWT input is not filtered. Finally, the effects of the TWT on an FDM/FM link at high SNR are considered.

3.1 TWT Effects on Sine Wave Plus Gaussian Noise

Suppose that the TWT input consists of the pure sinusoid $A \cos \omega_0 t$ corrupted by Gaussian noise

$$n(t) = n_c(t) \cos \omega_0 t - n_s(t) \sin \omega_0 t$$

where $n_c(t)$ and $n_s(t)$ are independent Gaussian processes, and $n(t)$, $n_c(t)$, and $n_s(t)$ all have zero mean and variance of σ^2 . It is well known that the resulting process can be written in envelope-phase form as

$$\begin{aligned} x(t) &= A \cos \omega_0 t + n(t) \\ &= E(t) \cos [\omega_0 t + \phi(t)] \end{aligned}$$

The envelope E and phase ϕ at any instant have the joint probability density function [3-1]

$$p(E, \phi) = \frac{E}{2\pi\sigma^2} \exp\left\{-(E^2 + A^2 - 2AE\cos\phi)/2\sigma^2\right\},$$

$$E \geq 0, \quad -\pi \leq \phi < \pi \quad (3.1-1)$$

while the marginal density function of E has the Rice-Nakagami form

$$p(E) = \frac{E}{\sigma^2} e^{-(E^2 + A^2)/2\sigma^2} I_0\left(\frac{AE}{\sigma^2}\right), \quad E \geq 0 \quad (3.1-2)$$

The first two moments of E are [3-1]

$$\bar{E} = \frac{A}{2} \sqrt{\frac{\pi}{\rho}} e^{-\rho/2} \left[(1+\rho) I_0(\rho/2) + \rho I_1(\rho/2) \right]$$

$$\overline{E^2} = A^2 (1 + 1/\rho)$$

where $\rho = A^2/2\sigma^2$ is the signal-to-noise ratio.

The density function of ϕ is an even function [3-1], indicating that $\bar{\phi} = 0$. The second moment $\overline{\phi^2}$ can be calculated by numerical integration. For future reference, several moments of E and ϕ are plotted in Figure 3.1-1. Note that for ρ in excess of 10 dB, excellent approximations are:

$$\bar{E}/A = 1 + 1/4\rho$$

$$\left(\overline{E^2} - \bar{E}^2 \right)^{1/2} / A = (2\rho)^{-1/2}$$

$$\left(\overline{\phi^2} \right)^{1/2} = (2\rho)^{-1/2} \quad (\text{radians})$$

The TWT distorts the amplitude and introduces an amplitude-dependent phase shift so that the output is

$$y(t) = F(E(t)) \cos[\omega_0 t + \phi(t) + G(E(t))] \quad (3.1-3)$$

It will be convenient to work with normalized TWT characteristics. Let R_0 denote the maximum value of $F(E)$, i.e., the saturation output, and let E_{sat} denote the input level which saturates the TWT. The normalized characteristics $f(\cdot)$ and $g(\cdot)$ are defined implicitly by

$$F(E) = R_0 f(E/E_{\text{sat}})$$

$$G(E) = g(E/E_{\text{sat}})$$

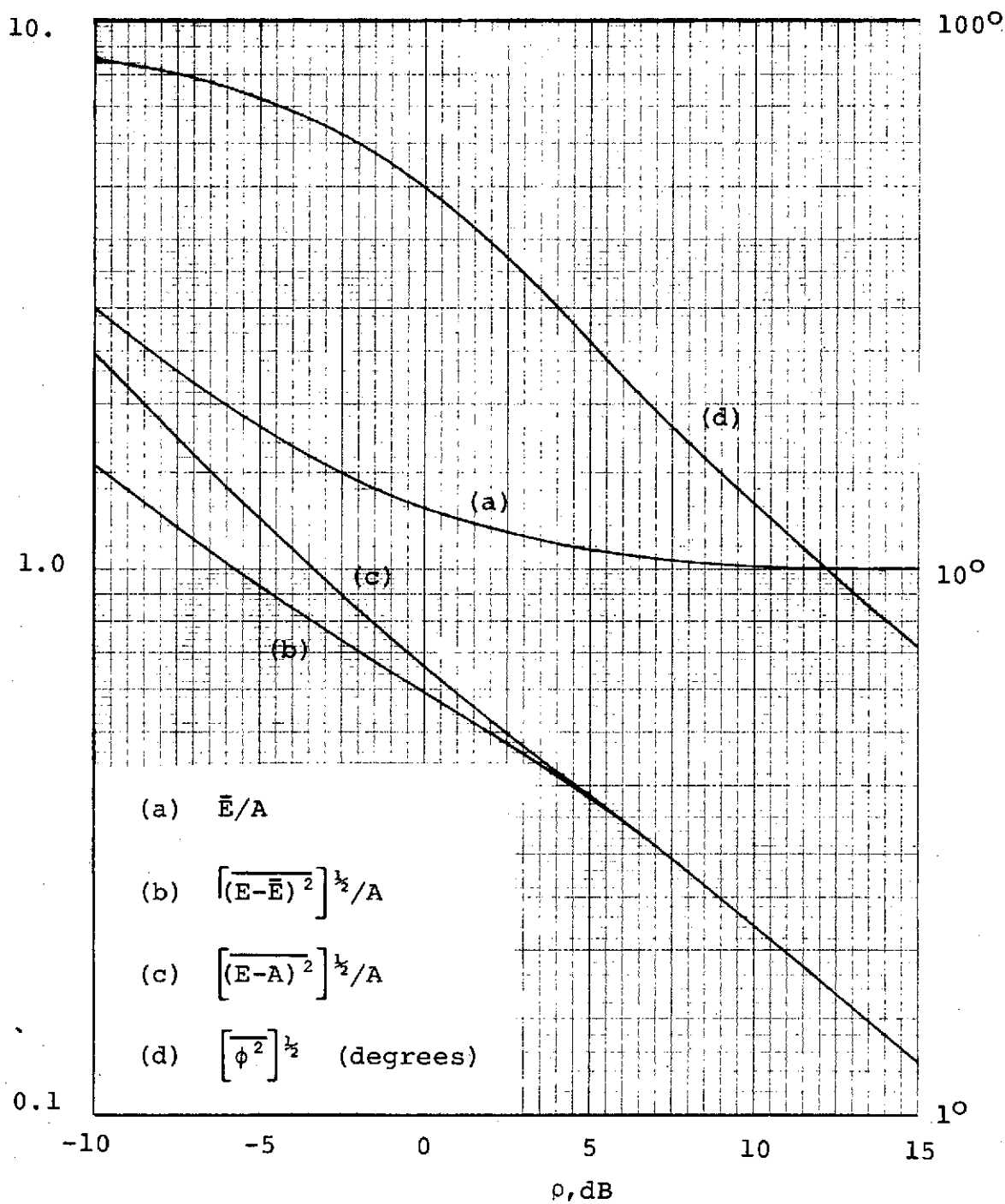


FIGURE 3.1-1. ENVELOPE AND PHASE MOMENTS FOR SINE WAVE PLUS GAUSSIAN NOISE.

Thus $f(1) = 1$ and $g(1) = G(E_{\text{sat}})$. The average output amplitude is, using Equation (3.1-2),

$$\begin{aligned}\overline{F(E)} &= \int_0^{\infty} F(E) \frac{E}{\sigma^2} e^{-(E^2+A^2)/2\sigma^2} I_0\left(\frac{AE}{\sigma^2}\right) dE \\ &= \frac{R_0}{\sigma^2} e^{-\rho} \int_0^{\infty} f\left(\frac{E}{E_{\text{sat}}}\right) E e^{-E^2/2\sigma^2} I_0\left(\frac{AE}{\sigma^2}\right) dE\end{aligned}$$

Making the change of variable $u=E/E_{\text{sat}}$ leads to

$$\overline{F(E)} = \frac{R_0}{\sigma^2} e^{-\rho E_{\text{sat}}^2} \int_0^{\infty} f(u) u e^{-E_{\text{sat}}^2 u^2/2\sigma^2} I_0\left(\frac{A E_{\text{sat}} u}{\sigma^2}\right) du$$

Finally, let $A = \beta E_{\text{sat}}$, where β is the "backoff," or fraction of saturating drive level at which the TWT is being operated nominally. Then the average output level, normalized to its maximum, is given by

$$\frac{\overline{F(E)}}{R_0} = \frac{2\rho}{\beta^2} e^{-\rho} \int_0^{\infty} u f(u) e^{-u^2\rho/\beta^2} I_0\left(\frac{2\rho u}{\beta}\right) du \quad (3.1-4)$$

Proceeding in the same manner, the normalized mean-square output amplitude is found to be

$$\frac{\overline{F^2(E)}}{R_0^2} = \frac{2\rho}{\beta^2} e^{-\rho} \int_0^{\infty} u f^2(u) e^{-u^2\rho/\beta^2} I_0\left(\frac{2\rho u}{\beta}\right) du \quad (3.1-5)$$

Equations (3.1-4) and (3.1-5) express the normalized average and mean-square output amplitude as functionals of the normalized amplitude characteristic $f(\cdot)$. For certain forms, they can be evaluated analytically. For example, if $f(u)$ is given by several terms of a power series expansion, each term can be integrated [3-2] to yield a series expression for $\overline{F(E)}/R_0$. More generally, however, whether $f(u)$ is given by a closed-form expression, a power series, or a table of values, Equations (3.1-4) and (3.1-5) can be integrated numerically; moreover, since the given characteristic is usually a "typical" characteristic, and not exact for a given TWT, the accuracy of numerical integration is not a limiting factor.

The output phase relative to that of the signal is, from Equation (3.1-3),

$$\theta(t) = \phi(t) + G(E(t))$$

with mean value $\bar{\theta} = \overline{G(E)}$. The mean square value is

$$\overline{\theta^2} = \overline{\phi^2} + 2\overline{\phi G(E)} + \overline{G^2(E)}$$

The mean square input phase $\overline{\phi^2}$ can be obtained from Figure 3.1-1. The mean and mean-square AM-to-PM conversion are averages only over E, and can be obtained, as before, by numerically carrying out the integrations indicated below:

$$\begin{aligned}\overline{G(E)} &= \frac{2\rho}{\beta^2} e^{-\rho} \int_0^{\infty} u g(u) e^{-\rho u^2/\beta^2} I_0\left(\frac{2\rho u}{\beta}\right) du \\ \overline{G^2(E)} &= \frac{2\rho}{\beta^2} e^{-\rho} \int_0^{\infty} u g^2(u) e^{-\rho u^2/\beta^2} I_0\left(\frac{2\rho u}{\beta}\right) du\end{aligned}$$

The cross term $\overline{\phi G(E)}$, however, must be computed as an average over both E and ϕ , using (3.1-1):

$$\overline{\phi G(E)} = \frac{1}{2\pi\sigma^2} \int_0^{\infty} E G(E) e^{-(E^2+A^2)/2\sigma^2} \int_{-\pi}^{\pi} \phi e^{AE \cos \phi / \sigma^2} d\phi dE$$

Since $e^{AE \cos \phi / \sigma^2}$ is an even function of ϕ , the integration on ϕ vanishes for all E, so that

$$\overline{\phi G(E)} = 0$$

Accordingly, the RMS phase jitter about its mean is

$$\sigma_{\theta} = \sqrt{\overline{\theta^2} - \bar{\theta}^2} = \left[\overline{\theta^2} + \overline{G^2(E)} - \overline{G(E)}^2 \right]^{1/2}$$

Various amplitude and phase moments for the typical TWT characteristics of Figure 2.2-1 have been obtained by numerical integration, and are plotted as functions of TWT input signal-to-noise ratio in Figures 3.1-2 through 3.1-4. Figure 3.1-2 illustrates the normalized average, mean square, and standard deviation of the output amplitude. Figure 3.1-3 indicates the average output phase $G(E)$ and the angle

$$\gamma = \tan^{-1} \left[\overline{F(E) \sin G(E)} / \overline{F(E) \cos G(E)} \right]$$

whose significance will be discussed in the next section. The total RMS phase jitter $(\overline{\theta^2} - \bar{\theta}^2)^{1/2}$, as well as the input jitter from Figure 3.1-1 and the jitter due to amplitude variations alone, $(\overline{G^2(E)} - \overline{G(E)}^2)^{1/2}$, are shown in Figure 3.1-4. Note that although the jitter due to AM-to-PM conversion is significant

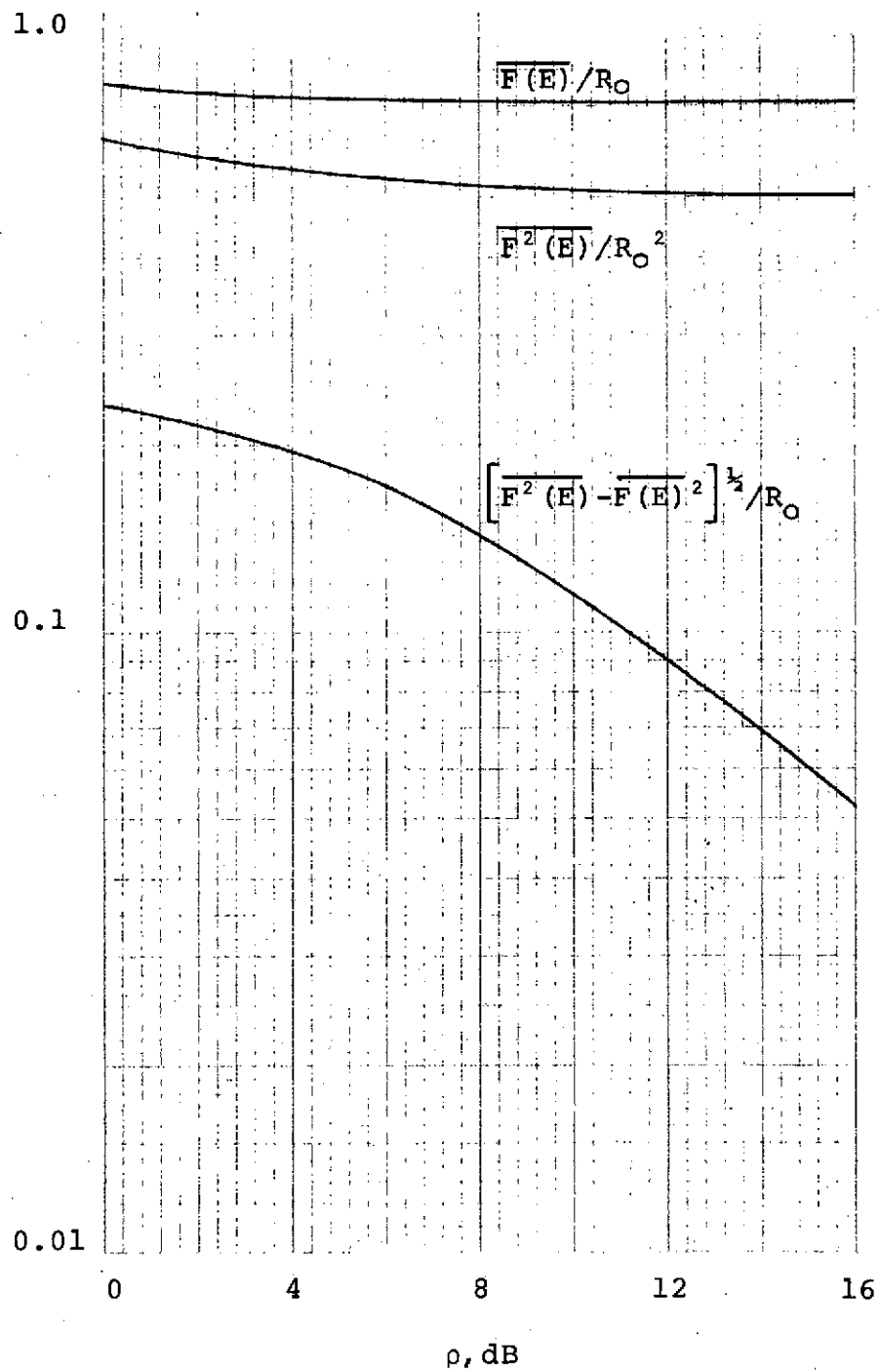


FIGURE 3.1-2. NORMALIZED AVERAGE, MEAN SQUARE, AND STANDARD DEVIATION OF TWT OUTPUT AMPLITUDE, $\beta=0.44$.

ORIGINAL PAGE IS
OF POOR QUALITY

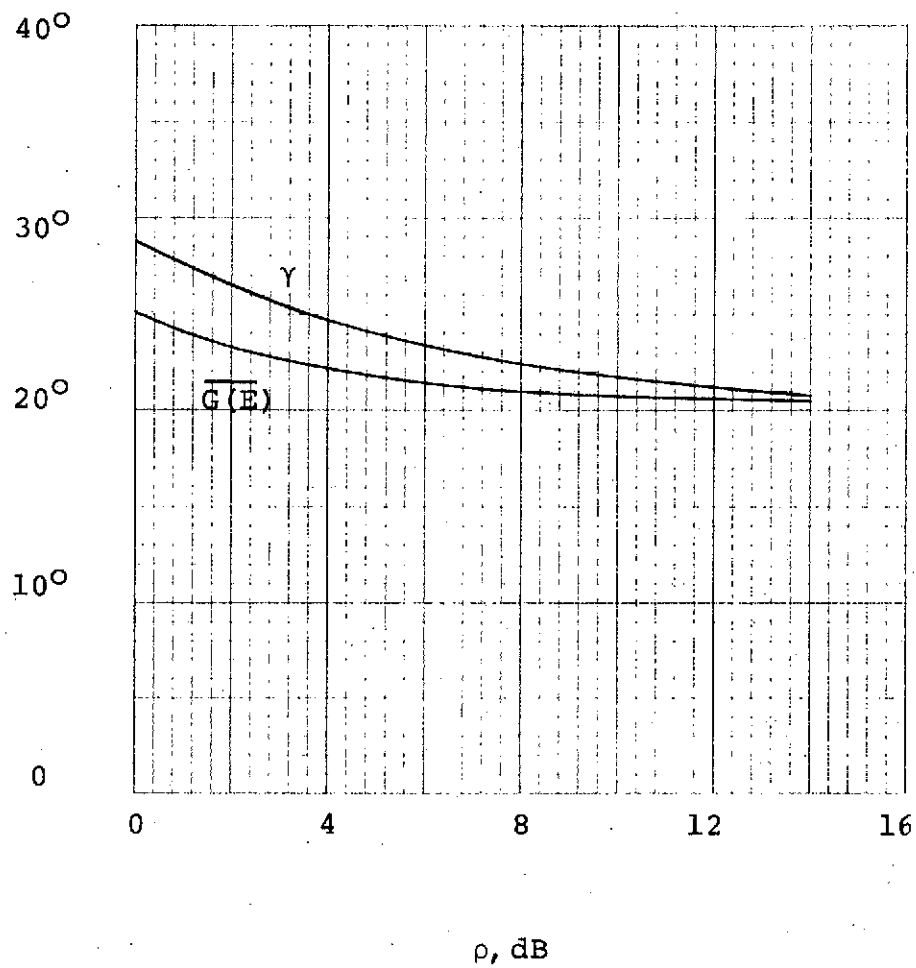


FIGURE 3.1-3. AVERAGE OUTPUT PHASE AND γ , $\beta=0.44$.

ORIGINAL PAGE IS
OF POOR QUALITY.

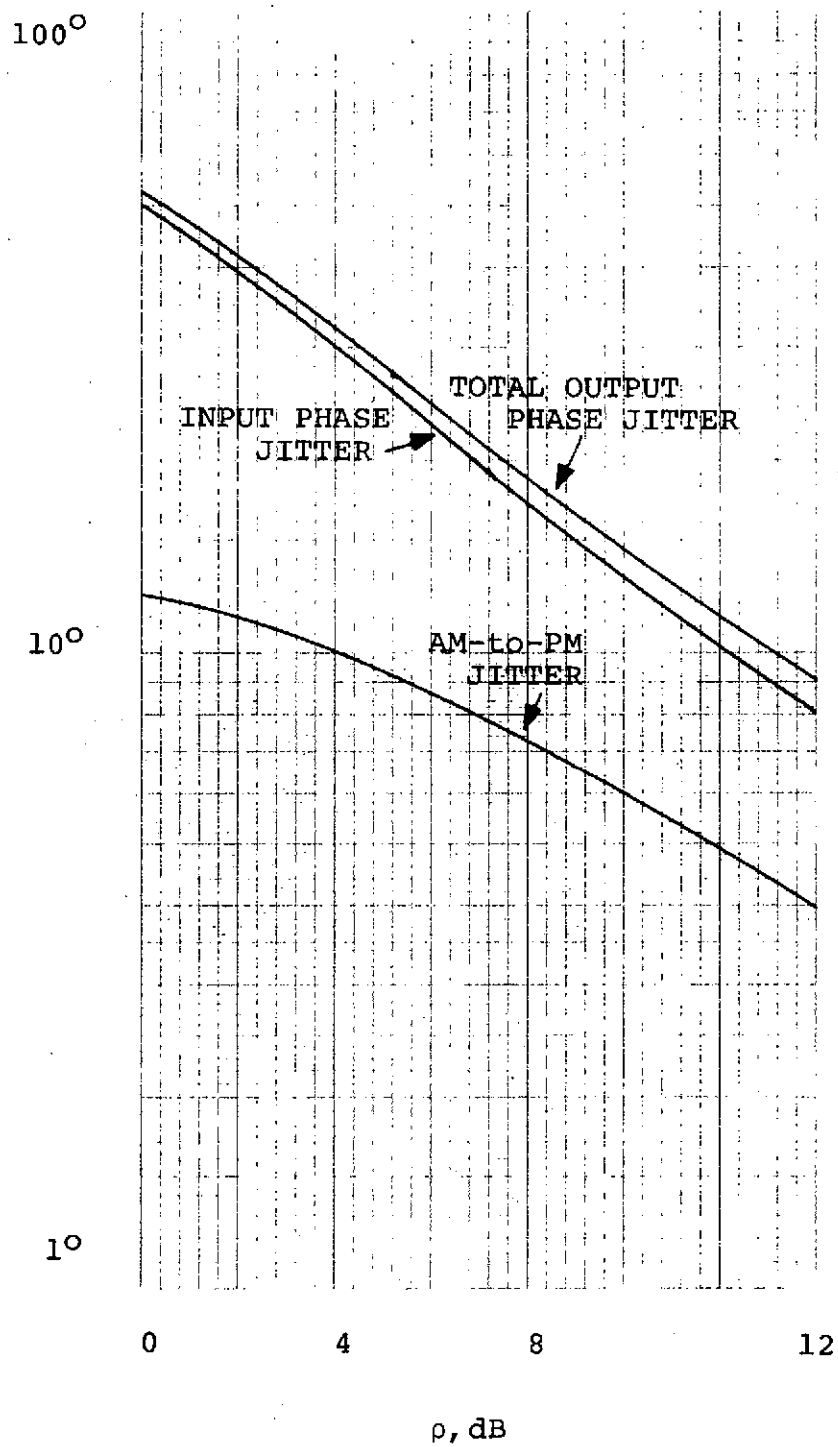


FIGURE 3.1-4. RMS PHASE JITTER AT TWT OUTPUT, $\beta=0.44$.

in comparison with the jitter due to input noise, it has no appreciable effect on the net phase jitter. The reason for this is that it is the variances which add, so that if the RMS values are in a ratio of 2:1, the presence of AM-to-PM conversion increases the net RMS phase jitter by only a factor $\sqrt{1.25}$.

In all the results presented, the backoff is selected at $\beta=0.44$. Reference to Figure 2.2-1 illustrates that this value of backoff corresponds to a nominal output level at 3 dB below saturation.

3.2 TWT Effects on PSK Detection

The effect of a bandpass nonlinearity on PSK error probability has been widely investigated. The model generally used is that illustrated in Figure 3.2-1, where it is assumed that the filters $H(f)$ are ideal filters of bandwidth $2W$, wide enough to pass the PSK signal $A_d(t)\cos\omega_c t$ without appreciable distortion. Under this assumption, the signal appears, over each bit time, as a constant-amplitude sinusoid in the presence of Gaussian noise, and many of the results of the previous section can be invoked. The receiver mixes with a phase-shifted version of the signal and samples the result at rate $2W$, ensuring that all the noise samples are independent. While all investigators have been forced to resort to analyzing such a discrete-time model of the detector, they differ on what the decision device does with the $2WT$ samples it receives for each data bit. Some, including Jain and Blachman [3-3], and Lyons [3-4], visualize a detector which makes a hard decision on each sample, then takes a vote among the $2WT$ hard decisions to arrive at an overall bit decision. Others, notably Aein [3-5], [3-6], and Davisson and Milstein [3-7] assume that the detector sums all $2WT$ samples and makes its decision according to the sign of the sum. The latter approach more closely approximates the integrate-and-dump detector implemented in practice, and its performance will, in general, be superior to that of the majority decision detector. However, for purposes of developing insight into the problem, both models are useful, and investigation along both lines has been carried out in the study.

For the majority-decision receiver, if P_e denotes the probability that a single hard decision is in error, then the probability of a bit error is the probability that more than half of the hard decisions are in error, or

$$P_E = 1 - \sum_{k=0}^{WT} \binom{2WT}{k} P_e^k (1-P_e)^{2WT-k}$$

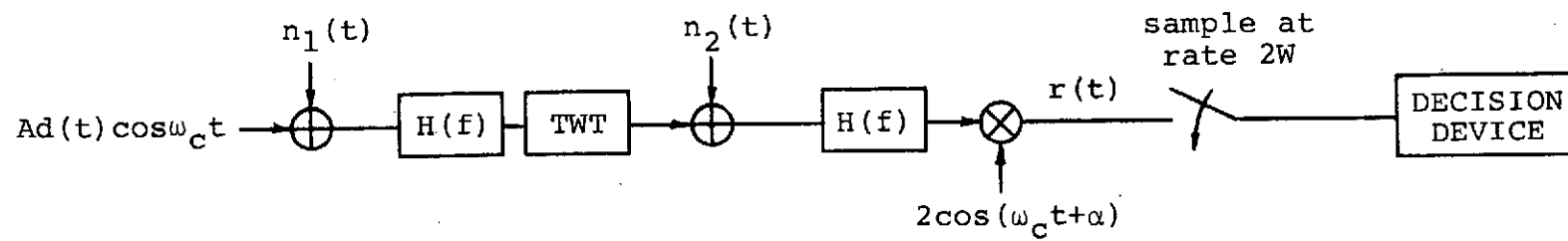


Figure 3.2-1. DISCRETE-TIME MODEL OF PSK COMMUNICATION LINK.

Paragraph 3.2.1 focuses on determination of the single-sample error probability P_e .

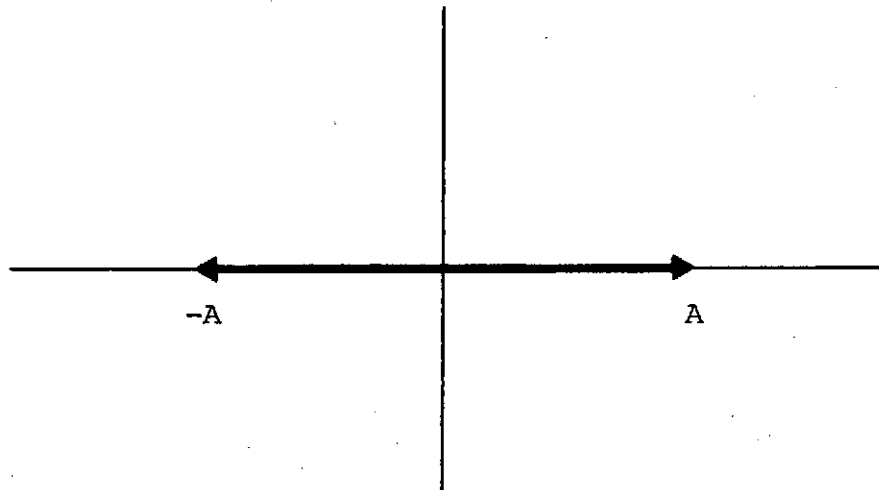
As detailed in paragraph 3.2.2, the probability density function of a single sample, in the absence of downlink noise, is determined. Besides being of interest in its own right, this density function forms the basis for analysis of the performance of the receiver which sums $2WT$ samples before making a bit decision.

Finally, it should be remarked that neither approach to performance analysis can be applied with confidence to the system of primary interest in this study, since the ratio of input bandwidth to data rate is small ($WT \approx 1$), and the TWT input filter introduces considerable amplitude variation. The following analyses are included not for the numerical results one can derive from them, but for the insight they provide into the effects of the nonlinearity in the system.

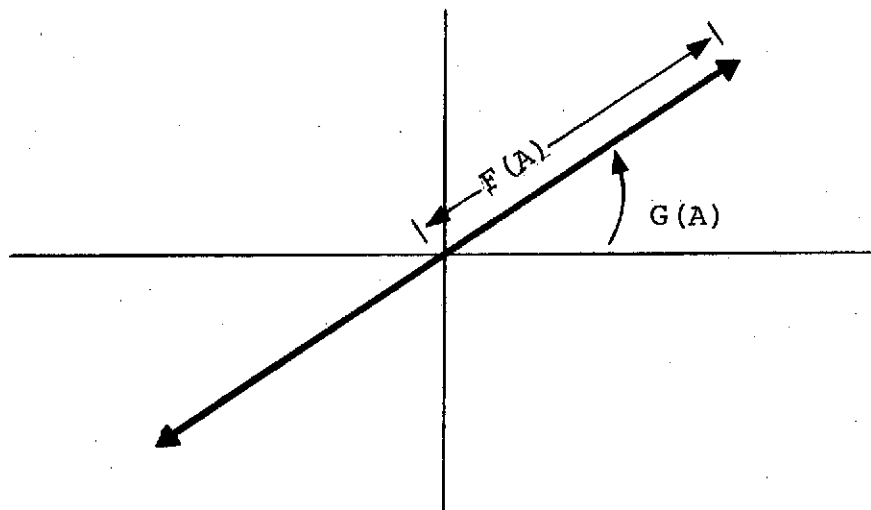
3.2.1 Single-Sample Error Probability

It is illuminating to use a phasor representation of the signals. The PSK signal can be viewed as one of the two antipodal phasors illustrated in Figure 3.2.1-1(a). Suppose, first, that there is no noise in the uplink. The effect of the TWT is to rotate the phase and change the amplitude, so that at the TWT output, the phasor diagram is as illustrated in Figure 3.2.1-1(b). The ground receiver sees one of these phasors in the presence of Gaussian noise; classical detection theory calls for correlating with a phasor at the angle $G(A)$ and making a decision according to the sign of the result.

When noise is present in the uplink, the situation becomes more complicated. The TWT input phasor is the sum of the signal phasor and a noise phasor whose components are independent Gaussian random variables. Equal-probability loci for the input phasor are circles centered at $\pm A$. The effect of the TWT is again to extend (or contract) and rotate the input phasor; however, since points on an equal-probability locus lie at different distances from the origin, the length variation and phase rotation induced by the TWT are different for different points on the locus. The locus is therefore distorted. As an example, an equal-probability circle about $A = 0.44E_{\text{sat}}$ and the corresponding locus which results when this signal is passed through the TWT of Figure 2.2-1, are illustrated in Figure 3.2.1-2.



(a) AT TWT INPUT



(b) AT TWT OUTPUT

FIGURE 3.2.1-1. PSK SIGNAL PHASOR REPRESENTATIONS.

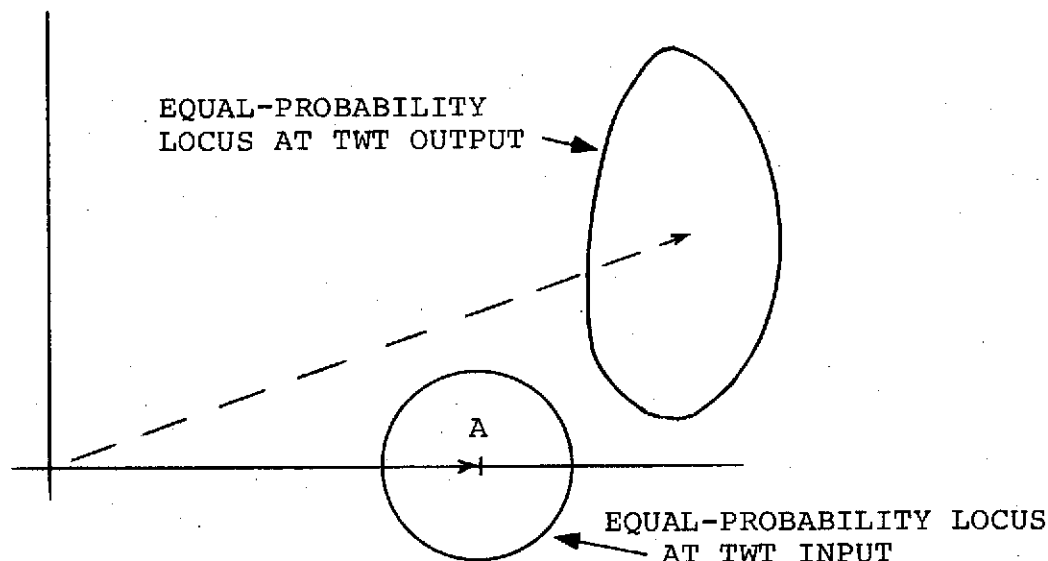


FIGURE 3.2.1-2. EQUAL-PROBABILITY LOCI
FOR INPUT SIGNAL PHASOR
 $A=0.44E_{SAT}$.

The signal at the TWT output is either the phasor

$$S_o(E, \phi) = F(E) \angle (G(E) + \phi)$$

or its negative. In principle, one can determine the optimum decision strategy for this so-called composite hypothesis test; the optimum receiver correlates the received phasor with $S_o(E, \phi)$, operates on the result with a certain nonlinear function, and averages over E and ϕ using Equation (3.1-1). The decision is made according to the sign of this average. While it is conceivable that this routine can be distilled down to an implementable operation, it appears to be unrewardingly complex. A much simpler approach, and one which would seem to be nearly as good at the signal-to-noise ratios of interest, is to correlate the received phasor with some "average" signal phasor. At high SNR, it is clear that this phasor should lie at an angle near $G(A)$. The exact optimum angle is not obvious, but since the correlation is relatively insensitive to small variations in this angle, it is not critical. Lyons [3-4] has suggested that the angle

$$\alpha = \tan^{-1} \left[\frac{\overline{F(E) \sin G(E)}}{\overline{F(E) \cos G(E)}} \right] \quad (3.2.1-1)$$

is appropriate, since this is the phase of the conditional expectation of the TWT output given the original input phasor $+A$. (The significance of this conditional expectation was pointed out by Blachman [3-8].)

In results reported in the sequel, the correlator phase given by Equation (3.2.1-1) is used; however, there is no guarantee that it minimizes error probability. Determination of the optimum choice of α , and study of the structure and performance of the optimum receiver alluded to previously, remain as interesting open problems.

The output of the receiver's mixer, neglecting the double-frequency term is

$$r = \pm F(E) \cos[\phi + G(E) - \alpha] + n$$

where n is a Gaussian random variable of variance σ_2^2 . The error probability is, therefore, given by

$$P_e = \int_0^{\infty} \int_{-\pi}^{\pi} Q\left(\frac{F(E) \cos[\phi + G(E) - \alpha]}{\sigma_2}\right) p(E, \phi) d\phi dE$$

where

$$Q(x) = \frac{1}{\sqrt{2\pi}} \int_x^{\infty} e^{-y^2/2} dy$$

Using (3.1-1) and normalizing as in the previous section, this becomes

$$P_e = \frac{\rho_1}{\pi \beta^2} \int_0^{\infty} \int_{-\pi}^{\pi} u \exp\left\{-\frac{\rho_1}{\beta^2}(u^2 - 2\beta u \cos\phi + \beta^2)\right\} Q(\sqrt{2\rho_2} f(u) \cos(\phi + g(u) - \alpha)) d\phi du$$

where $\beta = A/E_{\text{sat}}$, $\rho_1 = A^2/2\sigma_1^2$, and $\rho_2 = R_0^2/2\sigma_2^2$. Note that ρ_2 is the saturation output SNR, and that the actual downlink SNR is in general less than ρ_2 .

A computer program was written to carry out this double integration numerically. In order to check the accuracy of the computation, the special case of an ideal limiter was considered. For this example, $f(u)=1$, $g(u)=0$. The results are illustrated in Figure 3.2.1-3. These results agree with those of Jain and Blachman [3-3], who derived a series expansion for P_e and evaluated the result on a digital computer.

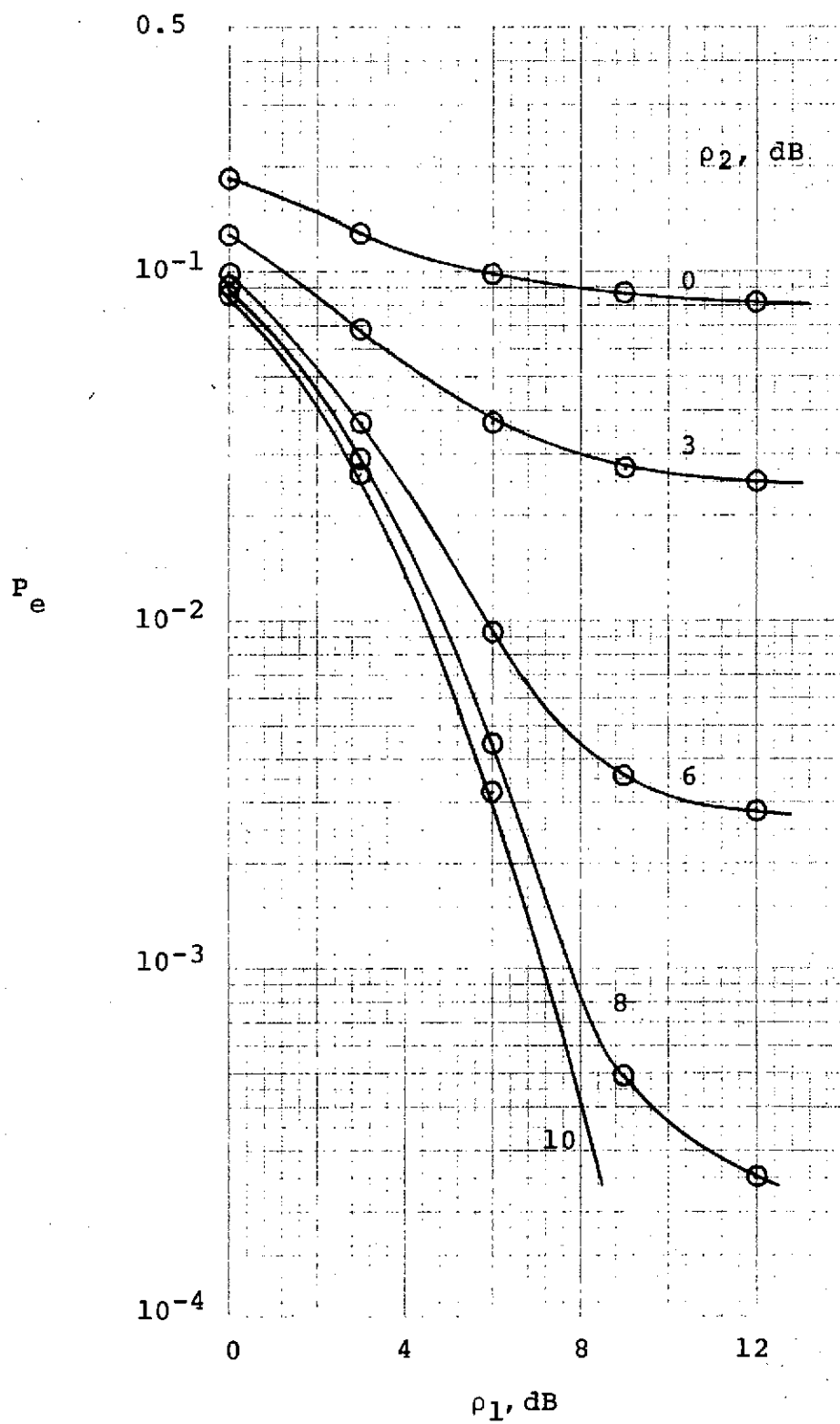


FIGURE 3.2.1-3. SINGLE-SAMPLE ERROR PROBABILITY FOR IDEAL HARD LIMITER.

Following this verification, the program was applied to the TWT described by Figure 2.2-1 with $\beta=0.44$. In this case, the saturation SNR ρ_2 is less physically meaningful, and it is preferable to have results in terms of the ratio of actual TWT output power P_T to noise power. In order to do this, note that

$$P_T = R_O^2 \overline{f^2(u)}/2$$

so that

$$\frac{P_T}{\sigma_2^2} = \rho_2 \overline{f^2(u)}$$

which is a function of ρ_1 . The results of paragraph 3.1 can be used to find $\overline{f^2(u)}$, so that for a given ρ_1 , data can be obtained as a function of P_T/σ_2^2 by choosing

$$\rho_2, \text{dB} = \left(\frac{P_T}{\sigma_2^2} \right) \text{dB} - 10 \log_{10} \overline{f^2(u)}$$

The appropriate adjustment factors, as well as the receiver phase α of (3.2.1-1), for various ρ_1 are given in Table 3.2.1-1. P_e curves showing variations with ρ_1 and P_T/σ_2^2 are specified in Figure 3.2.1-4.

Table 3.2.1-1

Adjustment Factor and Phase Offset

<u>ρ_1, dB</u>	<u>$-10 \log_{10} \overline{f^2(u)}$</u>	<u>$\alpha, \text{degrees}$</u>
0	2.06	28.7
3	2.46	25.6
6	2.71	23.4
9	2.85	22.0

3.2.2 Density Function of the Mixer Output

In the absence of downlink noise, the mixer output, neglecting the double frequency term, is

$$r = F(E) \cos [\phi + G(E) - \alpha] \quad (3.2.2-1)$$

which is a random variable. Since one approach to predicting error probability is to consider the detector statistic to be a sum of several independent random variables of this form and a Gaussian noise variable, it is of interest to determine the density function of r . To do this, define an auxiliary random variable

$$s = E \quad (3.2.2-2)$$

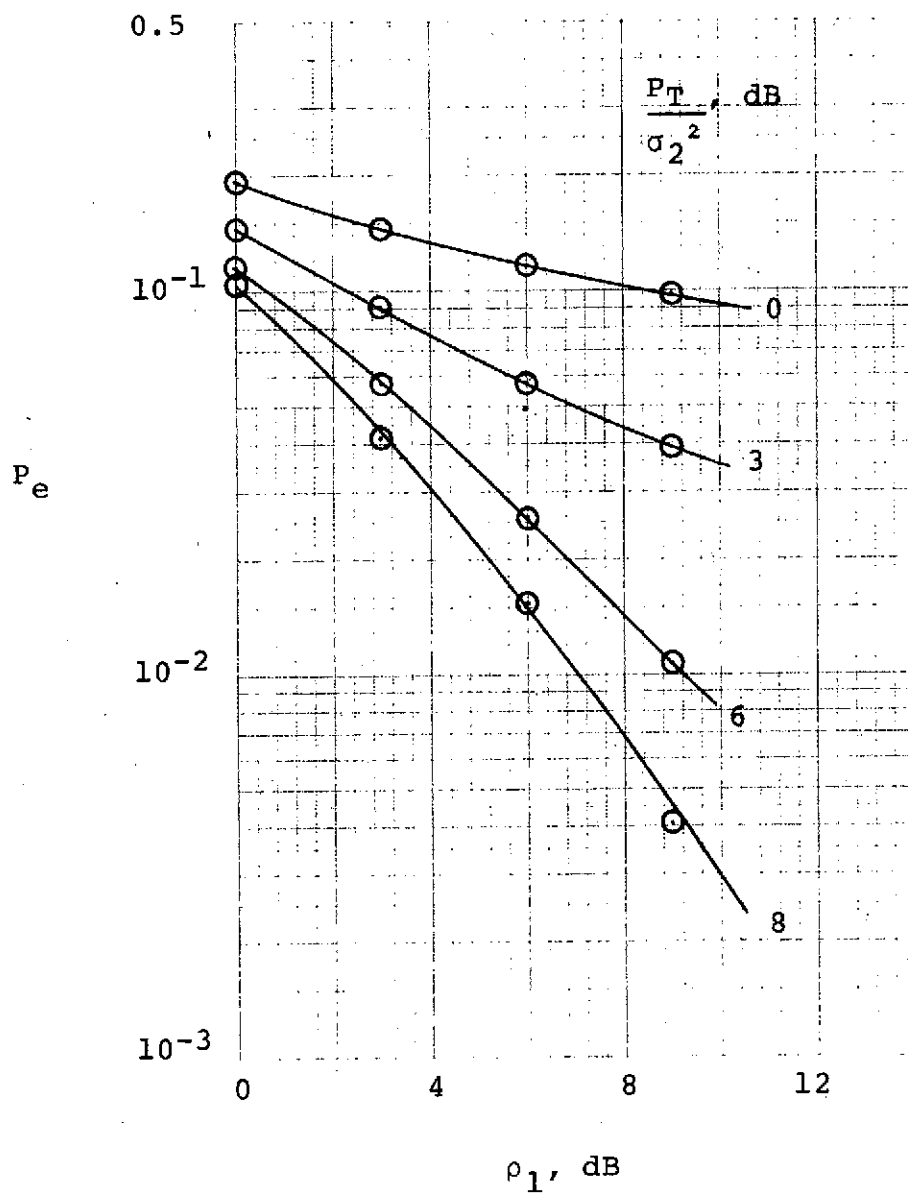


FIGURE 3.2.1-4. SINGLE-SAMPLE ERROR PROBABILITY
FOR TWT OF FIGURE 2.2-1, $\beta = 0.44$.

and consider the transformation of random variables (E, ϕ) to (r, s) induced by Equations (3.2.2-1) and (3.2.2-2). The domain and range of this transformation are as illustrated in Figure 3.2.2-1. The Jacobian of the transformation is

$$J = \begin{vmatrix} \frac{\partial r}{\partial E} & \frac{\partial r}{\partial \phi} \\ \frac{\partial s}{\partial E} & \frac{\partial s}{\partial \phi} \end{vmatrix} = F(E) \sin[\phi + G(E) - \alpha]$$

The inverse transformation $(r, s) \rightarrow (E, \phi)$ is

$$E = s$$

$$\phi = \cos^{-1}(r/F(s)) - G(s) + \alpha$$

This inverse transformation has two solutions, corresponding to the two solutions of $\cos^{-1}(r/F(s))$ in the range $[-\pi, \pi]$. The joint density function of r and s is, therefore, given by

$$p(r, s) = \frac{p(E_1, \phi_1)}{|J(E_1, \phi_1)|} + \frac{p(E_2, \phi_2)}{|J(E_2, \phi_2)|}$$

Note that

$$|J(E, \phi)| = \sqrt{F^2(s) - r^2}$$

for both (E_1, ϕ_1) and (E_2, ϕ_2) . Using Equation (3.1-1) and noting that the two solutions for ϕ yield

$$\begin{Bmatrix} \cos \phi_1 \\ \cos \phi_2 \end{Bmatrix} = \frac{r}{F(s)} \cos [G(s) - \alpha] \pm \sqrt{1 - \left(\frac{r}{F(s)}\right)^2} \sin [G(s) - \alpha]$$

one obtains

$$p(r, s) = \frac{se^{-(s^2 + A^2)/2\sigma^2}}{\pi\sigma^2\sqrt{F^2(s) - r^2}} \exp \left\{ \frac{Ars}{\sigma^2 F(s)} \cos [G(s) - \alpha] \right\} \\ \cdot \cosh \left\{ \frac{As}{\sigma^2} \sqrt{1 - \left(\frac{r}{F(s)}\right)^2} \sin [G(s) - \alpha] \right\}, \\ s \geq 0, \quad |r| \leq F(s)$$

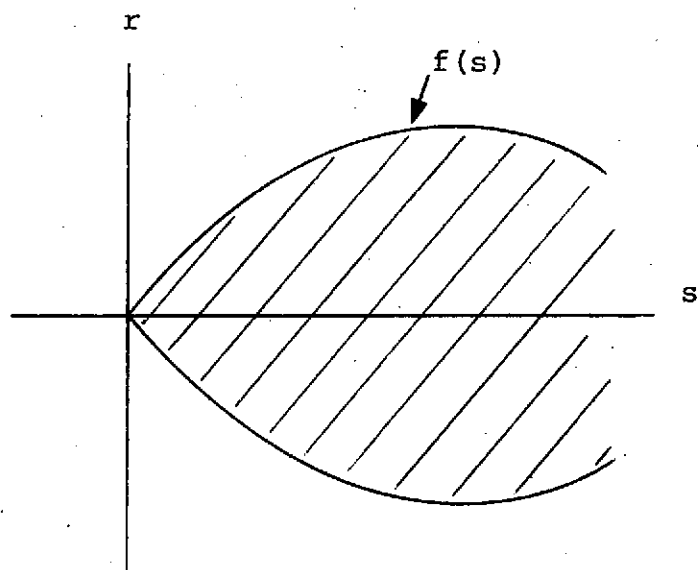
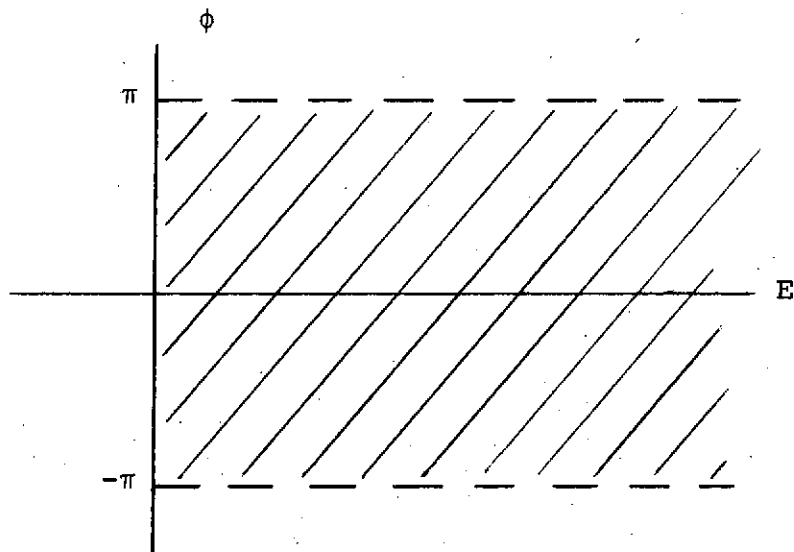


FIGURE 3.2.2-1. DOMAIN AND RANGE OF THE TRANSFORMATION $(E, \phi) \rightarrow (r, s)$.

The density function of r is obtained by integrating over all s for which $|r| \leq F(s)$:

$$p(r) = \frac{\int p(r,s) ds}{R(r)} \quad R(r) = \{s: F(s) \geq |r|\}$$

Normalizing as before, and letting $v=r/R_0$, yields for the probability density function of v ,

$$p(v) = \frac{2\rho}{\pi\beta^2} \int \frac{u}{\sqrt{f^2(u)-v^2}} \exp \left\{ -\frac{\rho}{\beta^2} \left[u^2 - 2 \frac{\beta uv}{f(u)} \cos [g(u) - \alpha] + \beta^2 \right] \right\} \frac{du}{R(v)} \\ \cdot \cosh \left\{ \frac{2\rho u}{\beta f(u)} \sqrt{f^2(u)-v^2} \sin [g(u) - \alpha] \right\} du, \quad |v| \leq 1 \quad (3.2.2-3)$$

where $R(v) = \{u: f(u) \geq |v|\}$.

A computer program was written to carry out the integration numerically. For the special case of a hard limiter with no AM-to-PM conversion, i.e., $f(u)=1$, $g(u)=0$, the density function at $\rho=0$ dB is illustrated in Figure 3.2.2-2. This result agrees with previous results for the density function of $\cos \phi$ (see e.g., Lyons [3-4]). For the TWT of Figure 2.2-1, the density function for the mixer output (in the absence of downlink noise) is given in Figure 3.2.2-3 for $\rho=0$ dB and $\beta=0.44$.

If the detector sums 2WT independent random variables, each with density function given by Equation (3.2.2-3), the density function of the sum is the 2WT-fold convolution of Equation (3.2.2-3). In principle, this operation can be carried out by taking the discrete Fourier transform of Equation (3.2.2-3), raising to the 2WT-th power, and inverting the transform. Moreover, since the effect of downlink noise is to add a Gaussian random variable to the sum of the v 's, this can be accounted for by multiplying by the appropriate Gaussian characteristic function before inverting the transform. The error probability is then obtained by numerically integrating the result over the negative values. In practice, the sharp peaks of Equation (3.2.2-3) and the fact that the convolution spreads the density function out by a factor of 2WT make this numerical procedure somewhat delicate, and results of reasonable accuracy are difficult to obtain. Since any results derived from such a procedure would be of only peripheral interest in this study, no attempts to refine the technique to yield accurate results were undertaken.

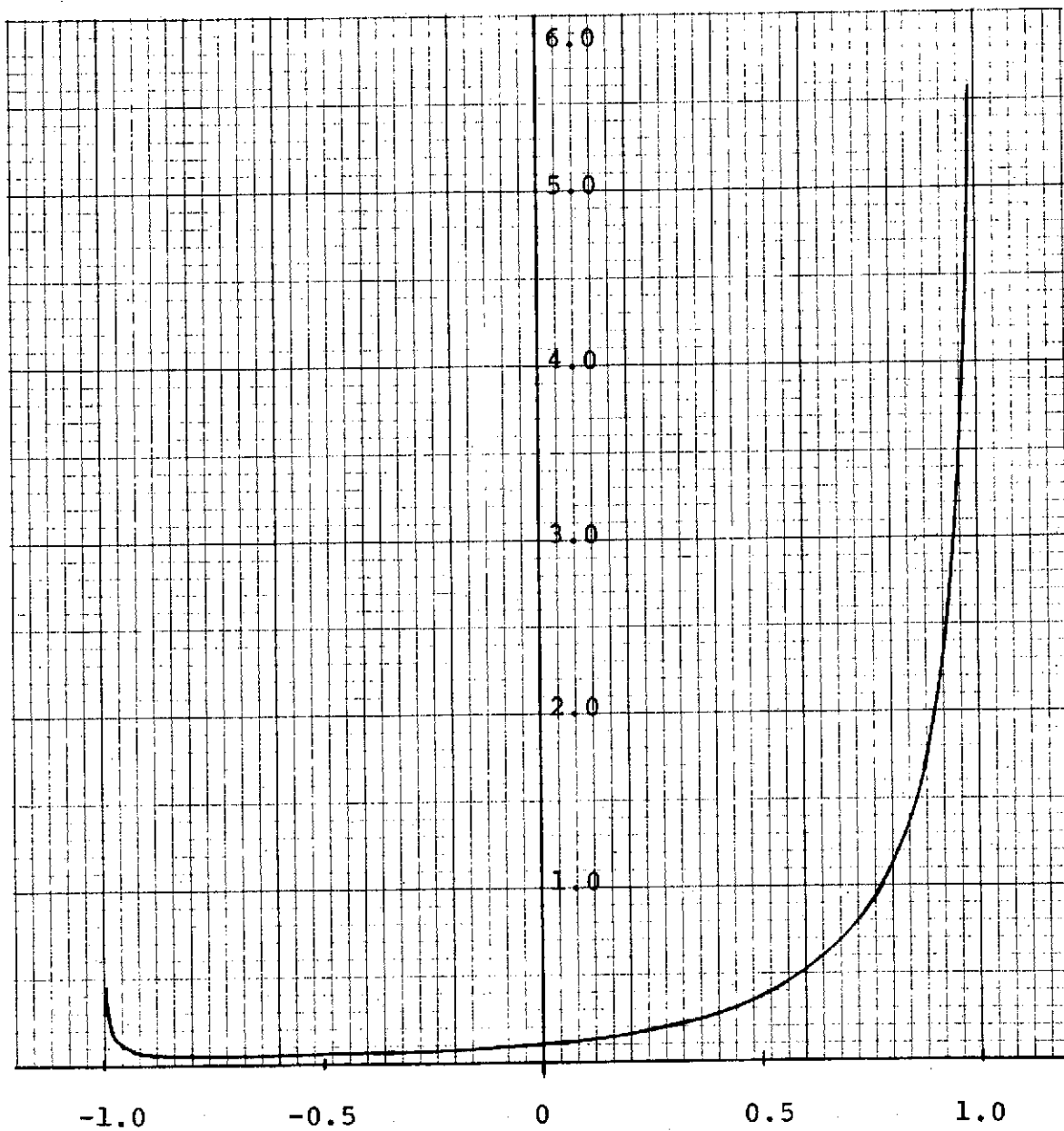


FIGURE 3.2.2-2. DENSITY FUNCTION OF $\cos\phi$
AT $\rho=0\text{dB}$.

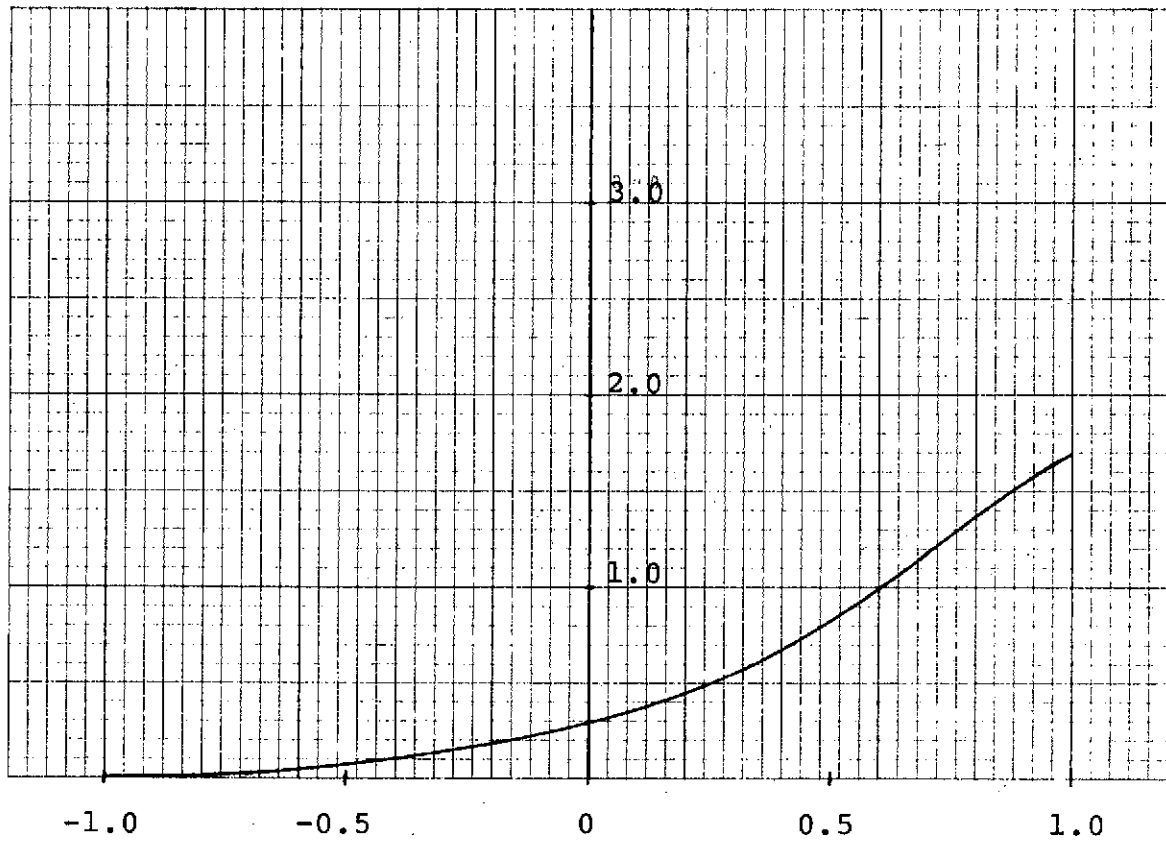


FIGURE 3.2.2-3. DENSITY FUNCTION OF v FOR TWT OF FIGURE 2.2-1 at $\rho=0\text{dB}$ and $\beta=0.44$.

3.3 The FDM/FM Link at High Signal-to-Noise Ratios

In this section, the FDM/FM system diagrammed in Figure 3.3-1 is addressed, under the assumption of high signal-to-noise ratio in both the uplink and downlink. The RF transmitted signal $x_1(t)$ is an FM signal

$$x_1(t) = A \cos[\omega_c t + \psi(t)]$$

where

$$\psi(t) = 2\pi \int_0^t [\Delta f_1 u_1(\tau) + \Delta f_2 u_2(\tau)] d\tau + \psi_0 \quad (3.3-1)$$

The baseband message signals $u_1(t)$ and $u_2(t)$ are assumed to be nonoverlapping in the frequency domain.

Since the repeater input bandwidth is typically much greater than the bandwidth of $\psi(t)$, it is legitimate [3-9] to expand the uplink noise into components in phase with and quadrature to the modulated carrier. Thus

$$\begin{aligned} y_1(t) &= [A + n_c(t)] \cos[\omega_c t + \psi(t)] - n_s(t) \sin[\omega_c t + \psi(t)] \\ &= E(t) \cos[\omega_c t + \phi(t)] \end{aligned}$$

where

$$E(t) = \left[(A + n_c(t))^2 + n_s^2(t) \right]^{1/2}$$

and

$$\phi(t) = \psi(t) + \tan^{-1} \frac{n_s(t)}{A + n_c(t)}$$

Then the TWT output is given by

$$x_2(t) = F(E(t)) \cos[\omega_c t + \phi(t) + G(E(t))]$$

At high SNR, $E(t) \approx A + n_c(t)$ and $\phi(t) \approx \psi(t) + n_s(t)/A$ with high probability. Expanding the TWT characteristics about $E=A$ and retaining only first-order terms yields

$$F(E(t)) \approx F(A) + a n_c(t)$$

$$G(E(t)) \approx G(A) + b n_c(t)$$

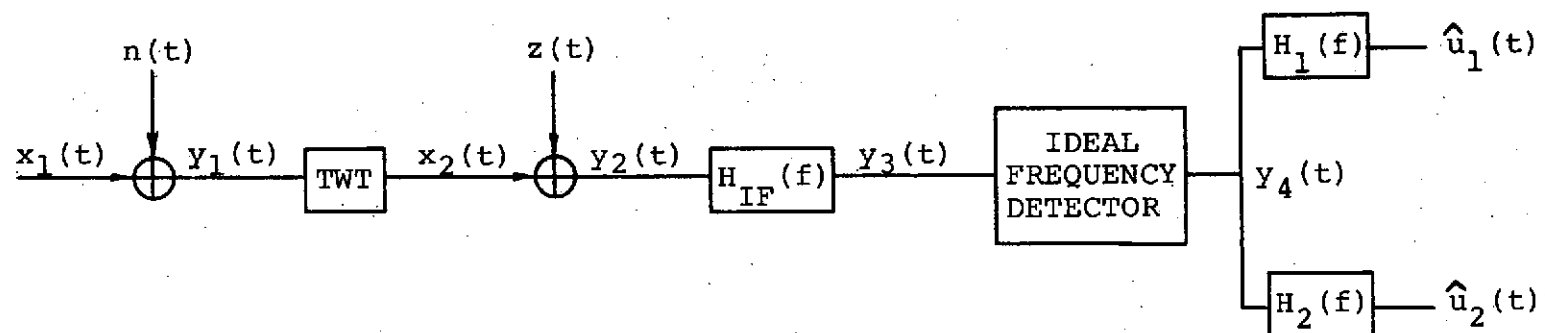


Figure 3.3-1. MODEL OF FDM/FM COMMUNICATION LINK.

where $a = F'(A)$ and $b = G'(A)$. Therefore

$$\begin{aligned} x_2(t) &= [F(A) + an_c(t)] \cos \left[\omega_c t + \psi(t) + G(A) + \frac{n_s(t)}{A} + bn_c(t) \right] \\ &= [F(A) + an_c(t)] \cos \left[\frac{n_s(t)}{A} + bn_c(t) \right] \cos [\omega_c t + \psi(t) + G(A)] \\ &\quad - [F(A) + an_c(t)] \sin \left[\frac{n_s(t)}{A} + bn_c(t) \right] \sin [\omega_c t + \psi(t) + G(A)] \end{aligned}$$

At high SNR, and with typical AM-to-PM conversion, both $n_s(t)/A$ and $bn_c(t)$ are small with high probability; thus $x_2(t)$ can be approximated as

$$\begin{aligned} x_2(t) &\approx [F(A) + an_c(t)] \cos [\omega_c t + \psi(t) + G(A)] \\ &\quad - F(A) \left[\frac{n_s(t)}{A} + bn_c(t) \right] \sin [\omega_c t + \psi(t) + G(A)] \end{aligned}$$

Since the IF filter must be wide enough to pass a constant-amplitude FM signal with negligible distortion, the filter effects on $x_2(t)$ are simply to lowpass filter the amplitudes of the quadrature components. But since $n_c(t)$ and $n_s(t)$ have constant spectral density N_0 for all $|f| < B_{TWT}/2$, the filtered versions of $n_c(t)$ and $n_s(t)$, denoted $\tilde{n}_c(t)$ and $\tilde{n}_s(t)$, have spectral density N_0 for all $|f| < B_{IF}/2$, and the IF filter output due to $x_2(t)$ alone is

$$\begin{aligned} y_3(t) \Big|_{z(t)=0} &\approx [F(A) + a\tilde{n}_c(t)] \cos [\omega_c t + \psi(t) + G(A)] \\ &\quad - F(A) \left[\frac{\tilde{n}_s(t)}{A} + b\tilde{n}_c(t) \right] \sin [\omega_c t + \psi(t) + G(A)] \\ &\approx [F(A) + a\tilde{n}_c(t)] \cos \left[\omega_c t + \psi(t) + G(A) + \frac{\tilde{n}_s(t)}{A} + b\tilde{n}_c(t) \right] \end{aligned}$$

(3.3-2)

Thus in the absence of downlink noise, the output of the ideal frequency detector, which is the derivative of the instantaneous phase of its input, is

$$y_4(t) \Big|_{z=0} \approx \frac{d\psi}{dt} + \frac{1}{A} \frac{d\tilde{n}_s}{dt} + b \frac{d\tilde{n}_c}{dt}$$

The effect of $z(t)$ on $y_4(t)$ is to add a noise term which, at high SNR, is independent of the "modulation" $\psi(t) + \tilde{n}_s(t)/A + b\tilde{n}_c(t)$ [3-10]. Therefore, to determine this contribution, $y_3(t)$ of Equation (3.3-2) can be replaced by an unmodulated sinusoid of amplitude $F(A)$. Adding the downlink noise in quadrature-carrier representation yields

$$y_3(t) = [F(A) + z_c(t)] \cos[\omega_c t + G(A)] - z_s(t) \sin[\omega_c t + G(A)]$$

where $z_c(t)$ and $z_s(t)$ have constant spectral density Z_0 for $|f| < B_{IF}/2$. The instantaneous phase of $y_3(t)$ is

$$\frac{d}{dt} \tan^{-1} \left\{ \frac{z_s(t)}{F(A) + z_c(t)} \right\} \approx \frac{1}{F(A)} \frac{dz_s}{dt}$$

Hence the total output $y_4(t)$ is given by

$$y_4(t) = \frac{d\psi}{dt} + e(t) \quad (3.3-3)$$

where

$$e(t) = \frac{1}{A} \frac{d\tilde{n}_s}{dt} + b \frac{d\tilde{n}_c}{dt} + \frac{1}{F(A)} \frac{dz_s}{dt} \quad (3.3-4)$$

The first term in $y_4(t)$ is the desired signal. The three error contributions are attributable to quadrature uplink noise, AM-to-PM conversion of inphase uplink noise, and quadrature downlink noise, respectively. Each noise term has a parabolic power spectral density over the range $|f| < B_{IF}/2$, and because of independence, they add incoherently. Thus the total error power spectrum is

$$S_e(f) = (2\pi)^2 \left[\frac{N_0}{A^2} + b^2 N_0 + \frac{Z_0}{(F(A))^2} \right] f^2 \quad |f| < B_{IF}/2$$

Observe that this is the same expression that would result if the message were transmitted by frequency-modulating a carrier of amplitude c , and transmitting over a white noise channel of one-sided spectral density n_0 , where

$$\frac{n_0}{c^2} = \frac{N_0}{A^2} + b^2 N_0 + \frac{Z_0}{(F(A))^2}$$

For simplicity of notation, this artifice of a "virtual channel" will be used in the sequel.

If message $u_1(t)$ is a lowpass signal of bandwidth W , and the demultiplexing filter $H_1(f)$ is an ideal lowpass filter, then the output noise power is

$$\overline{e_1^2} = 2 \int_0^W S_e(f) df = \frac{8\pi^2}{3} \frac{n_o}{c^2} W^3$$

The output signal-to-noise ratio is thus, using Equation (3.3-1),

$$SNR_1 = \frac{3}{2} \left(\frac{\Delta f_1}{W} \right)^2 \frac{\overline{u_1^2}}{\frac{n_o}{c^2} W} \quad (3.3-5)$$

Note that in the case of a quiet uplink ($N_o = 0$), this reduces to the familiar expression

$$SNR_1 = 3\beta_1^2 \overline{u_1^2} \rho$$

where β_1 is the FM deviation ratio and ρ is the signal-to-noise ratio in the message bandwidth.

The same technique can be applied to obtain the SNR at the output of $H_2(f)$; however, in the signal of interest, $u_2(t)$ is a PSK signal, and the quantity of primary concern is the error probability. The assumption that $u_1(t)$ and $u_2(t)$ are essentially non-overlapping in frequency implies that a matched-filter detector for $u_2(t)$ will respond negligibly to $u_1(t)$, so that the demultiplexing filter is not actually required (although it could conceivably serve a purpose in noise rejection). For analytical purposes, therefore, it is sufficient to consider as input to the PSK detector of Figure 3.3-2, the signal

$$y_4(t) = 2\pi\Delta f_2 u_2(t) + e(t)$$

where $u_2(t) = d(t)\sin\omega_{sc}(t)$, and $e(t)$ has power spectral density

$$S_e(f) = (2\pi)^2 \frac{n_o}{c^2} f^2 \quad |f| < B_{IF}/2 \quad (3.3-6)$$

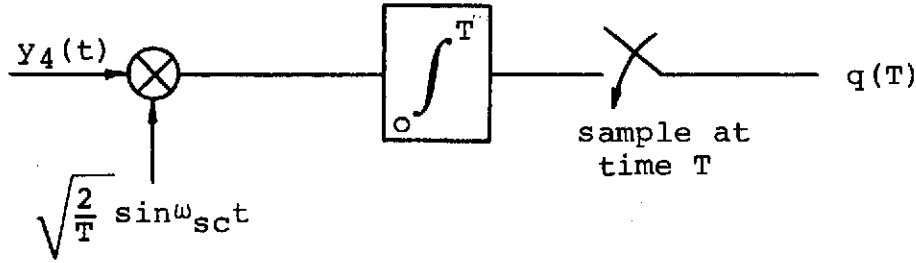


Figure 3.3-2. PSK DETECTOR.

Assume for simplicity that the subcarrier frequency is an integer multiple of the data rate. This assumption can be removed, but the generalization is somewhat complex. The detector output at the sampling time is

$$q(t) = \pm \sqrt{2T\pi\Delta f_2} + \zeta$$

where ζ is a zero-mean Gaussian random variable. The error probability is therefore

$$P_E = Q\left(\frac{\sqrt{2T\pi\Delta f_2}}{\sigma_\zeta}\right) \quad (3.3-7)$$

The variance of ζ is clearly overbounded if the restriction $|f| < B_{IF}/2$ of Equation (3.3-6) is relaxed and $S_e(f)$ is taken to be

$$S_e(f) = (2\pi)^2 \frac{n_o}{c^2} f^2 \quad \text{for all } f$$

Rewriting this as

$$S_e(f) = - (j2\pi f)^2 \frac{n_o}{c^2}$$

and noting that multiplying by $j2\pi f$ in the frequency domain corresponds to differentiating in the time domain, one obtains for the autocorrelation function of $e(t)$,

$$R_e(\tau) = - \frac{d^2}{d\tau^2} \left\{ \frac{n_o}{c^2} \delta(\tau) \right\} = - \frac{n_o}{c^2} \delta''(\tau)$$

Now since

$$\zeta = \sqrt{\frac{2}{T}} \int_0^T e(t) \sin \omega_{sc} t dt,$$

$$\begin{aligned} E \left\{ \zeta^2 \right\} &= \frac{2}{T} \int_0^T \int_0^T E \left\{ e(t) e(u) \right\} \sin \omega_{sc} t \sin \omega_{sc} u du dt \\ &= - \frac{2n_o}{c^2 T} \int_0^T \int_0^T \delta''(t-u) \sin \omega_{sc} t \sin \omega_{sc} u du dt \end{aligned}$$

But $\int \delta^{(n)}(t-u) f(u) du = \frac{d^n f(t)}{dt^n}$; therefore

$$E \left\{ \zeta^2 \right\} = - \frac{2}{T} \frac{n_o}{c^2} \int_0^T \sin \omega_{sc} t \frac{d^2}{dt^2} \sin \omega_{sc} t dt$$

Differentiating the pulsed sinusoid $\sin \omega_{sc} t$ twice results in impulses at times 0 and T, but $\sin \omega_{sc} t$ vanishes at these points, so that

$$\begin{aligned} E \left\{ \zeta^2 \right\} &= \frac{2}{T} \frac{n_o}{c^2} \omega_{sc}^2 \int_0^T \sin^2 \omega_{sc} t dt \\ &= (2\pi)^2 \frac{n_o}{c^2} f_{sc}^2 \end{aligned} \quad (3.3-8)$$

The standard deviation of ζ is therefore

$$\sigma_{\zeta} = 2\pi \frac{\sqrt{n_o}}{c} f_{sc}$$

Inserting this in Equation (3.3-7) yields

$$P_E = Q \left(\sqrt{\frac{c^2}{2N_o R} \beta_2^2} \right) \quad (3.3-9)$$

where $\beta_2 = \Delta f_2 / f_{sc}$ can be interpreted as the FM deviation ratio corresponding to $u_2(t)$, and $R = 1/T$ is the data rate.

Equation (3.3-9) relates the error probability in a simple way to the virtual channel's signal-to-noise ratio in a bit-rate bandwidth and to the RF deviation ratio. It seems to imply that for a fixed SNR, performance can be improved simply by increasing the deviation ratio, as might be expected from the "wideband noise improvement" typical of FM systems. However, the analysis leading to (4) is valid only above threshold, which implies an upper limit to the value of β for which the relationship is valid.

Note, from Equation (3.3-8) that the variance of ξ is exactly the same as it would be if the parabolic-spectrum process $e(t)$ were replaced by a white-noise process with spectral density equal to the parabola's value at the sub-carrier frequency, namely $2\pi^2 n_o f_{sc}^2 / c^2$. This suggests that error probability when operating below threshold could be approximated by assuming white noise of spectral density $S_e(f_{sc})$, where the spectral density of $e(t)$ is determined from one of several empirical expressions for FM noise spectral density below threshold. This approach overlooks the fact that below threshold the process $e(t)$ is no longer Gaussian, but is nevertheless a reasonable means of estimating performance.

As a final observation, an absolute lower bound on P_E for a PSK/FM system (leaving out, for simplicity, the other message $u_2(t)$) operating on a white Gaussian RF channel can be obtained as follows. In general, the RF signal corresponding to a data 0 is

$$s_0(t) = c \cos \left[\omega_c t + \frac{2\pi \Delta f}{\omega_{sc}} \cos(\omega_{sc} t + \theta_{sc}) + \theta_c \right] \quad 0 \leq t \leq T$$

while that corresponding to a data 1 is

$$s_1(t) = c \cos \left[\omega_c t - \frac{2\pi \Delta f}{\omega_{sc}} \cos(\omega_{sc} t + \theta_{sc}) + \theta_c \right] \quad 0 \leq t \leq T$$

A receiver which is able to establish phase coherence at both RF and subcarrier has error probability given by [3-11]

$$P_E = Q \left(\sqrt{\frac{E_b}{n_o} (1-\gamma)} \right)$$

where $E_b = c^2 / 2R$ and

$$\begin{aligned} \gamma &= \frac{1}{E_b} \int_0^T s_0(t) s_1(t) dt \\ &= R \int_0^T \cos \left[\frac{4\pi \Delta f}{\omega_{sc}} \cos(\omega_{sc} t + \theta_{sc}) \right] dt \end{aligned}$$

+ double-frequency term integrating to zero

Since the integrand has period $1/f_{sc}$, and since there are an integer number ($f_{sc}T$) of cycles in the interval of integration, this becomes

$$\gamma = f_{sc} \int_0^{1/f_{sc}} \cos \left[\frac{2\Delta f}{f_{sc}} \cos(\omega_{sc}t + \theta_{sc}) \right] dt = J_0(2\beta)$$

Therefore

$$P_E = Q \left(\sqrt{\frac{c^2}{2n_0 R}} (1 - J_0(2\beta)) \right)$$

Since $J_0(x) \approx 1 - x^2/4$ for small x ,

$$P_E \approx Q \left(\sqrt{\frac{c^2}{2n_0 R}} \beta^2 \right), \beta \ll 1$$

showing that the demodulator considered above is essentially optimum for small deviation ratios, and when operating above threshold.

3.4 References

- 3-1 Middleton, D., Introduction to Statistical Communication Theory, McGraw-Hill Book Co., 1960, Chapter 9.
- 3-2 Gradshteyn, I.S., and I.M. Ryzhik, Table of Integrals, Series, and Products, Academic Press, 1965, No. 6.631.
- 3-3 Jain, P.C., and N.M. Blachman, "Detection of a PSK Signal Transmitted Through a Hard-Limited Channel," IEEE Trans. Inform. Theory, Vol. IT-19, pp. 623-630, September 1973.
- 3-4 Lyons, R.G., "The Effect of a Bandpass Nonlinearity on Signal Detectability," IEEE Trans. Comm., Vol. COM-21, pp. 51-60, January 1973.
- 3-5 Aein, J.M., "Normal Approximations to the Error Rate for Hard-Limited Correlators," IEEE Trans. Comm. Tech., Vol. COM-15, pp. 44-51, February 1967.
- 3-6 Aein, J.M., "Error Rate for Peak-Limited Coherent Binary Channels," IEEE Trans. Comm. Tech., Vol. COM-16, pp. 35-44, February 1968.

- 3-7 Davisson, L.D., and L.B. Milstein, "On the Performance of Digital Communication Systems with Bandpass Limiters," IEEE Trans. Comm., Vol. COM-20, pp. 972-980, October 1972.
- 3-8 Blachman, N. M., "The Signal X Signal, Noise X Noise, and Signal X Noise Output of a Nonlinearity," IEEE Trans. Inform. Theory, Vol. IT-14, pp. 21-27, January 1968.
- 3-9 Viterbi, A. J. Principles of Coherent Communication, McGraw-Hill Book Co., 1966, p. 177.
- 3-10 Panter, P. F., Modulation, Noise, and Spectral Analysis, McGraw-Hill Book Co., 1965, Chapter 14.
- 3-11 Viterbi, A.J., Principles of Coherent Communication, McGraw-Hill Book Co., 1966, Chapter 7.

SECTION 4.0
SIMULATION OF THE RETURN LINK

The mathematical models developed in Section 2.0 form the basis for the digital computer simulation of the system. This section will describe the actual implementation of the models, giving specifics of filter design, signal flow, and so forth. Program details are relegated to Appendix E.

4.1

General Considerations

Discrete-time modeling of continuous systems poses some particular questions relative to selection of sampling rate and approximation of analog filters by digital filters. Since these considerations are common to all the simulations, they are dealt with separately in this section. Implementation of the nonlinearity is also discussed.

Selection of the sampling rate is primarily a trade-off between the necessity for accurate representation of the analog signals and the desire to obtain results with minimum computer run time. At the bare minimum, signals must be sampled at their Nyquist rate; that is, at least two samples per cycle of the highest frequency component must be taken. However, signals sampled at or near the Nyquist rate generally must be processed in a rather sophisticated fashion in order for the desired information to be recovered. This prohibits, for example, the use of such intuitively satisfying correspondences as replacing analog integrators by discrete-time summers. It is more realistic for simulation purposes to sample at several times the Nyquist rate, so that the sequence of samples closely resembles the analog waveform without elaborate processing. As a useful guideline, if linear interpolation between samples yields an accurate replica of the analog signal, the sampling rate is high enough for most simulation purposes. (Nyquist sampling, by contrast, requires interpolation using a $(\sin x)/x$ weighting function for accurate reconstitution of the analog signal.)

The implementation of filters is another consideration in constructing simulation programs. The approach taken depends basically upon whether the intention is simply to achieve some specified frequency response, or to accurately model a given analog filter. For the latter case, there are techniques for transforming a given analog transfer function $H(s)$ to a discrete-time transfer function $H'(z)$ whose frequency response, both amplitude and phase, closely approximates that of $H(s)$ for frequencies up to near the half-sampling rate. For the former case, there are design techniques which can be applied directly to design a digital filter whose characteristics approximate the desired characteristics. Both techniques are discussed in Appendix C.

In the simulations of this study, in some cases it was desired to closely model some given analog filter, such as a Butterworth filter, and the transformation technique was used. Examples of this are the IF and demultiplexing filters in the FDM/FM simulation. In other cases, such as for the TWT input filters, the only objective was to construct a filter with a prescribed passband, and the direct filter design technique was used.

The TWT nonlinearity is implemented in the simulations by way of a table look-up. There are two 151-entry tables, one for the normalized amplitude characteristic $f(u)$, the other for the normalized phase $g(u)$. The first entry in the table gives the value at $u=0$; the 101st entry gives the value at $u=1.0$ (i.e., $E=E_{\text{sat}}$). For a normalized input amplitude u , the index in the table is the integer part of $1+100u$. For input levels in excess of 150% of saturating drive level, the value at $u=1.5$, i.e., the 151st entry in the table, is used. (It is not anticipated that this will occur with any regularity.) Because the TWT characteristics are usually measured characteristics of a "typical" TWT, more accurate representation of $f(u)$ and $g(u)$ is not justified.

The amplitude and phase tables may be generated in any convenient way. The tables for the TWT of Figure 2.2-1 are read in from data cards. Alternatively, the table could be generated by a curve-fitting routine which passes curves through or near a small number of measured data points, or an analytical form for $f(u)$ and $g(u)$ may be assumed, and the tables generated by evaluating the functions at intervals of 0.01.

4.2 High-Rate PSK Simulations

Figure 4.2-1 illustrates in a general way how the signal processing implied by Figure 2.5-1 is organized into program modules in the NRZ PSK simulation. The objective in this and the other simulations is to achieve the maximum program modularity consistent with efficient operation. This facilitates changes or additions to the simulation. The sampling rate in this simulation is 1 GHz, which is large enough to accurately represent the required 112.5 MHz lowpass equivalent of the TDRS wideband input filter, and the 100 Mb/s PSK signal of interest.

FUNCTION SIGIN generates samples of the complex envelope of the PSK signal, using as data periodic repetition of the 63-bit pseudorandom sequence generated by the feedback shift register of Figure 4.2-2. FUNCTION TWTOUT simulates

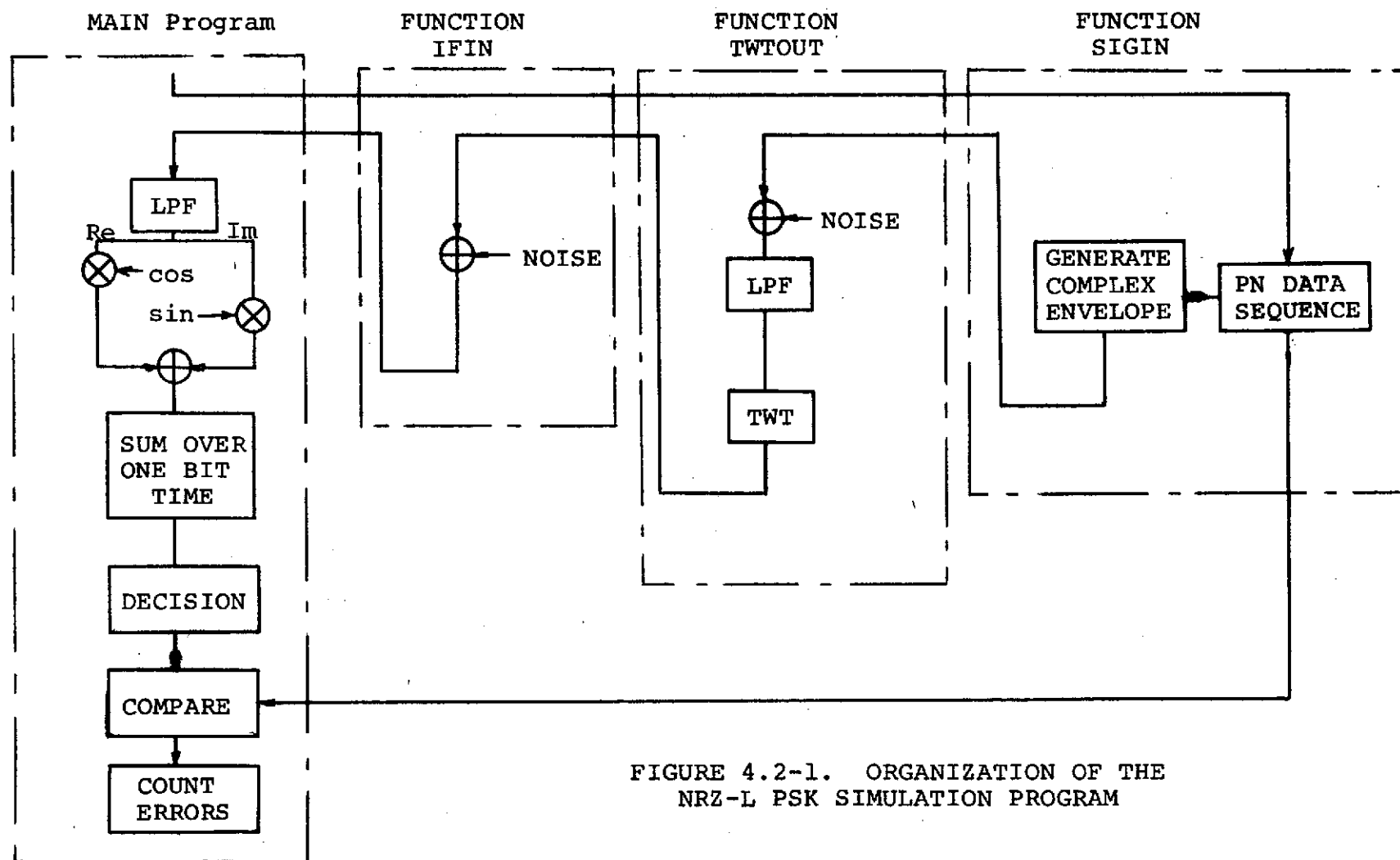


FIGURE 4.2-1. ORGANIZATION OF THE NRZ-L PSK SIMULATION PROGRAM

the addition of uplink noise, filtering, and nonlinear amplification by the TWT. Independent sequences $\{z_c(k)\}$, $\{z_s(k)\}$ of pseudo-Gaussian random variables are generated as sums of 12 uniform random variables [4-1]. Each sample has variance $N_0 f_s$, where N_0 is the one-sided uplink noise spectral density; the sequences thus represent samples of the quadrature components of white Gaussian noise of bandwidth equal to the sampling rate. The complex sequence $\{z_c(k) + jz_s(k)\}$ is added to the complex envelope sequence and passed through the TWT input filter. This filter is realized as a 41-stage nonrecursive digital filter with linear phase, as described in Appendix C. It has a design bandwidth of 112.5 MHz; its actual frequency response is illustrated by Figure 4.2-3.

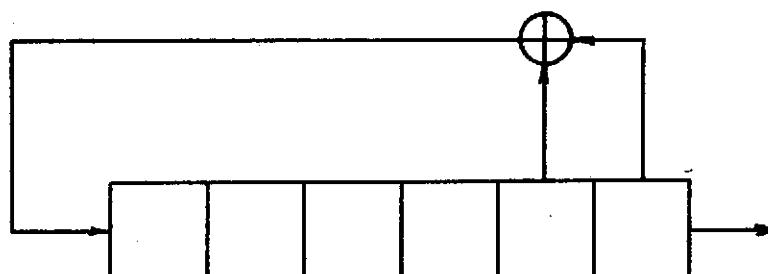


FIGURE 4.2-2.

PSEUDORANDOM DATA SEQUENCE GENERATOR

The output of the filter is the complex envelope of the TWT input. Its magnitude is used to access the amplitude nonlinearity and AM-to-PM conversion tables and the appropriate adjustment is then made to the complex envelope.

Complex downlink noise is generated in the same fashion as the uplink noise, and added to the complex envelope. This is carried out in FUNCTION IFIN.

The MAIN program receives from FUNCTION IFIN the complex envelope of the received signal. This is filtered by a representation of the RF and IF receiver stages, which for simplicity is taken to be the same filter as the TWT input filter. The real and imaginary parts of this filter's output are extracted and separately correlated with a phase angle which accounts for both the initial RF phase set in FUNCTION SIGIN and an offset to compensate for the rotation induced by AM-to-PM conversion in the TWT.

MAGNITUDE, dB

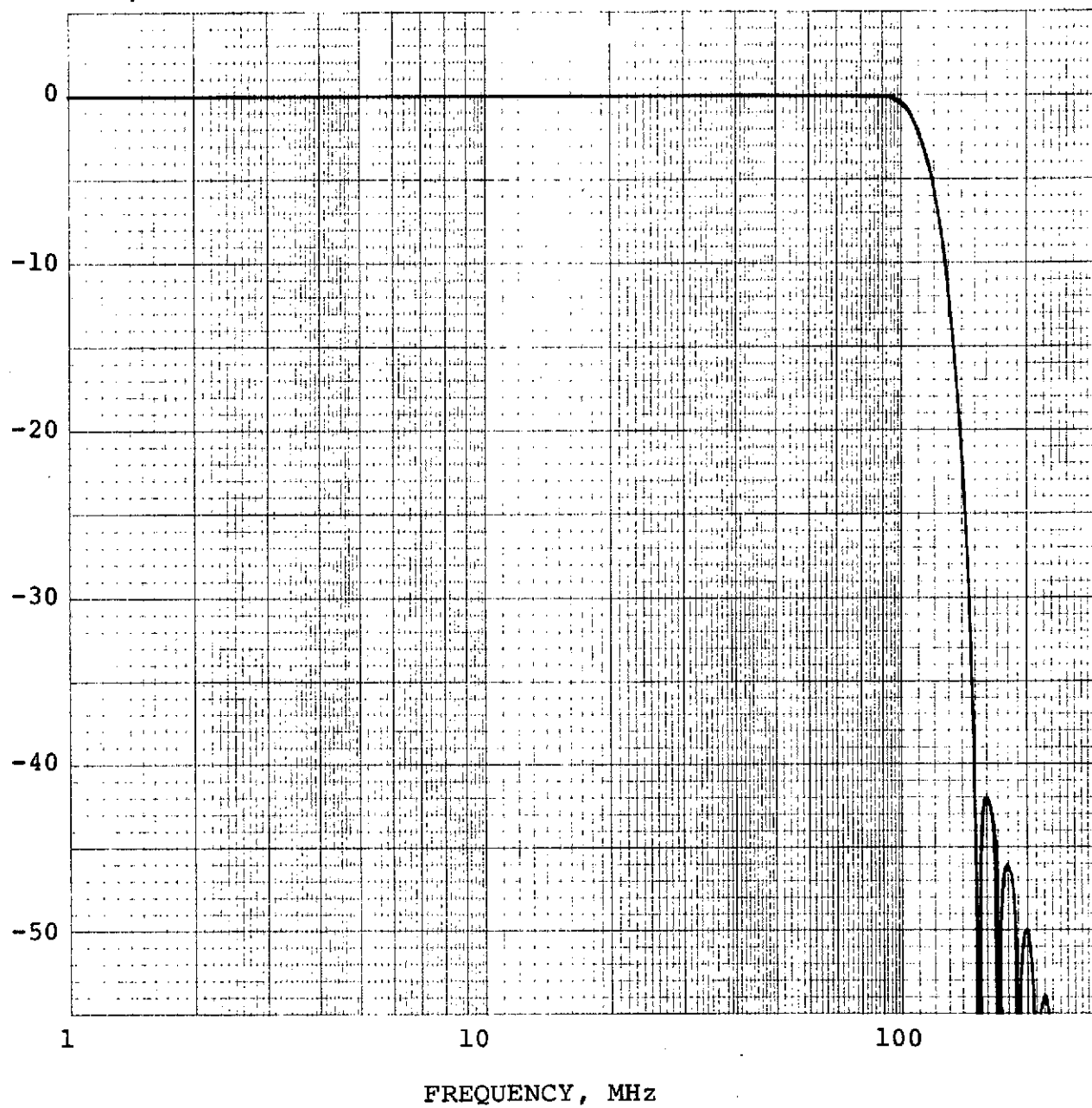


FIGURE 4.2-3. FREQUENCY RESPONSE OF LOWPASS EQUIVALENT OF WIDEBAND TDRS INPUT FILTER

Following a built-in delay to account for propagation time through the filters, the correlation results are summed over the duration of each bit, and decisions made according to the sign of the result. These decisions are compared to the original data sequence to determine error probability.

The split-phase PSK simulation is essentially the same as the NRZ PSK program, with several exceptions. FUNCTION SIGIN, naturally, generates a split-phase PSK signal, and the summation over a bit interval in the MAIN program actually adds over the first half-bit and subtracts over the second half-bit. The TWT and IF filters are again implemented as 41-tap digital filters, but the design bandwidth is 44 MHz, simulating the lowpass equivalent of the narrowband TDRS input filter. The frequency response of these filters is illustrated in Figure 4.2-4.

4.3 FDM/FM Simulation

The modular organization of the FDM/FM simulation is illustrated in Figure 4.3-1. Since the RF bandwidth is substantially greater than that of the FDM baseband, two sampling rates are used. In the MAIN program, all signals are at baseband and the sampling rate is 200 MHz; all other modules process RF complex envelopes and a sampling rate of 400 MHz is used. Interfacing the two rates is accomplished by executing FUNCTIONS IFOUT, IFIN, TWTOUT, and SIGIN twice per MAIN program sample time.

Generation of the signal's complex envelope is, as before, accomplished in FUNCTION SIGIN; however, it is a more complicated operation here than the case of the PSK signals. Figure 4.3-2 is a more detailed representation of the operation of this module, and the optional configurations which may be selected by the user. The analog signal, representing a television signal, consists of up to fifteen tones of variable frequency and amplitude. The PSK signal has variable subcarrier amplitude and data rate, with the same pseudorandom data sequence used in the NRZ-L and split-phase programs. Either or both may be filtered prior to multiplexing, in order to eliminate crosstalk. The TV filter is a digital approximation of an eighth-order Chebyshev lowpass filter cutting off at 4.2 MHz. The PSK filter is a digital approximation of a fourth-order Butterworth bandpass filter with 4 MHz passband. The transfer function of this filter is obtained from that of a lowpass Butterworth filter by a transformation which results in a passband which is geometrically symmetric about the center frequency. Under narrowband

MAGNITUDE, dB

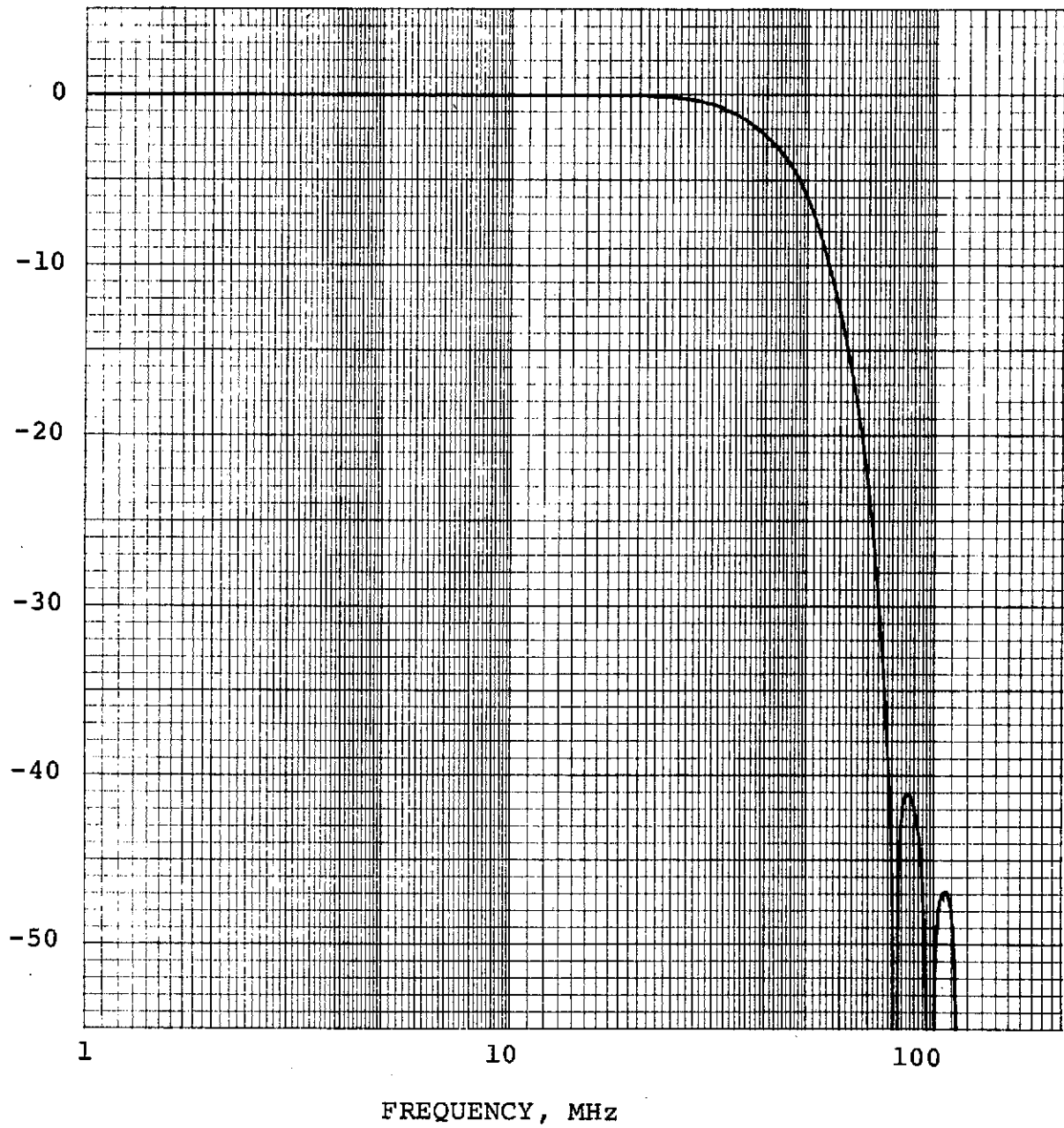


FIGURE 4.2-4. FREQUENCY RESPONSE OF LOWPASS EQUIVALENT OF NARROWBAND TDRS INPUT FILTER

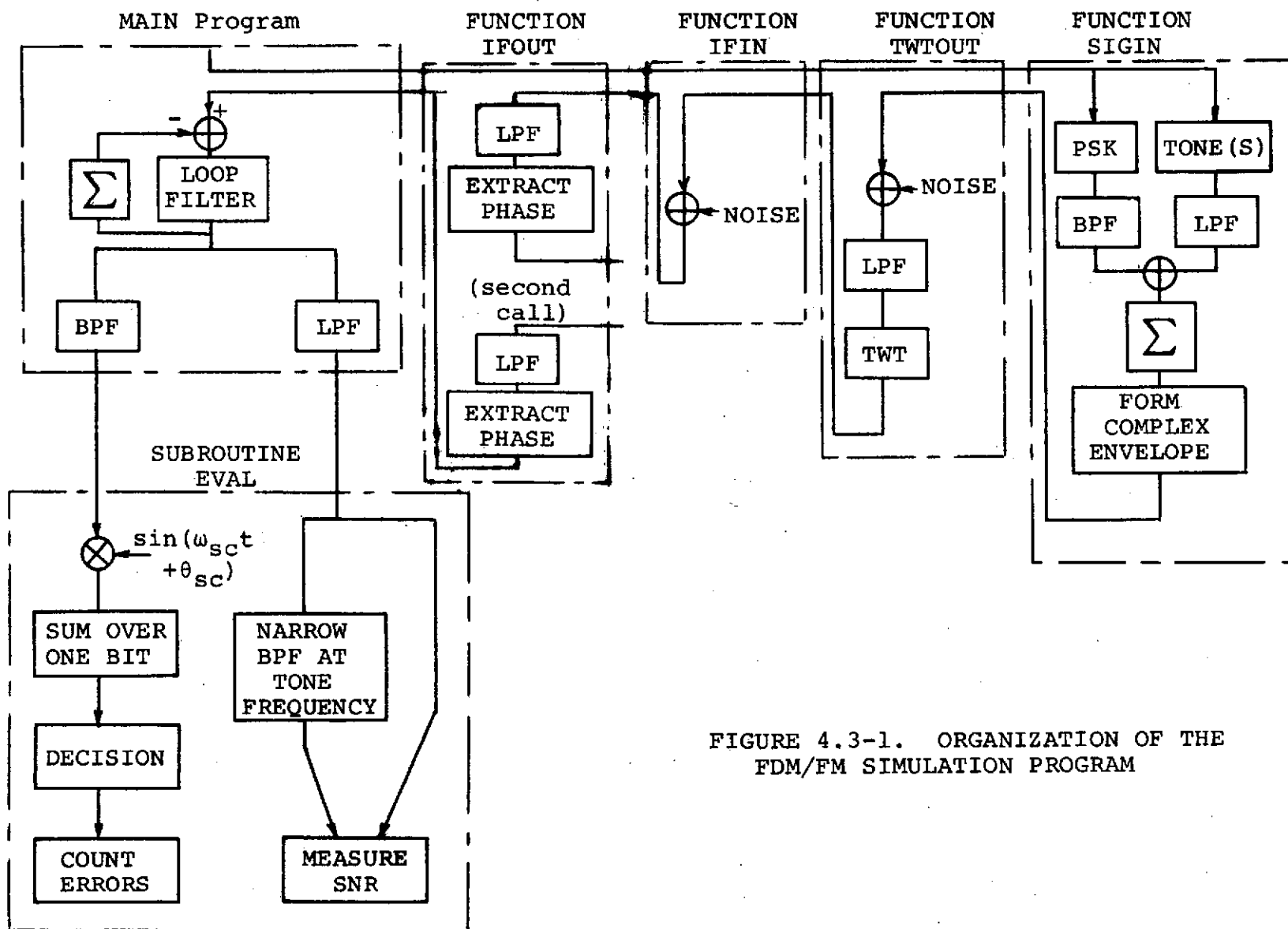


FIGURE 4.3-1. ORGANIZATION OF THE FDM/FM SIMULATION PROGRAM

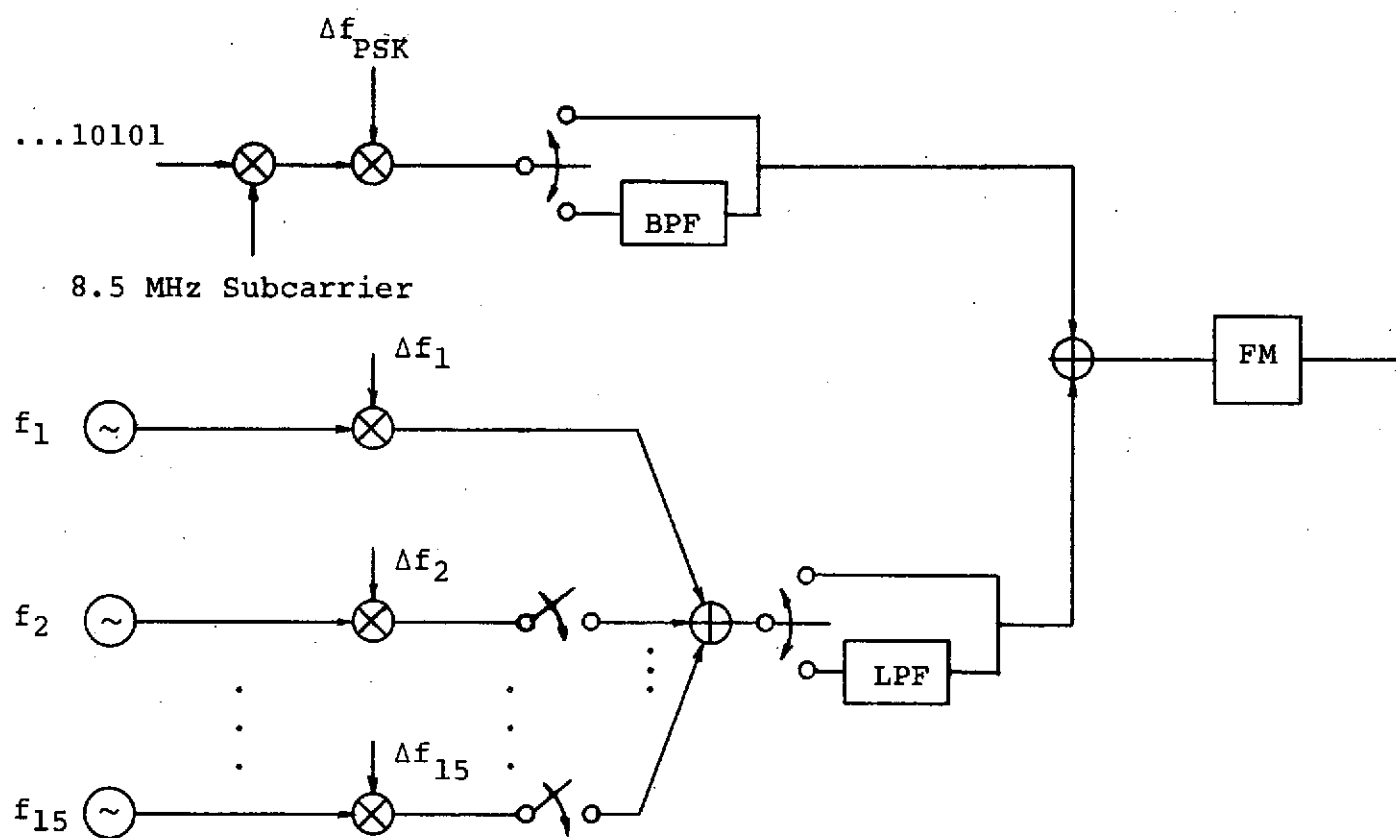


FIGURE 4.3-2. SIGNAL OPTIONS IN FDM/FM SIMULATION PROGRAM

conditions (center frequency much greater than bandwidth), the passband would be approximately arithmetically symmetric about the center frequency. For the PSK demultiplexing filter, however, the necessary bandwidth is a significant fraction of the subcarrier frequency, and the passband is not arithmetically symmetric about the design center frequency. Anticipating the selection $f_{sc} = 8.5$ MHz, it was desired to center the passband at 8.5 MHz. If the passband is taken to be the range between 3-dB points, then since the 3-dB points occur at αf_o and f_o/α , where f_o is the design center frequency and $\alpha < 1$, the passband is centered at 8.5 MHz if

$$\alpha f_o + \frac{1}{\alpha} f_o = 17 \text{ MHz} \quad (4.3-1)$$

But the bandwidth is 4 MHz, so that

$$\frac{1}{\alpha} f_o - \alpha f_o = 4 \text{ MHz} \quad (4.3-2)$$

Simultaneous solution of Equations (4.3-1) and (4.3-2) yields

$$f_o = (8.5)^2 - 4 = 8.26 \text{ MHz}$$

Therefore a design center frequency of 8.26 MHz was used in the lowpass-to-bandpass transformation to obtain the PSK filter.

The frequency responses of both the analog filters and the digital implementations are illustrated in Figures 4.3-3 and 4.3-4. The digital filters are obtained using the bilinear transformation technique discussed in Appendix C.

To obtain the phase of the FM signal, the sum of the analog and PSK signals is numerically integrated and the complex envelope of the input signal is formed in accordance with Equation (2.3.2-1). Note that the amplitudes selected for the constituent signals determine the RF frequency deviation of the FM signal.

FUNCTIONS TWTOUT and IFIN are similar to their counterparts in the PSK simulation programs, except that the TWT input filter can be selected to be either the 88 MHz narrowband input filter or the 225 MHz wideband input filter. The filters are realized as 17-tap nonrecursive digital filters.

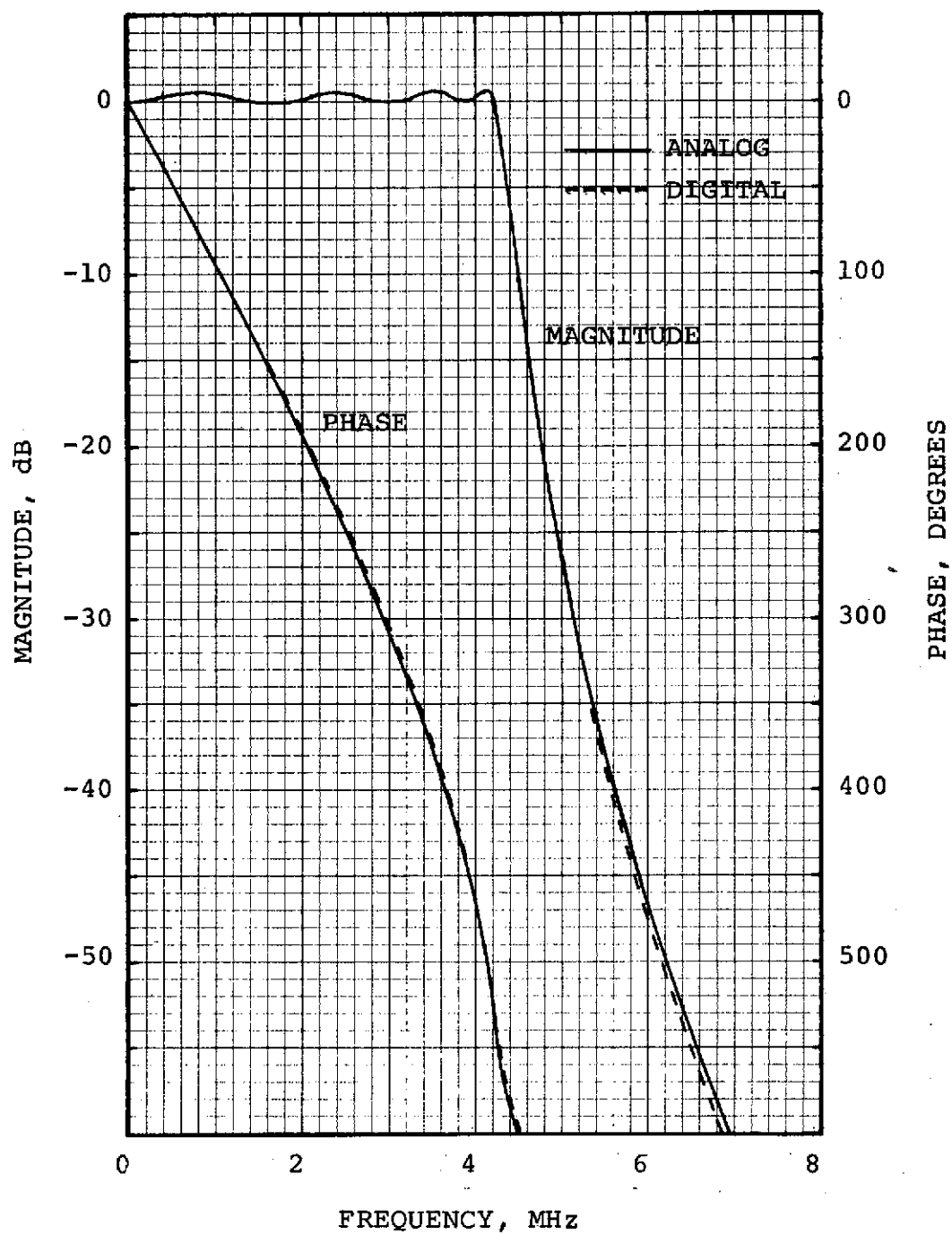


FIGURE 4.3-3. FREQUENCY RESPONSE OF LOWPASS PREMULPLEXING FILTER (EIGHTH-ORDER CHEBYSHEV)

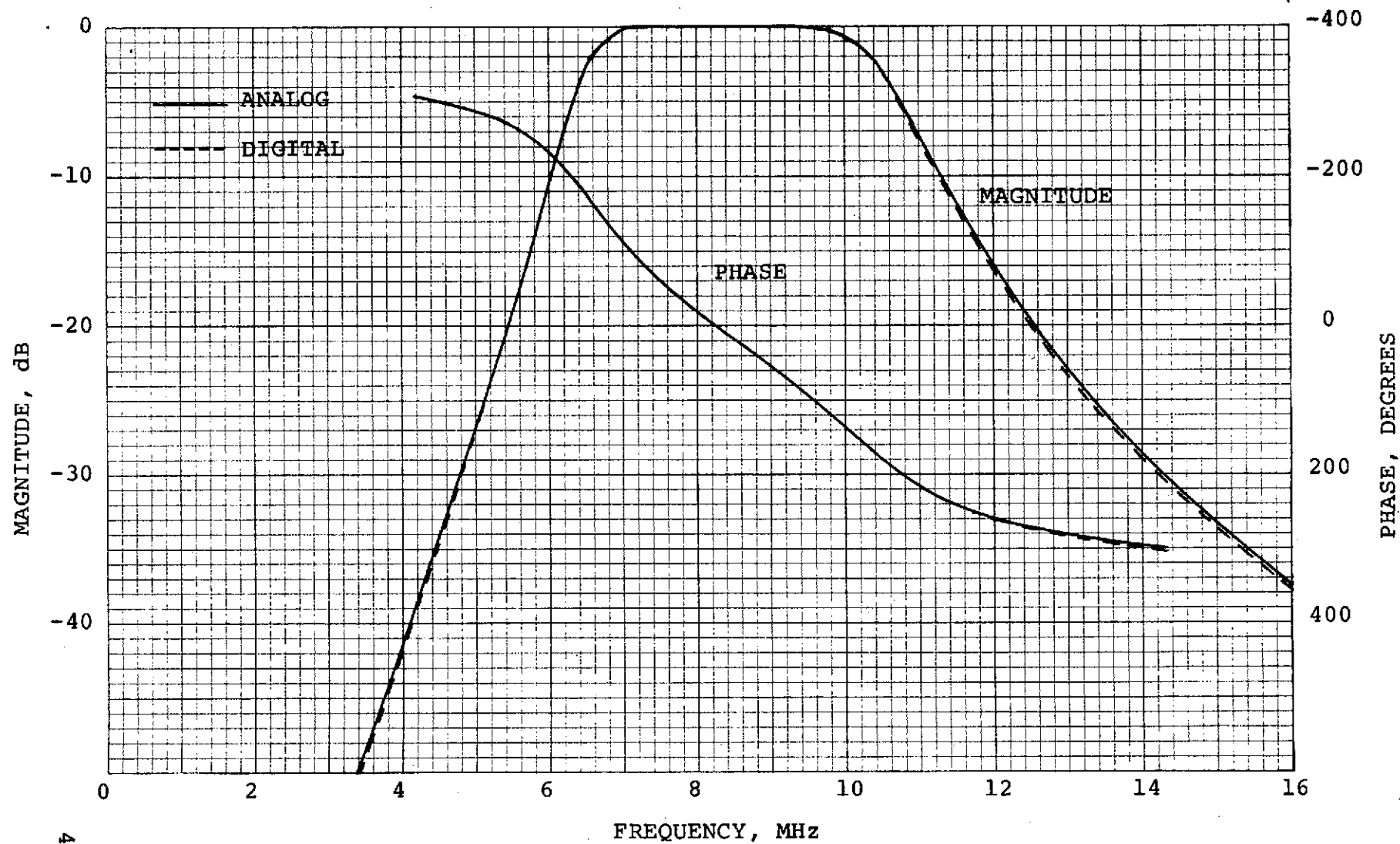


FIGURE 4.3-4. FREQUENCY RESPONSE OF BANDPASS PREMULPLEXING FILTER (FOURTH-ORDER BUTTERWORTH)

It is also possible to specify no input filter; because the sampling rate is 400 MHz, this is equivalent to assuming the presence of an ideal filter of 400 MHz bandwidth at the TWT input.

FUNCTION IFOUT performs the dual tasks of IF filtering and extracting the phase of the filter output. The IF filter is a digital approximation of a fourth-order Butterworth lowpass filter, whose frequency response is shown in Figure 4.3-5. This is the baseband equivalent of an IF filter with bandwidth 35 MHz. The output phase is obtained as the arctangent of the ratio of the imaginary and real parts of the filter output.

The MAIN program simulates FM demodulation by passing the IF output phase through the baseband PLL model of Figure 2.4.2-3. The loop filter has the form illustrated in Figure 4.3-6, with transfer function

$$F(s) = \frac{R_3}{R_1} \frac{R_2Cs + 1}{(R_2 + R_3)Cs + 1}$$

This loop filter, and the circuit parameters illustrated in Figure 4.3-6, were suggested by the Technical Monitor.

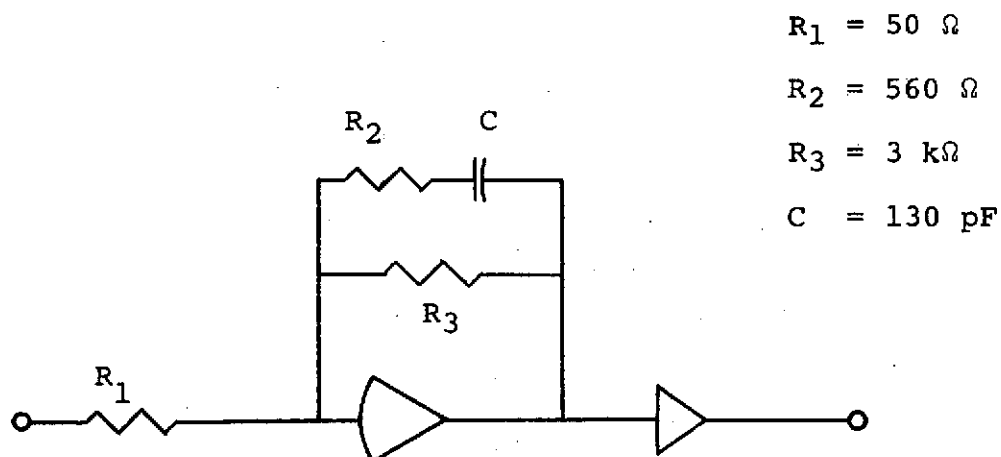


FIGURE 4.3-6. IMPLEMENTATION OF THE LOOP FILTER

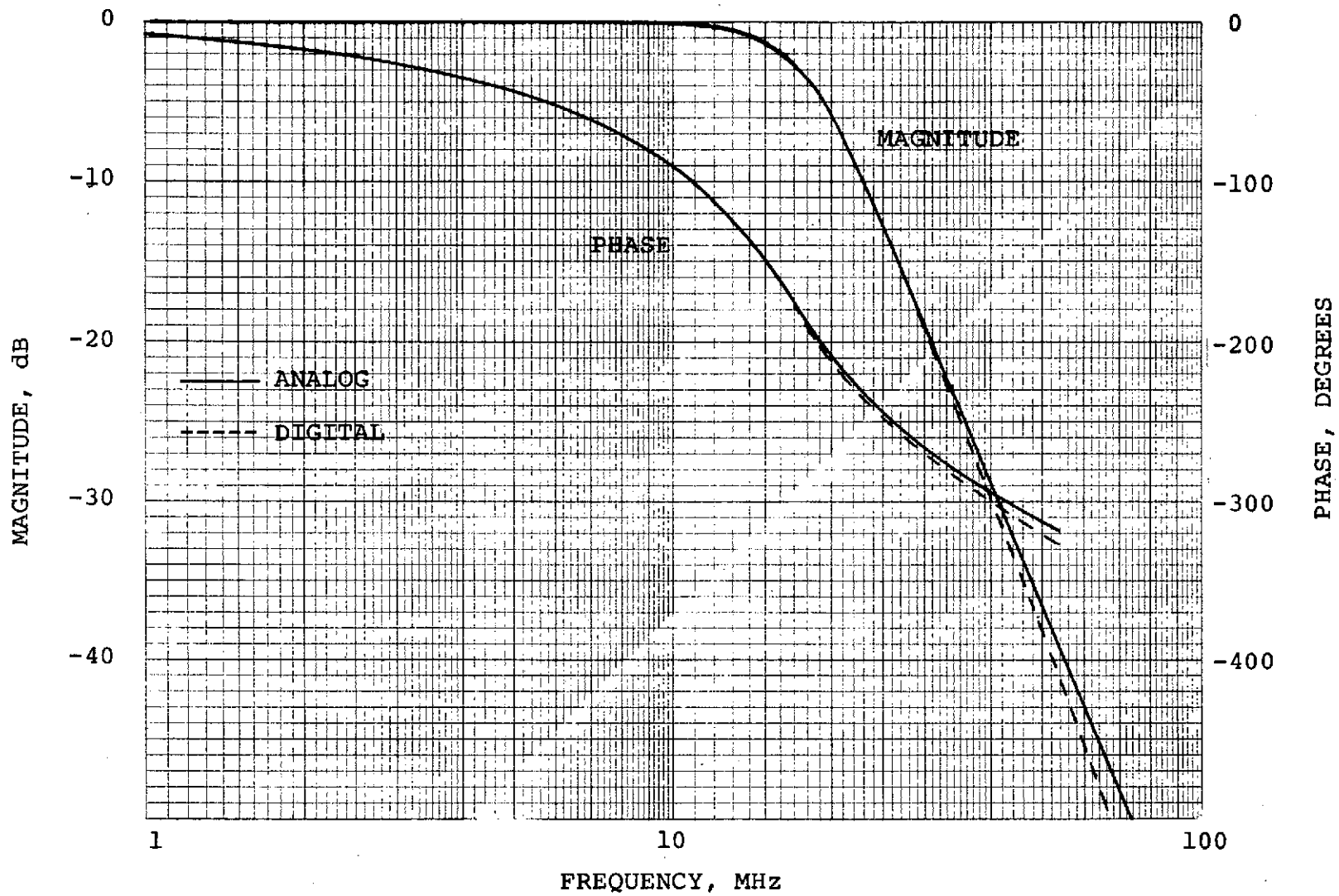


FIGURE 4.3-5. FREQUENCY RESPONSE OF THE
IF FILTER LOWPASS EQUIVALENT

Under linear operation, the closed-loop transfer function of the PLL is, using Equation (2.4.2-6),

$$\frac{\theta_2(s)}{\theta_1(s)} = \frac{G(R_2Cs+1)/((R_2+R_3)Cs+1)}{s + G(R_2Cs+1)/((R_2+R_3)Cs+1)} \quad (4.3-3)$$

where the loop filter's DC gain, R_3/R_1 has been absorbed into the PLL gain G . The frequency response is illustrated in Figure 4.3-7 for several values of loop gain and the circuit parameters specified in Figure 4.3-6.

The transfer function from input to output is given by

$$\frac{Y(s)}{\theta_1(s)} = s \frac{\theta_2(s)}{\theta_1(s)} \quad (4.3-4)$$

Since the transfer function of an ideal frequency detector is s , the closed-loop transfer function $\theta_2(s)/\theta_1(s)$ represents variation from an ideal frequency detector. The input-output frequency response for $G=2.7 \times 10^8$ is illustrated in Figure 4.3-8, along with the corresponding response of an ideal discriminator. In Figure 4.3-9, the location of the 3 dB point of Equation (4.3-3) as a function of PLL gain, for the circuit parameters of Figure 4.3-6, is given. From Equation (4.3-4), this frequency is also the point at which the input-output frequency response departs by 3 dB from that of an ideal discriminator.

In the simulation program, the loop filter is a digital approximation of the filter of Figure 4.3-6, obtained using the bilinear transformation. The integrator in the baseband PLL model is implemented as a simple rectangular integration. The PLL gain is variable on input.

The PLL output, which is the RF demodulator's estimate of the baseband signal, may be optionally passed through either or both of two demultiplexing filters to separate the TV and PSK portions of the signal. These filters are identical to the premultiplexing filters used in FUNCTION SIGIN, except for differences due to the difference in sampling rates. The TV and PSK signals are then passed to SUBROUTINE EVAL, which determines error probability in the PSK signal, and signal-to-noise ratio in the TV signal. This subroutine includes a PSK detection routine, which correlates the received signal with an appropriately delayed local subcarrier, sums over a bit interval, and checks the sequence of bit decisions against the known data sequence to determine the number of errors.

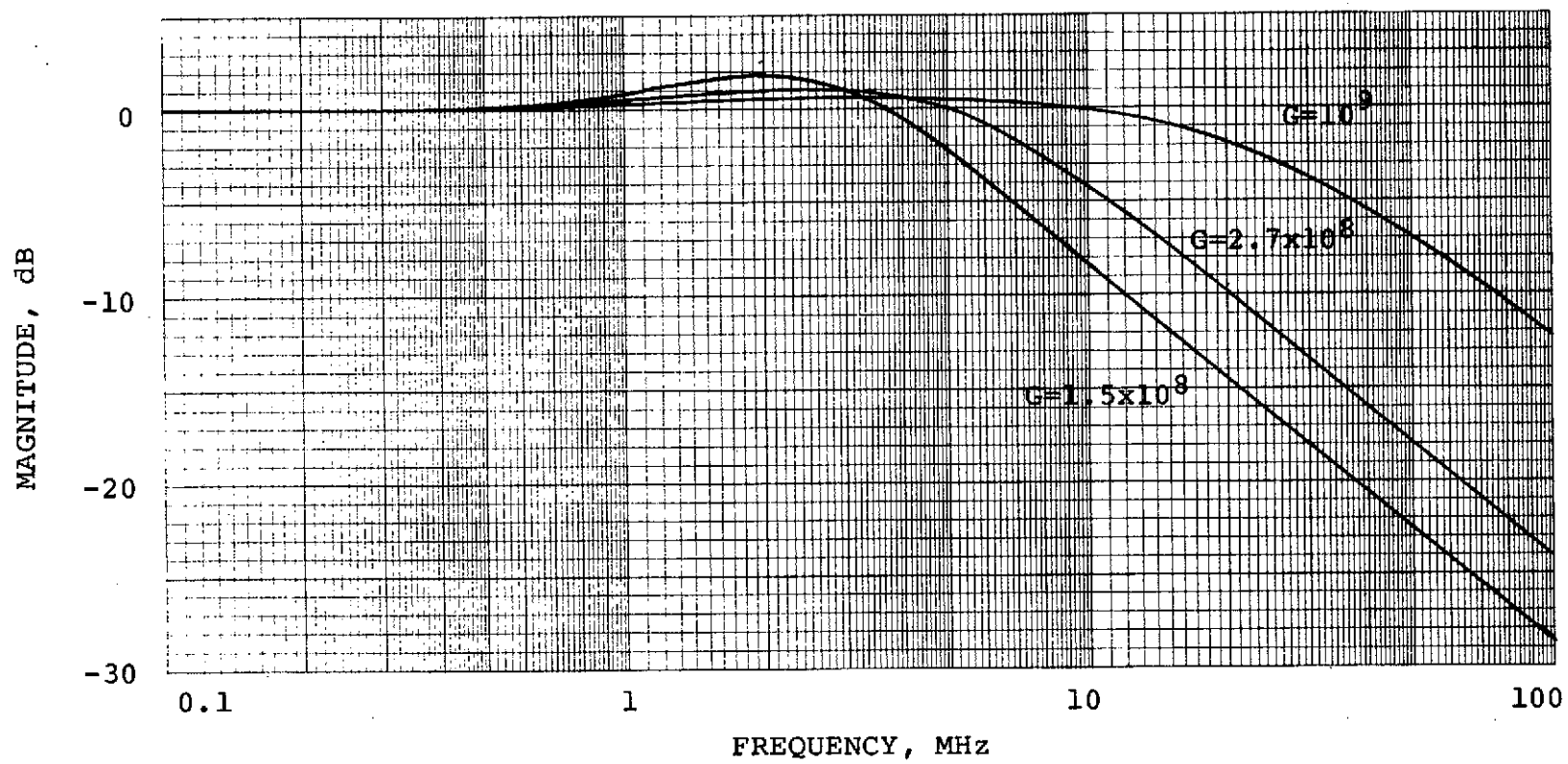


FIGURE 4.3-7. FREQUENCY RESPONSE OF THE LINEARIZED PLL

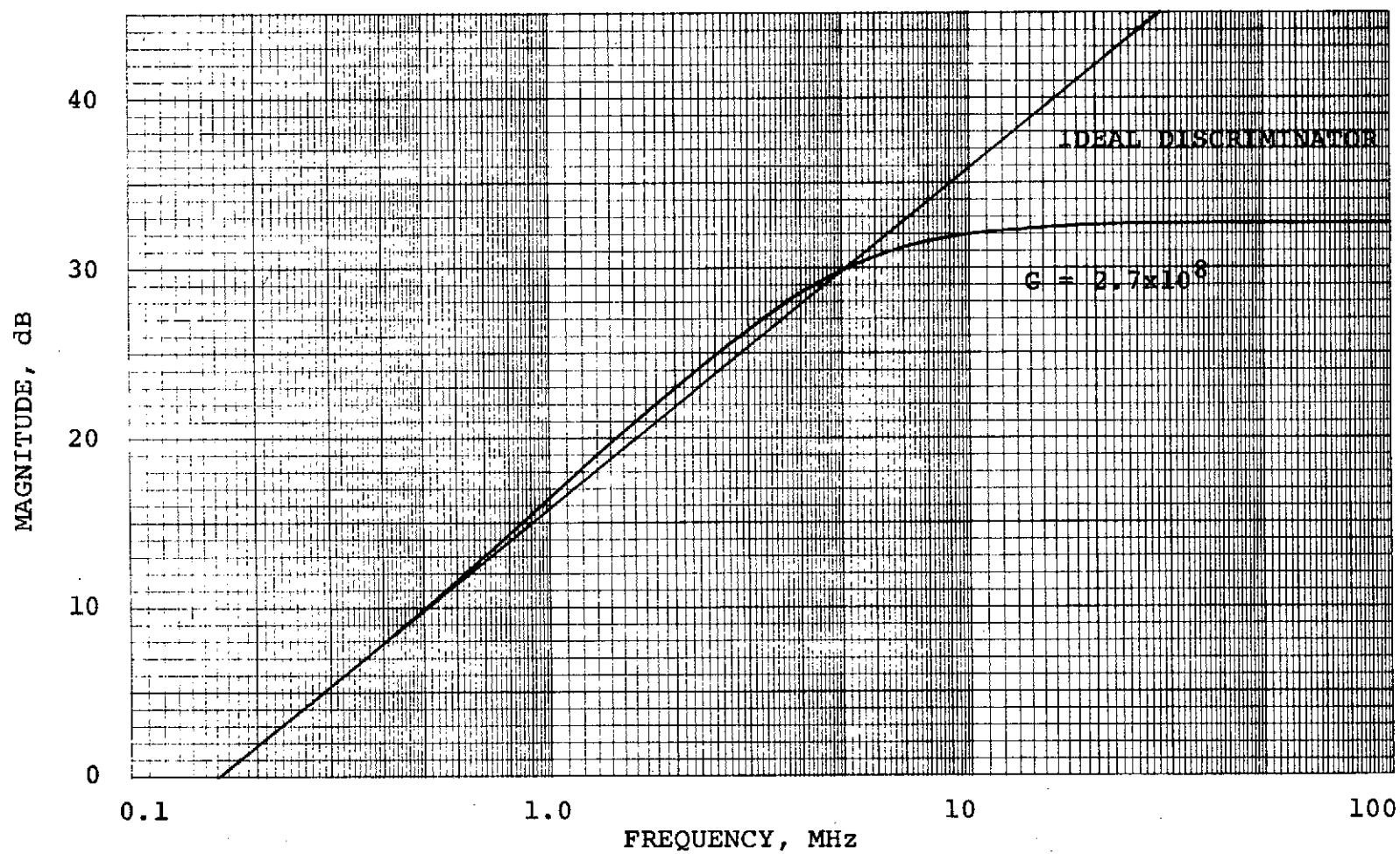


FIGURE 4.3-8. PLL FM DEMODULATOR CHARACTERISTIC

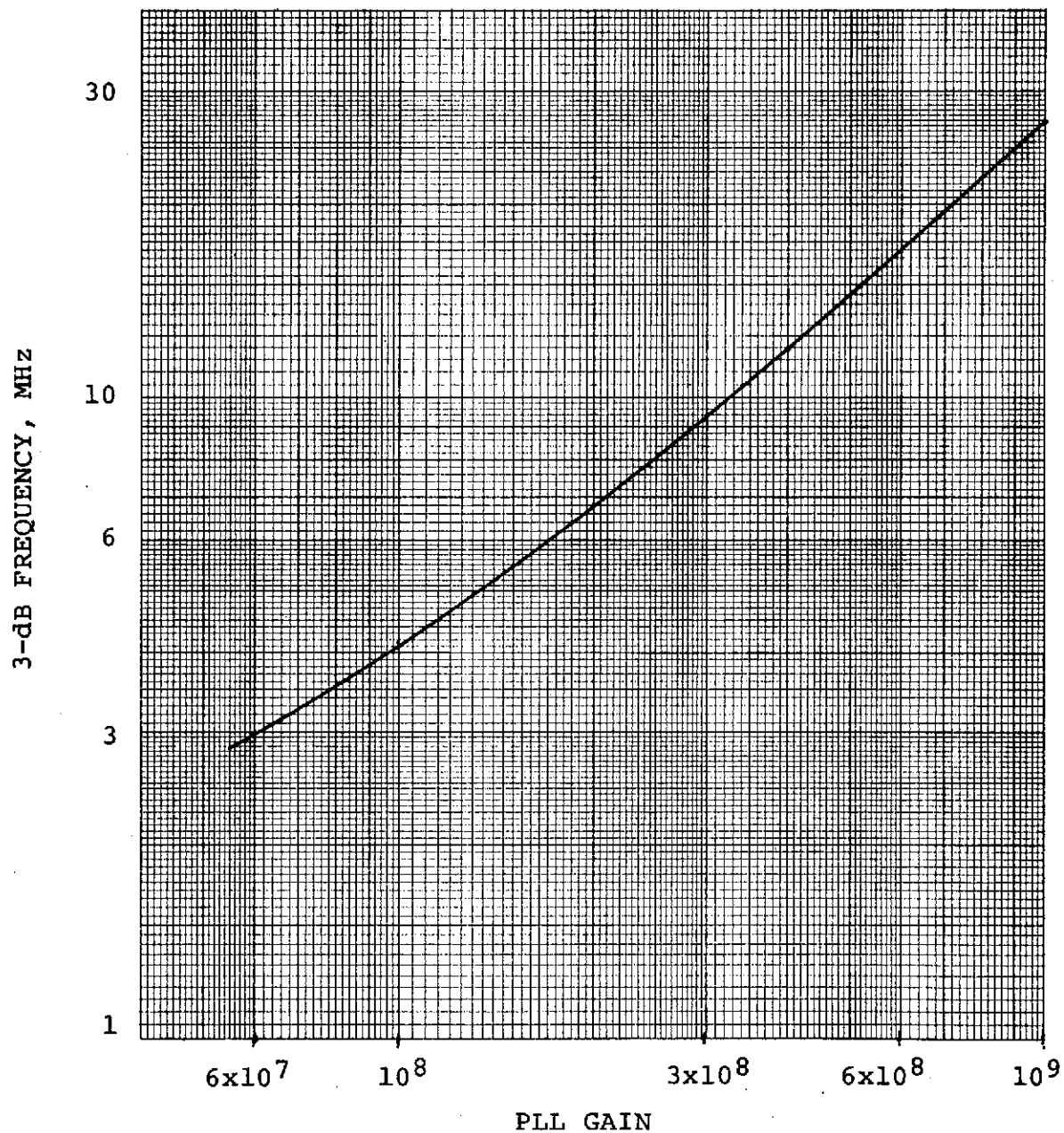


FIGURE 4.3-9. PHASE-LOCKED LOOP 3-dB POINT AS A FUNCTION OF LOOP GAIN

The analog portion of the subroutine measures test tone-to-noise ratio using a digital version of the device illustrated in Figure 4.3-10. The upper branch of this device in essence computes the power in the output of a narrowband filter centered at the specified frequency, whose bandwidth is of the order of the reciprocal of the total simulation run time T . If the input to this device is a pure tone $a \sin(\omega_1 t + \theta)$, then the "signal power" output can be shown to be

$$Y = \frac{a^2}{2} \left[1 + \left(\frac{\sin \omega_1 T}{\omega_1 T} \right)^2 - \frac{\sin(2\omega_1 T + 2\theta) - \sin 2\theta}{\omega_1 T} \right] \quad (4.3-5)$$

which is the actual signal power perturbed by error terms which diminish as T increases. When noise is present in the input, there is an additional contribution to Y . Thus, Y can be written

$$Y = \frac{a^2}{2} [1 + e_s(T)] + e_n(T)$$

where $e_s(T)$ consists of the error terms from Equation (4.3-5), and $e_n(T)$ accounts for the effects of noise (and depends on signal as well as noise). The magnitude of $e_n(T)$ is related to the noise bandwidth of the filter, which is, in turn, proportional to $1/T$.

The estimate of the noise power is obtained by subtracting Y from the total power Z . Thus, the estimate of signal-to-noise ratio is

$$\text{SNR}_{\text{est}} = \frac{Y}{Z - Y}$$

Letting $N = Z - \frac{a^2}{2}$ denote the true noise power, this becomes

$$\text{SNR}_{\text{est}} = \frac{a^2}{2N} \left[\frac{1 + e_s(T) + \frac{2}{a^2} e_n(T)}{1 - \frac{a^2}{2N} e_s(T) - \frac{1}{N} e_n(T)} \right]$$

Expanding in a two-variable Taylor series about $e_s(T)=0$ and $e_n(T)=0$, and letting $\rho = a^2/2N$ denote the true signal-to-noise ratio, this reduces to

$$\text{SNR}_{\text{est}} \approx \rho \left[1 + (1+\rho) e_s(T) + \frac{1}{N} \frac{\rho+1}{\rho} e_n(T) \right]$$

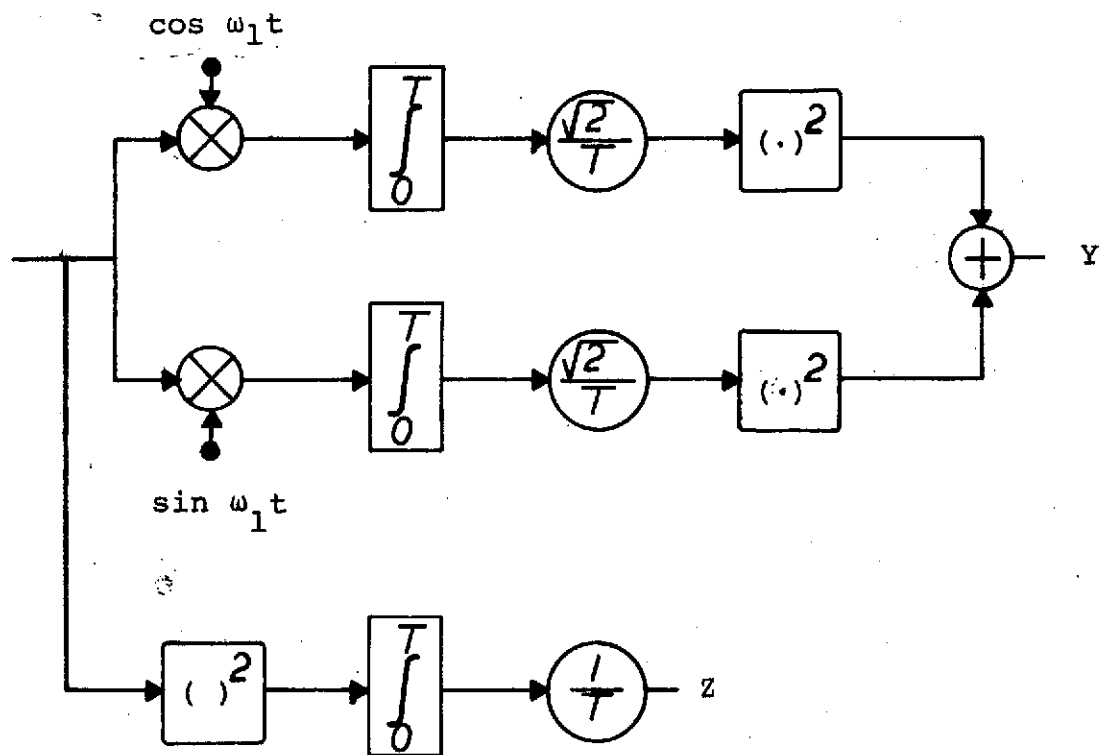


FIGURE 4.3-10. POWER MEASUREMENTS FOR DETERMINATION OF TEST-TONE-TO-NOISE RATIO

If T is an integer multiple of the period of the tone, then $e_s(T)$ vanishes; otherwise the error contribution from the term $(1+\rho)e_s(T)$ decreases slowly with T , and at high signal-to-noise ratios can seriously affect the accuracy of the measurement.

At high signal-to-noise ratio, $e_n(T)$ is dominated by signal X noise contributions, and is thus proportional to a and \sqrt{N} , and inversely proportional to T ; accordingly, the third term in the brackets is approximated as

$$\frac{1}{N} \frac{\rho+1}{\rho} e_n(T) \approx k \frac{a}{\sqrt{N}} \frac{1}{T} = \sqrt{2}k \sqrt{\rho}/T, \quad \rho \rightarrow \infty$$

where k is a proportionality constant. As the signal-to-noise ratio being measured is increased, therefore, to preserve the same accuracy, the simulation time must increase as the square root of the signal-to-noise ratio. At low signal-to-noise ratios, $e_n(T)$ is dominated by noise X noise, and is proportional to N and inversely proportional to T ; therefore

$$\frac{1}{N} \frac{\rho+1}{\rho} e_n(T) \approx k/\rho T \quad \rho \rightarrow 0$$

In this case, T must increase as $1/\rho$ as ρ is reduced.

The general conclusion is that T should be a large integer multiple of the tone period. An effective means of determining the required value of T for a given SNR is to increase T until no substantial change in the measured SNR is observed. The guidelines established above can then be applied to select run times for other SNR's.

4.4 Reference

- 4-1 Abramowitz, M., and I. A. Stegun, Handbook of Mathematical Functions (AMS-55), National Bureau of Standards, 1964, Section 26.8.

SECTION 5.0

QUANTITATIVE RESULTS FOR STUDY TASKS

5.0 QUANTITATIVE RESULTS FOR STUDY TASKS

This section addresses specifically the six tasks briefly introduced in Section 1.2, and presents the quantitative results applicable to these tasks. For the most part, the digital computer simulations discussed previously have been used to obtain these results. The efforts reported here furnish fairly complete and detailed examples of the use of the simulation programs. These results assume specific modulation parameters, filter bandwidths, and TWT characteristics, which were either obtained from existing TDRS and Shuttle documentation, or suggested as appropriate by the Technical Monitor. However, the flexibility and modularity of the programs facilitates carrying out similar runs for different parameters. The results of this section can be used as guidelines and examples for operating the simulation programs under different configurations.

Tasks 1 through 6 are discussed separately in Paragraphs 5.1 through 5.6.

5.1 Performance of the FDM/FM Link

The composite video-data signal is modeled as a pure tone of frequency 300 kHz multiplexed with a PSK signal of data rate 1.92 Mb/s and subcarrier frequency of 8.5 MHz. The test tone is a poor model of a video waveform for many purposes, but since the intention is only to measure output signal-to-noise ratio, this simple model is reasonable. (Accurate modeling of video signals was outside the scope of this study; however, with minor modifications of the programs, better signal models could be implemented, if desired.) The RF deviations chosen were $\Delta f_1 = 11$ MHz for the TV signal and $\Delta f_2 = 5.4$ MHz for the PSK signal. The constituent signals were filtered prior to multiplexing, as discussed in Paragraph 4.3, and the narrowband TDRS input bandwidth (88 MHz) was employed. The input signal amplitude was chosen as $0.44 E_{\text{sat}}$, resulting in a nominal output level 3 dB below the saturation output level. At the ground receiver, a phase-locked loop gain of 2.7×10^8 was used. From Figure 4.3-9, this places the 3 dB point of the loop frequency response at the subcarrier frequency, 8.5 MHz. It will be shown later that even at very high signal-to-noise ratios, the PLL does not operate in a fully linear mode with this loop gain, and that the gain must be increased significantly to achieve linearity. However, the increased noise bandwidth which results when higher gains are used actually leads to poorer performance.

The first step in operating the simulation is to determine the appropriate delay and phasing of the local subcarrier oscillator and bit synchronizer. While bit timing and

subcarrier phasing are known at the point of signal generation (FUNCTION SIGIN), the effects of filtering at various points of the system must be included. Unlike the actual receiver, the simulation program does not include routines for extracting synchronization from the PSK signal. This information must be determined in advance by the user. The most direct way to obtain this information is by inspection of a printout of the PSK signal at the demultiplexing filter output (or PLL output if no demultiplexing filter is used). Since the delay is independent of signal-to-noise ratio, a printout obtained under noiseless conditions can be used. The local correlator is programmed to correlate with a subcarrier in sine phase relative to the delayed starting time. Thus, the printout is inspected to find sine phases at bit transition times. In order to facilitate locating the data pattern, the starting point in the PN sequence is selected in such a way that the first several data bits are -1, +1, -1, +1, +1, +1,

The technique is illustrated in Figure 5.5-1, which shows a portion of the PSK demultiplexing filter output. Although it cannot be confidently verified from this relatively short segment, study of a long record shows that the first data bit begins at sample time 109. Thus a correlator delay of 108 samples should be used for this case, in which both premultiplexing and demultiplexing filters are present. When only one of these filters is used, the delay should be chosen as 60 samples, and when neither is used, the delay should be 12 samples. These values were found by inspection of the printouts and corroborated by considering the frequency responses of all filters in the system and verifying that the delays they introduce agree with the delays found by inspection.

For other filter characteristics and PLL parameters, the delays will be different, but the same technique can be applied. Establishment of synchronization by this method is somewhat tedious, but it avoids the need for complicated synchronization modules in the program, and the associated increase in run time.

With PSK detector timing established, the simulation can be run for as long as required to draw statistically sound conclusions. Generally, it is desirable to process a large integer number of cycles of the 300 kHz tone in order to make the SNR calculation as accurate as possible. The runs reported subsequently extend for 66,667 samples (following the 108-sample delay), which yields 100 cycles of the tone, and 639 bits of the PSK signal. Statistical significance with regard to error probability, for example, is thus limited to error rates of the order of 10^{-2} and higher, which is much greater than the

76
77
78
79
80
81
82
83
84
85
86
87
88
89
90
91
92
93
94
95
96
97
98
99
100
101
102
103
104
105
106
107
108
109
110
111
112
113
114
115
116
117
118
119
120
121
122
123
124
125
126
127
128
129
130
131
132
133
134
135
136
137
138
139
140
141
142
143
144
145
146
147
148
149
150
151
152
153
154
155
156
157
158
159
160
161
162
163
164
165
166
167
168
169
170
171
172
173
174
175
176
177
178

179
180
181
182
183
184
185
186
187
188
189
190
191
192
193
194
195
196
197
198
199
200
201
202
203
204
205
206
207
208
209
210
211
212
213
214
215
216
217
218
219
220
221
222
223
224
225
226
227
228
229
230
231
232
233
234
235
236
237
238
239
240
241
242
243
244
245
246
247
248
249
250
251
252
253
254
255
256
257
258
259
260
261
262
263
264
265
266
267
268
269
270
271
272
273
274
275
276
277
278
279
280
281
282
283
284
285
286
287

FIGURE 5.1-1.

ESTABLISHING PSK SYNCHRONIZATION BY
INSPECTION

range usually desired. However, as has been argued previously, making runs long enough to obtain credible measurements of error rates near 10^{-4} is not reasonable.

Figure 5.1-2 illustrates signal-to-noise ratio measured at the lowpass demultiplexing filter output for a variety of uplink and downlink signal-to-noise ratios. Uplink SNR is taken to be the ratio of input signal power to noise power in the 88 MHz TDRS input bandwidth. Downlink signal power is taken to be the power in a signal of nominal output amplitude level (i.e., TWT output amplitude when driven by the given input amplitude in the absence of uplink noise). Downlink SNR is the ratio of this power to the noise power in the receiver's IF bandwidth.

Equation (3.3-5) can be used to predict performance at high uplink and downlink signal-to-noise ratios. Upon substitution of the appropriate parameters, when the downlink SNR is much higher than the uplink SNR, Equation (3.3-5) indicates that the output SNR will exceed the uplink SNR by 22 dB. When the uplink SNR is much higher than the downlink SNR, the output SNR will exceed the downlink SNR by 19 dB. These asymptotes are also plotted in Figure 5.1-2. The simulation results are seen to be in reasonable agreement with these predictions.

Error probability in the PSK signal is illustrated by Figure 5.1-3. Comparison of these error probability and SNR results with those of a linear repeater is deferred to Paragraph 5.6.

Another quantity of interest in the FDM/FM system is the RMS phase tracking error of the PLL, which is an indicator of the linearity of the loop. The results, shown in Figure 5.1-4, indicate that substantial error exists even at high SNR. The reason for this is that the loop frequency response does not extend as far as the composite signal bandwidth. Increasing the PLL gain improves the linearity of the PLL by expanding the bandwidth, but actually degrades overall performance, except at high SNR. This effect is demonstrated in Table 5.1-1 in which error probability, output SNR, and loop tracking error are compared for PLL gains of 2.7×10^8 and 10^9 .

5.2 Performance of High Rate Digital Links

The NRZ-L PSK simulation program was run for various uplink and downlink signal-to-noise ratios for runs of 1000 bits to obtain the results shown in Figure 5.2-1. The data rate was selected as 100 Mb/s. Uplink SNR is defined, as before, as the

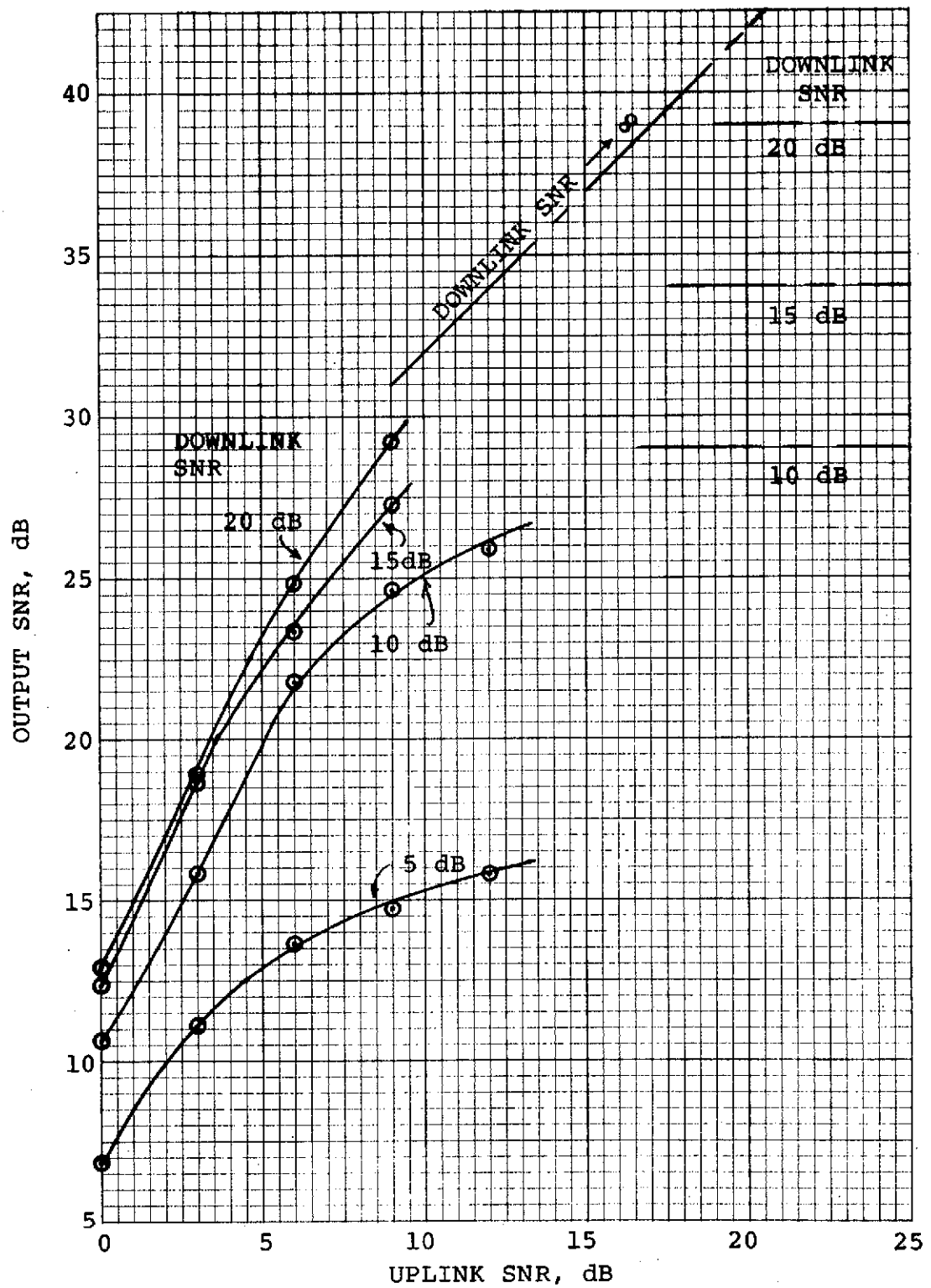


FIGURE 5.1-2. TEST TONE-TO-NOISE RATIO AT DEMULTIPLEXING FILTER OUTPUT

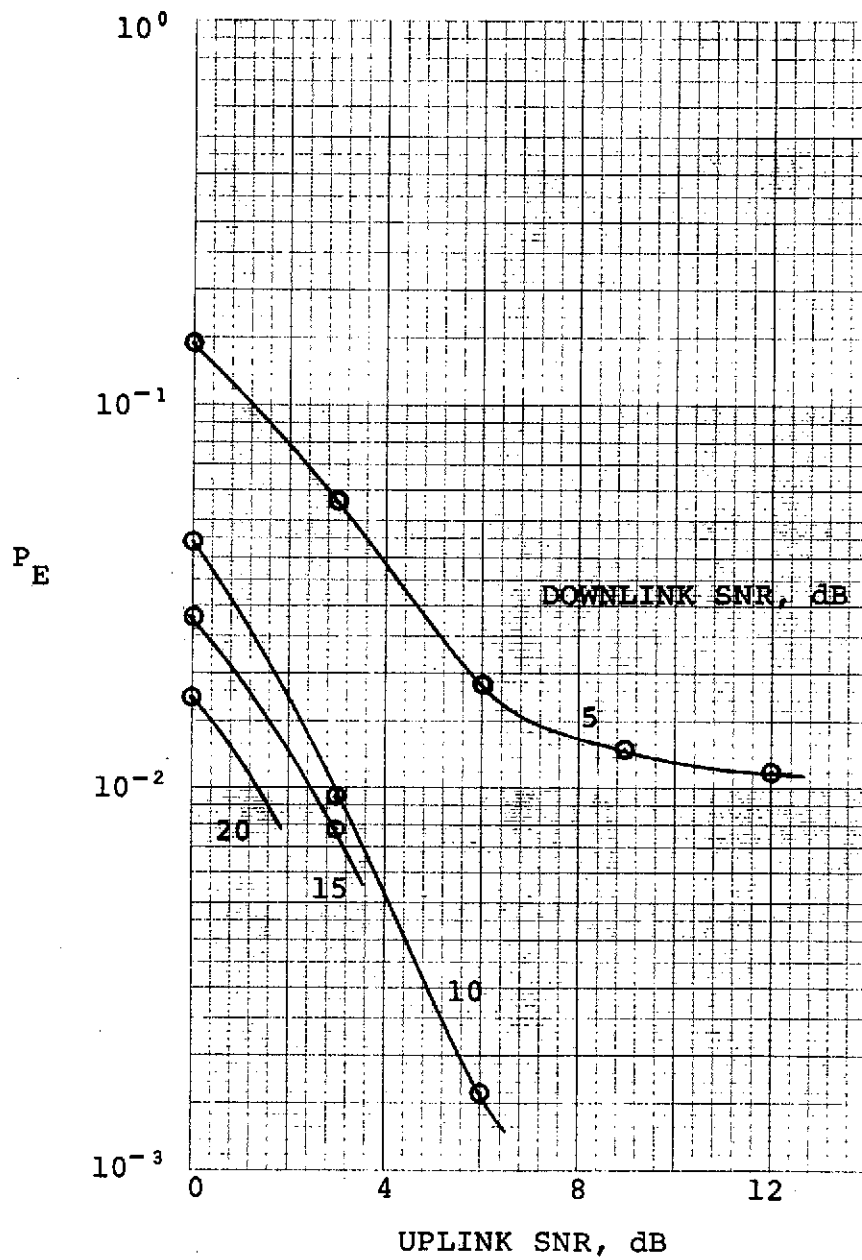


FIGURE 5.1-3. PSK ERROR PROBABILITY FOR THE FDM/FM SIGNAL

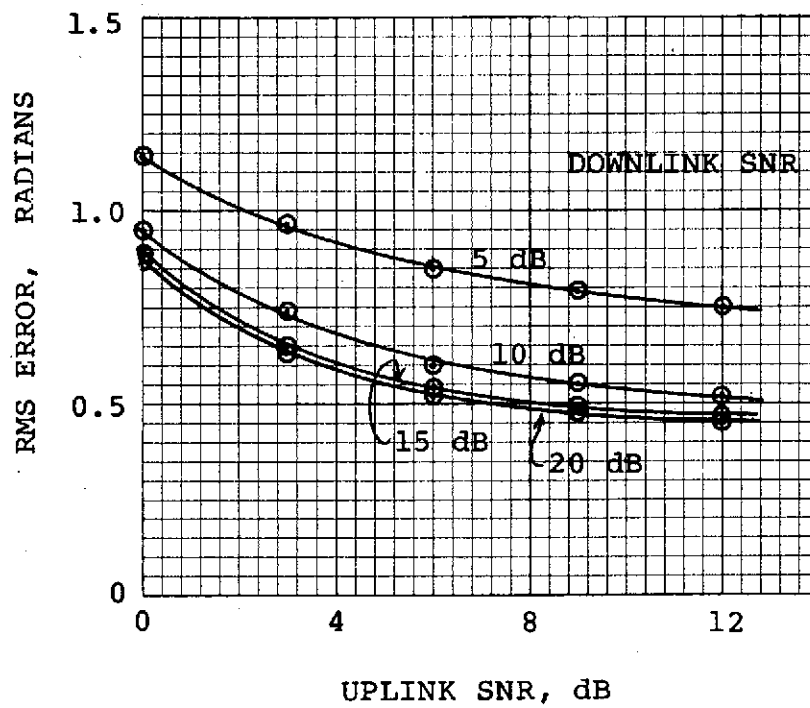


FIGURE 5.1-4. PLL RMS TRACKING ERROR

Table 5.1-1

System Performance as a Function of PLL Gain

Uplink SNR	Downlink SNR	Gain	
		2.7×10^8	10^9
3 dB	5 dB	$P_E = 0.077$ $SNR = 11.1 \text{ dB}$ $e_{RMS} = 0.97$	$P_E = 0.163$ $SNR = 5.6 \text{ dB}$ $e_{RMS} = 0.57$
9 dB	5 dB	$P_E = 0.019$ $SNR = 14.7 \text{ dB}$ $e_{RMS} = 0.79$	$P_E = 0.075$ $SNR = 9.5 \text{ dB}$ $e_{RMS} = 0.44$
9 dB	20 dB	$P_E = 0$ $SNR = 29.2 \text{ dB}$ $e_{RMS} = 0.48$	$P_E = 0$ $SNR = 29.3 \text{ dB}$ $e_{RMS} = 0.18$

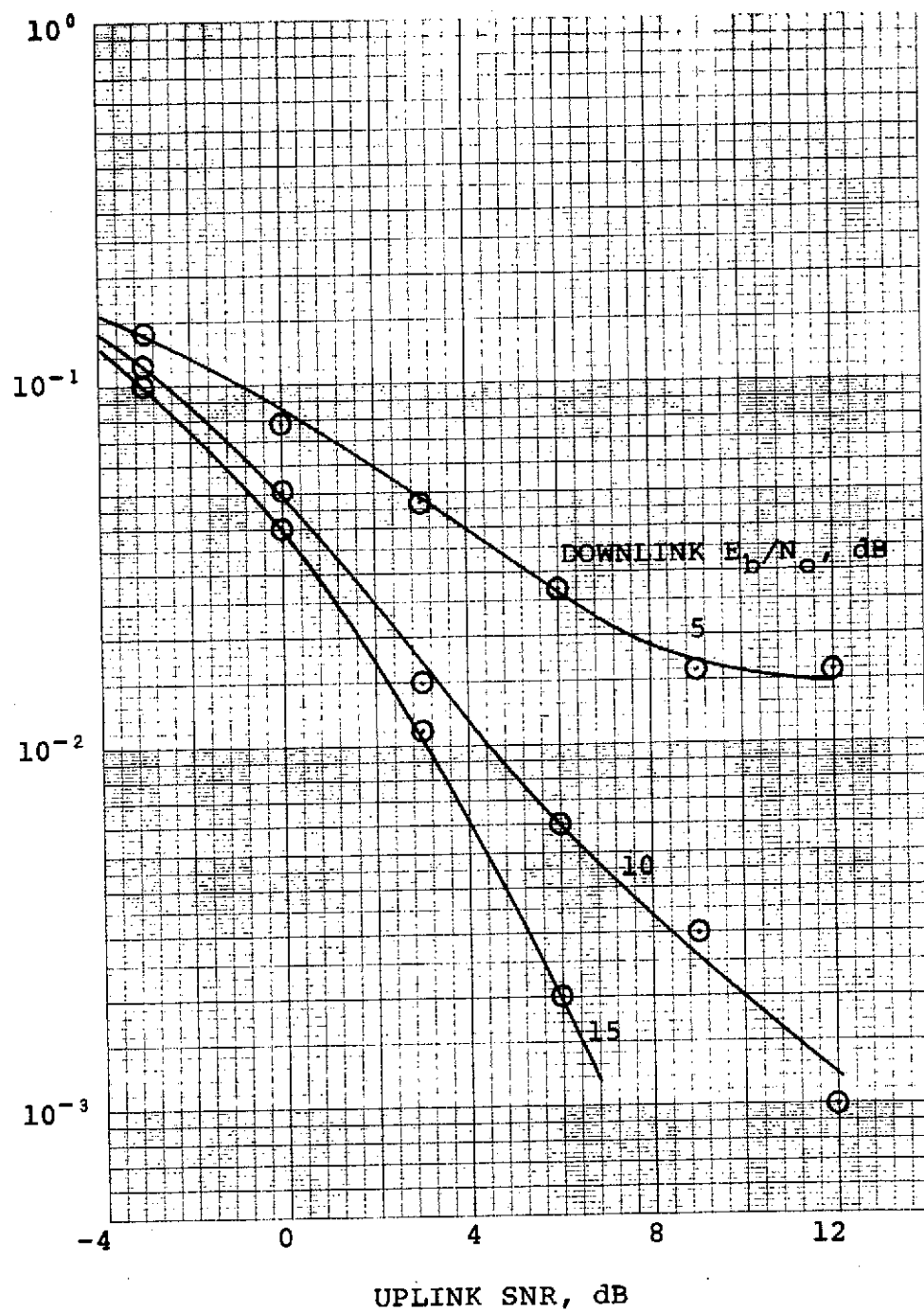


FIGURE 5.2-1. SIMULATED PERFORMANCE OF NRZ-L PSK SYSTEM

ratio of power in the input signal to noise power in the wide-band TDRS input bandwidth (225 MHz). In the downlink, E_b/N_o is the ratio of bit energy of a signal at the nominal TWT output amplitude to noise spectral density, or equivalently, the ratio of power in the nominal output signal to noise power in a bandwidth equal to the data rate (100 MHz). For these runs, a back-off of 0.44 was again used. The correlator phase is chosen as

$$\alpha = \tan^{-1}[\overline{f(E) \sin g(E)} / \overline{f(E) \cos g(E)}]$$

as discussed in Paragraph 3.2.1. This angle is a function of backoff and uplink SNR, and can be determined as discussed in Paragraph 3.1. For $\beta = 0.44$, the values of α for various uplink SNR's are listed in Table 5.2-1.

Table 5.2-1

Correlator Phase for Various SNR's

<u>Uplink SNR, dB</u>	<u>α</u>
-3	32.2°
0	28.7°
3	25.6°
6	23.4°
9	22.0°
12	21.2°

Figure 5.2-2 illustrates results for the split-phase PSK simulation runs. These are also 1000-bit runs, but with 30 Mb/s data rate and narrowband TDRS input (88 MHz). The backoff was again $\beta = 0.44$, and the correlator phases listed in Table 5.2-1 were used.

5.3 Performance of the Analog TV/FM Link

To study the TV/FM system, one simply sets the PSK deviation to zero in the FDM/FM simulation program. Lowpass demultiplexing filter output SNR is shown in Figure 5.3-1. For simplicity, only one downlink SNR is shown. The 300 kHz test-tone model for TV is again used, with deviation $\Delta f_1 = 11$ MHz.

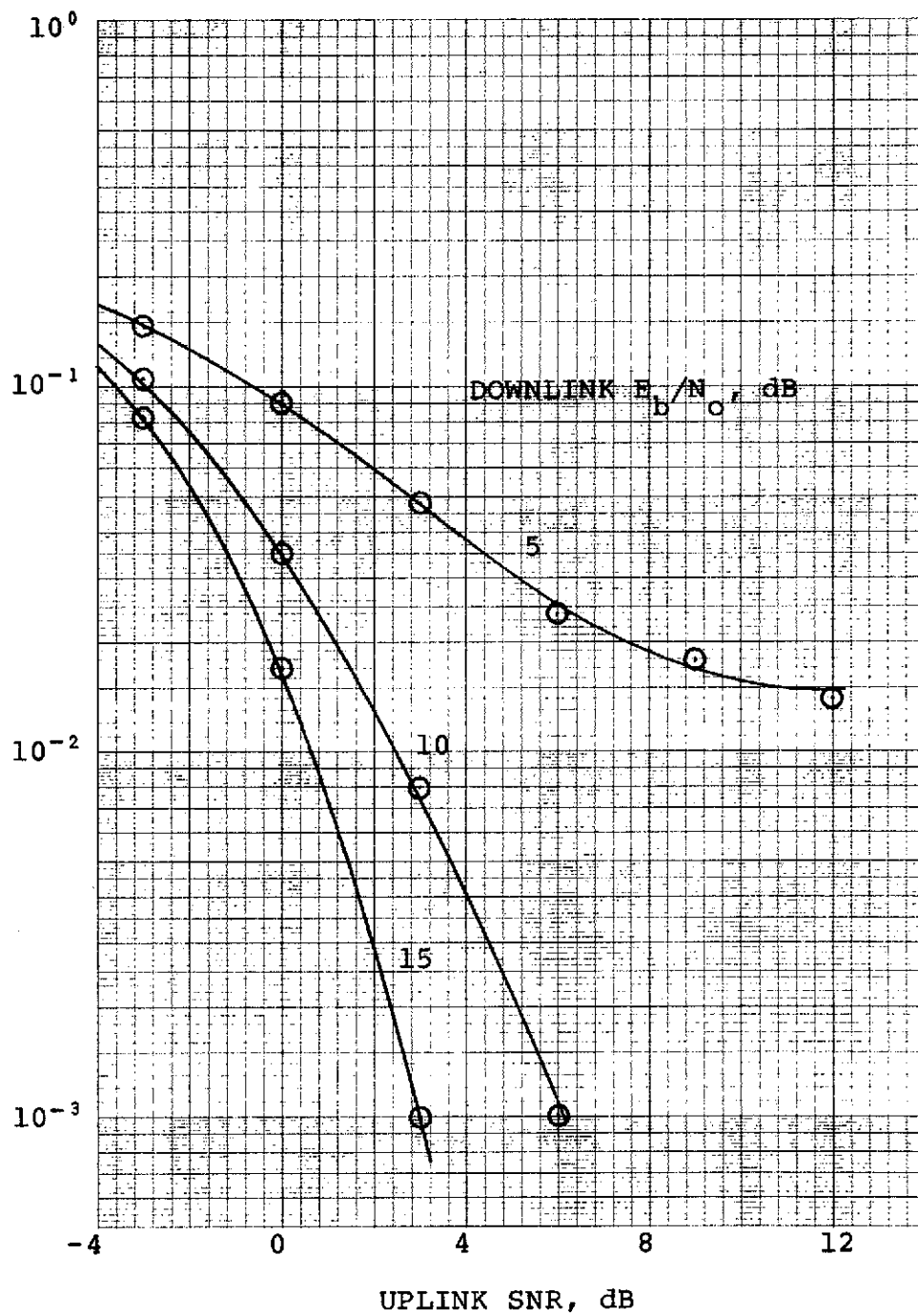


FIGURE 5.2-2. SIMULATED PERFORMANCE OF SPLIT-PHASE PSK SYSTEM

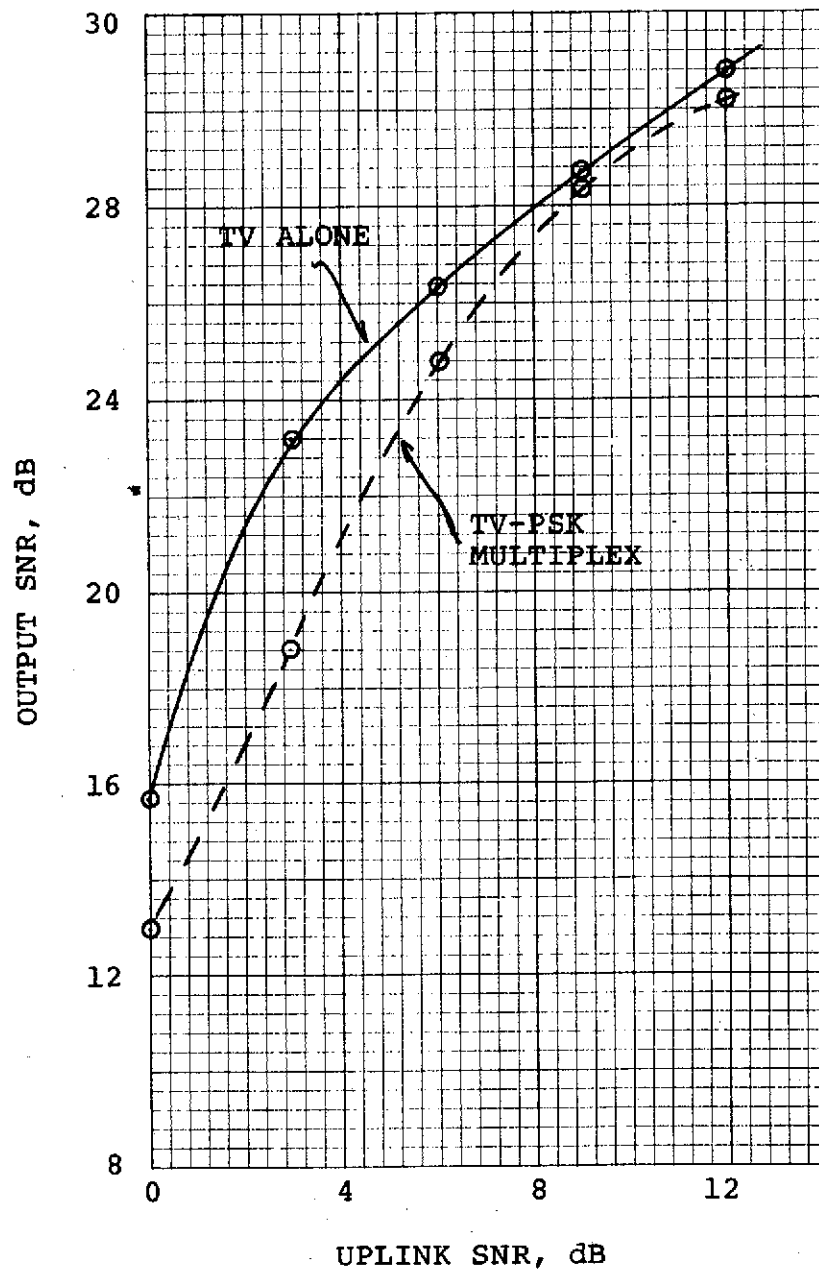


FIGURE 5.3-1. OUTPUT TEST TONE-TO-NOISE RATIO FOR ANALOG TV/FM SIGNAL, DOWNLINK SNR = 20 dB

As before, the backoff is $\beta = 0.44$, the narrowband TDRS input is used, and the PLL gain is 2.7×10^8 . The length of the run is 100 cycles of the tone.

For comparison, the corresponding curve from Figure 5.1-2 is included. As expected, at high SNR, performance is the same whether the PSK subcarrier is present or not, while at lower SNR, the presence of the subcarrier degrades the TV signal.

Figure 5.3-2 illustrates the PLL RMS error for this configuration, as well as the error when the PSK is included. The error is substantially smaller when the stressing by the 8.5 MHz subcarrier is removed.

5.4 Filtering and TWT Effects on Spread-Spectrum Signals

In contrast with the other study tasks, Task 4 is concerned with the forward link. In order to satisfy CCIR regulations on received power density at the earth's surface, the spectrum of the signal transmitted by TDRS must be spread over a wider band than that actually required for the baseband command data. Task 4 is concerned with the degradation due to the filtering and nonlinear amplification of this signal by TDRS. A model of the system under study is shown in Figure 5.4-1. The reasonable assumption is made that uplink noise is negligible.

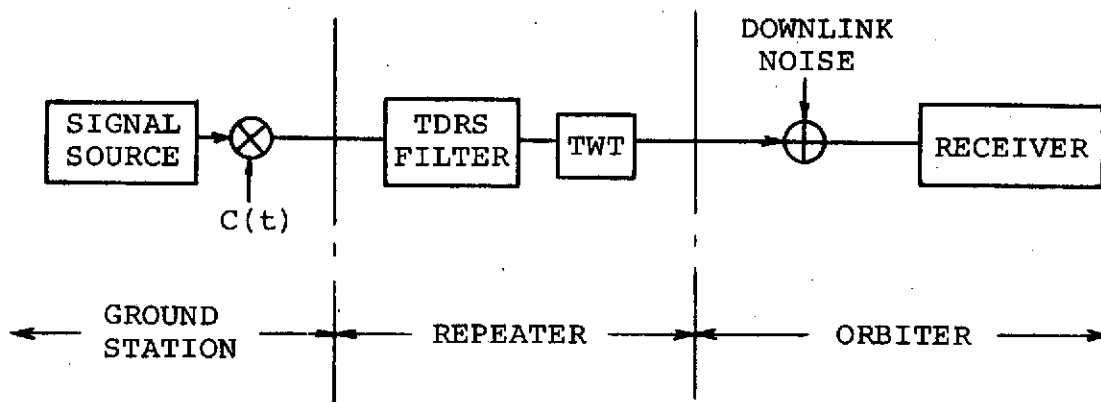


FIGURE 5.4-1. SIMPLIFIED MODEL OF THE FORWARD LINK

There are several system configurations to be considered, both at S- and K_u-band. In the S-band link, the data signal, which generally consists of time multiplexed command, synchronization, and digitized voice, has a data rate of either 32 kb/s or 72 kb/s. This baseband information signal is encoded

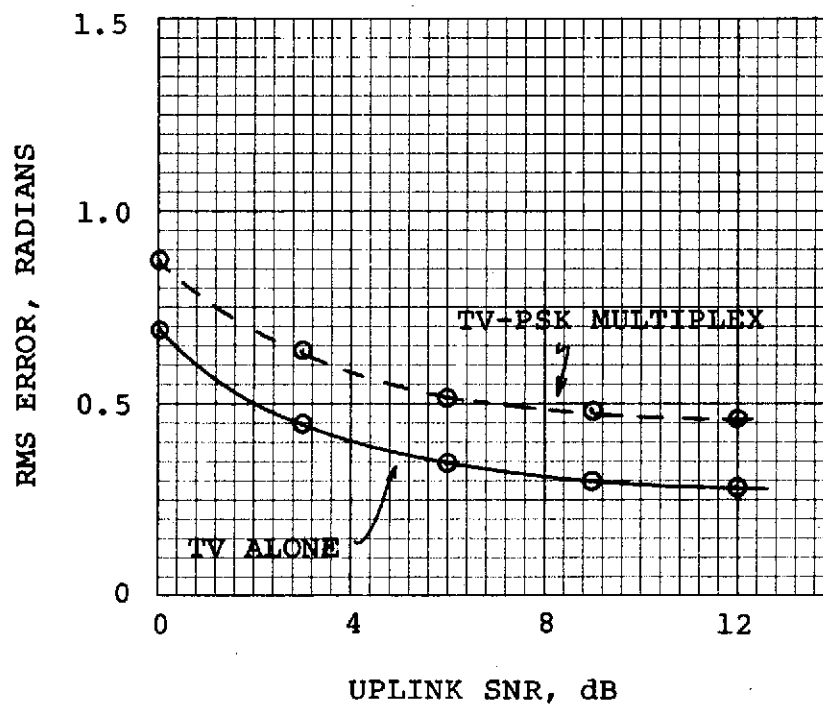


FIGURE 5.3-2. PLL RMS TRACKING ERROR,
DOWNLINK SNR = 20 dB

by a rate-1/3 convolutional encoder, yielding either 96 kb/s or 216 kb/s, and converted to split-phase. Spectrum spreading is achieved by mixing with a PN sequence of chip rate 10.368 Mc/s and period 2047. This results in a spreading ratio of 24 chips per half-bit of the high rate encoded sequence, or 54 chips per half-bit of the low rate encoded sequence. The S-band receive bandwidth of the repeater is 20 MHz. The K_u-band link data sequence has a rate of 972 kb/s, and is also encoded 3:1 to 2.916 Mb/s split-phase. This sequence is mixed with a PN sequence of rate 11.664 Mc/s for a spread ratio of 2 chips per half-bit. The K_u-band receive bandwidth is 50 MHz. These quantities are summarized in Table 5.4-1.

Table 5.4-1

Forward Link Spectrum-Spreading Parameters

<u>Link</u>	<u>Encoded Data Rate, kb/s</u>	<u>PN Code Chip Rate, Mc/s</u>	<u>Chips Per Half Bit</u>	<u>BW/Bit Rate</u>	<u>BW/Chip Rate</u>
S-band, low rate	96	10.368	54	208.33	1.93
S-band, high rate	216	10.368	24	92.59	1.93
K _u -band	2,916	11.664	2	17.15	4.29

Note that while the filter bandwidths are narrow with respect to the chip rate, they are wide with respect to the bit rate. Accordingly, while interchip interference will be substantial, interbit interference is negligible.

At the receiver, coherent mixing with a local oscillator is performed, including mixing with a synchronized replica of the PN sequence to despread the spectrum. The resulting waveform is split-phase integrated over a bit time. The integrator outputs are fed to a Viterbi decoder which decodes the rate-1/3 convolutional code and outputs the estimate of the data sequence. In order to avoid considering the encoder/decoder performance, the approach discussed in Paragraph 2.4.1 is again employed. That is, a system is hypothesized which makes hard decisions on each bit at the correlator output. While the performance of such a hard-decision device will be inferior to that of the soft-

decision receiver actually used, it is not anticipated that the degradation in performance due to filtering and nonlinear amplification will differ significantly for the two systems.

The assumption of hard bit decisions and the lack of appreciable interbit interference justifies looking at the system on a bit-by-bit basis. The general approach to the problem is best understood by reference to Figure 5.4-2. The component labelled "distorter" represents any function having the property

$$D(-s(t)) = -D(s(t))$$

so that the signals transmitted over the channel, although distorted, are still antipodal, and the receiver has the classical problem of deciding between $D(s_o(t))$ and $-D(s_o(t))$ received in the presence of white Gaussian noise. The optimum receiver consists of a filter matched to $D(s_o(t))$ with decisions made according to the sign of the response at the end of a bit interval; its error probability is given by

$$P_{E, \text{opt}} = Q\left(\sqrt{2\hat{E}/N_o}\right)$$

where \hat{E} is the energy in $D(s_o(t))$. Any reduction in signal energy as the signal passes through the distorter thus counts as degradation in the best achievable performance.

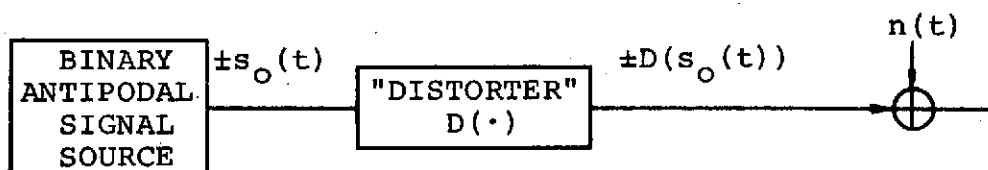


FIGURE 5.4-2. MODEL FOR DEGRADATION CALCULATIONS

The receiver actually used, however, is often not matched to $D(s_o(t))$, but rather to $s_o(t)$. This mismatch causes additional performance degradation over that attributable to energy reduction. That is, if

$$s_o(t) = \sqrt{E} u(t)$$

where $u(t)$ has unit energy, and $D(s_o(t))$ is written in the form

$$D(s_o(t)) = \sqrt{\hat{E}} \hat{u}(t)$$

where $\hat{u}(t)$ has unit energy, then a filter matched to $u(t)$ will have average output

$$\bar{v} = \rho \sqrt{\hat{E}}$$

where $\rho = \int_0^T u(t) \hat{u}(t) dt$, and the error probability will thus be

$$P_E = Q\left(\sqrt{2\hat{E}\rho^2/N_o}\right)$$

with a total degradation in decibels given by

$$d = -10 \log_{10} \left\{ \rho^2 \hat{E}/E \right\}$$

relative to the optimum receiver for the nondistorted signal. Of this amount, $-10 \log_{10} (\hat{E}/E)$ dB is attributable to energy loss and $-10 \log_{10} \rho^2$ dB is attributable to receiver mismatch.

To apply this abstract model to a specific situation of interest, suppose first that the distorter consists only of an ideal lowpass filter of bandwidth W , and that $s_o(t)$ is a baseband pseudorandom sequence of +1 and -1 chips of chip rate C . Assume that there are N such chips in $s_o(t)$. Since the N -chip sequence is random (although known to the receiver) the energy loss in filtering is a random variable. For a particular sequence with output energy \hat{E} , the error probability of the optimum receiver is given by

$$P_E = Q\left(\sqrt{2\hat{E}/N_o}\right);$$

therefore, the average error probability is given by

$$\bar{P}_E = Q\left(\sqrt{2\hat{E}/N_o}\right)$$

(This is an average over an ensemble of signals and receivers, and therefore of little practical significance, except as a bound on the performance of any given receiver.) It is reasonable to define degradation as the energy loss which would make error probability equal to this average. This quantity is difficult to evaluate exactly, but is easy to bound, arguing as follows. Since $Q(\cdot)$ is a convex function

$$Q\left(\left[2\hat{E}/N_0\right]^{1/2}\right) \geq Q\left(\left[2\bar{E}/N_0\right]^{1/2}\right)$$

Hence, the degradation d , as defined above, is bounded by

$$d \geq -10 \log_{10} (\bar{E}/E)$$

But the average output energy \bar{E} is simply the bit duration N/C times the average power in the output of an ideal filter of bandwidth W driven by a random binary sequence of rate C and average power EC/N . Such a signal has power spectral density given by

$$S(f) = \frac{E}{N} \left(\frac{\sin \pi f/C}{\pi f/C} \right)^2$$

so that

$$d \geq -10 \log_{10} \left\{ \frac{2}{C} \int_0^W \left(\frac{\sin \pi f/C}{\pi f/C} \right)^2 df \right\}$$

This simple bound on the degradation due to filtering a baseband signal is plotted in Figure 5.4-3.

In applying the technique to the model of Figure 5.4-1, the distorter consists of the cascade of TDRS input filter and TWT. Note that since signaling is coherent, the baseband model can be used, with the filter represented as a lowpass filter and the TWT as an operation on the complex envelope. Because the TWT introduces a phase shift, the correlator phase at the receiver must be adjusted to be in approximate coherence with the TWT output signal. The input filter was arbitrarily modelled as a 51-tap nonrecursive lowpass digital filter with linear phase and variable bandwidth. The TWT characteristics of Figure 2.2-1 were used. To generate a PN sequence of length 2047, the maximal-length shift register shown in Figure 5.4-4 was used, and various

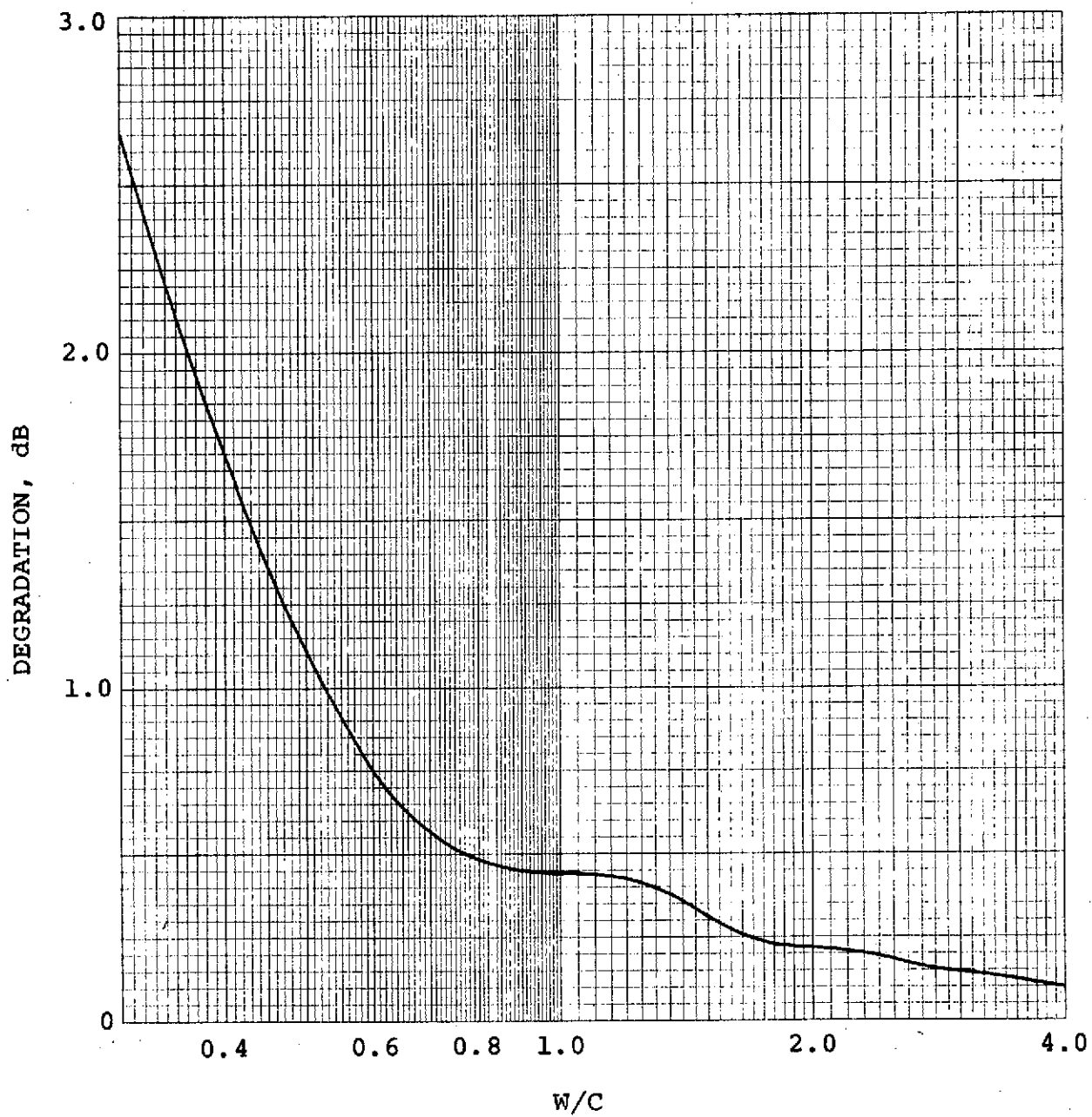


FIGURE 5.4-3. LOWER BOUND TO DEGRADATION FOR IDEAL FILTERING OF A BASEBAND PSEUDORANDOM SIGNAL

48-chip segments of the sequence were considered as the signal sequence (with the second 24 chips appearing as complements because of the split-phasing). Use of 24 chips per half-bit corresponds to the high-rate S-band link configuration. The TDRS input signal level was taken to be E_{sat} ; that is, the TWT is operated at saturation except for the effects of the filter on TWT input amplitude. Since the AM-to-PM conversion at saturation is 42° , the correlator phase is adjusted to this value. This is not the best choice of correlator phase when the signal is heavily filtered, and should be replaced by some "average" phase shift, but it is not clear exactly what this average should be.

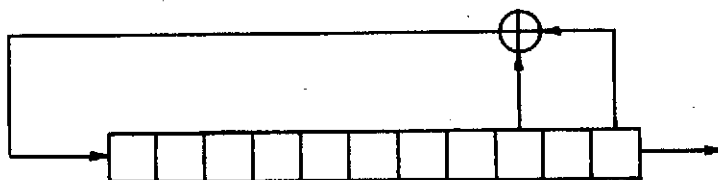


FIGURE 5.4-4. GENERATOR FOR PN SEQUENCE OF LENGTH 2047.

It is desired to bound the degradation as before by finding the average energy reduction and receiver mismatch upon passing split-phase PN sequence segments through the filter-TWT cascade. It can be argued that the TWT actually amplifies the signal and thus enhances rather than reduces signal energy, in spite of the filtering and nonlinearity. This difficulty can be partially circumvented by using the normalized characteristics (unity output amplitude at saturation), but the normalized curves still yield somewhat greater output power than input power if the TWT is operated at or below saturation. The degradation results obtained using this model can be interpreted as degradation vis-a-vis an unfiltered linear repeater with unity output amplitude at unity input amplitude; the degradation relative to an unfiltered linear repeater with the same average power gain as the TWT may be greater.

Exact determination of the average energy reduction and mismatch would require averaging the results for each of the 2047 possible starting chips in the PN sequence, which would involve considerable computation. Instead, a Monte Carlo technique was used, in which 50 starting points were selected randomly and the average energy reduction and mismatch for these 50 signals was computed for various ratios of filter bandwidth

to chip rate. The results are plotted versus the ratio of the filter's one-sided equivalent white-noise bandwidth W_{EQ} to the chip rate, as the curve labelled "partial average" in Figure 5.4-5. Provided that this partial average accurately reflects the actual average energy reduction and mismatch, this curve is a lower bound to degradation due to the filter-TWT cascade.

It is clear that the degradation can be upper bounded by finding the maximum energy reduction and mismatch over all possible signal sequences. This maximum was also obtained for the same 50 random starting points and the results are shown as the curve labelled "partial maximum" in Figure 5.4-5. Since this is a maximum over a relatively small number of signals, however, it is not a true upper bound on degradation.

As a check on these Monte Carlo results, the entire set of 2047 possible starting points was exhaustively searched for a bandwidth-to-chip rate ratio of 1.096. The average and maximum are shown as the points labelled "true average" and "true maximum" on Figure 5.4-5. It can be inferred from this that the average computed by the Monte Carlo technique is quite accurate, and that the partial average curve is, therefore, a reliable lower bound to degradation. It is also reasonable to believe that the partial maximum curve is within a few tenths of a decibel of the true upper bound.

For the high-rate S-band link, Table 5.4-1 indicates a bandwidth to chip rate ratio of 1.93. Thus, the equivalent lowpass ratio is $W_{EQ}/C = 0.965$. Referring to Figure 5.4-5, the degradation using this particular filter and TWT is expected to be approximately 0.9 dB. There is no reason to suspect that the difference in number of chips per bit would have any considerable effect, and thus the low-rate S-band link would suffer similar degradation (limited Monte Carlo runs with 54 chips per half bit support this claim.) In the K_u -band link, the bandwidth to chip rate ratio is large enough that degradation is negligible.

Finally it should be remarked that the degradation due to the filter - TWT cascade is actually slightly less than that due to the filter alone. That is, insertion of the TWT improves the situation with regard to the quantity being measured. There are two reasons why the TWT has this effect. First, as noted above, the energy at the TWT output is slightly greater than at its input. Secondly, the amplitude characteristic of the TWT is such that it attempts to restore some of the squareness of the pulses which was smoothed out by filtering. Thus, the TWT partially ameliorates the effect of the filter on the signal.

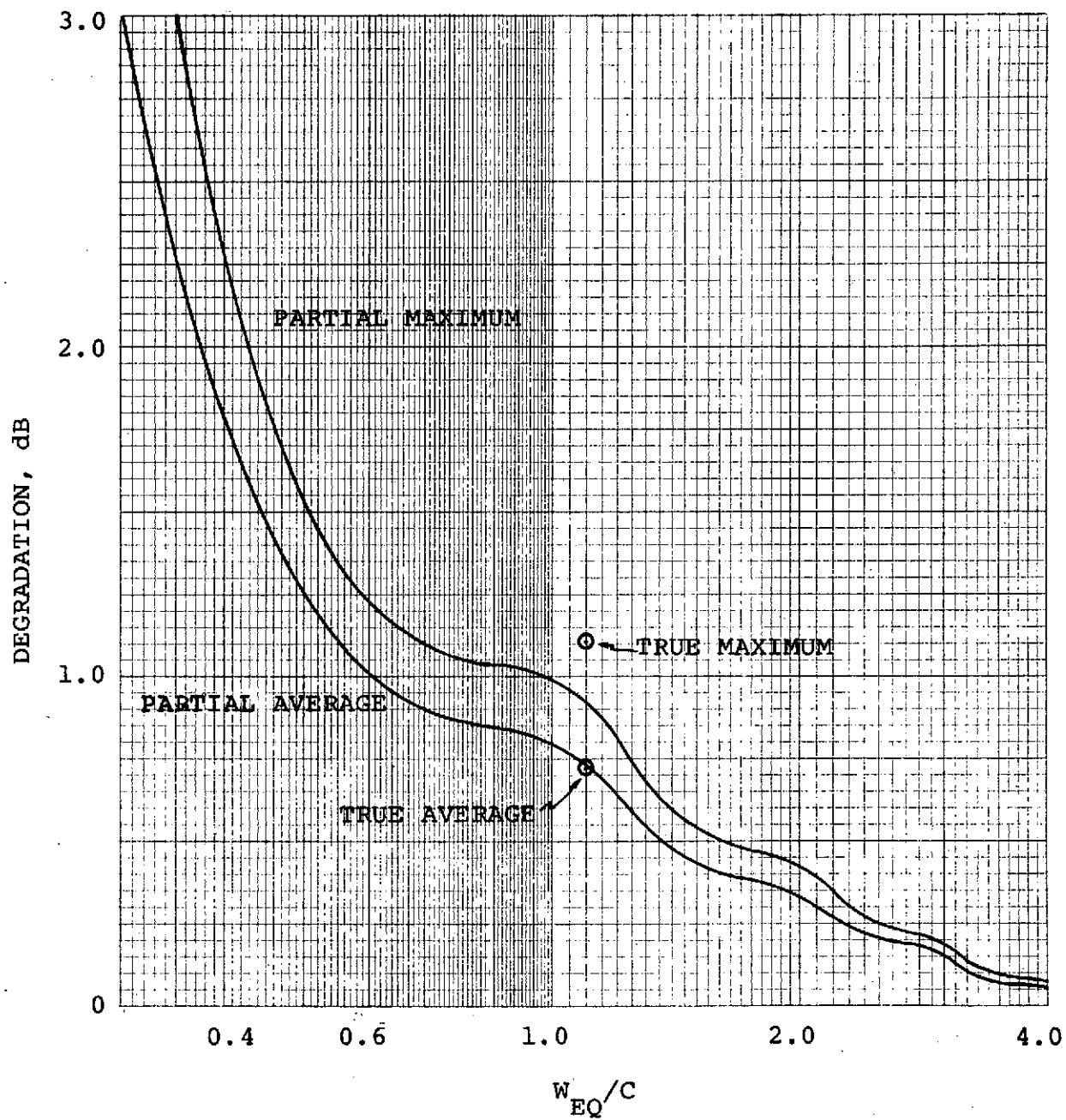


FIGURE 5.4-5. BOUNDS ON DEGRADATION FOR A FILTER-TWT CASCADE

The phenomenon of communication blackout during re-entry is familiar to even the most casual follower of the manned space program. The cause of this phenomenon lies in the interaction of the electromagnetic field of the transmitting antenna with the plasma sheath which surrounds the vehicle. The blackout problem has received attention from NASA for a number of years, and several techniques have been proposed to reduce the attenuation, including the use of high carrier frequencies. One example is the design and fabrication by Radiation Incorporated (now HARRIS Electronic Systems Division) of a tracking and telemetry receiving system operating at 35 GHz. This system was delivered in 1965 to NASA Marshall Space Flight Center under Contract No. NAS 8-11857.

This section contains a brief tutorial discussion of the plasma blackout problem and shows why the use of Ku-band and higher carrier frequencies can reduce the blackout. For reasons which will become apparent, accurate determination of the extent to which blackout can be reduced will require experimental investigation.

When a vehicle enters the earth's atmosphere at high speed, typically several km/s, intense heat is built up near the surface because of friction. The heat is sufficient to ionize molecules of the atmosphere. The "gas" of ionized particles surrounding the vehicle constitutes a plasma. Ions in a plasma oscillate with a resonant frequency which is proportional to the square root of the ion density and inversely proportional to the square root of the ion mass. Since electrons are much lighter than positive ions, the resonant frequency for electrons is much higher than that for positive ions and is typically the dominant consideration. An external electromagnetic wave oscillating at a frequency near the plasma frequency combines with the plasma in such a way that the energy is almost completely reflected and does not penetrate the plasma. For frequencies less than the plasma frequency, a severely attenuated signal passes through the plasma. However, if the field frequency is greater than the plasma frequency, the plasma has very little effect. The rapidity with which the attenuation decreases as the field frequency increases past the plasma frequency depends, to some extent, on the frequency of particle collisions in the plasma but is typically quite rapid. Therefore, a general rule is that carrier frequencies in excess of the plasma frequency will be relatively immune to blackout.

As noted above, the plasma frequency is related to the ion density in the plasma. At the beginning of reentry, where the atmosphere is rare, there are relatively few molecules and,

hence, ion density is small. As the atmosphere becomes denser, the ion density increases and the plasma frequency increases. The vehicle slows as it penetrates deeper into the atmosphere, however, and this reduced velocity induces less heat. Eventually, although molecule density is high, a relatively small fraction is ionized and the plasma frequency decreases. Thus, over the reentry time, the plasma frequency builds up to a maximum and then diminishes. The interval over which the plasma frequency exceeds the carrier frequency is the blackout interval. If the carrier frequency is greater than the maximum plasma frequency, there is essentially no blackout.

The maximum plasma frequency depends on such particulars as the shape and angle of attack of the vehicle. Moreover, the maximum plasma frequency will be different at different parts of the vehicle. Analysis is hopeless for all but trivial shapes. A considerable body of literature exists describing experimental measurements of maximum plasma frequency. For example, the Apollo reentry vehicle, whose reentry velocity is approximately 11 km/s, has been found to have a maximum plasma frequency of 250 GHz at the worst point on the capsule surface. However, at the antenna location on the capsule, the maximum plasma frequency is 15 GHz. Because of the aerodynamic design of the Shuttle Orbiter, the maximum plasma frequency is likely to be smaller for similar reentry velocity.

In summary, plasma blackout during Orbiter reentry depends on reentry velocity, attitude, and placement of the antenna on board the vehicle as well as the carrier frequency. While these dependencies prevent certain prediction of the blackout phenomenon, past experience suggests that the use of a K_u -band carrier (at 15 GHz) may well eliminate blackout or hold the duration to a short time.

A lucid discussion of the blackout problem and a summary of experimental plasma measurements and techniques to reduce its effects is given by Rybak and Churchill [5-1].

5.6 Degradation Due to Repeater Nonlinearity

Task 6 has as its chief objective the comparison of a communication link using a TWT repeater with a link using a purely linear repeater. It should be noted parenthetically that a nonlinear repeater is not necessarily worse than a linear repeater; Jain and Blachman [5-2], for example, cite cases in which an ideal hard limiter outperforms a linear repeater. However, the results to be presented in this section all show some degradation in comparison with linear repeaters.

There is some ambiguity in the concept of equivalence between linear and nonlinear repeaters. For the purposes of this section, a linear repeater will be said to be equivalent to a given TWT at a specified backoff β , if the voltage gain of the linear repeater equals that of the nonlinear repeater at that backoff. This is illustrated in Figure 5.6-1. There are other, equally valid, definitions of equivalence. For example, the repeaters could be considered equivalent if the total output powers were equal when driven at the same level with the same input signal-to-noise ratio. A disadvantage of the latter definition is that the gain of the equivalent linear repeater depends upon the input SNR as well as the nominal drive level (backoff), whereas in the former definition, it depends only on the nominal drive level. The point is that different definitions of equivalence will lead to different measurements of degradation. The results reported here will assume the definition implied by Figure 5.6-1.

Figure 5.6-2(a) illustrates a model of a linear relay link. Assuming that $H(f)$ is an ideal filter of bandwidth $2W$ centered at the carrier frequency, this system is equivalent to the one-link model of Figure 5.6-2(b); the equivalent noise process $n_{eq}(t)$ has a one-sided power spectrum in the vicinity of f_c , as illustrated by Figure 5.6-2(c). If the filter is wide enough that the signal $s(t)$ passes undistorted, then the SNR in the receiver's IF bandwidth B_{IF} is

$$SNR = \frac{K^2 \overline{s^2(t)}}{(Z_o + K^2 N_o) B_{IF}}$$

If uplink noise dominates, ($K^2 N_o \gg Z_o$), the repeater has no real effect, while if downlink noise dominates ($Z_o \gg K^2 N_o$), the SNR is improved by a factor equal to the power gain K^2 .

Of the signals of interest in this study, only the FDM/FM signal's bandwidth is such that it passes the TDRS input filter essentially undistorted. The TWT degradation is best seen by referring to the "virtual channel" concept introduced in Paragraph 3.3 in which the noise spectral density n_o and carrier amplitude c satisfy

$$\frac{n_o}{c^2} = \frac{N_o}{A^2} + b^2 N_o + \frac{Z_o}{(F(A))^2} \quad (5.6-1)$$

Similarly, the model of Figure 5.6-2(b) can be thought of as a virtual channel for which the noise spectral density (over the

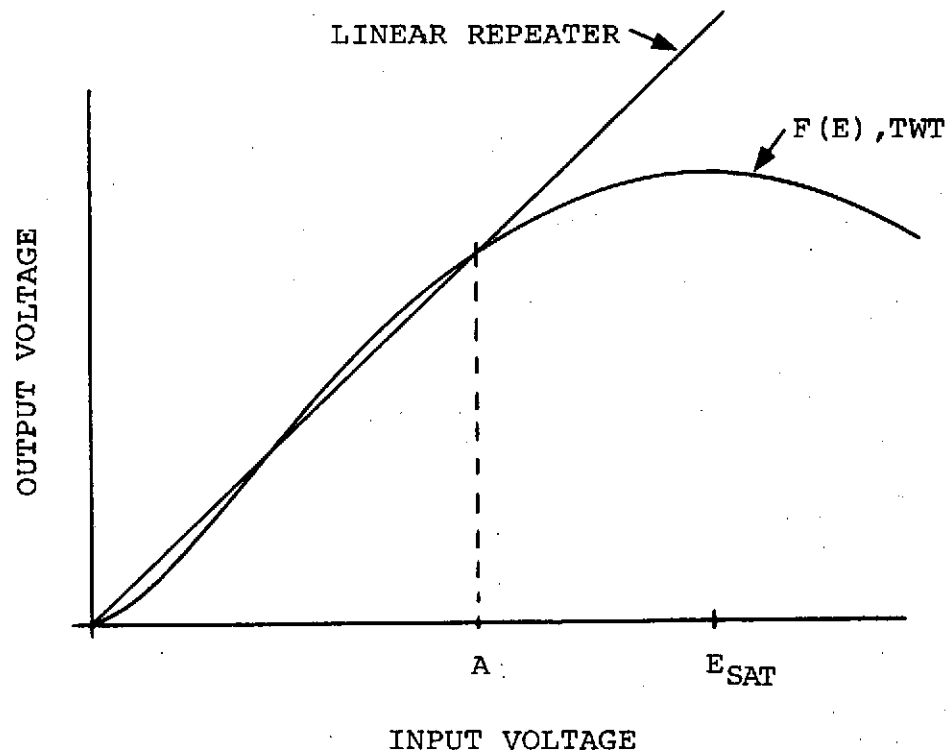
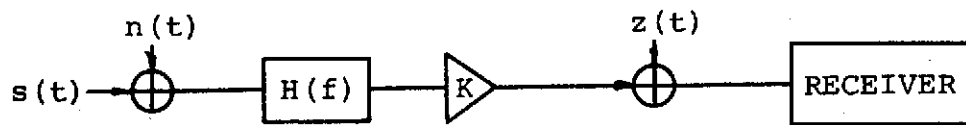
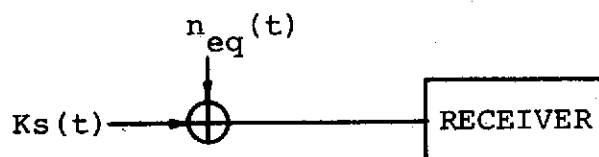


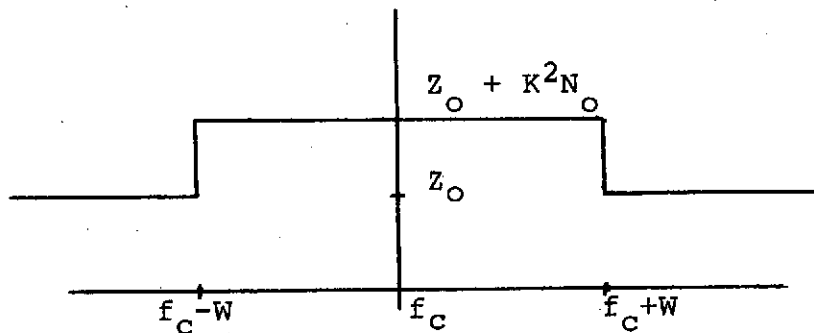
FIGURE 5.6-1. A TYPICAL TWT CHARACTERISTIC AND ITS LINEAR EQUIVALENT AT OPERATING POINT A.



(a)



(b)



(c)

FIGURE 5.6-2. MODEL OF A LINEAR REPEATER LINK. (a) LINEAR REPEATER LINK. (b) EQUIVALENT MODEL. (c) ONE-SIDED POWER SPECTRAL DENSITY OF $n_{eq}(t)$.

bandwidth of interest) is $n_o' = K^2 N_o + Z_o$, and the carrier amplitude is $c' = AK$; therefore

$$\frac{n_o'}{(c')^2} = \frac{K^2 N_o + Z_o}{A^2 K^2}$$

Moreover, the definition of equivalence implies that $F(A) = KA$; thus

$$\frac{n_o'}{(c')^2} = \frac{N_o}{A^2} + \frac{Z_o}{(F(A))^2} \quad (5.6-2)$$

comparison of Equation (5.6-1) and Equation (5.6-2) shows that the degradation induced by the TWT appears as an additional additive term in the noise power spectrum, whose magnitude is related to the slope of the AM-to-PM conversion characteristic at the operating point.

When the downlink noise dominates, this contribution is negligible, but when uplink noise dominates, the degradation due to the nonlinearity is

$$\frac{n_o/c^2}{n_o'/(c')^2} = \frac{b^2 + 1/A^2}{1/A^2} = 1 + A^2 b^2$$

At the operating point $\beta = 0.44$ which has been assumed heretofore, reference to Figure 2.2-1(b) reveals that the slope of $G(E)$ is approximately $60^\circ/E_{\text{sat}}$ degrees per volt, or about $1/E_{\text{sat}}$ radians per volt. Degradation is thus

$$\frac{n_o/c^2}{n_o'/(c')^2} = 1 + \frac{(0.44)^2 E_{\text{sat}}^2}{E_{\text{sat}}^2} \approx 1.194$$

or about 0.8 dB. This estimate applies only at high signal-to-noise ratio, where the "virtual channel" concept is valid.

To determine degradation at lower signal-to-noise ratios, the simulation program can be used. A linear repeater is implemented by selecting the normalized amplitude nonlinearity $f(u) = Ku$, and the normalized AM-to-PM conversion $g(u) = 0$.

The results for a high downlink SNR are illustrated in Figure 5.6-3, along with the corresponding curve from Figure 5.1-2.

While the same analytical approach followed above can be used to find the performance of a PSK system using a wideband linear repeater, the results are somewhat misleading in the present application because the PSK signals accessing the repeater are actually significantly affected by the TDRS input filter. Thus, use of the simulation program with a linear repeater characteristic provides a better estimate.

Figure 5.6-4 illustrates error probability for the NRZ-L PSK signal curves for the TWT and an equivalent linear repeater with the same filters. Figure 5.6-5 is a similar set of results for the split-phase PSK signal. These results are obtained from the simulations. Also shown is the error probability for an equivalent linear repeater without significant filtering. Although there is substantial degradation between the unfiltered linear link and the TWT link, most of the degradation is due to filtering rather than to the nonlinearity. For clarity, only a downlink E_b/N_0 of 10 dB is shown. The apparent crossover of the TWT and linear repeater curves in Figure 5.6-5 occurs in a region of very low confidence and should probably be ignored.

The general conclusion of these analytical and simulation results is that the degradation due to the nonlinearity is of the order of 1 dB relative to an equivalent linear repeater with the same nominal gain at the drive level.

5.7 References

- 5-1 Rybak, J. P., and R. J. Churchill, "Progress in Reentry Communications," IEEE Trans. Aerospace and Elect. Syst., Vol. AES-7, pp 879-894, September 1971.
- 5-2 Jain, P. C., and N. M. Blachman, "Detection of a PSK Signal Transmitted Through a Hard-Limited Channel," IEEE Trans. Inform. Theory, Vol. IT-19, pp 623-630, September 1973.

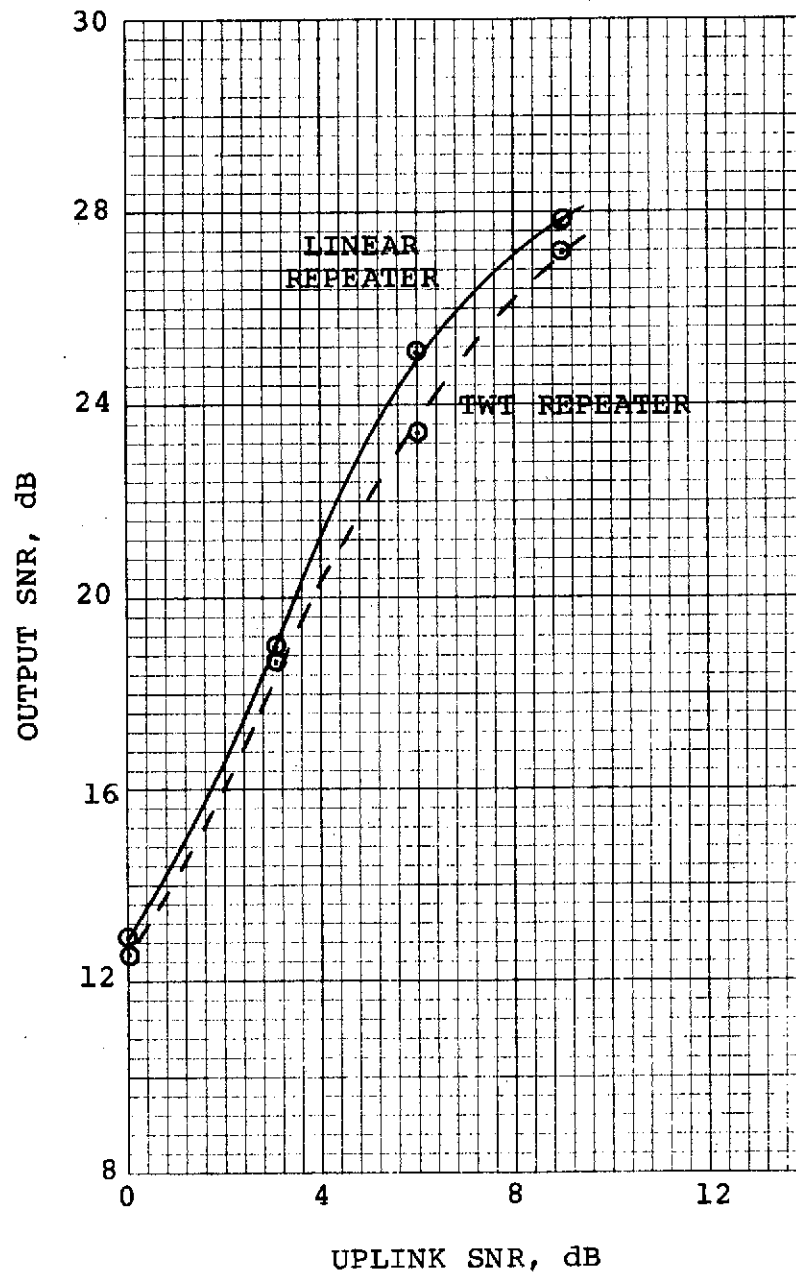


FIGURE 5.6-3. TEST TONE-TO-NOISE RATIO AT LOWPASS DEMULTIPLEXING FILTER OUTPUT FOR FDM/FM SIGNAL, DOWNLINK SNR = 15 dB

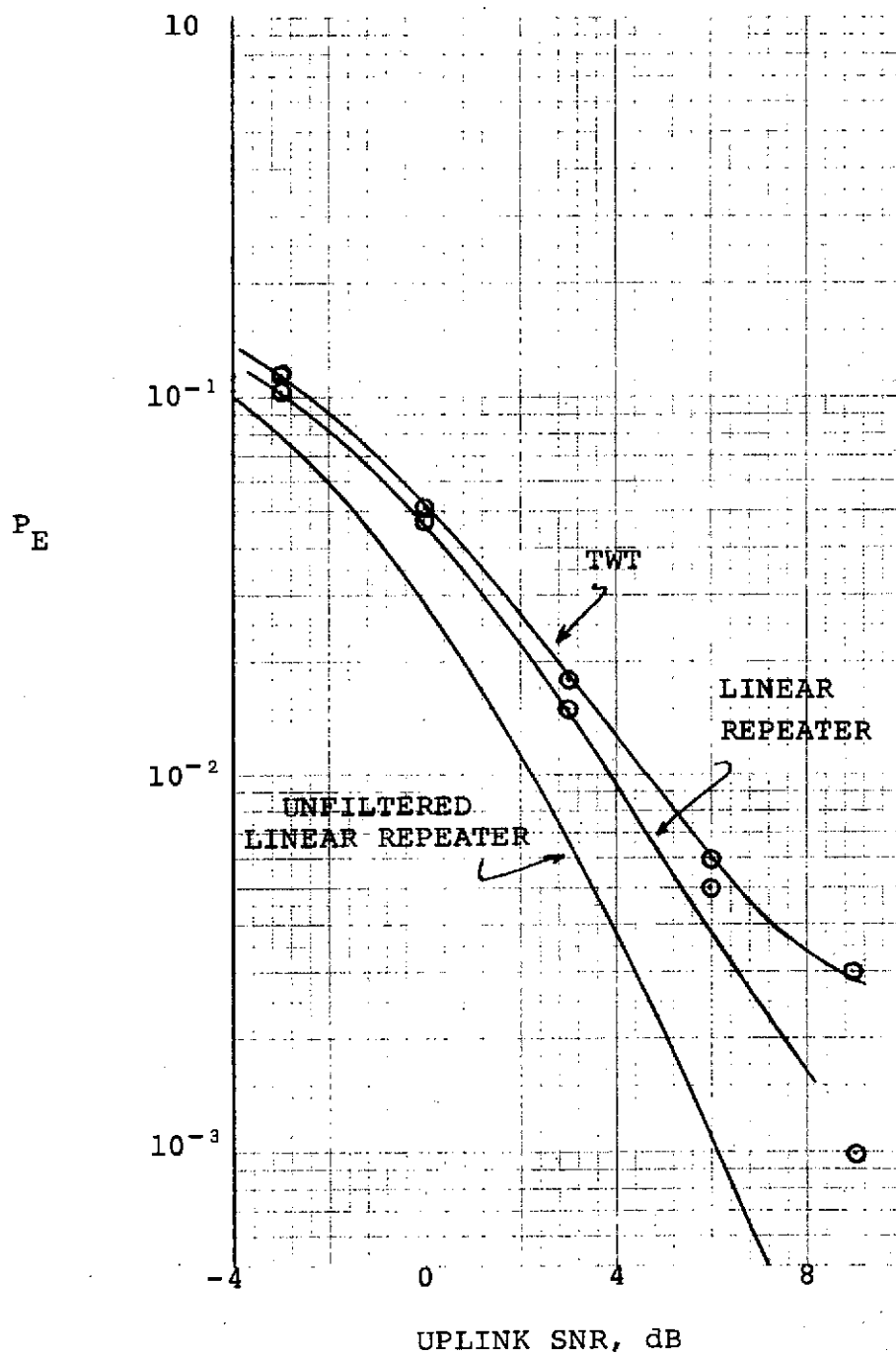


FIGURE 5.6-4. COMPARISON OF TWT AND LINEAR REPEATER FOR NRZ-L PSK SIGNAL, DOWNLINK $E_b/N_o = 10$ dB

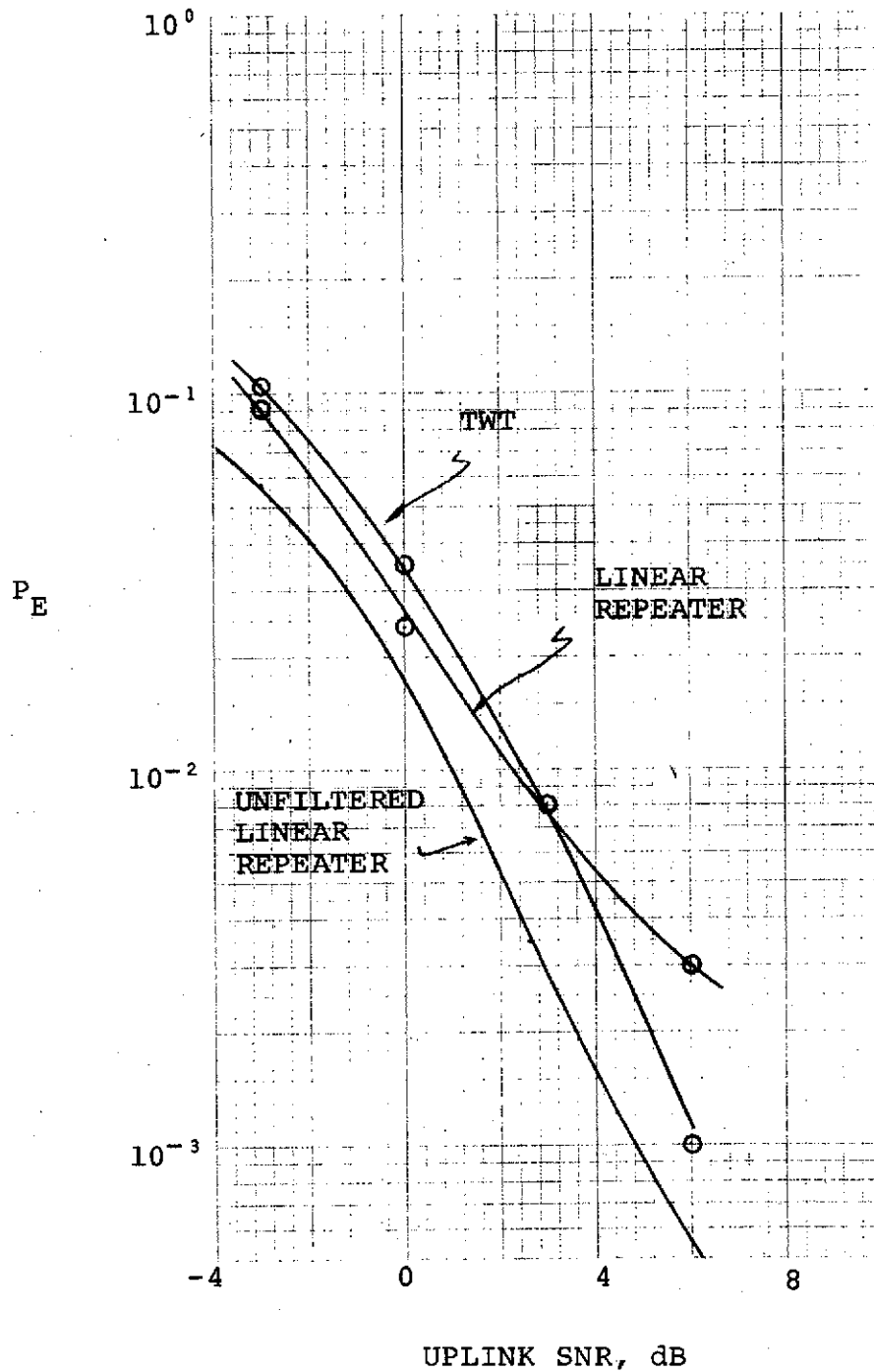


FIGURE 5.6-5. COMPARISON OF TWT AND LINEAR REPEATER FOR SPLIT-PHASE PSK SIGNAL, DOWNLINK $E_b/N_o = 10$ dB

APPENDIX A

EQUIVALENT BASEBAND REPRESENTATION OF AN RF SYSTEM

APPENDIX A

EQUIVALENT BASEBAND REPRESENTATION OF AN RF SYSTEM

In order to present a practical approach to digital computer simulation of an RF system, it is necessary to remove the RF frequency dependence from the simulation problem. This objective is realized through use of an equivalent baseband system representation. Such a representation of a linear, time invariant, bandpass system is developed in this appendix. In addition, an equivalent baseband filter function which is representative of common bandpass filter types is presented.

Of general interest is the system illustrated by Figure A-1, which has impulse response $h(t)$. This system is assumed to have an input passband centered at frequency f_o . The system is excited by an angle modulated carrier characterized as a narrowband signal. The frequency of the modulated carrier is denoted as f_c and it is assumed offset from the system input band-center according to $f_c = f_o - \delta$. This situation is illustrated in Figure A-2.

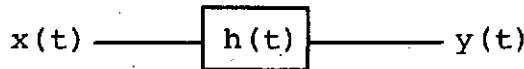


FIGURE A-1. BANDPASS SYSTEM

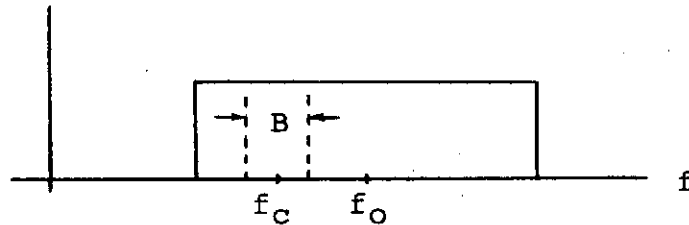


FIGURE A-2. SYSTEM INPUT PASSBAND

A general expression for the input signal with bandwidth B is

$$x(t) = R(t) \cos [\omega_o t + \phi(t)]$$

with $\phi(t)$ representing an angle modulated carrier at frequency f_c . The output of the system is given by the convolution integral

$$\begin{aligned} y(t) &= \int_{-\infty}^{\infty} R(t - \tau) \cos [\omega_o(t - \tau) + \phi(t - \tau)] h(\tau) d\tau \\ &= \text{Re} \left\{ e^{j\omega_o t} \int_{-\infty}^{\infty} R(t - \tau) e^{j\phi(t - \tau)} \hat{h}(\tau) d\tau \right\} \end{aligned}$$

where

$$\hat{h}(t) = h(t) e^{-j\omega_o t} \quad (\text{A-1})$$

Defining

$$X(t) = R(t) e^{j\phi(t)},$$

$$Y(t) = \int_{-\infty}^{\infty} X(t - \tau) \hat{h}(\tau) d\tau \quad (\text{A-2})$$

is the complex envelope of the output signal. In terms of the complex envelope, the real output signal is given by

$$y(t) = |Y(t)| \cos \left[\omega_o t + \tan^{-1} \left| \text{Im}(Y(t)) / \text{Re}(Y(t)) \right| \right]$$

For purposes of system simulation, the bandpass system reduces to the baseband system shown in Figure A-3.

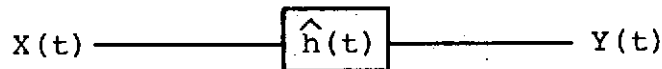


FIGURE A-3. EQUIVALENT BASEBAND SYSTEM

Baseband Equivalent of a Bandpass Filter

Bandpass filter design is often accomplished in terms of a lowpass filter characteristic which is subsequently transformed to a bandpass filter. For simulation purposes, the

bandpass filter undergoes another transformation to yield the desired baseband equivalent filter function. The various frequency variables of interest here are defined as follows:

p = lowpass complex frequency

s = bandpass complex frequency

q = equivalent baseband complex frequency

A commonly used lowpass-to-bandpass transformation is

$$p = \frac{s^2 + \omega_c^2}{s} \quad (\text{A-3})$$

while the conversion of bandpass to equivalent baseband implied by Equation (A-1) is accomplished by the transformation

$$s = q + j\omega_o \quad (\text{A-4})$$

A lowpass filter function exhibiting unit DC gain can be expressed as

$$H(p) = \frac{p_1 p_2 \cdots p_n}{(p + p_1) \cdots (p + p_n)}$$

Considering transformation of a single factor according to Equation (A-3),

$$H_i(p) = \frac{p_i}{p + p_i} \rightarrow \frac{p_i s}{s^2 + p_i s + \omega_c^2} = H_i(s)$$

Using Equation (A-4), $H_i(s)$ transforms to the baseband equivalent

$$H_i(s) \rightarrow \frac{p_i (q + j\omega_o)}{(q + q_1)(q + q_2)} = H_i(q)$$

where

$$q_{1,2} = \frac{p_i}{2} + j\omega_o \pm \sqrt{\left(\frac{p_i}{2}\right)^2 - j\frac{p_i}{2}\omega_o - \omega_c^2}$$

If, as is usually the case, $p_i \ll \omega_0$ and $p_i \ll \omega_c$, $H_i(q)$ is closely approximated by

$$H_i(q) = \frac{p_i(q + j\omega_0)}{\left[q + \frac{p_i}{2} + j(\omega_0 - \omega_c)\right] \left[q + \frac{p_i}{2} + j(\omega_0 + \omega_c)\right]}$$

The equivalent baseband filter now becomes

$$H(q) = \prod_{i=1}^n H_i(q)$$

The magnitude of the filter frequency response as the filter undergoes transformation according to Equations (A-3) and (A-4) is represented by Figure A-4.

Simplifications Under Narrowband Conditions

Solving Equation (A-3) for the bandpass frequency variable s yields

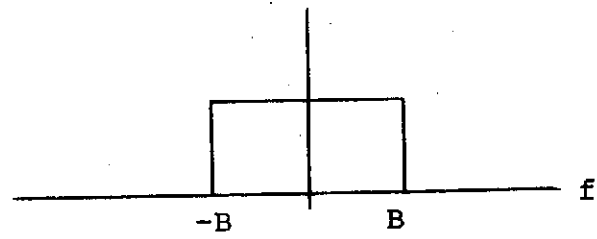
$$s = \frac{p}{2} \pm \sqrt{\left(\frac{p}{2}\right)^2 - \omega_c^2} \quad (\text{A-5})$$

Under narrowband conditions, complex frequencies p in the passband of the lowpass filter satisfy $|p| \ll \omega_c$. Accordingly, over the passband of the bandpass filter, Equation (A-5) becomes

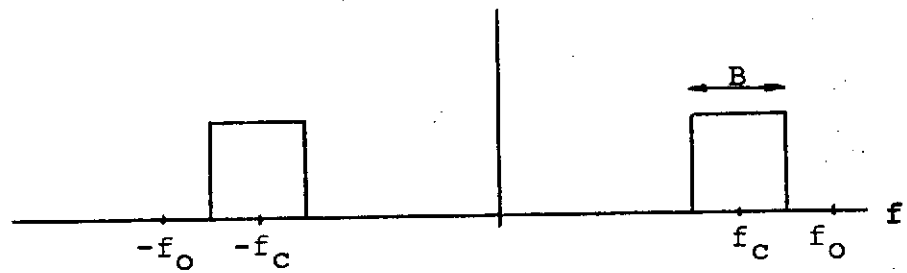
$$s \approx \frac{p}{2} \pm j\omega_c$$

so that to a good approximation, the passband is linearly translated to $\pm\omega_c$ (and halved in width). The transformation of Equation (A-4) is another linear translation of the passband, which leaves the bandwidth invariant. Thus the overall effect on the passband is to halve the width, move the center from DC to $f_c - f_0$, and generate an image of the passband at $-(f_0 + f_c)$.

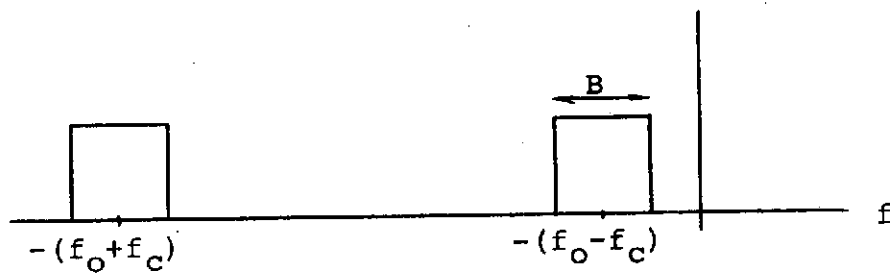
Since the complex envelope is to be passed through this filter, in accordance with Equation (A-2), the image at $-(f_0 + f_c)$ can be disregarded because the complex envelope is a



(a) Lowpass



(b) Bandpass



(c) Equivalent Baseband

FIGURE A-4. FILTER TRANSFORMATIONS

baseband signal. In addition, if $f_c = f_o$, as always assumed in this study, then the baseband equivalent is centered at DC. Therefore, the baseband equivalent of a filter obtained by applying Equation (A-3) to a lowpass filter, can be taken to be this original lowpass filter with its bandwidth reduced by one-half.

APPENDIX B

REPRESENTATION OF NONLINEARITIES

APPENDIX B

REPRESENTATION OF NONLINEARITIES

The simplest representation of a nonlinear component in a system is by means of a functional equation relating input to output. If the input and output are time functions, such a relationship has the form

$$y(t) = f(x(t)) \quad (B-1)$$

A nonlinearity representable in this way is said to be memoryless, since the output at time t is determined entirely by the input at the same time.

It often happens that the signals of interest are narrowband signals, representable in the form

$$x(t) = R(t) \cos [\omega_c t + \theta(t)] \quad (B-2)$$

When such a signal is input to a memoryless nonlinearity, experience suggests that the output will consist of modulated harmonics of the carrier frequency; thus one is led to assume an output of the form

$$y(t) = \sum_{k=0}^{\infty} R_k(t) \cos [k\omega_c t + k\theta(t)] \quad (B-3)$$

Blachman^[B-1] has shown that the amplitudes of the harmonics $R_k(t)$ are nonlinear functions of the input amplitude $R(t)$,

$$R_k(t) = F_k(R(t))$$

where the amplitude functions $F_k(\cdot)$ are obtained from the input-output function $f(\cdot)$ by the Chebyshev transform:

$$F_k(R) = \frac{\epsilon_k}{\pi} \int_0^{\pi} f(R \cos \psi) \cos k\psi d\psi$$

where $\epsilon_0 = 1$ and $\epsilon_k = 2, k > 0$. This transform, together with the inversion technique developed by Blachman, provide a relatively straightforward means of relating the instantaneous voltage characteristic to envelope characteristics. For bandpass nonlinearities, the first harmonic term of (B-2) is the term of interest, with the other harmonics effectively suppressed by a zonal filter. The output of a memoryless bandpass nonlinearity with a narrowband input is therefore,

$$y(t) = F_1(R(t)) \cos[\omega_c t + \theta(t)]$$

where the amplitude nonlinearity is given by

$$F_1(R) = \frac{2}{\pi} \int_0^{\pi} f(R \cos \psi) \cos \psi d\psi$$

A traveling-wave tube driven by a signal of the form of Equation (B-2) is known to have output given by

$$y(t) = F(R(t)) \cos[\omega_c t + \theta(t) + G(R(t))] \quad (B-4)$$

To see that such a nonlinearity cannot be correctly modelled as a single memoryless nonlinearity, note that whenever $\omega_c t + \theta(t) = \pm\pi/2$, $x(t) = 0$ so that a memoryless nonlinearity, as given by Equation (B-1), would exhibit the same output $y(t) = f(0)$ at all such times. However, Equation (B-4) shows that the output at such times is actually

$$y(t) = F(R(t)) \cos\left[\pm \frac{\pi}{2} + G(R(t))\right] = \pm F(R(t)) \sin G(R(t))$$

Kaye, George and Eric ^[B-2] have shown how much a nonlinearity can be modelled as a pair of "quadrature" memoryless nonlinearities. This is accomplished by rewriting Equation (B-4) in the form

$$y(t) = F(R(t)) \cos G(R(t)) \cos[\omega_c t + \theta(t)] \\ - F(R(t)) \sin G(R(t)) \sin[\omega_c t + \theta(t)]$$

Each of the "quadrature" amplitude nonlinearities

$$F_c(R) = F(R) \cos G(R)$$

$$F_s(R) = F(R) \sin G(R)$$

is memoryless and the corresponding instantaneous voltage transfer characteristic could be obtained, if desired, by inverting the Chebyshev transform. The TWT is then modelled as illustrated in Figure B-1.

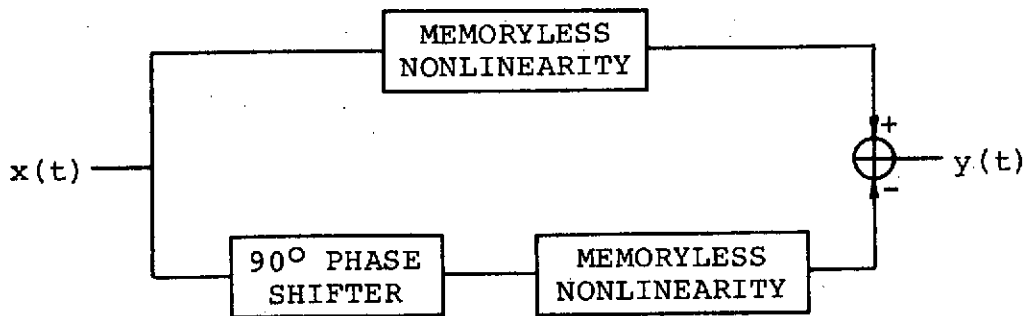


FIGURE B-1. QUADRATURE MODEL OF A TWT NONLINEARITY

This representation of the TWT is useful in applications where, for some reason, it is desired to work with instantaneous voltage signals. In this study, the use of complex envelope signal representations permits a simpler and more direct model of the TWT effects. The complex envelope of a signal of the form of Equation (B-2), given by

$$X(t) = R(t) \exp(j\theta(t))$$

is mapped into

$$Y(t) = F(R(t)) \exp(j\theta(t) + jG(R(t)))$$

which is the complex envelope of Equation (B-4).

References

- B-1 Blachman, N. M., "Detectors, Bandpass Nonlinearities, and Their Optimization: Inversion of the Chebyshev Transform," IEEE Trans. Inform. Theory, Vol. IT-17, pp. 398-404, July 1974.
- B-2 Kaye, A. R., D. A. George, and M. J. Eric, "Analysis and Compensation of Bandpass Nonlinearities for Communications," IEEE Trans. Comm., Vol. COM-20, pp. 965-972, October 1972.

APPENDIX C

IMPLEMENTATION OF DIGITAL FILTERS

APPENDIX C

IMPLEMENTATION OF DIGITAL FILTERS

Simulation of an analog filter on a digital computer can be accomplished through use of digital filtering techniques. The degree to which the simulation agrees with the analog filter characteristics is basically a function of the sampling rate and it is usually traded off against computer run-time requirements for simulating a given system. Two types of digital filters, recursive and nonrecursive, are briefly discussed in this appendix along with the implementation approaches found useful in simulating the communications systems of interest in this study.

Recursive Lowpass Digital Filters

An n th order lowpass analog filter with unit DC gain is described in the complex frequency domain by

$$H(p) = \prod_{i=1}^n \frac{p_i}{p + p_i} \quad (C-1)$$

where the p_i are either real or occur in complex conjugate pairs (if the impulse response is real). Combining the conjugate pole pairs leads to second-order factors of the form

$$\frac{p_i p_i^*}{(p + p_i)(p + p_i^*)} = \frac{|p_i|^2}{p^2 + 2\operatorname{Re}|p_i|p + |p_i|^2} \quad (C-2)$$

Thus, $H(p)$ can be represented as a product of first-order factors of the form $p_i/(p + p_i)$ (associated with real poles) and second-order factors of the form of Equation (C-2) (associated with conjugate poles).

In a straightforward manner, each factor can be transformed into a first- or second-order digital filter via one of several transformations. In the development presented here, the bilinear z -transform [C-1]

$$p = \frac{z - 1}{z + 1} \quad (C-3)$$

is utilized. This transformation maps the $j\omega$ axis of the p -plane onto the unit circle of the z -plane, with the left-half p -plane

mapped into the interior of the unit circle, preserving stability. The bilinear transform induces a nonlinear warping of the frequency scale, so that the critical frequencies used in filter design must be prewarped according to

$$\omega_c' = \tan (\omega_c T/2)$$

where ω_c represents a desired critical frequency, ω_c' is the corresponding prewarped analog filter critical frequency, and T is the sampling interval. The analog filter is designed to the prewarped critical frequencies, and transformation by Equation (C-3) follows. The overall filter implementation is a cascade of first- and second-order digital filters.*

Applying the bilinear transformation to a first-order factor of the form

$$H_i(p) = \frac{p_i}{p + p_i}$$

yields

$$H_i(z) = \frac{A_i(z + 1)}{z + B_i}$$

and the corresponding first-order difference equation is

$$y_i(kT) = -B_i y_i(kT - T) + A_i x_i(kT) + A_i x_i(kT - T) \quad (C-4)$$

with

$$A_i = p_i / (p_i + 1)$$

*It is also possible to implement the filter as a parallel combination, and it has been shown that a parallel realization is slightly less susceptible to computational error than a cascade realization. However, the parallel realization carries a greater computational time requirement. It has been verified experimentally during this study effort that a cascade of first- and second-order elemental stages performs quite satisfactorily for filter orders as high as 12, when programmed in floating point arithmetic on a 24-bit machine. Thus, the cascade realization is utilized here.

and

$$B_i = (p_i - 1)/(p_i + 1)$$

Transforming a second-order factor of the form of Equation (C-2) yields

$$H_i(z) = \frac{K_i(z^2 + 2z + 1)}{z^2 + C_i z + D_i}$$

The corresponding difference equation is

$$\begin{aligned} y_i(kT) = & -[C_i y_i(kT - T) + D_i y_i(kT - 2T)] \\ & + K_i [x_i(kT) + 2x_i(kT - T) + x_i(kT - 2T)] \quad (C-5) \end{aligned}$$

where

$$K_i = |p_i|^2 / \beta_i$$

$$C_i = 2(|p_i|^2 - 1) / \beta_i$$

$$D_i = (1 - 2\operatorname{Re}[p_i] + |p_i|^2) / \beta_i$$

$$\beta_i = (1 + 2\operatorname{Re}[p_i] + |p_i|^2)$$

Equations (C-4) and (C-5) are the equations actually programmed in the software implementation of the filters. Programs for determining the constants A_i , B_i , C_i , D_i , and K_i for digital Butterworth and Chebyshev lowpass filters have been developed. Instructions for the use of these programs are given in Appendix D.

Recursive Bandpass Digital Filters

As noted in Appendix A, one method of designing bandpass filters is through the use of a lowpass-to-bandpass transformation. Thus, an elemental first-order factor (real or complex)

of a given lowpass transfer function undergoes transformation as follows:

$$\frac{p_i}{p + p_i} \rightarrow \frac{p_i s}{s^2 + p_i s + \omega_c^2} = \frac{p_i s}{(s + s_i)(s + s_i^*)} \quad (C-6)$$

where ω_c is the bandpass center frequency. If p_i is real, the poles in the s -domain resulting from this transformation are a conjugate pair. If p_i is complex, the two poles of Equation (C-6) are not conjugates, but the four poles obtained by applying Equation (C-6) to both p_i and p_i^* occur in two conjugate pairs. For example, referring to Figure C-1, the real pole at $-p_1$ transforms to poles at $-s_1$ and $-s_1^* = -s_1$. The complex pole at $-p_2$ transforms to poles at $-s_2$ and $-s_2^*$, which are not conjugates. However, the poles resulting from transforming the pole at $-p_3$ are at $-s_3^* = -s_2^*$ and $-s_3 = -s_2$. Thus, three conjugate pairs result.

In similar fashion, transformation of any n -pole low-pass filter by the lowpass-to-bandpass transformation of Equation (C-6) will result in a transfer function whose poles occur in n complex conjugate pairs. Each such pair corresponds to a real second-order section, with the overall transfer function realized as the cascade of these n second-order sections. Each such section has the form

$$H_i(s) = \frac{|p_i|s}{(s + s_i)(s + s_i^*)} \quad (C-7)$$

Upon applying the bilinear transformation to (C-7), a discrete-time transfer function

$$H_i(z) = \frac{K_i(z^2 - 1)}{z^2 + C_i z + D_i}$$

is obtained, with corresponding difference equation

$$y_i(kT) = -[C_i y_i(kT - T) + D_i y_i(kT - 2T)] \\ + K_i [x_i(kT) - x_i(kT - 2T)]$$

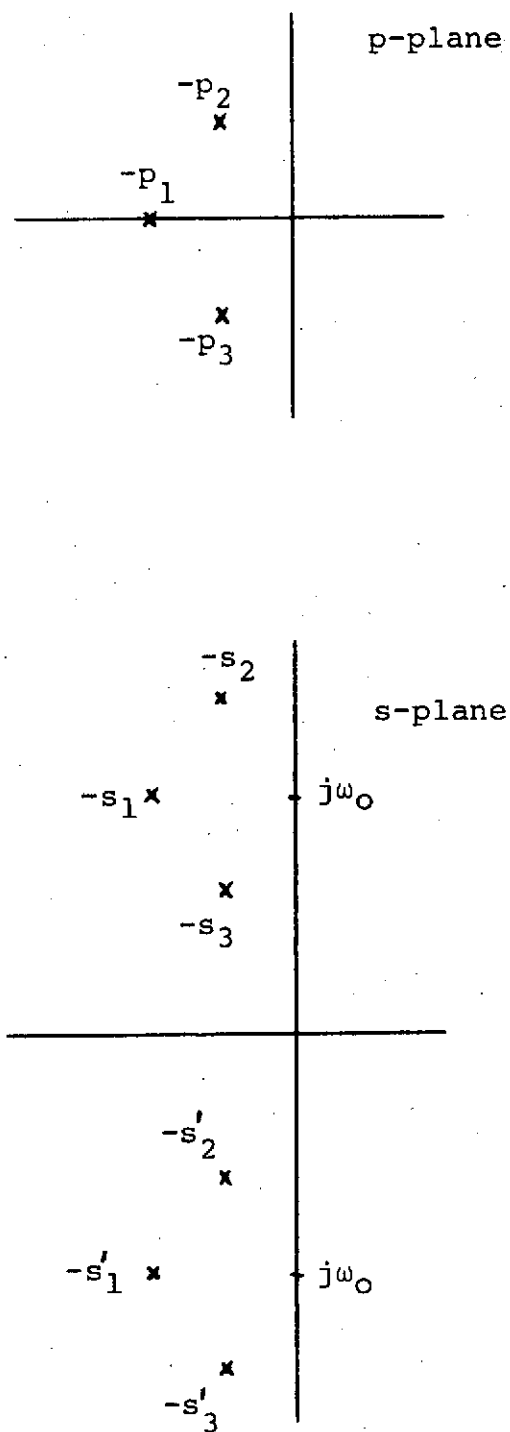


FIGURE C-1. EFFECT OF LOWPASS-TO-BANDPASS TRANSFORMATION

The constants above are

$$K_i = |p_i|/\beta_i$$

$$C_i = -2/\beta_i$$

$$D_i = (1 - 2\operatorname{Re}\{s_i\} + |s_i|^2)/\beta_i$$

$$\beta_i = 1 + 2\operatorname{Re}\{s_i\}$$

Programs for constructing bandpass Butterworth filters have been developed and are discussed in Appendix D.

Nonrecursive Lowpass Digital Filters

The difference equations developed above show that in general the output of recursive digital filters at time kT is a linear combination of both past inputs and past outputs. Nonrecursive digital filters, in contrast, have outputs depending only on past inputs; thus the difference equation for such a filter has the form

$$y(kT) = \sum_{j=0}^N h_j x((k-j)T) \quad (C-8)$$

Such filters have no poles and are, therefore, always stable. It is possible, by proper selection of the constants h_j , to obtain precisely linear phase. The major drawback of these filters is that they generally require more arithmetic operations to obtain a given selectivity than recursive filters.

Assume for simplicity, that N in Equation (C-8) is even, so that the sum contains an odd number of terms. If the constants h_j are even about $h_{N/2}$, i.e.,

$$h_{N/2-j} = h_{N/2+j} \quad j = 0, 1, \dots, N/2 \quad (C-9)$$

then the frequency response of the filter can be shown to have phase which is linear with frequency, so that no delay distortion results when a signal is passed through the filter.

For design of linear-phase lowpass filters, the constants $h_{N/2}$, $h_{N/2 + 1}$, ..., h_N are selected to be samples of an ideal lowpass filter impulse response $(\sin(\alpha t)/\alpha t)$ weighted by a "window" function to restrict the response to finite duration. Thus

$$h_{N/2 + j} = w(jT) \frac{\sin \alpha jT}{\alpha jT} \quad j = 0, 1, \dots, N/2$$

where the constant α determines the cutoff frequency. The constants h_0 , h_1 , ..., $h_{N/2 - 1}$ are chosen to satisfy Equation (C-9).

The selection of the window function has considerable effect on the frequency response. A common function is the Kaiser window

$$w(t) = \begin{cases} \frac{1}{I_0(\beta)} I_0(\beta \sqrt{1 - (2t/NT)^2}) & |t| < NT/2 \\ 0 & \text{otherwise} \end{cases}$$

The constant β governs the amount of out-of-band rejection of the filter.

A program to construct nonrecursive lowpass filters with a Kaiser window with $\beta = 3.384$ (yielding 40 dB out-of-band attenuation) has been written and its use is discussed in Appendix D. The theory of both recursive and nonrecursive digital filter designs is discussed thoroughly by Luntz, Osborne, and Zahm [C-2].

References

- C-1 Gold, B., and C. M. Rader, Digital Processing of Signals, McGraw-Hill Book Co., 1969.
- C-2 Luntz, M. B., W. P. Osborne, and C. L. Zahm, Digital Filter Design, Technical Report No. 50, Harris Corporation, Electronic Systems Division, October 1974.

APPENDIX D

FILTER GENERATION PROGRAMS AND THEIR USE

APPENDIX D

FILTER GENERATION PROGRAMS AND THEIR USE

This appendix contains program listings, sample outputs, and instructions for use of the filter generation programs discussed in Appendix C. The programs are listed in FORTRAN suitable for execution on the Datacraft 6024/5 computer. Card decks, listings, and sample runs in UNIVAC 1108-compatible FORTRAN have been delivered separately.

Chevyshev Lowpass Filters

To use this program, the user must specify a cutoff frequency (FREQC), the passband ripple (RIPPLE) in decibels, and the sampling rate (FREQS). The stopband characteristics are determined either by the specification of the filter order (PN) or by specifying a frequency (FREQ2) in the stopband by which the magnitude response is down by a specified amount (DBDOWN) in decibels. The program will determine analog filter pole locations, prewarp and transform to find digital filter pole locations, and print out analog and digital filter poles and difference equation coefficients for the digital filter cascade realization. The program then evaluates and outputs the analog and digital filter frequency response between specified limits (FSTRT and FSTOP) at a specified increment (FINC). The user may optionally call for a printout of the time response of the filter to a sinusoidal input. If this is called for (by setting TRSP≠0.), the excitation tone frequency is specified as a fraction of the cutoff frequency (that is, the excitation frequency is SCALE*FREQC).

Several filter generations may be accomplished in one run by including several sets of data cards. Each filter generation requires two data cards. Parameters on both cards are floating point values in free format, separated by commas. The order and meaning of the input data are as follows:

Card 1

FREQC	Cutoff frequency
FREQ2	A frequency (greater than FREQC) at which the response is to be down, in decibels, by the amount indicated by the next input
DBDOWN	Rejection in decibels at FREQ2

FREQS	Sampling rate
RIPPLE	Passband ripple in decibels
PN	Filter order. If $PN = 0$, the order will be determined from FREQ2 and DBDOWN. If $PN \neq 0$, it determines the filter order and FREQ2 and DBDOWN are ignored. The maximum filter order is 12.

Card 2

FSTRT	Beginning frequency value for frequency response printout
FSTOP	Final frequency value for frequency response printout
FINC	Frequency increment
TRSP	Time response option specification. If $TRSP = 0$, no time response computation will be made, and the next two inputs are ignored. If $TRSP \neq 0$, time response to a tone input will be calculated and output.
PMAX	Maximum number of time response samples to be output
SCALE	Excitation frequency as a fraction of FREQC

A program listing and a sample output are given in the following pages. The sample output shows the filter constants and frequency response of the TV demultiplexing filter used in the FDM/FM simulation program. (The quantities listed as poles of the analog and digital filters are actually negatives of the poles of these filters.)

C CHEBYSHEV LOWPASS FILTER GENERATOR

C
C

```

COMPLEX S,SW,Z,CONSTS,CONSTZ,ZZ,RL,RM
COMMON /BLK1/ LDO,LDI
COMMON /BLK2/ N,TS,CONSTS,CONSTZ
COMMON /BLK3/ Z(24),ZZ(24)
COMMON /BLK5/ S(24),SW(24)
COMMON /BLK6/ CON(6),C(6),D(6),CONA,ZA
DIMENSION V(50)
LDO = 6
LDI = 7
PI = 3.1415926536
TWOPI = 2. * PI
5 READ (LDI,-) FREQC,FREQ2,DBDOWN,FREQS,RIPPLE,PN
  READ (LDI,-) FSTRT,FSTOP,FINC,TRSP,PMAX,SCALE
  RIPPLE = ABS(RIPPLE)
  DBDOWN = ABS(DBDOWN)
  TS = 1. / FREQS
  AA = PI * FREQC * TS
  AB = PI * FREQ2 * TS

```

C

```

C***** WARP FREQUENCY SCALE *****
OMEGC = SIN(AA) / COS(AA)
OMEG2 = SIN(AB) / COS(AB)
K = PN
IF(K,EQ,0) GO TO 11
FREQ2 = 0.
DBDOWN = 0.
E = 1./((10.**(.1*RIPPLE))-1)
GO TO 10

```

C

```

C***** DETERMINE FILTER ORDER *****
11 AC = OMEG2 / OMEGC
  AD = 0.1 * DBDOWN
  AE = 10.**AD - 1.
  DD = 10.**(.1*RIPPLE)
  E = 1/(DD-1)
  TEST = E * AE
  V(1) = AC
  V(2) = 2 * (V(1)**2) - 1
  VK2 = AC*AC
  IF(VK2.LT.TEST) GO TO 12
  K = 1
  GO TO 10
12 VK2 = V(2)**2
  IF(VK2.LT.TEST) GO TO 14
  K = 2
  GO TO 10
14 K = 2
15 K = K+1
  V(K) = 2*AC*V(K-1) - V(K-2)
  VK2 = V(K)**2
  IF(VK2.LT.TEST) GO TO 15
10 N = K

```

```

C
C***** N IS ORDER OF FILTER *****
      WRITE(LD0,201) FREQC,FREQ2,DBDOWN,FREQS,RIPPLE
201  FORMAT (1H1,4X,'LOW PASS CHEBYSHEV FILTER'//5X,
1' CUTOFF FREQUENCY = ',F6.2,' HERTZ'/5X,'AT',F6.2,
2' HERTZ, RESPONSE IS DOWN',F7.2,' DB'/5X,'SAMPLING FREQUENCY = '
3F7.2,'/5X,'PASSBAND RIPPLE = ',F5.2,' DB')
      WRITE(LD0,202) N
202  FORMAT (5X,'FILTER ORDER = ',I2//11X,'POLES OF H(S)',44X,
2' POLES OF H(Z)')//)
      IF(N.EQ.0.OR.N.GT.12) GO TO 300
      EH = E**.5
      EX = (E+1.)**.5 + EH
      EN = 1./N
      X1 = EX**EN
      X2 = 1/X1
      EAA = .5 * (X1-X2)
      EBB = .5 * (X1+X2)

C
C***** DETERMINE POLES OF H(S) AND H(Z) *****
      N2 = 2 * N
      DO 20 I = 1,N
      THE = PI * FLOAT(2*I-1+N) / FLOAT(N2)
C***** S(I) = POLES OF H(S) *****
C***** SW(I) = POLES OF H'(S) (WARPED FREQUENCY SCALE) *****
C***** Z(I) = POLES OF H(Z) (TRANSFORMATION OF SW(I)) *****
      RL = -EAA * OMEGC * CEXP(CMPLX(0.,THE))
      RM = -EBB * OMEGC * CEXP(CMPLX(0.,THE))
      SW(I) = CMPLX(REAL(RL),AIMAG(RM))
      S(I) = SW(I) * TWOPI * FREQC / OMEGC
20  Z(I) = (SW(I) - CMPLX(1.,0.)) / (SW(I) + CMPLX(1.,0.))
C***** DETERMINE MULTIPLICATIVE CONSTANT FOR H(S) AND H(Z) *****
      CONSTS = CMPLX(1.,0.)
      CONSTZ = CMPLX(1.,0.)
      DO 22 I = 1,N
      ZZ(I) = CMPLX(1.,0.)
      CONSTS = CONSTS * S(I)
      CONSTZ = CONSTZ * (SW(I) / (SW(I) + CMPLX(1.,0.)))
22  WRITE(LD0,203) I,S(I),I,Z(I)
203  FORMAT(3X,'S(',I2,') = ',2E15.8,20X,'Z(',I2,') = ',2E15.8)
      WRITE(LD0,204) CONSTS,CONSTZ
204  FORMAT(/3X,'MULT. CONST. = ',2E15.8,13X,'MULT. CONST. = ',2E15.8)

C
C***** DETERMINE COMPLEX COEFFICIENTS REQ FOR TIME RESPONSE CALC. *****
      WRITE(LD0,208)
208  FORMAT(/,22X,'LOW PASS CHEBYSHEV DIGITAL FILTER COEFFICIENTS')/
      CALL LPCOEF

C
C***** TIME RESPONSE REQUIRED? *****
      IF(TRSP.EQ.0.) GO TO 250

C
C***** YES, CALCULATE TIME RESPONSE *****
      MAXIN = PMAX
      WRITE(LD0,205) SCALE,MAXIN
205  FORMAT(1H1,4X,'TIME RESPONSE FOR LOW PASS CHEBYSHEV DIGITAL FILTER

```

```

1'//,5X,'SCALE FACTOR = ',F15.5,/,5X,'NUMBER OF SAMPLES = ',I5,/)
TFREQ = FREQC * SCALE
CALL LPCCOE (TFREQ,MAXIN)

```

C

```

C***** DETERMINE FREQUENCY RESPONSE FOR H(S) AND H(Z) *****
250 CALL FRESP(FREQC,FSTRT,FSTOP,FINC)
GO TO 5
300 WRITE(LDO,301)
301 FORMAT(3X,'FILTER ORDER IS ZERO OR GREATER THAN 12',/,1H1)
GO TO 5
END

```

```

SUBROUTINE LPCOEF
COMPLEX S,SW,CONSTS,CONSTZ
COMMON /BLK1/LDO,LDI
COMMON /BLK2/N,TS,CONSTS,CONSTZ
COMMON /BLK5/ S(24),SW(24)
COMMON /BLK6/CON(6),C(6),D(6),CONA,ZA
NJ = N/2
NX = 2*NJ
WRITE(LDO,45)
45 FORMAT(16X,'I',9X,'K(I)',13X,'C(I)',14X,'D(I)')//)
DO 40 I=1,NJ
D1 = CABS(SW(I)**2) + 2. * REAL(SW(I)) + 1.
CON(I) = CABS(SW(I))**2/D1
C(I) = 2. * (CABS(SW(I))**2-1.)/D1
D(I) = (CABS(SW(I))**2 - 2.*REAL(SW(I))+1.)/D1
WRITE(LDO,48)I,CON(I),C(I),D(I)
40 CONTINUE
48 FORMAT(15X,I2,3(3X,E15.8))
IF(NX.EQ.N) GO TO 41
IT = NJ+1
CONA = REAL(SW(IT)/(SW(IT)+1.))
ZA = REAL((SW(IT)-1.)/(SW(IT)+1.))
WRITE(LDO,48)IT,CONA,ZA
41 RETURN
END

```

```

SUBROUTINE FRESP(FC,STRT,STP,DELF)
COMPLEX S,Z,ZZ,CS,CZ,PA,PD,ZD,VARS,VARZ,HS,HZ,SW
COMMON /BLK1/ LDO,LDI
COMMON /BLK2/ N,TS,CS,CZ
COMMON /BLK3/ Z(24),ZZ(24)
COMMON /BLK5/ S(24),SW(24)
PI = 3.1415926536
TWOPI = 2. * PI
FREQ = -DELF
RCS = REAL(CS)
RCZ = REAL(CZ)

```

```

WRITE(LD0,201)
5 FREQ = FREQ + DELF
IF(FREQ.GT.STP) RETURN
C***** COMPUTE RESPONSE FOR H(S)
AS = TWOPI * FREQ
VARS = CMPLX(0.,AS)
PA = CMPLX(1.,0.)
DO 12 J = 1,N
12 PA = PA * (VARS + S(J))
HS = RCS / PA
SMAG = CABS(HS)
SANG = ATAN2(AIMAG(HS),REAL(HS)) * 180./PI
SDB = 20. * ALOG10(SMAG)
C***** COMPUTE RESPONSE FOR H(Z) *****
AZ = TWOPI * FREQ * TS
VARZ = CEXP(CMPLX(0.,AZ))
PD = CMPLX(1.,0.)
ZD = CMPLX(1.,0.)
DO 14 K = 1,N
PD = PD * (VARZ + Z(K))
14 ZD = ZD * (VARZ + ZZ(K))
HZ = RCZ * ZD / PD
ZMAG = CABS(HZ)
ZANG = ATAN2(AIMAG(HZ),REAL(HZ)) * 180. / PI
ZDB = 20. * ALOG10(ZMAG)
IF(FREQ.GE.STRT)WRITE (LD0,202) FREQ,SMAG,SDB,SANG,ZMAG,ZDB,ZANG
GO TO 5
201 FORMAT(1H1,5X,'FREQUENCY RESPONSE OF LOW PASS CHEBYSHEV FILTER',//
1 17X,'-----ANALOG FILTER RESPONSE-----'9X'-----DIGIT
2AL FILTER RESPONSE-----'//3X,'FREQUENCY AMPLITUDE AMPL
3ITUDE PHASE AMPLITUDE AMPLITUDE PHASE'//4X,
4'(HERTZ)'25X,'(DB) (DEG)',30X,'(DB) (DEG)'//)
202 FORMAT(3X,F9.2,5X,E14.8,3X,F7.2,3X,F7.2,10X,E15.8,3X,F7.2,3X,
1F7.2)
END

```

```

SUBROUTINE LPCCDE(FREQ,MAXIN)
COMPLEX CONSTS,CONSTZ
COMMON /BLK1/LD0,LDI
COMMON /BLK2/N,TS,CONSTS,CONSTZ
COMMON /BLK6/CON(6),C(6),D(6),CONA,ZA
DIMENSION Y(24)
PI = 3.1415926536
OLDY = 0.
OLDX = 0.
YY = 0.
NJ = N/2
NX = 2*NJ
41 WRITE(LD0,49)
49 FORMAT(///,7X,'K',12X,'X(KT)',15X,'Y(KT)'//)
DEL = 2.*PI*FREQ*TS
DO 50 J = 1,24

```

```

50 Y(J) = 0.
   DO 70 L=1,MAXIN
     LL = L-1
     J=3
     Y(3) = COS(DEL*LL)
     DO 55 I = 1,NJ
       J = J + 3
       J1 = J-1
       J2 = J-2
       J3 = J-3
       J4 = J-4
       J5 = J-5
55  Y(J) = -C(I)*Y(J1)-D(I)*Y(J2) + CON(I)*(Y(J3)+Y(J4)+Y(J4)+Y(J5))
     YZ = Y(J)
     IF(NX.EQ.N) GO TO 58
     YY = -ZA*OLDY + CONA*(Y(J)+OLDX)
     YZ = YY
58  WRITE(LD0,44) LL,Y(3),YZ
44  FORMAT(3X,I5,2(5X,E16.8))
C***** SHIFT INPUT AND OUTPUT VALUES
     OLDY = YY
     OLDX = Y(J)
     DO 60 K = 1,J,3
       K1 = K + 1
       K2 = K + 2
       Y(K) = Y(K1)
60  Y(K1) = Y(K2)
70  CONTINUE
     RETURN
     END

```

LOW PASS CHEBYSHEV FILTER

CUTOFF FREQUENCY = 4.20 HERTZ
 AT 5.50 HERTZ, RESPONSE IS DOWN 35.00 DB
 SAMPLING FREQUENCY = 200.00
 PASSBAND RIPPLE = .50 DB
 FILTER ORDER = 8

POLES OF H(S)

S(1) =	.11511023E	1	-.26521375E	2
S(2) =	.32780749E	1	-.22483734E	2
S(3) =	.49059824E	1	-.15023161E	2
S(4) =	.57870028E	1	-.52754386E	1
S(5) =	.57870046E	1	.52754289E	1
S(6) =	.49059843E	1	.15023137E	2
S(7) =	.32780788E	1	.22483723E	2
S(8) =	.11511108E	1	.26521371E	2

MULT. CONST. = .55719834E 10 -.12896000E 5

POLES OF H(Z)

Z(1) =	-.98554884E	0	-.13146117E	0
Z(2) =	-.97755474E	0	-.11041243E	0
Z(3) =	-.97300836E	0	-.73309286E	-1
Z(4) =	-.97110279E	0	-.25662052E	-1
Z(5) =	-.97110279E	0	.25662015E	-1
Z(6) =	-.97300836E	0	.73309196E	-1
Z(7) =	-.97755474E	0	.11041242E	0
Z(8) =	-.98554884E	0	.13146120E	0

MULT. CONST. = .79059641E-11 -.14636729E-16

LOW PASS CHEBYSHEV DIGITAL FILTER COEFFICIENTS

I	K(I)	C(I)	D(I)
1	.43727169E -2	-.19710976E 1	.98858843E 0
2	.31736721E -2	-.19551096E 1	.96780426E 0
3	.15256969E -2	-.19460172E 1	.95212002E 0
4	.37339903E -3	-.19422053E 1	.94369894E 0

ORIGINAL PAGE IS
 OF POOR QUALITY

FREQUENCY RESPONSE OF LOW PASS CHEBYSHEV FILTER

-----ANALOG FILTER RESPONSE-----

FREQUENCY (HERTZ)	AMPLITUDE		AMPLITUDE (DB)	PHASE (DEG)
0.00	.99999975E	0	-.00	.00
.42	.10292922E	1	.25	-37.86
.84	.10591499E	1	.50	-79.50
1.26	.10235936E	1	.20	-121.55
1.68	.10012260E	1	.01	-161.17
2.10	.10434591E	1	.37	156.39
2.52	.10479326E	1	.41	107.77
2.94	.10003498E	1	.00	59.24
3.36	.10479328E	1	.41	5.42
3.78	.10111910E	1	.10	-63.10
4.20	.10000040E	1	.00	-162.58
4.62	.17200546E	0	-15.29	105.03
5.04	.41701451E	-1	-27.60	80.54
5.46	.14277688E	-1	-36.91	67.84
5.88	.58951118E	-2	-44.59	59.44
6.30	.27479814E	-2	-51.22	53.26
6.72	.13972612E	-2	-57.09	48.45
7.14	.75912459E	-3	-62.39	44.56
7.56	.43473109E	-3	-67.24	41.32
7.98	.25993894E	-3	-71.70	38.57
8.40	.16115224E	-3	-75.86	36.19
8.82	.10304232E	-3	-79.74	34.12
9.24	.67672400E	-4	-83.39	32.29
9.66	.45497408E	-4	-86.84	30.66
10.08	.31229967E	-4	-90.11	29.19
10.50	.21837305E	-4	-93.22	27.87
10.92	.15525898E	-4	-96.18	26.67
11.34	.11206189E	-4	-99.01	25.58
11.76	.81999501E	-5	-101.72	24.57
12.18	.60758761E	-5	-104.33	23.64
12.60	.45541385E	-5	-106.83	22.79
13.02	.34499515E	-5	-109.24	21.99
13.44	.26392892E	-5	-111.57	21.25
13.86	.20376104E	-5	-113.82	20.56
14.28	.15865178E	-5	-115.99	19.92
14.70	.12451228E	-5	-118.10	19.32
15.12	.98447415E	-6	-120.14	18.75
15.54	.78383069E	-6	-122.12	18.21
15.96	.62818099E	-6	-124.04	17.71

-----DIGITAL FILTER RESPONSE-----

AMPLITUDE		AMPLITUDE (DB)	PHASE (DEG)
.10000005E	1	.00	.00
.10292225E	1	.25	-37.81
.10591694E	1	.50	-79.38
.10237871E	1	.20	-121.39
.10011637E	1	.01	-160.97
.10431989E	1	.37	156.64
.10481953E	1	.41	108.05
.10003999E	1	.00	59.49
.10476626E	1	.40	5.69
.10114123E	1	.10	-62.92
.10000482E	1	.00	-162.58
.17102901E	0	-15.34	104.90
.41317941E	-1	-27.68	80.42
.14099587E	-1	-37.02	67.71
.58017915E	-2	-44.73	59.30
.26948736E	-2	-51.39	53.12
.13651328E	-2	-57.30	48.30
.73874303E	-3	-62.63	44.39
.42130106E	-3	-67.51	41.14
.25080626E	-3	-72.01	38.38
.15477446E	-3	-76.21	36.00
.98486218E	-4	-80.13	33.92
.64352731E	-4	-83.83	32.08
.43036492E	-4	-87.32	30.44
.29377491E	-4	-90.64	28.96
.20423598E	-4	-93.80	27.63
.14433650E	-4	-96.81	26.42
.10352825E	-4	-99.70	25.32
.75264631E	-5	-102.47	24.30
.55393944E	-5	-105.13	23.37
.41231295E	-5	-107.70	22.50
.31009585E	-5	-110.17	21.70
.23546461E	-5	-112.56	20.95
.18038850E	-5	-114.88	20.25
.13933886E	-5	-117.12	19.59
.10846096E	-5	-119.29	18.98
.85033476E	-6	-121.41	18.40
.67115863E	-6	-123.46	17.86
.53308197E	-6	-125.46	17.35

ORIGINAL PAGE IS
OF POOR QUALITY

Butterworth Lowpass and Bandpass Filters

The Butterworth lowpass filter program is similar to the Chebyshev lowpass filter program, except that only one data card is required for each filter design. The nine input parameters must contain decimal points, and must be separated by commas. Input parameter order, and meaning of each parameter, is as given below:

FREQC	Filter cutoff frequency
FREQ2	A frequency value (greater than FREQC) at which the response is to be down, in decibels, by the amount indicated by the next input
DBDOWN	Rejection in decibels at FREQ2
FREQS	Sampling rate
FREQO	Dummy variable (set to 0.)
PN	Filter order. If PN = 0., the order of the filter will be determined from the input data.
TRSP	Time response indicator. A zero value suppresses time response output.
PMAX	Number of time response samples to be printed
SCALE	Excitation frequency scale factor

For the Butterworth bandpass filter, the input parameters are the same as for the lowpass filter, except that FREQC becomes the design bandwidth of the passband, and FREQO is the design center frequency of the passband. FREQ2 and DBDOWN, if used, refer to the stopband characteristics of the lowpass filter from which the bandpass filter is obtained by the transform of Equation (C-6).

The frequency response output from the lowpass filter program extends from zero to four times the cutoff frequency, in increments of one-tenth of the cutoff frequency. For the bandpass filter, the response is output for a region eight times the bandwidth, centered at FREQO, at increments of one-tenth the bandwidth.

Program listing and sample outputs for these two programs are given in the following pages.

C BUTTERWORTH LOWPASS FILTER GENERATOR

C
C

```

COMPLEX S,SW,Z,CONSTS,CONSTZ,ZZ
COMMON /BLK1/ LDO,LDI
COMMON /BLK2/ N,TS,CONSTS,CONSTZ
COMMON /BLK3/ Z(12),ZZ(12)
COMMON /BLK5/ S(24),SW(24)
COMMON /BLK6/ CON(6),C(6),D(6),CONA,ZA
LDI = 7
LDO = 6
PI = 3.1415926536
TWOPI = 2. * PI
5 READ(LDI, )FREQC,FREQ2,DBDOWN,FREQS,FREQ0,PN,TRSP,PMAXIN,SCALE
DBDOWN = ABS(DBDOWN)
TS = 1. / FREQS
AA = PI * FREQC * TS
AB = PI * FREQ2 * TS

```

C

C***** WARP FREQUENCY SCALE *****

```

OMEGC = SIN(AA) / COS(AA)
OMEG2 = SIN(AB) / COS(AB)

```

C

C***** DETERMINE FILTER ORDER *****

```

IF(PN.EQ.0) GO TO 10
FREQ2 = 0.
DBDOWN = 0.
N=PN
GO TO 15
10 AC = OMEG2 / OMEGC
AD = 0.1 * DBDOWN
AE = 10.**AD - 1.
AN = .5 * ALOG(AE) / ALOG(AC)

```

C

C***** N IS ORDER OF FILTER *****

```

N = INT(AN) + 1
15 WRITE(LDO,201) FREQC,FREQ2,DBDOWN,FREQS
201 FORMAT (1H1,4X, 'LOW PASS BUTTERWORTH FILTER',//5X,
1'CUTOFF FREQUENCY = ',F15.5,' HERTZ'/5X,'AT',F15.5,
2' HERTZ, RESPONSE IS DOWN',F7.2,' DB'/5X,'SAMPLING FREQUENCY = '
3F15.5)
WRITE(LDO,202) N
202 FORMAT (5X,'FILTER ORDER = ',I3///11X,'POLES OF H(S)',44X,
2'POLES OF H(Z)'//)
IF(N.LT.1.OR.N.GT.12) GO TO 300

```

C

C***** DETERMINE POLES OF H(S) AND H(Z) *****

```

N2 = 2 * N
DO 20 I = 1,N
THE = PI * FLOAT(2*I-1+N) / FLOAT(N2)
C***** S(I) = POLES OF H(S) *****
C***** SW(I) = POLES OF H'(S) (WARPED FREQUENCY SCALE) *****
C***** Z(I) = POLES OF H(Z) (TRANSFORMATION OF SW(I)) *****
S(I) = -TWOPI * FREQC * CEXP(CMPLX(0.,THE))
SW(I) = -OMEGC * CEXP(CMPLX(0.,THE))

```

```

      20 Z(I) = (SW(I) - CMPLX(1.,0.)) / (SW(I) + CMPLX(1.,0.))
C
C***** DETERMINE MULTIPLICATIVE CONSTANTS FOR H(S) AND H(Z)
      CONSTS = CMPLX(1.,0.)
      CONSTZ = CMPLX(1.,0.)
      DO 22 I = 1,N
        CONSTS = CONSTS * S(I)
        CONSTZ = CONSTZ * (SW(I)/(SW(I) + CMPLX(1.,0.)))
      22 WRITE(LD0,203) I,S(I),I,Z(I)
      203 FORMAT(3X,'S(',I2,') = ',2E15.8,20X,'Z(',I2,') = ',2E15.8)
        WRITE(LD0,208) CONSTS,CONSTZ
      208 FORMAT(//3X,'MULT. CONST = ',2E15.8,13X,'MULT. CONST = ',2E15.8/)
        WRITE(LD0,204)
C
C***** DETERMINE COMPLEX COEFFICIENTS REQ'D FOR TIME RESP. CALCULATIONS
      204 FORMAT(//22X,'LOW PASS BUTTERWORTH DIGITAL FILTER COEFFICIENTS'//)
        CALL LPCOEF
C
C***** TIME RESPONSE OUTPUT REQUIRED?
      41 IF(TRSP.EQ.0) GO TO 250
C
C***** TIME RESPONSE OUTPUT *****
      MAXIN = PMAXIN
      WRITE(LD0,205) SCALE,MAXIN
      205 FORMAT(1H1,4X,'TIME RESPONSE FOR LOW PASS BUTTERWORTH FILTER',//
        15X,'SCALE FACTOR = ',F15.5,/,5X,'NUMBER OF SAMPLES = ',I5/)
      TFREQ = SCALE * FREQC
      CALL LPCCDE(TFREQ,MAXIN)
C
C***** DETERMINE FREQUENCY RESPONSE FOR H(S) AND H(Z) *****
      250 CONTINUE
        DO 24 I = 1,N
          24 ZZ(I) = CMPLX(1.,0.)
          CALL FRESP(S,Z,ZZ,FREQC)
          GO TO 5
      300 WRITE(LD0,301)
      301 FORMAT(3X,'FILTER ORDER IS ZERO OR GREATER THAN 12')
        GO TO 5
      END

      SUBROUTINE LPCOEF
        COMPLEX S,SW,CONSTS,CONSTZ
        COMMON /BLK1/LD0,LDI
        COMMON /BLK2/N,TS,CONSTS,CONSTZ
        COMMON /BLK5/ S(24),SW(24)
        COMMON /BLK6/CON(6),C(6),D(6),CONA,ZA
        NJ = N/2
        NX = 2*NJ
        WRITE(LD0,45)
      45 FORMAT(16X,'I',9X,'K(I)',13X,'C(I)',14X,'D(I)'//)
        DO 40 I=1,NJ
          D1 = CABS(SW(I)**2) + 2. * REAL(SW(I)) + 1.

```

```

CON(I) = CABS(SW(I))*2/D1
C(I) = 2. * (CABS(SW(I))*2-1.)/D1
D(I) = (CABS(SW(I))*2 - 2.*REAL(SW(I))+1.)/D1
WRITE(LD0,48)I,CON(I),C(I),D(I)
40 CONTINUE
48 FORMAT(15X,I2,3(3X,E15.8))
IF(NX,EQ,N) GO TO 41
IT = NJ+1
CONA = REAL(SW(IT)/(SW(IT)+1.))
ZA = REAL((SW(IT)-1.)/(SW(IT)+1.))
WRITE(LD0,48)IT,CONA,ZA
41 RETURN
END

```

```

SUBROUTINE LPCCDE(FREQ,MAXIN)
COMPLEX CONSTS,CONSTZ
COMMON /BLK1/LD0,LDI
COMMON /BLK2/N,TS,CONSTS,CONSTZ
COMMON /BLK6/CON(6),C(6),D(6),CONA,ZA
DIMENSION Y(24)
PI = 3.1415926536
OLDY = 0.
OLDX = 0.
YY = 0.
NJ = N/2
NX = 2*NJ
41 WRITE(LD0,49)
49 FORMAT(///,7X,'K',12X,'X(KT)',15X,'Y(KT)'//)
DEL = 2. * PI * FREQ * TS
DO 50 J = 1,24
50 Y(J) = 0.
DO 70 L=1,MAXIN
LL = L-1
J=3
Y(3) = COS(DEL*LL)
DO 55 I = 1,NJ
J = J + 3
J1 = J-1
J2 = J-2
J3 = J-3
J4 = J-4
J5 = J-5
55 Y(J) = -C(I)*Y(J1)-D(I)*Y(J2) + CON(I)*(Y(J3)+Y(J4)+Y(J4)+Y(J5))
YZ = Y(J)
IF(NX,EQ,N) GO TO 58
YY = -ZA*OLDY + CONA*(Y(J)+OLDX)
YZ = YY
58 WRITE(LD0,44) LL,Y(3),YZ
44 FORMAT(3X,I5,2(5X,E16.8))
C***** SHIFT INPUT AND OUTPUT VALUES
OLDY = YY
OLDX = Y(J)
DO 60 K = 1,J,3

```

```

K1 = K + 1
K2 = K + 2
Y(K) = Y(K1)
60 Y(K1) = Y(K2)
70 CONTINUE
RETURN
END

```

```

SUBROUTINE FRESP(S,Z,ZZ,FC)
COMPLEX S,Z,ZZ,CS,CZ,PA,PD,ZD,VARS,VARZ,HS,HZ
COMMON /BLK1/LDO,LOI
COMMON /BLK2/N,TS,CS,CZ
DIMENSION S(12),Z(12),ZZ(12)
PI = 3.1415926536
TWOPI = 2. * PI
DELF = 0.1 * FC
RCS = REAL(CS)
RCZ = REAL(CZ)
WRITE(LDO,201)
DO 20 I = 1,41
FREQ = DELF * FLOAT(I-1)
C***** COMPUTE RESPONSE FOR H(S)
AS = TWOPI * FREQ
VARS = CMPLX(0.,AS)
PA = CMPLX(1.,0.)
DO 12 J = 1,N
12 PA = PA * (VARS + S(J))
HS = RCS / PA
SMAG = CABS(HS)
SANG = ATAN2(AIMAG(HS),REAL(HS)) * 180./PI
SDB = 20. * ALOG10(SMAG)
C***** COMPUTE RESPONSE FOR H(Z) *****
AZ = TWOPI * FREQ * TS
VARZ = CEXP(CMPLX(0.,AZ))
PD = CMPLX(1.,0.)
ZD = CMPLX(1.,0.)
DO 14 K = 1,N
PD = PD * (VARZ + Z(K))
14 ZD = ZD * (VARZ + ZZ(K))
HZ = RCZ * ZD / PD
ZMAG = CABS(HZ)
ZANG = ATAN2(AIMAG(HZ),REAL(HZ)) * 180. / PI
ZDB = 20. * ALOG10(ZMAG)
20 WRITE(LDO,202) FREQ,SMAG,SDB,SANG,ZMAG,ZDB,ZANG
201 FORMAT(1H1,5X,'FREQUENCY RESPONSE OF LOW PASS BUTTERWORTH FILTER'
1 //17X,'-----ANALOG FILTER RESPONSE-----'9X'-----DIGIT
2AL FILTER RESPONSE-----'//3X,'FREQUENCY AMPLITUDE AMPL
3ITUDE PHASE AMPLITUDE AMPLITUDE PHASE'//4X,
4'(HERTZ),'25X,'(DB) (DEG)',30X,'(DB) (DEG)'//)
202 FORMAT(3X,F9.2,5X,E15.8,3X,F6.2,3X,F7.2,10X,E15.8,3X,F6.2,3X,
1F7.2)
RETURN
END

```

C BUTTERWORTH BANDPASS FILTER GENERATOR

C
C

```

COMPLEX S,SW,Z,CONSTS,CONSTZ,ZZ,F2,PIT,P,PW
COMMON /BLK1/ LDO,LDI
COMMON /BLK2/ N,TS,CONSTS,CONSTZ
COMMON /BLK3/ Z(24),ZZ(24)
COMMON /BLK5/ S(24),SW(24)
COMMON /BLK6/ CON(12),C(12),D(12)
COMMON /BLK7/ P(12),PW(12)
LDI = 7
PI = 3.1415926536
LDO = 6
TWOPI = 2. * PI
5 READ(LDI,-)FREQC,FREQ2,DBDOWN,FREQS,FREQO,PN,TRSP,PMAX,SCALE
DBDOWN = ABS(DBDOWN)
TS = 1. / FREQS
AA = PI * FREQC * TS
AB = PI * FREQ2 * TS
BB = PI * FREQO * TS
C***** WARP FREQUENCY SCALE *****
OMEGC = SIN(AA) / COS(AA)
OMEG2 = SIN(AB) / COS(AB)
OMEGO = SIN(BB)/COS(BB)
C***** DETERMINE FILTER ORDER *****
IF(PN.EQ.0) GO TO 10
FREQ2 = 0.
DBDOWN = 0.
N=PN
GO TO 15
10 AC = OMEG2 / OMEGC
AD = 0.1 * DBDOWN
AE = 10.**AD - 1.
AN = .5 * ALOG(AE) / ALOG(AC)
C***** N IS ORDER OF FILTER *****
N = INT(AN) + 1
15 WRITE(LDO,201) FREQC,FREQ2,DBDOWN,FREQS,FREQO
201 FORMAT (1H1,4X,'EQUIVALENT BAND PASS BUTTERWORTH FILTER',//5X,
1'CUTOFF FREQUENCY = ',F15.5,' HERTZ'/5X,'AT',F15.5,
2' HERTZ, RESPONSE IS DOWN',F7.2,' DB'/5X,'SAMPLING FREQUENCY = '
3F15.5//5X,'CENTER FREQUENCY = ',F15.5)
WRITE(LDO,202) N
202 FORMAT (5X,'FILTER ORDER = ',I3///11X,'POLES OF H(S)',44X,
2'POLES OF H(Z)')//)
IF(N.LT.1.OR.N.GT.12) GO TO 300
C***** DETERMINE POLES OF H(S) AND H(Z) *****
N2 = 2 * N
CONSTZ = CMPLX(1.,0.)
CONSTS = CMPLX(1.,0.)
DO 20 I = 1,N
THE = PI * FLOAT(2*I-1+N) / FLOAT(N2)
C***** S(I) = POLES OF H(S) *****
C***** SW(I) = POLES OF H'(S) (WARPED FREQUENCY SCALE) *****
C***** Z(I) = POLES OF H(Z) (TRANSFORMATION OF SW(I)) *****
P(I) = -TWOPI * FREQC * CEXP(CMPLX(0.,THE))

```

```

PW(I) = -OMEGC * CEXP(CMPLX(0.,THE))
PIT = .5 * P(I)
F2 = P(I)**2-4.*CMPLX((TWOPI*FREGO)**2,0.)
F2 = .5*CSQRT(F2)
I2 = 2*I
I1 = I2-1
S(I1) = PIT + F2
S(I2) = PIT - F2
PIT = .5 * PW(I)
F2 = PW(I)**2-4.*CMPLX(OMEGO*OMEGO,0.)
F2 = .5*CSQRT(F2)
SW(I1) = PIT + F2
SW(I2) = PIT - F2
Z(I1) = (SW(I1)+CMPLX(-1.,0.))/(SW(I1)+CMPLX(1.,0.))
Z(I2) = (SW(I2)+CMPLX(-1.,0.))/(SW(I2)+CMPLX(1.,0.))
WRITE(LD0,203) I1,S(I1),I1,Z(I1)
WRITE(LD0,203) I2,S(I2),I2,Z(I2)
ZZ(I2) = CMPLX(1.,0.)
ZZ(I1) = CMPLX(-1.,0.)
C***** DETERMINE MULTIPLICATIVE CONSTANT FOR H(S) AND H(Z) *****
CONSTS = CONSTS * P(I)
CONSTZ = CONSTZ * PW(I) / (PW(I) + CMPLX(OMEGO*OMEGO+1.,0.))
20 CONTINUE
203 FORMAT(3X,'S(' ,I2,') = ',2E15.8,20X,'Z(' ,I2,') = ',2E15.8)
WRITE (LD0,204) CONSTS,CONSTZ
204 FORMAT(/3X,'MULT. CONST. = ',2E15.8,13X,'MULT. CONST. = ',2E15.8)
C
C
C***** DETERMINE REAL COEFFICIENTS
WRITE(LD0,208)
208 FORMAT(/17X,'BAND PASS BUTTERWORTH DIGITAL FILTER COEFFICIENTS'/)
CALL BPCOEF
C
C***** TIME RESPONSE REQUIRED? *****
IF(TRSP.EQ.0) GO TO 250
C
C***** TIME RESPONSE OUTPUT *****
MAXIN = PMAX
WRITE(LD0,205) SCALE,MAXIN,FREGO
205 FORMAT(1H1,4X,'TIME RESPONSE FOR BAND PASS BUTTERWORTH FILTER',//
15X,'SCALE FACTOR = ',F15.5,/,5X,'NUMBER OF SAMPLES = ',I5/,
25X,'CENTER FREQUENCY = ',F15.5,/)
TFREQ = SCALE * FREGO
CALL BPCCDE(TFREQ,MAXIN)
C
C*****
C***** DETERMINE FREQUENCY RESPONSE FOR H(S) AND H(Z) *****
250 CALL FRESP1(FREGC,FREGO)
GO TO 5
300 WRITE(LD0,301)
301 FORMAT(3X,'FILTER ORDER IS ZERO OR GREATER THAN 12')
GO TO 5
END

```



```

SUBROUTINE BPCOEF
COMPLEX CONSTS,CONSTZ,S,SW,Z,ZZ,PW,P
COMMON /BLK1/LDO,LDI
COMMON /BLK2/N,TS,CONSTS,CONSTZ
COMMON /BLK3/Z(24),ZZ(24)
COMMON /BLK5/ S(24),SW(24)
COMMON /BLK6/ CON(12),C(12),D(12)
COMMON /BLK7/P(12),PW(12)
NJ = N/2
I2 = 0
DO 25 I=1,NJ
I2 = 2*I
I1 = I2-1
CON(I1) = CABS(PW(I))/CABS(SW(I1) + CMPLX(1.,0.))**2
CON(I2) = CABS(PW(I))/CABS(SW(I2) + CMPLX(1.,0.))**2
C(I1) = 2. * REAL(Z(I1))
C(I2) = 2. * REAL(Z(I2))
D(I1) = CABS(Z(I1))**2
D(I2) = CABS(Z(I2))**2
WRITE (LDO,330)I1,CON(I1),I1,C(I1),I1,D(I1)
WRITE (LDO,330)I2,CON(I2),I2,C(I2),I2,D(I2)
25 CONTINUE
IF(I2.EQ.N) GO TO 30
I2 = I2+1
K = NJ+1
CON(I2) = CABS(PW(K))/CABS(SW(I2)+CMPLX(1.,0.))**2
C(I2) = 2. * REAL(Z(I2))
D(I2) = CABS(Z(I2))**2
WRITE(LDO,330) I2,CON(I2),I2,C(I2),I2,D(I2)
30 CONTINUE
330 FORMAT(17X,'CON('',I2,'') = ',E15.8,'   C('',I2,'') = ',E15.8,'   D('',
1I2,'') = ',E15.8)
RETURN
END

```

```

SUBROUTINE BPCCDE(FREQ,MAXIN)
COMPLEX CONSTS,CONSTZ
COMMON /BLK1/ LDO,LDI
COMMON /BLK2/ N,TS,CONSTS,CONSTZ
COMMON /BLK6/ CON(12),C(12),D(12)
DIMENSION Y(39)
PI = 3.1415926536
DEL = 2. * PI * FREQ * TS
DO 50 J = 1,39
50 Y(J) = 0.
DO 70 L=1,MAXIN
LL = L-1
J=3
Y(3) = COS(DEL*LL)
DO 55 I = 1,N
J = J + 3
J1 = J-1

```

```

J2 = J-2
J3 = J-3
J4 = J-4
J5 = J-5
55 Y(J) = -C(I)*Y(J1)-D(I)*Y(J2) + CON(I)*(Y(J3)-Y(J5))
58 WRITE(LD0,44) LL,Y(3),Y(J)
44 FORMAT(3X,I5,2(5X,E16.8))
C***** SHIFT INPUT AND OUTPUT VALUES
DO 60 K = 1,J,3
K1 = K + 1
K2 = K + 2
Y(K) = Y(K1)
60 Y(K1) = Y(K2)
70 CONTINUE
RETURN
END

```

```

SUBROUTINE FRESP1(FC,F0)
COMPLEX S,Z,ZZ,CS,CZ,PA,PD,ZD,VARS,VARZ,HS,HZ,SW
COMMON /BLK1/LD0,LDI
COMMON /BLK2/N,TS,CS,CZ
COMMON /BLK3/ Z(24),ZZ(24)
COMMON /BLK5/ S(24),SW(24)
PI = 3.1415926536
TWOPI = 2. * PI
DELF = 0.1 * FC
RCS = REAL(CS)
RCZ = REAL(CZ)
WRITE(LD0,201)
DO 20 I = 1,83
J = I-42
FREQ = DELF * FLOAT(J) + F0
C***** COMPUTE RESPONSE FOR H(S)
AS = TWOPI * FREQ
VARS = CMPLX(0.,AS)
PA = CMPLX(1.,0.)
N2 = 2*N
DO 12 J = 1,N2
12 PA = PA * (VARS + S(J))
HS = RCS * (VARS**N)/PA
SMAG = CABS(HS)
SANG = ATAN2(AIMAG(HS),REAL(HS)) * 180./PI
SDB = 20. * ALOG10(SMAG)
C***** COMPUTE RESPONSE FOR H(Z) *****
AZ = TWOPI * FREQ * TS
VARZ = CEXP(CMPLX(0.,AZ))
PD = CMPLX(1.,0.)
ZD = CMPLX(1.,0.)
DO 14 K = 1,N2
PD = PD * (VARZ + Z(K))
14 ZD = ZD * (VARZ + ZZ(K))
HZ = RCZ * ZD / PD
ZMAG = CABS(HZ)

```

```

      ZANG = ATAN2(AIMAG(HZ),REAL(HZ)) * 180. / PI
      ZDB = 20. * ALOG10(ZMAG)
20  WRITE(LD0,202) FREQ,SMAG,SDB,SANG,ZMAG,ZDB,ZANG
201  FORMAT(1H1,5X,'FREQUENCY RESPONSE OF EQUIVALENT BAND PASS BUTTERWO
      1RTH FILTER'//17X'-----ANALOG FILTER RESPONSE-----'9X'-----DIGIT
      2AL FILTER RESPONSE-----'//3X,'FREQUENCY          AMPLITUDE      AMPL
      3ITUDE  PHASE          AMPLITUDE      AMPLITUDE  PHASE'/4X,
      4'(HERTZ)'25X,'(DB)          (DEG)',30X,'(DB)          (DEG)'//)
202  FORMAT(3X,F9.2,5X,E15.8,3X,F6.2,3X,F7.2,10X,E15.8,3X,F6.2,3X,
      1F7.2)
      RETURN
      END

```

LOW PASS BUTTERWORTH FILTER

CUTOFF FREQUENCY = 17.50000 HERTZ
 AT 35.00000 HERTZ, RESPONSE IS DOWN 20.00 DB
 SAMPLING FREQUENCY = 400.00000
 FILTER ORDER = 4

POLES OF H(S)

S(1) = .42078165E 2 -.10158586E 3
 S(2) = .10158589E 3 -.42078267E 2
 S(3) = .10158589E 3 .42078165E 2
 S(4) = .42078328E 2 .10158589E 3

POLES OF H(Z)

Z(1) = -.87188720E 0 -.22717970E 0
 Z(2) = -.76948511E 0 -.83048951E -1
 Z(3) = -.76948511E 0 .83048759E -1
 Z(4) = -.87188720E 0 .22717982E 0

MULT. CONST = .14617461E 9 -.33600000E 3

MULT. CONST = .25523384E -3 -.55297278E -9

LOW PASS BUTTERWORTH DIGITAL FILTER COEFFICIENTS

I	K(I)	C(I)	D(I)
1	.17005865E -1	-.17437749E 1	.81179839E 0
2	.15008558E -1	-.15389702E 1	.59900437E 0

ORIGINAL PAGE IS
 OF POOR QUALITY

FREQUENCY RESPONSE OF LOW PASS BUTTERWORTH FILTER

-----ANALOG FILTER RESPONSE-----

FREQUENCY (HERTZ)	AMPLITUDE		AMPLITUDE (DB)	PHASE (DEG)
0.00	.99999969E	0	-.00	.00
1.75	.99999997E	0	-.00	-14.99
3.50	.99999886E	0	-.00	-30.11
5.25	.99996745E	0	-.00	-45.51
7.00	.99967307E	0	-.00	-61.37
8.75	.99805350E	0	-.02	-77.96
10.50	.99170765E	0	-.07	-95.66
12.25	.97236685E	0	-.24	-114.89
14.00	.92538370E	0	-.67	-135.86
15.75	.83610731E	0	-1.55	-158.06
17.50	.70710832E	0	-3.01	-180.00
19.25	.56401183E	0	-4.97	160.10
21.00	.43438069E	0	-7.24	143.18
22.75	.33045857E	0	-9.62	129.23
24.50	.25191362E	0	-11.97	117.78
26.25	.19378667E	0	-14.25	108.29
28.00	.15084213E	0	-16.43	100.31
29.75	.11888138E	0	-18.50	93.51
31.50	.94830673E	-1	-20.46	87.63
33.25	.76508756E	-1	-22.33	82.50
35.00	.62378339E	-1	-24.10	77.96
36.75	.51351112E	-1	-25.79	73.93
38.50	.42649539E	-1	-27.40	70.31
40.25	.35711815E	-1	-28.94	67.04
42.00	.30127177E	-1	-30.42	64.07
43.75	.25591636E	-1	-31.84	61.37
45.50	.21877769E	-1	-33.20	58.89
47.25	.18813444E	-1	-34.51	56.61
49.00	.16267127E	-1	-35.77	54.50
50.75	.14137248E	-1	-36.99	52.55
52.50	.12344748E	-1	-38.17	50.73
54.25	.10827498E	-1	-39.31	49.04
56.00	.95363175E	-2	-40.41	47.46
57.75	.84319695E	-2	-41.48	45.98
59.50	.74829452E	-2	-42.52	44.59
61.25	.66637452E	-2	-43.53	43.29
63.00	.59536405E	-2	-44.50	42.06
64.75	.53356476E	-2	-45.46	40.89
66.50	.47957990E	-2	-46.38	39.79
68.25	.43225268E	-2	-47.29	38.75
70.00	.39062236E	-2	-48.16	37.77

-----DIGITAL FILTER RESPONSE-----

AMPLITUDE		AMPLITUDE (DB)	PHASE (DEG)
.99999899E	0	-.00	.00
.10000003E	1	.00	-14.90
.99999852E	0	-.00	-29.93
.99996977E	0	-.00	-45.24
.99968647E	0	-.00	-61.03
.99812491E	0	-.02	-77.56
.99196846E	0	-.07	-95.22
.97304348E	0	-.24	-114.44
.92658785E	0	-.66	-135.46
.83731652E	0	-1.54	-157.82
.70710623E	0	-3.01	-180.00
.56195645E	0	-5.01	159.82
.43044109E	0	-7.32	142.66
.32531127E	0	-9.75	128.51
.24619029E	0	-12.17	116.90
.18791284E	0	-14.52	107.26
.14506578E	0	-16.77	99.15
.11333449E	0	-18.91	92.22
.89575871E	-1	-20.96	86.23
.71569429E	-1	-22.91	80.98
.57756099E	-1	-24.77	76.33
.47035753E	-1	-26.55	72.19
.38625021E	-1	-28.26	68.46
.31959409E	-1	-29.91	65.09
.26627451E	-1	-31.49	62.01
.22325565E	-1	-33.02	59.20
.18827109E	-1	-34.50	56.62
.15961215E	-1	-35.94	54.23
.13597542E	-1	-37.33	52.02
.11635860E	-1	-38.68	49.96
.99983117E	-2	-40.00	48.04
.86239590E	-2	-41.29	46.25
.74646918E	-2	-42.54	44.56
.64822427E	-2	-43.77	42.98
.56460194E	-2	-44.97	41.49
.49313291E	-2	-46.14	40.08
.43181978E	-2	-47.29	38.74
.37902826E	-2	-48.43	37.48
.33342283E	-2	-49.54	36.28
.29390070E	-2	-50.64	35.13
.25955002E	-2	-51.72	34.04

ORIGINAL PAGE IS
OF POOR QUALITY

EQUIVALENT BAND PASS BUTTERWORTH FILTER

CUTOFF FREQUENCY = 4.00000 HERTZ
 AT 8.00000 HERTZ, RESPONSE IS DOWN 20.00 DB
 SAMPLING FREQUENCY = 200.00000
 CENTER FREQUENCY = 8.26000
 FILTER ORDER = 4

POLES OF H(S)

S(1) = .58628531E 1 -.64584236E 2
 S(2) = .37550135E 1 .41364616E 2
 S(3) = .12708332E 2 -.55632774E 2
 S(4) = .10511295E 2 .46014885E 2
 S(5) = .12708334E 2 .55632759E 2
 S(6) = .10511301E 2 -.46014885E 2
 S(7) = .58628740E 1 .64584236E 2
 S(8) = .37550287E 1 -.41364601E 2

MULT. CONST. = .39898788E 6 -.90625000E 0

POLES OF H(Z)

Z(1) = -.92196466E 0 -.30728192E 0
 Z(2) = -.96050315E 0 .20218227E 0
 Z(3) = -.90339794E 0 -.25796552E 0
 Z(4) = -.92421955E 0 .21703873E 0
 Z(5) = -.90339794E 0 .25796546E 0
 Z(6) = -.92421955E 0 -.21703870E 0
 Z(7) = -.92196477E 0 .30728193E 0
 Z(8) = -.96050315E 0 -.20218218E 0

MULT. CONST. = .12459860E -4 -.26452800E -10

BAND PASS BUTTERWORTH DIGITAL FILTER COEFFICIENTS

CON(1) = .59585995E -1 C(1) = -.18439293E 1 D(1) = .94444083E 0
 CON(2) = .61097219E -1 C(2) = -.19210063E 1 D(2) = .96344355E 0
 CON(3) = .58030448E -1 C(3) = -.18067959E 1 D(3) = .88267400E 0
 CON(4) = .58978208E -1 C(4) = -.18484391E 1 D(4) = .90128712E 0

ORIGINAL PAGE IS
 OF POOR QUALITY

FREQUENCY RESPONSE OF EQUIVALENT BAND PASS BUTTERWORTH FILTER

-----ANALOG FILTER RESPONSE-----				-----DIGITAL FILTER RESPONSE-----		
FREQUENCY (HERTZ)	AMPLITUDE	AMPLITUDE (DB)	PHASE (DEG)	AMPLITUDE	AMPLITUDE (DB)	PHASE (DEG)
-8.14	.10000004E 1	.00	-9.05	.10000057E 1	.00	-9.19
-7.74	.99998636E 0	-.00	-40.66	.99999295E 0	-.00	-41.28
-7.34	.99837199E 0	-.01	-76.06	.99819129E 0	-.02	-77.27
-6.94	.96472626E 0	-.31	-119.51	.96082525E 0	-.35	-121.60
-6.54	.74454318E 0	-2.56	-174.23	.72637487E 0	-2.78	-177.08
-6.14	.38637776E 0	-8.26	136.84	.36947789E 0	-8.65	134.57
-5.74	.17656187E 0	-15.06	105.22	.16809926E 0	-15.49	103.65
-5.34	.83407276E -1	-21.58	84.51	.79431928E -1	-22.00	83.36
-4.94	.41298046E -1	-27.68	69.70	.39373158E -1	-28.10	68.81
-4.54	.21152114E -1	-33.49	58.37	.20190318E -1	-33.90	57.66
-4.14	.11039237E -1	-39.14	49.29	.10549117E -1	-39.54	48.71
-3.74	.57868428E -2	-44.75	41.75	.55356006E -2	-45.14	41.28
-3.34	.30028380E -2	-50.45	35.32	.28751359E -2	-50.83	34.93
-2.94	.15174352E -2	-56.38	29.71	.14541053E -2	-56.75	29.39
-2.54	.73163728E -3	-62.71	24.72	.70160552E -3	-63.08	24.46
-2.14	.32715711E -3	-69.70	20.19	.31392067E -3	-70.06	19.98
-1.74	.12985132E -3	-77.73	16.01	.12466120E -3	-78.09	15.84
-1.34	.42378965E -4	-87.46	12.09	.40701466E -4	-87.81	11.97
-.94	.97175357E -5	?	8.36	.93356835E -5	?	8.28
-.54	.10219169E -5	?	4.76	.98194973E -6	?	4.72
-.14	.45437208E -8	?	1.23	.43664074E -8	?	1.22
.26	.54202038E -7	?	-2.28	.52085995E -7	?	-2.27
.66	.22998616E -5	?	-5.83	.22098155E -5	?	-5.77
1.06	.15939315E -4	-95.95	-9.47	.15311779E -4	-96.30	-9.37
1.46	.60946869E -4	-84.30	-13.24	.58527920E -4	-84.65	-13.11
1.86	.17412041E -3	-75.18	-17.23	.16713715E -3	-75.54	-17.05
2.26	.42073215E -3	-67.52	-21.50	.40363964E -3	-67.88	-21.28
2.66	.91648296E -3	-60.76	-26.16	.87868117E -3	-61.12	-25.89
3.06	.18694964E -2	-54.57	-31.32	.17910516E -2	-54.94	-30.99
3.46	.36632449E -2	-48.72	-37.15	.35065266E -2	-49.10	-36.74
3.86	.70267880E -2	-43.06	-43.88	.67197245E -2	-43.45	-43.38
4.26	.13402423E -1	-37.46	-51.82	.12803113E -1	-37.85	-51.21
4.66	.25785751E -1	-31.77	-61.49	.24604380E -1	-32.18	-60.74
5.06	.50776614E -1	-25.89	-73.70	.48392773E -1	-26.30	-72.75
5.46	.10389743E 0	-19.67	-89.95	.98921716E -1	-20.09	-88.69
5.86	.22312994E 0	-13.03	-113.23	.21253259E 0	-13.45	-111.48
6.26	.48378450E 0	-6.31	-149.61	.46442635E 0	-6.66	-147.10
6.66	.84043641E 0	-1.51	157.19	.82661960E 0	-1.65	159.93
7.06	.98424754E 0	-.14	105.25	.98242663E 0	-.15	107.03
7.46	.99950009E 0	-.00	64.86	.99944801E 0	-.00	65.86
7.86	.99999610E 0	-.00	30.89	.10000098E 1	.00	31.36
8.26	.99999716E 0	-.00	.00	.10000079E 1	.00	-.00
8.66	.99999577E 0	-.00	-29.41	.10000018E 1	.00	-29.89
9.06	.99976863E 0	-.00	-58.52	.99974666E 0	-.00	-59.56
9.46	.99950620E 0	-.04	-88.77	.99943479E 0	-.05	-90.53
9.86	.95991590E 0	-.36	-122.06	.95414702E 0	-.41	-124.83
10.26	.83325767E 0	-1.58	-158.63	.81351707E 0	-1.79	-162.42
10.66	.61383629E 0	-4.24	166.76	.58415818E 0	-4.67	162.77
11.06	.40831520E 0	-7.78	139.75	.38159353E 0	-8.37	136.20
11.46	.26824693E 0	-11.43	120.27	.24820760E 0	-12.10	117.21
11.86	.18097746E 0	-14.85	106.02	.16644793E 0	-15.57	103.34
12.26	.12640179E 0	-17.96	95.20	.11573060E 0	-18.73	92.78
12.66	.91222431E -1	-20.80	86.67	.83193614E -1	-21.60	84.45
13.06	.67748445E -1	-23.38	79.76	.61554608E -1	-24.21	77.68
13.46	.51569028E -1	-25.75	74.01	.46680742E -1	-26.62	72.04
13.86	.40091330E -1	-27.94	69.15	.36155239E -1	-28.84	67.26
14.26	.31740921E -1	-29.97	64.97	.28515299E -1	-30.90	63.15
14.66	.25530303E -1	-31.86	61.33	.22846058E -1	-32.82	59.56
15.06	.20820744E -1	-33.63	58.13	.18556894E -1	-34.63	56.40
15.46	.17187975E -1	-35.30	55.29	.15256100E -1	-36.33	53.60
15.86	.14343151E -1	-36.87	52.74	.12677185E -1	-37.94	51.08
16.26	.12085054E -1	-38.36	50.45	.10635035E -1	-39.47	48.81
16.66	.10270842E -1	-39.77	48.38	.89983196E -2	-40.92	46.76
17.06	.87973780E -2	-41.11	46.49	.76722045E -2	-42.30	44.88
17.46	.75887241E -2	-42.40	44.75	.65871751E -2	-43.63	43.16
17.86	.65883562E -2	-43.62	43.16	.56914264E -2	-44.90	41.57
18.26	.57536070E -2	-44.80	41.69	.49459078E -2	-46.12	40.11
18.66	.50517955E -2	-45.93	40.33	.43207919E -2	-47.29	38.75
19.06	.44576891E -2	-47.02	39.06	.37930137E -2	-48.42	37.48
19.46	.39515081E -2	-48.06	37.88	.33446169E -2	-49.51	36.30
19.86	.35177202E -2	-49.07	36.77	.29614259E -2	-50.57	35.20
20.26	.31439202E -2	-50.05	35.74	.26321812E -2	-51.59	34.16
20.66	.28201987E -2	-50.99	34.76	.23478746E -2	-52.59	33.18
21.06	.25384921E -2	-51.91	33.85	.21012156E -2	-53.55	32.26
21.46	.22922720E -2	-52.79	32.98	.18862814E -2	-54.49	31.39
21.86	.20761760E -2	-53.65	32.17	.16982292E -2	-55.40	30.57
22.26	.18857677E -2	-54.49	31.39	.15330651E -2	-56.29	29.79
22.66	.17173959E -2	-55.30	30.66	.13874755E -2	-57.16	29.05
23.06	.15679856E -2	-56.09	29.96	.12587148E -2	-58.00	28.34
23.46	.14349716E -2	-56.86	29.30	.11444694E -2	-58.83	27.67
23.86	.13161936E -2	-57.61	28.66	.10427990E -2	-59.64	27.03
24.26	.12098208E -2	-58.35	28.06	.95206302E -3	-60.43	26.41
24.66	.11142843E -2	-59.06	27.48	.87086443E -3	-61.20	25.83

Nonrecursive Lowpass Filters

This program can be used to generate filters with an odd number of taps, up to 51, weighted by a Kaiser window with $\beta = 3.384$. The required input parameters for each filter design are as follows:

FREQC	"Cutoff" frequency
FREQS	Sampling frequency
PNMAX	Number of taps to the right (or left) of the center tap. ($N/2$ in the notation of Appendix C.)

These parameters are input on one data card as floating point numbers, separated by commas. The frequency FREQC is not the actual design cutoff frequency of the filter. It is in fact the 6 dB point of the filter, and must be chosen properly to place the 3 dB point of the filter at the desired cutoff frequency. The details of selecting FREQC are discussed in Section 4 of [C-2]. In general, FREQC will be somewhat greater than the desired 3-dB cutoff frequency.

The program gives as output the tap weights $h_{N/2+j}$, $j=0, 1, \dots, N/2$, with the remaining $N/2$ chosen by symmetry. The program also outputs the equivalent white-noise bandwidth of the filter, which serves as a useful check on the bandwidth, and the frequency response from zero to four times FREQC at increments of one-tenth FREQC. A listing and a sample output is given in the following pages.

C NONRECURSIVE LOWPASS FILTER GENERATOR WITH KAISER WINDOW
C
C

```

      REAL IOLOW
      DIMENSION C(25)
      PI=3.1415926
      LDI=7
      LDO=6
1    READ (LDI,-) FC,FS,PMAX
      NMAX=PMAX
      IF (NMAX.GT.25) NMAX=25
      FCT=FC/FS
      BETA=3.384
      WRITE (LDO,603) FS,FC
603  FORMAT (1H1,/,7X,27HNONRECURSIVE LOWPASS FILTER,/,
      $10X,16HSAMPLING RATE = ,F9.3,3H HZ,/,
      $10X,17H6-DB FREQUENCY = ,F8.3,3H HZ,/,
      $13X,1HJ,5X,6HWINDOW,10X,4HSINC,10X,8HH(N/I+J),/)
      N=0
      WN=1.
      HN=2.*FCT
      CO=HN
      ENBW=CO*CO
      WRITE (LDO,601) N,WN,HN,CO
      AI=IOLOW(BETA)
      XNSQ=FLOAT(NMAX)**2
      DO 100 N=1,NMAX
      XN=N
      FACT=SQRT(1.-XN*XN/XNSQ)
      ARG=FACT*BETA
      WN=IOLOW(ARG)/AI
      XX=2.*PI*XN*FCT
      HN=2.*FCT*SIN(XX)/XX
      C(N)=WN*HN
      ENBW=ENBW+2.*C(N)**2
100  WRITE (LDO,601) N,WN,HN,C(N)
601  FORMAT (10X,I4,3E15.6)
      ENBW=ENBW*FS
      WRITE (LDO,604) ENBW
604  FORMAT (/,10X,33HTWO-SIDED WHITE NOISE BANDWIDTH =,F9.3,3H HZ)
      WRITE (LDO,605)
605  FORMAT (1H1,10X,20HFREQUENCY RESPONSE--,/)
      $17X,9HFREQUENCY,7X,9HAMPLITUDE,/
      $18X,7H(HERTZ),11X,4H(DB),/)
      FINC=0.1*FC
      FMAX=4.*FC
      F=-FINC
150  F=F+FINC
      IF (F.GT.FMAX) GO TO 1
      WT=2.*PI*F/FS
      H=2.*FCT
      DO 200 N=1,NMAX
200  H=H+2.*C(N)*COS(N*WT)
      HH=H*H
      HDB=10.*ALOG10(HH)

```

```
WRITE (LD0,602) F,HDB
602 FORMAT (10X,2F15.3)
GO TO 150
END
```

```
REAL FUNCTION IOLOW(BFARG)
DATA A1,A2,A3,A4,A5,A6/3.5156229,3.0899424,1.2067492,
$ 0.2659732,0.0360768,0.0045813/
T=BFARG/3.75
TT=T*T
IOLOW=((((A6*TT+A5)*TT+A4)*TT+A3)*TT+A2)*TT+A1)*TT+1.
RETURN
END
END$
```

NONRECURSIVE LOWPASS FILTER

SAMPLING RATE = 1000.000 HZ

6-DB FREQUENCY = 121.000 HZ

J	WINDOW		SINC		H(N/I+J)	
0	.100000E	1	.242000E	0	.242000E	0
1	.996473E	0	.219352E	0	.218578E	0
2	.985947E	0	.158954E	0	.156720E	0
3	.968583E	0	.804648E	-1	.779368E	-1
4	.944648E	0	.798661E	-2	.754453E	-2
5	.914505E	0	-.390188E	-1	-.356829E	-1
6	.878612E	0	-.524496E	-1	-.460829E	-1
7	.837508E	0	-.372856E	-1	-.312270E	-1
8	.791804E	0	-.794628E	-2	-.629190E	-2
9	.742174E	0	.187629E	-1	.139254E	-1
10	.689338E	0	.308309E	-1	.212529E	-1
11	.634050E	0	.252699E	-1	.160224E	-1
12	.577085E	0	.787936E	-2	.454706E	-2
13	.519222E	0	-.108410E	-1	-.562891E	-2
14	.461232E	0	-.213434E	-1	-.984428E	-2
15	.403864E	0	-.194754E	-1	-.786541E	-2
16	.347830E	0	-.778620E	-2	-.270827E	-2
17	.293794E	0	.656336E	-2	.192827E	-2
18	.242360E	0	.159050E	-1	.385473E	-2
19	.194066E	0	.159654E	-1	.309835E	-2
20	.149371E	0	.766743E	-2	.114529E	-2

TWO-SIDED WHITE NOISE BANDWIDTH = 226.625 HZ

FREQUENCY RESPONSE--

FREQUENCY (HERTZ)	AMPLITUDE (DB)
0.000	.039
12.100	-.004
24.200	-.039
36.300	.014
48.400	.039
60.500	-.032
72.600	-.029
84.700	.070
96.800	-.295
108.900	-2.021
121.000	-6.043
133.100	-13.653
145.200	-28.876
157.300	-41.612
169.400	-64.177
181.500	-47.916
193.600	-55.243
205.700	-53.495
217.800	-56.301
229.900	-58.041
242.000	-58.109
254.100	-61.939
266.200	-59.998
278.300	-65.430
290.400	-61.863
302.500	-68.734
314.600	-63.682
326.700	-72.003
338.800	-65.495
350.900	-75.497
363.000	-67.328
375.100	-79.535
387.200	-69.272
399.300	-85.214
411.400	-71.337
423.500	-96.882
435.600	-73.761
447.700	-92.987
459.800	-76.781
471.900	-85.166
484.000	-81.121

APPENDIX E

USE OF THE SIMULATION PROGRAMS

APPENDIX E

USE OF THE SIMULATION PROGRAMS

This appendix contains program listings and detailed instructions for use of the three simulation programs. The programs are listed in FORTRAN suitable for execution on the Datacraft 6024/5 digital computer. Card decks, listings, and sample runs in UNIVAC 1108-compatible FORTRAN have been delivered separately.

General Remarks on Program Input

All input to the FDM/FM, NRZ/PSK, and SP/PSK Programs are field-formatted and must contain decimals.

For each program, the TWT amplitude and phase data is input on cards and must appear only once in a set of simulations. The amplitude and phase data consists of two 151-entry tables of normalized amplitude and phase characteristics corresponding to input levels 0.0 through 1.50 at discrete intervals of 0.01. Each table is contained on 16 cards using FORTRAN Format 10F8.4. Note that the amplitude table is expressed as normalized output voltage versus normalized input voltage, and the phase table is expressed in degrees versus normalized input voltage.

The remainder of the required card input is dependent on the program being run and is described below. The simulations are time-scaled by a factor 10^6 ; thus data rates should be entered in megabits per second, frequencies in MHz, and the PLL gain (in the FDM/FM program) in MHz per volt.

Input for FDM/FM Program

CARD 1

- | | |
|---------|-------------------------------------------------------------------------------------------------------------|
| CC 1-10 | Total number of samples for this simulation. |
| CC11-20 | Number of samples to process prior to or plotting. |
| CC21-30 | Output options:

= 0. No plot desired.

= 1. Generates plot of Butterworth bandpass PSK filter. |

- = 2. Plots Chebyshev lowpass TV filter output.
- = 3. Plots phase-lock loop output.
- = 4. Intermediate print option (Diagnostic).

Signal to noise ratio computations and bit error probabilities are included with each output selection.

CC31-40 Filter selection:

- = 0. Bypass TV and PSK filters.
- = 1. Pass PLL output through Butterworth PSK filter.
- = 2. Pass PLL output through Chebyshev lowpass TV filter.
- = 3. Pass PLL output through both PSK and TV filters.

CC41-50 Plot scale factor. This field may be left blank if plotting not requested.

CC51-60 PLL gain in MHz/volt.

Data parameters on Card 2 are required by FUNCTION SIGIN to generate samples of the complex envelope. Both the analog and PSK signals may be filtered prior to multiplexing.

CARD 2

- CC 1-10 PSK bit data rate of input signal, Mb/s.
- CC11-20 Zero-peak deviation of PSK input signal, MHz.
- CC21-30 Carrier amplitude.
- CC31-40 Filter selection:
 - = 0. Do not filter input signal.
 - = 1. Filter PSK signal with 4th order Butterworth bandpass filter.

- = 2. Filter analog with 8th order Chebyshev low pass filter.
- = 3. Filter both incoming signals prior to multiplexing.

CC41-50 Number of tones in analog signal (TV).

For each tone in analog signal, one Card 2A is required to define its frequency and zero-peak deviation. If no tones are requested, Card 2A must be omitted. The maximum number of tones which may be specified is 15.

CARD 2A

CC 1-10 Tone frequency, MHz.

CC11-20 Zero-peak deviation in MHz.

Card 3 specifies the uplink noise and filter selection required by FUNCTION TWTOUT to compute the complex envelope of the TWT input.

CARD 3

CC 1-10 Uplink noise spectral density.

CC11-20 Seven digit odd number.

CC21-30 Seven digit odd number.

CC31-40 TWT input filter selection:

- 0. = 400 MHz bandwidth filter at TWT input.
- 1. = 225 MHz bandwidth filter at TWT input.
- 2. = 88 MHz bandwidth filter at TWT input.

Card 4 inputs the downlink noise spectral density required to compute the complex envelope of the IF filter input (FUNCTION IFIN).

CARD 4

CC 1-10 Downlink noise spectral density.
CC11-20 Seven digit odd number.
CC21-30 Seven digit odd number.

The last card specifies correlator delay, and print interval of the evaluator module, SUBROUTINE EVAL, which determines error probability of PSK signal and signal-to-noise ratios of each of the tone frequencies.

CARD 5

CC 1-10 Correlator delay, samples.
CC11-20 Print option:
 0. = Suppress intermediate PSK correlation results.
 1. = Print correlation results.
 Enter 0. if plotted output requested or only bit error computations desired.
CC21-30 Correlation print interval, bits.

A typical input deck is illustrated in Figure E-1. Cards 1 through 5 represent one simulation. Multiple simulations using the same TWT amplitude and phase data are accomplished by repeating cards 1-5. A listing of the program is given below.

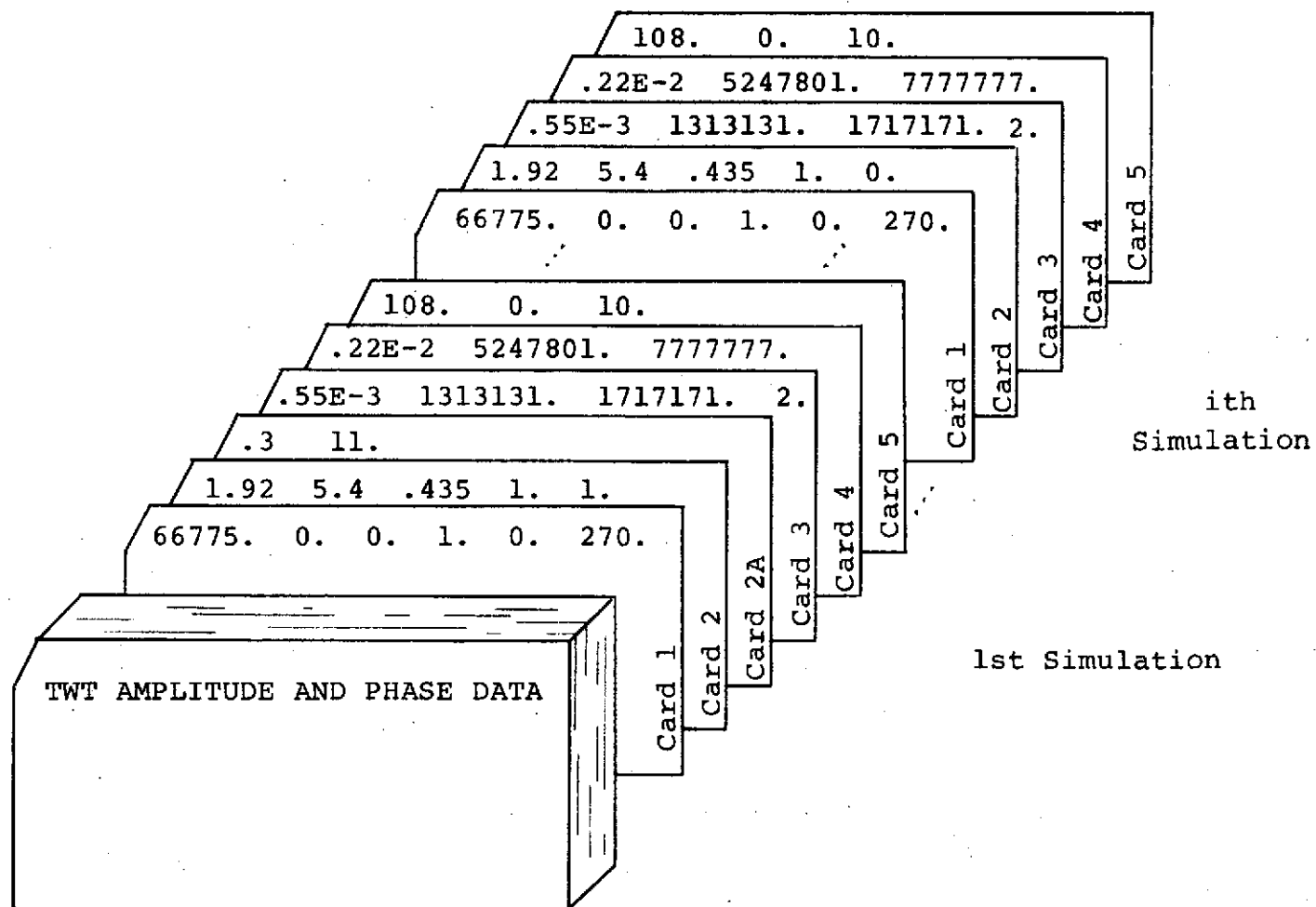


FIGURE E-1. SAMPLE INPUT DECK FOR FDM/FM SIMULATION

IF (NFILT.EQ.2) GO TO 12
IF(NFILT.EQ.0) GO TO 20

8.5 HZ DEMUX FILTER (CENTERED AT 8.26 HZ)

4TH ORDER BANDPASS BUTTERWORTH FILTER, 4HZ BANDWIDTH

11 UA=Y
VA = .18439293E+01 * VA1 - .94444083E+00 * VA2 + .59585995E-01
1 * (UA - UA2)
VB = .19210063E+01 * VB1 - .96344355E+00 * VB2 + .61097219E-01
1 * (VA - VA2)
VC = .18067959E+01 * VC1 - .88267400E+00 * VC2 + .58030448E-01
1 * (VB - VB2)
VD = .18484391E+01 * VD1 - .90128712E+00 * VD2 + .58978208E-01
1 * (VC - VC2)

UA2 = UA1
UA1 = UA
VA2 = VA1
VA1 = VA
VB2 = VB1
VB1 = VB
VC2 = VC1
VC1 = VC
VD2 = VD1
VD1 = VD
YPSK = VD

IF(NFILT.NE.3) GO TO 20

TV DEMUX FILTER

8TH ORDER CHERYSHEV LOWPASS FILTER WITH 4.2 HZ BANDWIDTH

12 PA=Y
QA = 0.19710976E+01 * QA1 - 0.98858843E+00 * QA2
1 + 0.43727169E-02 * (PA + PA1 + PA1 + PA2)
QB = 0.19551096E+01 * QB1 - 0.96780426E+00 * QB2
1 + 0.31736721E-02 * (QA + QA1 + QA1 + QA2)
QC = 0.19460172E+01 * QC1 - 0.95212002E+00 * QC2
1 + 0.15256969E-02 * (QB + QB1 + QB1 + QB2)
QD = 0.19422053E+01 * QD1 - 0.94369894E+00 * QD2
1 + 0.37339903E-03 * (QC + QC1 + QC1 + QC2)

PA2 = PA1
PA1 = PA
QA2 = QA1
QA1 = QA
QB2 = QB1
QB1 = QB
QC2 = QC1
QC1 = QC
QD2 = QD1
QD1 = QD

YTONES = QD

20 CONTINUE

IF (NN.LE.NHOLD) GO TO 100

IF (NP.EQ.0) GO TO 100

IF (NP.EQ.4) GO TO 80

SELECTIVE FILTER PLOT OUTPUT

IF (NP.EQ.1) ZZ = SCAF*YPSK + 41.5

IF (NP.EQ.2) ZZ = SCAF*YTONES + 41.5

IF (NP.EQ.3) ZZ = SCAF*Y + 41.5

NZ=ZZ

IF (NZ.GT.81) NZ=81

IF (NZ.LT.1) NZ=1

NGRAPH(41)=JDOT

NGRAPH(NZ)=JPLL

WRITE(LD0,601) NN,NGRAPH,ER,Y,YPSK,YTONES

601 FORMAT(I5,81A1,2X,4F9.4)

NGRAPH(NZ)=JBLANK

GO TO 100

80 WRITE(LD0,999) NN,YMSGG,YMSG,SIGC,SIGS,TINC,TINS,AIN,AOUT,PHOUT,

1 TOUTC,TOUTS,CIFIN,SIFIN,YR,YI,THETA,ER,Y,VD

999 FORMAT (I6,9F12.6,/,5X,10F12.6)

100 CALL EVAL(NN,UNC,UNS,DNC,DNS,ER,YPSK,YTONES,KOUNT)

CALL EVAL(-1,UNC,UNS,DNC,DNS,ER,YPSK,YTONES,KOUNT)

GO TO 1

END

READ TWT INPUT AMPLITUDE AND PHASE

SUBROUTINE TWTSET

COMMON AMPNL(151),PHNL(151)

COMMON /LUNITS/ LDI,LD0

READ(LDI,701) AMPNL

READ(LDI,701) PHNL

701 FORMAT (10F8.4)

RETURN

END

SUBROUTINE EVAL(NN,UNC,UNS,DNC,DNS,ER,Y,YF,KOUNT)

COMMON/QSIG/YMSGG,YMSG,AMP,S1,S2,BRATE

COMMON/QXTRA/FREQQ,FQ(15),NTONES

COMMON /LUNITS/ LDI,LD0

DIMENSION NBIT(63)

```

:      63 BIT PN DATA SEQUENCE
:
DATA NBIT/ 1,1,1,1,1,1,-1,-1,-1,-1,-1,1,-1,-1,-1,-1,1,1,
$ -1,-1,-1,1,-1,1,-1,-1,1,1,1,-1,1,-1,-1,-1,1,1,1,-1,-1,-1,
$ 1,-1,1,1,-1,1,1,1,-1,1,1,-1,-1,1,1,-1,1,-1,1/
:
IF(NN.EQ.0) GO TO 3
IF(NN.GT.NSKIP) GO TO 1
IF(NN.LT.0) GO TO 2
RETURN
:
3 PDNC=0.
  PDNS=0.
  PUNC=0.
  PUNS=0.
  ERSQ=0.
  PYF=0.
  PYFC=0.
  PYFS=0.
  NBITS = 0
  NERR = 0
  IBIT = 60
  CORR = 0.
  T=1./200.
  TBIT=1./BRATE
  TIME=-T
  READ(LDI,667) DNSKIP,DNP,DIPRNT
667 FORMAT(8F10.5)
  NSKIP = DNSKIP
  NP = DNP
  IPRINT = DIPRNT
  FCOR = FQ(1)
  IF(NTONES.EQ.0) FCOR=FREQQ
  XD = 6.2831853072*T
  DEL=XD*FQ(1)
  DELPSK=XD*FREQQ
  WRITE(LDO,603) NSKIP
603 FORMAT(20X,'CORRELATOR DELAY = ',I5,' SAMPLES'//)
  IF (NP.NE.0) WRITE (LDO,600)
600 FORMAT(/,15X,'TIME'9X'QERSQ',4X'POPS'3X'BITS   ERRS'
  $11X,'QYF',10X,'QYFCOR'/)
  RETURN
:
1 PDNC=PDNC+DNC*DNC
  PDNS=PDNS+DNS*DNS
  PUNC=PUNC+UNC*UNC
  PUNS=PUNS+UNS*UNS
  ERSQ=ERSQ+ER*ER
  PYF=PYF+YF*YF
  NDEL = NN-NSKIP
  XNORM=1./FLOAT(NDEL)
  X=DELPSK*FLOAT(NDEL)
  CORR = CORR + Y*SIN(X)*T
  IF(NTONES.LE.0) GO TO 20
  TME=FLOAT(NN)*DEL

```

```

C=COS(TME)
S=SIN(TME)
PYFC=PYFC+YF*C
PYFS=PYFS+YF*S
20 TIME=TIME+T
IF(TIME.LT.TBIT)RETURN
TIME = TIME - TBIT
MBIT = 1
IF(CORR.LT.0) MBIT = -1
IBIT = IBIT + 1
IF(IBIT.GT.63) IBIT=1
IF(MBIT.NE.NBIT(IBIT)) NERR=NERR+1
NBITS=NBITS+1
CORR=0.
IF(NP.NE.1) RETURN
IF(IPRINT.EQ.0) GO TO 2
IF(MOD(NBITS,IPRINT).NE.0) RETURN

2 QDNC=PDNC*XNORM
QDNS=PDNS*XNORM
QUNC=PUNC*XNORM
QUNS=PUNS*XNORM
QERSQ=ERSQ*XNORM
QYF=PYF*XNORM
QYFCOR=2.*XNORM*XNORM*(PYFC*PYFC+PYFS*PYFS)
IF(NN.NE.-1)
$WRITE(LD0,601)NN,QERSQ,KOUNT,NBITS,NERR,QYF,QYFCOR
601 FORMAT(9X,I10,2X,F12.4,3(2X,I5),2(2X,F14.4))
IF(NN.GT.0) RETURN

4 ACTNUP=0.5*(QUNC+QUNS)/400.
ACTNDN=0.5*(QDNC+QDNS)/400.
ACTIF=ACTNDN*35.*1.026
RMSER=SQRT(QERSQ)
PFNONS=QYF-QYFCOR
SNRFDB = -99.99
IF(PFNONS.LE.0.0) SNRFDB = 999.99
IF((QYFCOR.NE.0.).AND.(SNRFDB.LT.0.)) SNRFDB =
110.*ALOG10(QYFCOR/PFNONS)
ERR = NERR
BITS=NBITS
PE=ERR/BITS
WRITE(LD0,602)ACTNUP,ACTNDN,ACTIF,RMSER
602 FORMAT (//,25X,'ACTUAL UPLINK NOISE SPECTRAL DENSITY =',E13.6,//
$ 25X,'ACTUAL DOWNLINK NOISE SPECTRAL DENSITY =',E13.6,//
$ 25X,'ACTUAL NOISE POWER IN IF =',E13.6,//
$ 25X,'PLL RMS PHASE ERROR =',F8.4,/)
IF(NTONES.NE.0) WRITE(LD0,609) FCOR,SNRFDB
609 FORMAT(25X,'SIGNAL POWER MEASURED AT 'F7.3,' HZ'//
$ 25X,'DEMUX FILTER OUTPUT SNR =',F6.2,' DB',/)
WRITE(LD0,610) NBITS,PE
610 FORMAT(25X,'ERROR PROBABILITY AFTER ',I5,' BITS: ',E12.6)
RETURN
END

```


COMPLEX FUNCTION SIGIN(I)

COMPLEX SIG
COMMON/QSIG/YMSGG,YMSG,AMP,SIG,BRATE
COMMON/QXTRA/FREQQ,FREQ(15),NTONES
COMMON /LUNITS/ LDI,LDO
DIMENSION DEV(15),DEL(15),NBIT(63)

63 BIT PN DATA SEQUENCE

DATA NBIT/ 1,1,1,1,1,1,-1,-1,-1,-1,-1,1,-1,-1,-1,-1,1,1,
\$ -1,-1,-1,1,-1,1,-1,-1,1,1,1,1,-1,1,-1,-1,-1,1,1,-1,-1,
\$ 1,-1,1,1,-1,1,1,1,-1,1,1,-1,-1,1,1,-1,1,-1/

IF (I.GT.0) GO TO 1
TWOPI = 6.2831853072
YINT=0.
FREQQ = 8.5
T=1./400.
IBIT = 61
DTV = 0.
VA1 = 0.
VA2 = 0.
UA1 = 0.
UA2 = 0.
VB1 = 0.
VB2 = 0.
VC1 = 0.
VC2 = 0.
VD=0.
VD1=0.
VD2 = 0.
PA1 = 0.0
PA2 = 0.0
QA1 = 0.0
QA2 = 0.0
QB1 = 0.0
QB2 = 0.0
QC1 = 0.0
QC2 = 0.0
QD1 = 0.0
QD2 = 0.0
YMSG = 0.
YMSGG = 0.

PSK/FM DATA
READ(LDI,600) BRATE,DEVV,AMP,DTYPE,DTONES
NTYPE = DTYPE
NTONES = DTONES
600 FORMAT(8F10.5)
NFLAG = NTYPE +1

```

      AMP100=100.*AMP
      WRITE(LD0,601) FREQQ,BRATE,DEVV
601  FORMAT(1H1,/,/,20X,'MULTIPLEX PSK-TONE FM SIGNAL',/,/,
      $20X,'SUBCARRIER FREQUENCY =',F7.3,' HZ',/
      $20X,'DATA RATE =',F7.3,' BITS PER SECOND',/
      $20X,'ZERO-PEAK DEVIATION =',F7.3,' HZ')
      IF(NTYPE.EQ.1.OR.NTYPE.EQ.3) WRITE(LD0,607)
607  FORMAT(20X,'BANDPASS FILTER (4 HZ PASSBAND)')
      DELL = TWOPI*FREQQ*T
      TIME=-T
      SIGN = TWOPI*DEVV
      MULTIPLEX TONE DATA
      IF(NTONES.EQ.0) GO TO 55
      WRITE(LD0,604)
604  FORMAT(/,20X'TONE NUMBER'5X'TONE FREQUENCY'5X,
      $5X,'ZERO-PEAK DEVIATION')
605  FORMAT(24X,I2,13X,F8.3,14X,F8.3)
      DO 5 K=1,NTONES
      READ(LDI,600) FREQ(K),DEV(K)
      WRITE(LD0,605) K,FREQ(K),DEV(K)
      DEV(K) = TWOPI*DEV(K)
      5 DEL(K) = TWOPI * FREQ(K) * T
      55 TBIT=1./BRATE
      IF(NTYPE.EQ.3.OR.NTYPE.EQ.2) WRITE(LD0,608)
608  FORMAT(20X,'LOWPASS FILTER (4.2 HZ CUTOFF)')
      WRITE(LD0,606) AMP100
606  FORMAT(/20X,'CARRIER AMPLITUDE = 'F7.2,' PERCENT OF SATURATING VAL
      $UE')
      SIGIN=CMPLX(AMP,0.)
      RETURN
C
      1 FLOATI = FLOAT(I)
      Z4=YMSGG
      Z3=YMSG
      X=DELL*FLOATI
      TIME=TIME+T
      IF (TIME.LT.TBIT) GO TO 2
      TIME=TIME-TBIT
      IBIT = IBIT + 1
      IF(IBIT.GT.63) IBIT = 1
      2 YMSGG = SIGN*NBIT(IBIT)*SIN(X)
      UA = YMSGG
      Z2=YMSGG
C
      GO TO (200,100,200,100),NFLAG
C
C
C
C
      14107AUG74      4TH ORDER BANDPASS BUTTERWORTH FILTER
      FREQC = 4HZ., FREQO = 8.26HZ., FREQS = 400HZ.
C
      100 VA = .19454935E+01 * VA1 - .97129095E+00 * VA2 + .30772486E-01
      1 * (UA - UA2)
      VB = .19707495E+01 * VB1 - .98143707E+00 * VB2 + .31050632E-01
      1 *(VA - VA2)
      VC = .19190234E+01 * VC1 - .93870344E+00 * VC2 + .30308505E-01

```

```

1 *(VB -VB2)
VD = .19353782E+01 * VD1 - .94894032E+00 * VD2 + .30517427E-01
1 *(VC - VC2)

```

C

```

UA2 = UA1
UA1 = UA
VA2 = VA1
VA1 = VA
VB2 = VB1
VB1 = VB
VC2 = VC1
VC1 = VC
VD2 = VD1
VD1 = VD
Z2=VD
Z4=VD2

```

C

```

200 YMSG=0.
DO 10 K=1,NTONES
X=FLOATI*DEL(K)
10 YMSG = YMSG + COS(X) * DEV(K)
PA = YMSG
Z1=YMSG

```

C

```

GO TO (1000,1000,300,300),NFLAG

```

C

C

C

C

```

212829MAY74      8TH ORDER CHERYSHEV LOWPASS FILTER
FREQC = 4.2 HZ., FREQS = 400 HZ.

```

```

300 QA = 0.19898751E+01 * QA1 - 0.99426523E+00 * QA2
1 + 0.10975364E-02 * (PA + PA1 + PA1 + PA2)
QB = 0.19805498E+01 * QB1 - 0.98375002E+00 * QB2
1 + 0.80004320E-03 * (QA + QA1 + QA1 + QA2)
QC = 0.19742253E+01 * QC1 - 0.97576796E+00 * QC2
1 + 0.38565702E-03 * (QB + QB1 + QB1 + QB2)
QD = 0.19710921E+01 * QD1 - 0.97147012E+00 * QD2
1 + 0.94504691E-04 * (QC + QC1 + QC1 + QC2)

```

C

```

PA2 = PA1
PA1 = PA
QA2 = QA1
QA1 = QA
QB2 = QB1
QB1 = QB
QC2 = QC1
QC1 = QC
QD2 = QD1
QD1 = QD
Z1=QD
Z3=QD2

```

C

```

1000 DTV = DTV + .5 * T *(Z1+Z2+Z3+Z4)
SIG=AMP*CEXP(CMPLX(0.,DTV))
SIGIN=SIG
RETURN

```

END

```
C
C GENERATE COMPLEX ENVELOPE OF TWT OUTPUT
C
C COMPLEX FUNCTION TWTOUT(I)
C
  COMPLEX TWTIN,SIGIN,EPHASE(151)
  COMPLEX TOUT,R,R1,R2,R3,R4,R5,R6,R7,R8,R9,R10,R11,R12,R13,R14,
  # R15,R16
  COMMON AMP(151),PHASE(151)
  COMMON/QTWT/ XC,XS,TWTIN,TAMP,F,G,TOUT
  COMMON /LUNITS/ LDI,LDO
  DIMENSION C225(9),C88(9)
  DATA C225,C88/.6050,.294555,-.0892072,-.0474876,.0531323,
  # -.0027382,-.0196636,.0081931,.0028632,.2495,.219805,.145547,
  # .0614483,.0003447,-.0244838,-.0214247,-.0087023,-.0000747/

  IF (I.GT.0) GO TO 1
  TWTIN=SIGIN(I)
  R = CMPLX(0.,0.)
  R1= CMPLX(0.,0.)
  R2 = CMPLX(0.,0.)
  R3 = CMPLX(0.,0.)
  R4 = CMPLX(0.,0.)
  R5 = CMPLX(0.,0.)
  R6 = CMPLX(0.,0.)
  R7 = CMPLX(0.,0.)
  R8 = CMPLX(0.,0.)
  R9 = CMPLX(0.,0.)
  R10= CMPLX(0.,0.)
  R11= CMPLX(0.,0.)
  R12= CMPLX(0.,0.)
  R13= CMPLX(0.,0.)
  R14= CMPLX(0.,0.)
  R15= CMPLX(0.,0.)
  R16= CMPLX(0.,0.)
  AIN=REAL(TWTIN)
  INDEX=IFIX(100.*AIN)+1
  AOUT=AMP(INDEX)
  A100=100.*AOUT
  READ(LDI,600) UNOISE,UI,UJ,UNFTWT
  ISTART = UI
  JSTART = UJ
  NFTWT = UNFTWT
600 FORMAT(8F10.5)
  IF(NFTWT.EQ.0) NBWIN = 400
  IF(NFTWT.EQ.1) NBWIN = 225
  IF(NFTWT.EQ.2) NBWIN = 88
  WRITE(LDO,601) UNOISE, ISTART,JSTART,NBWIN,A100
601 FORMAT (/20X,'UPLINK NOISE SPECTRAL DENSITY =' ,E13.6, /
  $20X,'UPLINK NOISE SEEDS:',I8,I9, //
  $20X,'TWT INPUT BANDWIDTH = ' ,I4, ' HZ', //
```

```

$20X,'NOMINAL OUTPUT AMPLITUDE =',F7.2,' PERCENT OF SATURATION',/)
CC = 3.1415926536/180.
DO 10 N=1,151
10 EPHASE(N)=CEXP(CMPLX(0.,CC*PHASE(N)))
ALPHA=400.*UNOISE
ALPHA=SQRT(ALPHA)
IF(NFTWT.EQ.0) RETURN

C
IF(NFTWT.EQ.1) GO TO 11
C0 = C88(1)
C1 = C88(2)
C2 = C88(3)
C3 = C88(4)
C4 = C88(5)
C5 = C88(6)
C6 = C88(7)
C7 = C88(8)
C8 = C88(9)
RETURN

C
11 C0 = C225(1)
C1 = C225(2)
C2 = C225(3)
C3 = C225(4)
C4 = C225(5)
C5 = C225(6)
C6 = C225(7)
C7 = C225(8)
C8 = C225(9)
RETURN

C
1 XC=ALPHA*RNG(ISTART)
XS=ALPHA*RNG(JSTART)
TWTIN=SIGIN(I)+CMPLX(XC,XS)
IF(NFTWT.EQ.0) GO TO 2
R = TWTIN
TWTIN = C8*(R+R16) + C7*(R1+R15) + C6*(R2+R14) + C5*(R3+R13) +
$ C4*(R4+R12) + C3*(R5+R11) + C2*(R6+R10) + C1*(R7+R9) + C0*R8

C
R16 = R15
R15=R14
R14=R13
R13=R12
R12=R11
R11=R10
R10=R9
R9=R8
R8=R7
R7=R6
R6=R5
R5=R4
R4=R3
R3=R2
R2=R1
R1=R

```

C

```

2 TAMP=CABS(TWTIN)
  INDEX=IFIX(100.*TAMP)+1
  IF (INDEX.GT.151) INDEX=151
  F=AMP(INDEX)
  G=PHASE(INDEX)
  TOUT=F*TWTIN*EPHASE(INDEX)/TAMP
  TWTOUT=TOUT
  RETURN
  END

```

C

C GENERATE COMPLEX ENVELOPE OF IF FILTER INPUT

C

COMPLEX FUNCTION IFIN(I)

C

```

COMPLEX TWTOUT
COMPLEX IFFF
COMMON/QIFIN/ XC,XS,IFFF
COMMON /LUNITS/ LDI,LDO

```

C

```

IF (I.GT.0) GO TO 1
IFIN=TWTOUT(I)
READ(LDI,600) DNOISE,D1,DJ
600 FORMAT(8F10.5)
  ISTART = DI
  JSTART = DJ
  WRITE (LDO,601) DNOISE,ISTART,JSTART
601 FORMAT (20X,'DOWNLINK NOISE SPECTRAL DENSITY =',E13.6,/,
$20X,'DOWNLINK NOISE SEEDS:',I8,I9,/)
  ALPHA=400.*DNOISE
  ALPHA=SQRT(ALPHA)
  RETURN

```

C

```

1 XC=ALPHA*RNG(ISTART)
  XS=ALPHA*RNG(JSTART)
  IFFF=TWTOUT(I)+CMPLX(XC,XS)
  IFIN=IFFF
  RETURN
  END

```

C

GENERATE PHASE OF IF FILTER OUTPUT

C

REAL FUNCTION IFOUT(I)

C

```

COMPLEX XA,XA1,XA2,YA,YA1,YA2,YR,YB1,YB2
COMPLEX IFIN
COMMON/QIFOUT/ YR,YI
COMMON /LUNITS/ LDI,LDO

```

C

```

IF (I.GT.0) GO TO 1

```

```

PI = 3.1415926536
FREQS = 400.
TS = 1./FREQS
TWOPI = 2.*PI
IRAD = 0
IPREV = 1
XA1 = CMPLX(0.0,0.0)
XA2 = CMPLX(0.0,0.0)
YA1 = CMPLX(0.0,0.0)
YA2 = CMPLX(0.0,0.0)
YB1 = CMPLX(0.0,0.0)
YB2 = CMPLX(0.0,0.0)
XA=IFIN(I)
WRITE(LDD,600)
600 FORMAT (20X,'IF BANDWIDTH = 35 HZ',/)
NF=-1
RETURN

C
C THIS ROUTINE IS EXECUTED TWICE PER CALL
C
1 II=2*(I-1)
2 II=II+1
NF=NF+1

C
C OBTAIN COMPLEX ENVELOPE OF IF FILTER INPUT
C
XA=IFIN(II)

C
C LOWPASS VERSION OF IF FILTER
C
C 222724MAY74 4TH ORDER BUTTERWORTH LOWPASS FILTER
C FREQC = 17.5 HZ., FREQS = 400 HZ.
C
YA = 0.17437749E+01 * YA1 - 0.81179839E+00 * YA2
1+0.17005865E-01 * (XA + XA1 + XA1 + XA2)
YB = 0.15389702E+01 * YB1 - 0.59900437E+00 * YB2
1+0.15008558E-01 * (YA + YA1 + YA1 + YA2)
XA2 = XA1
XA1 = XA
YA2 = YA1
YA1 = YA
YB2 = YB1
YB1 = YB
YR = REAL(YB)
YI = AIMAG(YB)

C
C COMPUTE ANGLE OF OUTPUT, INCLUDING MULTIPLES OF 2*PI
C
IF(YR .NE. 0.0 .AND. YI .NE. 0.0) GO TO 7
RAD = 0.0
IF(IPREV .EQ. -1) IRAD=IRAD+1
IFLAG = 1
GO TO 15
7 IF(YR .NE. 0.0) GO TO 8
RAD = 0.0

```

```

      GO TO 9
8 RAD=ATAN(ABS(YI/YR))
9 IFLAG = 1
  IF(YR .GE. 0.0 .AND. YI .GE. 0.0) GO TO 13
  IF(YR .GE. 0.0 .AND. YI .LE. 0.0) GO TO 11
  IF(YR .LE. 0.0 .AND. YI .GE. 0.0) GO TO 12
10 RAD = RAD + PI
  IFLAG = 4
  GO TO 13
12 RAD = PI - RAD
  IFLAG = 2
  GO TO 13
11 RAD = TWOPI - RAD
  IFLAG = -1
13 IF(IFLAG + IPREV) 15,14,15
14 IRAD = IRAD + IFLAG
15 IPREV = IFLAG
  RAD = RAD + FLOAT(IRAD) * TWOPI
  IFOUT=RAD
  IF (NF.EQ.0) GO TO 2
  NF=-1
  RETURN
  END

```

```

C
C GENERATE A PSEUDOGAUSSIAN RANDOM NUMBER
C
C   FUNCTION RNG(ISEED)
C
C   Z=0.
C   DO 10 I=1,12
C     ISEED=4099*ISEED
C     IF (ISEED.LE.0) ISEED=ISEED+8388607+1
C     WW=ISEED
C     WW=WW*1.192093E-7
10  Z=Z+WW
C   RNG=Z-6.
C   RETURN
C   END

```


Input for NRZ-L and Split-Phase PSK Programs

The amplitude and phase tables precede the following cards.

CARD 1

CC 1-10	Total number of samples for the simulation.
CC11-20	Number of samples to process prior to printing.
CC21-30	Output option: = 0. No plot desired. = 1. Plots IF filter output. = 2. Intermediate print (Diagnostic).
CC31-40	Correlator phase angle, degrees.
CC41-50	Plot scale factor.

CARD 2

CC 1-10	PSK bit data rate, Mb/s.
CC11-20	Carrier amplitude.
CC21-30	RF phase angle, degrees.

CARD 3

CC 1-10	Uplink noise spectral density.
CC11-20	Seven digit odd number.
CC21-30	Seven digit odd number.

CARD 4

CC 1-10	Downlink noise spectral density.
CC11-20	Seven digit odd number.
CC21-30	Seven digit odd number.

Multiple simulations are made by repeating Cards 1 through 4, as illustrated by the sample input deck of Figure E-2. Listing of the programs are given in subsequent pages.

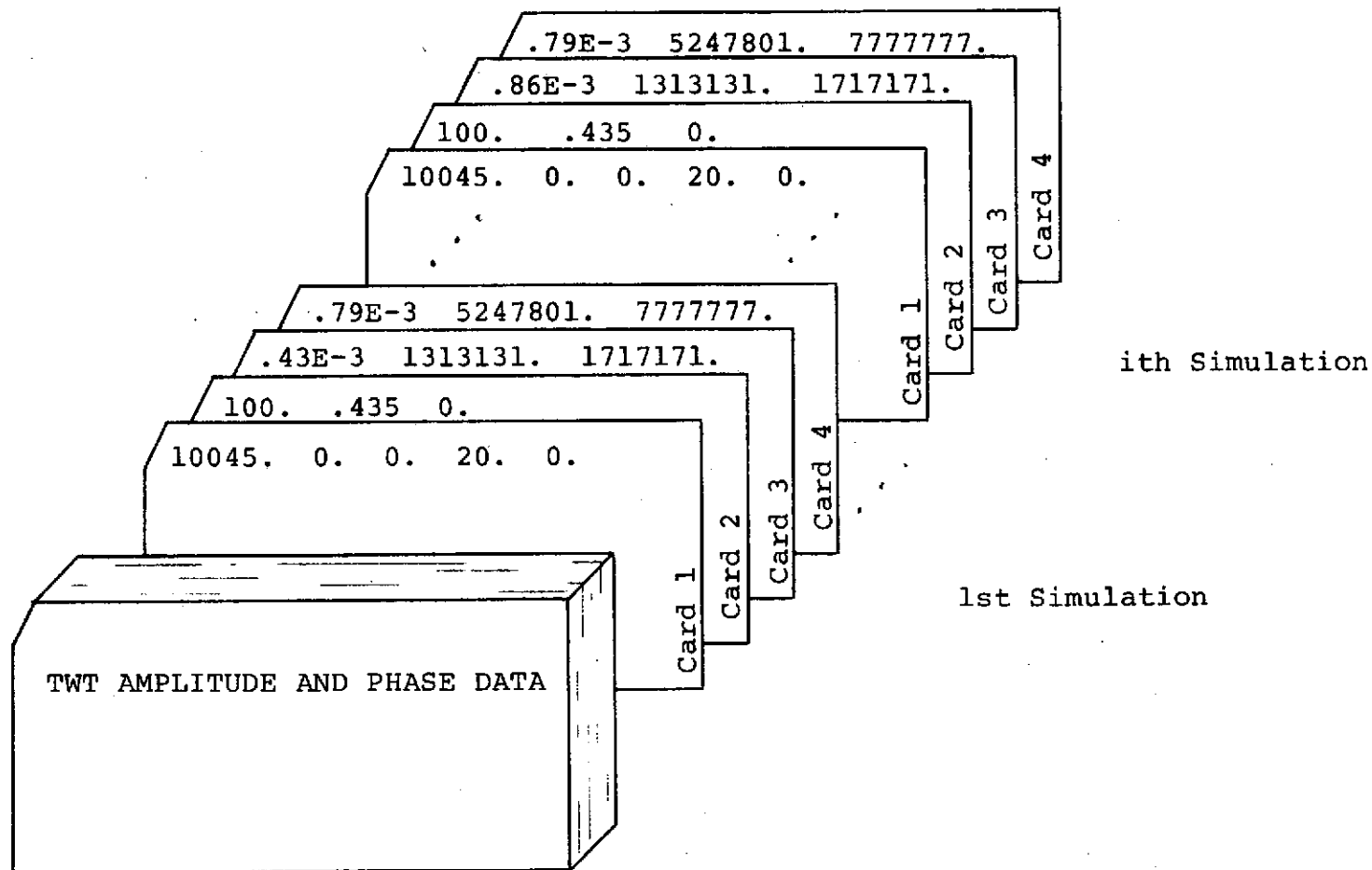


FIGURE E-2. SAMPLE INPUT DECK FOR NRZ-L PSK SIMULATION

SIMULATION PROGRAM FOR NRZ/PSK SIGNAL

NAME NRZPSK

COMPLEX SIG,IFIN
COMMON /LUNITS/ LDI,LDO
COMPLEX Y

COMPLEX Z(40),R,R1,R2,R3,R4,R5,R6,R7,R8,R9,R10,R11,R12,R13,R14,
R15,R16,R17,R18,R19,R20,R21,R22,R23,R24,R25,R26,R27,R28,R29,
R30,R31,R32,R33,R34,R35,R36,R37,R38,R39,R40
EQUIVALENCE (Z(1),R1),(Z(2),R2),(Z(3),R3),(Z(4),R4),
1 (Z(5),R5),(Z(6),R6),(Z(7),R7),(Z(8),R8),(Z(9),R9),(Z(10),R10),
1 (Z(11),R11),(Z(12),R12),(Z(13),R13),(Z(14),R14),(Z(15),R15),
1 (Z(16),R16),(Z(17),R17),(Z(18),R18),(Z(19),R19),(Z(20),R20),
1 (Z(21),R21),(Z(22),R22),(Z(23),R23),(Z(24),R24),(Z(25),R25),
1 (Z(26),R26),(Z(27),R27),(Z(28),R28),(Z(29),R29),(Z(30),R30),
1 (Z(31),R31),(Z(32),R32),(Z(33),R33),(Z(34),R34),(Z(35),R35),
1 (Z(36),R36),(Z(37),R37),(Z(38),R38),(Z(39),R39),(Z(40),R40)
DIMENSION NGRAPH(81)
DIMENSION NBIT(63)

SYSTEM TEST POINTS MAINTAINED IN LABELLED COMMON

COMMON AMPNL(151),PHNL(151)
COMMON/QTWT/ UNC,UNS,TINC,TINS,AIN,AOUT,PHOUT,TOUTC,TOUTS
COMMON/QIFIN/ DNC,DNS,CIFIN,SIFIN
COMMON /OSIG/ AMP,BRATE,RFRAD,SIG

COEFFICIENTS FOR 225 HZ IF FILTER

DATA C0,C1,C2,C3,C4,C5,C6,C7,C8,C9,C10,C11,C12,C13,C14,C15,C16,
C17,C18,C19,C20 / .242,.218578,.156720,.779368E-1,.754453E-2,
-.356829E-1, -.460829E-1, -.312270E-1, -.629190E-2,.139254E-1,
.212529E-1,.160224E-1,.454706E-02, -.562891E-2, -.984428E-2,
-.786541E-2, -.270827E-2,.192827E-2,.385473E-2,.309835E-2,
.114529E-2/

63 BIT PN DATA SEQUENCE

DATA NBIT/ 1,1,1,1,1,1,-1,-1,-1,-1,-1,1,-1,-1,-1,-1,1,1,
\$ -1,-1,-1,1,-1,1,-1,-1,1,1,1,1,-1,1,-1,-1,1,1,1,-1,-1,
\$ 1,-1,1,1,-1,1,1,1,-1,1,1,-1,-1,1,1,-1,1,-1,1,-1/
DATA JBLANK, JDOT, JPLL/1H ,1H.,1H*/

LDI = 7
LDO = 6

READ IN TWT AMPLITUDE AND PHASE NONLINEARITIES

CALL TWTSET
PI = 3.1415926536
TWOPI = 2.*PI

```

      T=1./1000.
      DO 8 I=1,81
      8 NGRAPH(I)=JBLANK
C
      1 CONTINUE
      READ(LDI,666) DN,DNHOLD,DNP,PHASE,FSCALE
666  FORMAT(5F10.5)
      N = DN
      NHOLD = DNHOLD
      NP = DNP
      NH=NHOLD+1
      R=CMPLX(0.,0.)
      DO 5 J=1,40
      5 Z(J)=CMPLX(0.,0.)
      R=IFIN(-1)
      WRITE(LDO,602) PHASE
602  FORMAT(20X,'CORRELATOR PHASE ANGLE = ',F7.3,' DEGREES'//)
      PHASE=PHASE*TWOPI/360.
      PSUM=0.
      IBIT=0
      PE=0.
      NERR=0
      IBITS=0
      TBIT=1./BRATE
      TIME=-T
C
      DO 100 NN=1,N
      R=IFIN(NN)
C
C      FILTER RECEIVED SIGNAL
C
      Y = C20*(R+R40)+C19*(R1+R39)+C18*(R2+R38)+C17*(R3+R37)+C16*(R4+
1 R36)+C15*(R5+R35)+C14*(R6+R34)+C13*(R7+R33)+C12*(R8+R32)+
1 C11*(R9+R31)+C10*(R10+R30)+
1 C9*(R11+R29)+C8*(R12+R28)+C7*(R13+R27)+C6*(R14+R26)+C5*(R15+R25)+
1 C4*(R16+R24)+C3*(R17+R23)+C2*(R18+R22)+C1*(R19+R21)+C0*R20
C
      R40=R39
      R39=R38
      R38=R37
      R37=R36
      R36=R35
      R35=R34
      R34=R33
      R33=R32
      R32=R31
      R31=R30
      R30=R29
      R29=R28
      R28=R27
      R27=R26
      R26=R25
      R25=R24
      R24=R23
      R23=R22

```

```

R22=R21
R21=R20
R20=R19
R19=R18
R18=R17
R17=R16
R16 = R15
R15=R14
R14=R13
R13=R12
R12=R11
R11=R10
R10=R9
R9=R8
R8=R7
R7=R6
R6=R5
R5=R4
R4=R3
R3=R2
R2=R1
R1=R

C
C   MULTIPLY BY LOCAL OSCILLATOR
C
C   YR=REAL(Y)
C   YI=AIMAG(Y)
C   THETA=YR*COS(PHASE)+YI*SIN(PHASE)

C
C   WAIT 40 SAMPLES TO ACCOUNT FOR FILTER DELAY
C
C   IF(NN.LE.40) GO TO 50
C   TIME=TIME+T

C
C   INTEGRATE OVER ONE BIT INTERVAL
C
C   PSUM=PSUM+THETA
C   IF(TIME.LT.TBIT) GO TO 50

C
C   MAKE BIT DECISION
C
C   TIME=TIME-TBIT
C   IBITS=IBITS+1
C   IBIT=IBIT+1
C   IF(IBIT.GT.63) IBIT =1
C   MBIT=1
C   IF(PSUM.LT.0) MBIT=-1

C
C   COMPARE WITH KNOWN DATA SEQUENCE
C
C   IF(MBIT.NE.NBIT(IBIT)) NERR=NERR+1
C   PSUM=0.
50 IF(NN.LE.NHOLD) GO TO 100
C   IF (NP.NE.1) GO TO 80

```

```

C      PLOT IF FILTER OUTPUT
C
      NZ=FSCALE*THETA + 41.5
      IF (NZ.GT.81) NZ=81
      IF (NZ.LT.1) NZ=1
      NGRAPH(41)=JDOT
      NGRAPH(NZ)=JPLL
      WRITE(LDO,601) NN,NGRAPH,THETA
601  FORMAT (I9,81A1,5X,3F10.5)
      NGRAPH(NZ)=JBLANK
      80 CONTINUE
      IF (NP.NE.2) GO TO 100
      IF (NN.EQ.NH) WRITE(LDO,501)
501  FORMAT(//,4X,'N',7X,'THETA',7X,'AMP',9X'*** SIG ***',9X'TINC',7X'TINS',
$ 7X'AOUT',6X,'PHOUT',6X'TOUTC',6X'TOUTS'//)
      WRITE(LDO,500) NN,THETA,AMP,SIG,TINC,TINS,AOUT,PHOUT,TOUTC,TOUTS
500  FORMAT(1X,I5,10F11.5)
100  CONTINUE
C
      TERR=NERR
      TBITS=IBITS
      IF (IBITS.NE.0) PE=TERR/TBITS
      WRITE(LDO,610) IBITS,PE
610  FORMAT(//,25X,'ERROR PROBABILITY AFTER ',I6,' BITS :',E12.6)
      GO TO 1
      END

C
C      READ TWT INPUT AMPLITUDE AND PHASE
C
C
C      SUBROUTINE TWTSET

      COMMON AMPNL(151),PHNL(151)
      COMMON /LUNITS/ LDI,LDO
C
      READ(LDI,701) AMPNL
      READ(LDI,701) PHNL
701  FORMAT (10F8.4)
      RETURN
      END

C
C      GENERATE COMPLEX ENVELOPE OF IF FILTER INPUT
C
C      COMPLEX FUNCTION IFIN(I)
C
      COMPLEX TWTOUT
      COMPLEX IFFF
      COMMON/QIFIN/ XC,XS,IFFF
      COMMON /LUNITS/ LDI,LDO

```

C

```

      IF (I.GT.0) GO TO 1
      IFIN=TWTOUT(I)
      READ(LDI,600) DNOISE,DI,DJ
600  FORMAT(5F10.5)
      ISTART = DI
      JSTART = DJ
      WRITE(LDO,601) DNOISE,ISTART,JSTART
601  FORMAT (20X,'DOWNLINK NOISE SPECTRAL DENSITY =',E13.6,/,
    $20X,'DOWNLINK NOISE SEEDS:',I8,I9,/)
      ALPHA=1000.*DNOISE
      ALPHA=SQRT(ALPHA)
      RETURN

```

C

```

1  XC=ALPHA*RNG(ISTART)
   XS=ALPHA*RNG(JSTART)
   IFFF=TWTOUT(I)+CMPLX(XC,XS)
   IFIN=IFFF
   RETURN
   END

```

C

C

GENERATE COMPLEX ENVELOPE OF TWT OUTPUT

C

COMPLEX FUNCTION TWTOUT(I)

C

```

      COMPLEX SIGIN
      COMPLEX TWTIN,EPHASE(151)
      COMPLEX TOUT,R,R1,R2,R3,R4,R5,R6,R7,R8,R9,R10,R11,R12,R13,R14,
    # R15,R16,R17,R18,R19,R20,R21,R22,R23,R24,R25,R26,R27,R28,R29,
    # R30,R31,R32,R33,R34,R35,R36,R37,R38,R39,R40,Z(40)
      COMMON AMP(151),PHASE(151)
      COMMON/QTWT/ XC,XS,TWTIN,TAMP,F,G,TOUT
      COMMON /LUNITS/ LDI,LDO
      EQUIVALENCE (Z(1),R1),(Z(2),R2),(Z(3),R3),(Z(4),R4),
1  (Z(5),R5),(Z(6),R6),(Z(7),R7),(Z(8),R8),(Z(9),R9),(Z(10),R10),
1  (Z(11),R11),(Z(12),R12),(Z(13),R13),(Z(14),R14),(Z(15),R15),
C  (Z(16),R16),(Z(17),R17),(Z(18),R18),(Z(19),R19),(Z(20),R20),
1  (Z(21),R21),(Z(22),R22),(Z(23),R23),(Z(24),R24),(Z(25),R25),
1  (Z(26),R26),(Z(27),R27),(Z(28),R28),(Z(29),R29),(Z(30),R30),
1  (Z(31),R31),(Z(32),R32),(Z(33),R33),(Z(34),R34),(Z(35),R35),
1  (Z(36),R36),(Z(37),R37),(Z(38),R38),(Z(39),R39),(Z(40),R40)
      DATA C0,C1,C2,C3,C4,C5,C6,C7,C8,C9,C10,C11,C12,C13,C14,C15,C16,
    # C17,C18,C19,C20 / .242,.218578,.156720,.779368E-1,.754453E-2,
    # -.356829E-1,-.460829E-1,-.312270E-1,-.629190E-2,.139254E-1,
    # .212529E-1,.160224E-1,.454706E-02,-.562891E-2,-.984428E-2,
    # -.786541E-2,-.270827E-2,.192827E-2,.385473E-2,.309835E-2,
    # .114529E-2/

```

C

```

      IF (I.GT.0) GO TO 1
      TWTIN=SIGIN(I)
      R=CMPLX(0.,0.)
      DO 5 J=1,40

```



```

5  Z(J)=CMPLX(0.,0.)
   AIN=REAL(TWTIN)
   INDEX=IFIX(100.*AIN)+1
   AOUT=AMP(INDEX)
   A100=100.*AOUT
   READ(LDI,600)UNOISE,UI,UJ
600 FORMAT(3F10.5)
   ISTART = UI
   JSTART = UJ
   WRITE(LDO,601) UNOISE,ISTART,JSTART,A100
601 FORMAT (/20X,'UPLINK NOISE SPECTRAL DENSITY =',E13.6,/,
$20X,'UPLINK NOISE SEEDS:',I8,I9,/,
$20X,'TWT INPUT BANDWIDTH = 225 HZ',/,
$20X,'NOMINAL OUTPUT AMPLITUDE =',F7.2,' PERCENT OF SATURATION',/,
   CC = 3.1415926536/180.
   DO 10 N=1,151
10  EPHASE(N)=CEXP(CMPLX(0.,CC*PHASE(N)))
   ALPHA=1000.*UNOISE
   ALPHA=SQRT(ALPHA)
   RETURN
C
1  XC=ALPHA*RNG(ISTART)
   XS=ALPHA*RNG(JSTART)
   TWTIN=SIGIN(I) + CMPLX(XC,XS)
   R=TWTIN
C
   TWTIN=C20*(R+R40)+C19*(R1+R39)+C18*(R2+R38)+C17*(R3+R37)+C16*(R4+
1  R36)+C15*(R5+R35)+C14*(R6+R34)+C13*(R7+R33)+C12*(R8+R32)+
1  C11*(R9+R31)+C10*(R10+R30)+
1  C9*(R11+R29)+C8*(R12+R28)+C7*(R13+R27)+C6*(R14+R26)+C5*(R15+R25)+
1  C4*(R16+R24)+C3*(R17+R23)+C2*(R18+R22)+C1*(R19+R21)+C0*R20
C
   R40=R39
   R39=R38
   R38=R37
   R37=R36
   R36=R35
   R35=R34
   R34=R33
   R33=R32
   R32=R31
   R31=R30
   R30=R29
   R29=R28
   R28=R27
   R27=R26
   R26=R25
   R25=R24
   R24=R23
   R23=R22
   R22=R21
   R21=R20
   R20=R19
   R19=R18
   R18=R17

```

```

R17=R16
R16 = R15
R15=R14
R14=R13
R13=R12
R12=R11
R11=R10
R10=R9
R9=R8
R8=R7
R7=R6
R6=R5
R5=R4
R4=R3
R3=R2
R2=R1
R1=R

```

C

```

2 TAMP=CABS(TWTIN)
  INDEX=IFIX(100.*TAMP)+1
  IF (INDEX.GT.151) INDEX=151
  F=AMP(INDEX)
  G=PHASE(INDEX)
  TOUT=F*TWTIN*EPHASE(INDEX)/TAMP
  TWTOUT=TOUT
  RETURN
  END

```

C

C

GENERATE COMPLEX ENVELOPE OF NRZ-L PSK SIGNAL

C

COMPLEX FUNCTION SIGIN(I)

C

```

  COMPLEX SIG,S1,SIGIN
  COMMON /GSIG/AMP,BRATE,RFRAD,SIG
  COMMON /LUNITS/ LDI,LDO
  DIMENSION NBIT(63)
  DATA NBIT/ 1,1,1,1,1,1,-1,-1,-1,-1,-1,1,-1,-1,-1,-1,1,1,
$ -1,-1,-1,1,-1,1,-1,-1,1,1,1,1,-1,1,-1,-1,-1,1,1,1,-1,-1,
$ 1,-1,1,1,-1,1,1,1,-1,1,1,-1,-1,1,1,-1,1,-1/

```

C

```

  IF(I.GT.0) GO TO 10
  K=1
  TWOPI=6.2831853072
  T=1./1000.
  TIME = -T
  READ(LDI,600) BRATE,AMP,RFPHSE
600 FORMAT(3F10.5)
  AMP100=AMP*100.
  TBIT=1./BRATE
  RFRAD = RFPHSE * TWOPI / 360.
  SI=CEXP(CMPLX(0.,RFRAD))*CMPLX(AMP,0.)
  SIGIN=CMPLX(AMP,0.)

```

```

        WRITE(LD0,601) BRATE,AMP100,RFPHSE
601  FORMAT(1H1,/,/,20X,'HIGH RATE NRZ PSK SIGNAL',/,/,
120X,'DATA RATE = ',F7.3,' BITS PER SECOND',/
120X,'CARRIER AMPLITUDE = ',F7.2,' PERCENT OF SATURATING VALUE',
1/,20X,'RF PHASE ANGLE = ',F7.3,' DEGREES')
        RETURN

```

C

```

10  TIME = TIME + T
    IF (TIME.LT.TBIT) GO TO 30
    TIME=TIME-TBIT
    K=K+1
    IF (K.GT.63) K=K-63
30  SIG=SI*NBIT(K)
    SIGIN=SIG
    RETURN
    END

```

C

C GENERATE A PSEUDOGAUSSIAN RANDOM NUMBER

C

```

        FUNCTION RNG(ISEED)

```

C

```

        Z=0.
        DO 10  I=1,12
        ISEED=4099*ISEED
        IF (ISEED.LE.0) ISEED=ISEED+8388607+1
        WW=ISEED
        WW=WW*1.192093E-7
10  Z=Z+WW
        RNG=Z-6.
        RETURN
        END

```



```

      DO 8 I=1,81
      8 NGRAPH(I)=JBLANK
C
      1 CONTINUE
      READ(LDI,666) DN,DNHOLD,DNP,PHASE,FSCALE
666  FORMAT(5F10.5)
      N = DN
      NHOLD = DNHOLD
      NP = DNP
      NH=NHOLD+1
      R=CMPLX(0.,0.)
      DO 5 J=1,40
      5 Z(J)=CMPLX(0.,0.)
      R=IFIN(-1)
      WRITE(LDO,602) PHASE
602  FORMAT(20X,'CORRELATOR PHASE ANGLE = ',F7.3,' DEGREES'//)
      PHASE=PHASE*TWOPI/360.
      PSUM=0.
      IBIT=0
      PE=0.
      NERR=0
      IBITS=0
      TBIT=1./BRATE
      T2=.5*TBIT
      KSIGN=1
      TIME=-I
      DO 100 NN=1,N
      R=IFIN(NN)
C
C      FILTER RECEIVED SIGNAL
C
      Y = C20*(R+R40)+C19*(R1+R39)+C18*(R2+R38)+C17*(R3+R37)+C16*(R4+
1 R36)+C15*(R5+R35)+C14*(R6+R34)+C13*(R7+R33)+C12*(R8+R32)+
1 C11*(R9+R31)+C10*(R10+R30)+
1 C9*(R11+R29)+C8*(R12+R28)+C7*(R13+R27)+C6*(R14+R26)+C5*(R15+R25)+
1 C4*(R16+R24)+C3*(R17+R23)+C2*(R18+R22)+C1*(R19+R21)+C0*R20
C
      R40=R39
      R39=R38
      R38=R37
      R37=R36
      R36=R35
      R35=R34
      R34=R33
      R33=R32
      R32=R31
      R31=R30
      R30=R29
      R29=R28
      R28=R27
      R27=R26
      R26=R25
      R25=R24
      R24=R23
      R23=R22

```

```

R22=R21
R21=R20
R20=R19
R19=R18
R18=R17
R17=R16
R16 = R15
R15=R14
R14=R13
R13=R12
R12=R11
R11=R10
R10=R9
R9=R8
R8=R7
R7=R6
R6=R5
R5=R4
R4=R3
R3=R2
R2=R1
R1=R

C
C   MULTIPLY BY LOCAL OSCILLATOR
C
    YR=REAL(Y)
    YI=AIMAG(Y)
    THETA=YR*COS(PHASE)+YI*SIN(PHASE)

C
C   WAIT 40 SAMPLES TO ACCOUNT FOR FILTER DELAY
C
    IF(NN.LE.40) GO TO 50
    TIME=TIME+T

C
C   SPLIT-PHASE INTEGRATE OVER ONE BIT INTERVAL
C
    IF(TIME.GE.T2) KSIGN=-1
    PSUM=PSUM+THETA*KSIGN
    IF(TIME.LT.TBIT) GO TO 50

C
C   MAKE BIT DECISION
C
    TIME=TIME-TBIT
    IBITS=IBITS+1
    IBIT=IBIT+1
    IF(IBIT.GT.63) IBIT =1
    MBIT=1
    IF(PSUM.LT.0) MBIT=-1

C
C   COMPARE WITH KNOWN DATA SEQUENCE
C
    IF(MBIT.NE.NBIT(IBIT)) NERR=NERR+1
    PSUM=0.
    KSIGN=1
50 IF(NN.LE.NHOLD) GO TO 100

```

```

      IF (NP.NE.1) GO TO 80
C
C      PLOT IF FILTER OUTPUT
C
      NZ=FSCALE*THETA + 41.5
      IF (NZ.GT.81) NZ=81
      IF (NZ.LT.1) NZ=1
      NGRAPH(41)=JDOT
      NGRAPH(NZ)=JPLL
      WRITE(LDO,601) NN,NGRAPH,THETA
601  FORMAT (I9,81A1,5X,3F10.5)
      NGRAPH(NZ)=JBLANK
      80 CONTINUE
      IF (NP.NE.2) GO TO 100
      IF (NN.EQ.NH) WRITE(LDO,501)
501  FORMAT(//,4X,'N',7X,'THETA'7X'AMP'9X'*** SIG ***'9X'TINC'7X'TINS'
      $ 7X'AOUT'6X,'PHOUT'6X'TOUTC'6X'TOUTS'//)
      WRITE(LDO,500) NN,THETA,AMP,SIG,TINC,TINS,AOUT,PHOUT,TOUTC,TOUTS
500  FORMAT(1X,I5,10F11.5)
      100 CONTINUE
C
      TERR=NERR
      TBITS=IBITS
      IF (IBITS.NE.0) PE=TERR/TBITS
      WRITE(LDO,610) IBITS,PE
610  FORMAT(//,25X,'ERROR PROBABILITY AFTER ',I6,' BITS :',E12.6)
      GO TO 1
      END

C
C      READ TWT INPUT AMPLITUDE AND PHASE
C
C      SUBROUTINE TWTSET
C
      COMMON AMPNL(151),PHNL(151)
      COMMON /LUNITS/ LDI,LDO
C
      READ(LDI,701) AMPNL
      READ(LDI,701) PHNL
701  FORMAT (10F8.4)
      RETURN
      END

C
C      GENERATE COMPLEX ENVELOPE OF IF FILTER INPUT
C
      COMPLEX FUNCTION IFIN(I)
C
      COMPLEX TWTOUT
      COMPLEX IFFF
      COMMON/QIFIN/ XC,XS,IFFF

```

```

COMMON /LUNITS/ LDI,LDO
C
  IF (I.GT.0) GO TO 1
  IFIN=TWTOUT(I)
  READ(LDI,600) DNOISE,DI,DJ
600 FORMAT(5F10.5)
  ISTART = DI
  JSTART = DJ
  WRITE(LDO,601) DNOISE,ISTART,JSTART
601 FORMAT (20X,'DOWNLINK NOISE SPECTRAL DENSITY =',E13.6,/,
$20X,'DOWNLINK NOISE SEEDS:',I8,I9,/)
  ALPHA=1000.*DNOISE
  ALPHA=SQRT(ALPHA)
  RETURN
C
1 XC=ALPHA*RNG(ISTART)
  XS=ALPHA*RNG(JSTART)
  IFFF=TWTOUT(I)+CMPLX(XC,XS)
  IFIN=IFFF
  RETURN
END

C
C GENERATE COMPLEX ENVELOPE OF TWT OUTPUT
C
  COMPLEX FUNCTION TWTOUT(I)
C
  COMPLEX SIGIN
  COMPLEX TWTIN,EPHASE(151)
  COMPLEX TOUT,R,R1,R2,R3,R4,R5,R6,R7,R8,R9,R10,R11,R12,R13,R14,
# R15,R16,R17,R18,R19,R20,R21,R22,R23,R24,R25,R26,R27,R28,R29,
# R30,R31,R32,R33,R34,R35,R36,R37,R38,R39,R40,Z(40)
  COMMON AMP(151),PHASE(151)
  COMMON/QTWT/ XC,XS,TWTIN,TAMP,F,G,TOUT
  COMMON /LUNITS/ LDI,LDO
  EQUIVALENCE (Z(1),R1),(Z(2),R2),(Z(3),R3),(Z(4),R4),
1 (Z(5),R5),(Z(6),R6),(Z(7),R7),(Z(8),R8),(Z(9),R9),(Z(10),R10),
1 (Z(11),R11),(Z(12),R12),(Z(13),R13),(Z(14),R14),(Z(15),R15),
C (Z(16),R16),(Z(17),R17),(Z(18),R18),(Z(19),R19),(Z(20),R20),
1 (Z(21),R21),(Z(22),R22),(Z(23),R23),(Z(24),R24),(Z(25),R25),
1 (Z(26),R26),(Z(27),R27),(Z(28),R28),(Z(29),R29),(Z(30),R30),
1 (Z(31),R31),(Z(32),R32),(Z(33),R33),(Z(34),R34),(Z(35),R35),
1 (Z(36),R36),(Z(37),R37),(Z(38),R38),(Z(39),R39),(Z(40),R40)
  DATA C0,C1,C2,C3,C4,C5,C6,C7,C8,C9,C10,C11,C12,C13,C14,C15,C16,
$ C17,C18,C19,C20 / .0998,.0978266,.0920746,.0830285,.0714349,
$ .0582189,.0443845,.0309087,.018646,.825247E-2,.137890E-3,
$ -.554897E-2, -.890396E-2, -.102239E-1, -.994462E-2, -.856989E-2,
$ -.660235E-2, -.448471E-2, -.255823E-2, -.104153E-2, -.298784E-4/
C
  IF (I.GT.0) GO TO 1
  TWTIN=SIGIN(I)
  R=CMPLX(0.,0.)
  DO 5 J=1,40

```



```

5 Z(J)=CMPLX(0.,0.)
  AIN=REAL(TWTIN)
  INDEX=1FIX(100.*AIN)+1
  AOUT=AMP(INDEX)
  A100=100.*AOUT
  READ(LDI,600)UNOISE,UI,UJ
600 FORMAT(3F10.5)
  ISTART = UI
  JSTART = UJ
  WRITE(LDO,601) UNOISE,ISTART,JSTART,A100
601 FORMAT (/20X,'UPLINK NOISE SPECTRAL DENSITY =',E13.6,/,
$20X,'UPLINK NOISE SEEDS:',I8,I9,/,
$20X,'TWT INPUT BANDWIDTH = 88 HZ',/,
$20X,'NOMINAL OUTPUT AMPLITUDE =',F7.2,' PERCENT OF SATURATION',/)
  CC = 3.1415926536/180.
  DO 10 N=1,151
10 EPHASE(N)=CEXP(CMPLX(0.,CC*PHASE(N)))
  ALPHA=1000.*UNOISE
  ALPHA=SQRT(ALPHA)
  RETURN
C
1 XC=ALPHA*RNG(ISTART)
  XS=ALPHA*RNG(JSTART)
  TWTIN=SIGIN(I) + CMPLX(XC,XS)
  R=TWTIN
C
  TWTIN=C20*(R+R40)+C19*(R1+R39)+C18*(R2+R38)+C17*(R3+R37)+C16*(R4+
1 R36)+C15*(R5+R35)+C14*(R6+R34)+C13*(R7+R33)+C12*(R8+R32)+
1 C11*(R9+R31)+C10*(R10+R30)+
1 C9*(R11+R29)+C8*(R12+R28)+C7*(R13+R27)+C6*(R14+R26)+C5*(R15+R25)+
1 C4*(R16+R24)+C3*(R17+R23)+C2*(R18+R22)+C1*(R19+R21)+C0*R20
C
  R40=R39
  R39=R38
  R38=R37
  R37=R36
  R36=R35
  R35=R34
  R34=R33
  R33=R32
  R32=R31
  R31=R30
  R30=R29
  R29=R28
  R28=R27
  R27=R26
  R26=R25
  R25=R24
  R24=R23
  R23=R22
  R22=R21
  R21=R20
  R20=R19
  R19=R18
  R18=R17

```

```

R17=R16
R16 = R15
R15=R14
R14=R13
R13=R12
R12=R11
R11=R10
R10=R9
R9=R8
R8=R7
R7=R6
R6=R5
R5=R4
R4=R3
R3=R2
R2=R1
R1=R

```

C

```

2 TAMP=CABS(TWTIN)
  INDEX=IFIX(100.*TAMP)+1
  IF (INDEX.GT.151) INDEX=151
  F=AMP(INDEX)
  G=PHASE(INDEX)
  TOUT=F*TWTIN*EPHASE(INDEX)/TAMP
  TWTOUT=TOUT
  RETURN
  END

```

C

C

GENERATE COMPLEX ENVELOPE OF SPLIT-PHASE PSK SIGNAL

C

COMPLEX FUNCTION SIGIN(I)

C

```

COMPLEX SIG,SI,SIGIN
COMMON /QSIG/AMP,BRATE,RFRAD,SIG
COMMON /LUNITS/ LDI,LDO
DIMENSION NBIT(63)
DATA NBIT/ 1,1,1,1,1,1,-1,-1,-1,-1,-1,1,-1,-1,-1,-1,1,1,
$ -1,-1,-1,1,-1,1,-1,-1,1,1,1,1,-1,1,-1,-1,-1,1,1,1,-1,-1,1,-1,
$ 1,-1,1,1,-1,1,1,1,-1,1,1,-1,-1,1,1,-1,1,-1,1,-1/

```

C

```

IF(I.GT.0) GO TO 10
K=1
TWOPI=6.2831853072
T=1./1000.
TIME = -T
READ(LDI,600) BRATE,AMP,RFPHSE
600 FORMAT(3F10.5)
AMP100=AMP*100.
TBIT=1./BRATE
T2=.5*TBIT
M=NBIT(K)
RFRAD = RFPHSE * TWOPI / 360.

```

```

        SI=CEXP(CMPLX(0.,RFRAD))*CMPLX(AMP,0.)
        SIGIN=CMPLX(AMP,0.)
        WRITE(L00,601) BRATE,AMP100,RFPHSE
601  FORMAT(1H1, '//, 20X, 'HIGH RATE SPLIT PHASE PSK SIGNAL', '//,
        120X, 'DATA RATE = ', F7.3, ' BITS PER SECOND', /
        120X, 'CARRIER AMPLITUDE = ', F7.2, ' PERCENT OF SATURATING VALUE',
        1/, 20X, 'RF PHASE ANGLE = ', F7.3, ' DEGREES')
        RETURN

```

```

C
10  TIME=TIME+T
    IF (TIME.GE.T2) M=-NBIT(K)
    IF (TIME.LT.TBIT) GO TO 30
    TIME=TIME-TBIT
    K=K+1
    IF (K.GT.63) K=1
    M=NBIT(K)

```

```

C
30  SIG = M*SI
    SIGIN=SIG
    RETURN
    END

```

```

C
C  GENERATE A PSEUDOGAUSSIAN RANDOM NUMBER
C

```

```

        FUNCTION RNG(ISEED)
C
        Z=0.
        DO 10  I=1,12
            ISEED=4099*ISEED
            IF (ISEED.LE.0) ISEED=ISEED+8388607+1
            WW=ISEED
            WW=WW*1.192093E-7
10  Z=Z+WW
        RNG=Z-6.
        RETURN
        END

```